

DISCOVERING NEW VACCINES AND THERAPEUTICS TO TREAT  
CHIKUNGUNYA VIRUS INFECTIONS: CHARACTERIZATION OF AN  
ANTIVIRAL, A THERAPY, AND A VACCINE

**By Rebecca Broeckel**

A DISSERTATION

Presented to the Department of Molecular Microbiology and Immunology and the  
Oregon Health & Science University School of Medicine in partial fulfillment of the  
requirements for the degree of

Doctor of Philosophy

October 2017

**School of Medicine**  
**Oregon Health & Science University**  
CERTIFICATE OF APPROVAL

---

This is to certify that the PhD dissertation thesis of

**Rebecca Broeckel**

has been approved

---

Advisor / Daniel Streblov, PhD

---

Committee Chair / Victor DeFilippis, PhD

---

Committee Member / William Messer, PhD

---

Committee Member / Jonah Sacha, PhD

---

Committee Member / Alec Hirsch, PhD

## ABSTRACT

Chikungunya virus (CHIKV) is a mosquito-borne alphavirus that causes acute febrile illness and long-lasting joint and muscle pain. The 2013-2016 CHIKV outbreaks in the Americas is one example of how CHIKV can rapidly spread through areas of CHIKV seronegative individuals and cause widespread severe and debilitating arthritic disease. Since there is no currently available licensed vaccine or antiviral for preventing or treating CHIKV and other alphaviruses, there is urgent need to understand the basic processes of viral replication and viral immunity to develop effective prophylactic and therapeutic treatments. In my dissertation, I describe three different strategies to uncover new aspects of CHIKV biology by testing a small molecule inhibitor, a monoclonal antibody therapy, and a novel T cell vaccine. Chapter One of this document contains a comprehensive overview of alphaviruses, their replication strategies, diseases they cause, and immunity.

Chapter Two of my dissertation is a study showing that manipulating cellular kinases and their signaling cascades can have significant impacts on viral replication. Although, the basic steps of viral replication (entry, RNA replication, translation, assembly, and release) are known, the reliance of each of these steps on host cellular proteins and host kinase signaling events is not well understood. Importantly, knowledge of the host-virus interactions could be used for the development of antivirals directed against CHIKV and other alphaviruses. I used the small molecule inhibitor dasatinib, also known as BMS-354825 or Sprycel, to show that the Src Family Kinases are required during alphavirus replication. I found that addition of dasatinib to cell culture medium at two hours post CHIKV infection inhibited viral replication at the level of structural protein synthesis, resulting in a 10-fold reduction in viral replication. Interestingly, I found that dasatinib blocked translation of replication complex-derived viral subgenomic mRNAs but it did not inhibit translation of host mRNAs or the viral genomic mRNA. These data imply that dasatinib treatment of CHIKV infected cells prevented translation of alphavirus subgenomic

mRNAs in the context of active infection. Src Family Kinases are therefore linked to translation of alphavirus subgenomic mRNAs. Importantly, this work facilitates the development of antivirals that target the translation step of alphavirus replication.

Chapter Three of my dissertation details results of our study aimed at developing a humanized monoclonal antibody therapy for CHIKV. Anti-CHIKV monoclonal antibody therapies have been effective in mouse models, and they could potentially be used to treat CHIKV infections in humans. The Streblow lab, in collaboration with the laboratories of Dr. Michael Diamond, Dr. James Crowe, and Sanofi, have previously shown the efficacy of a combination mouse monoclonal antibody therapy in blocking viremia in rhesus macaques. To further the development of a monoclonal antibody therapeutic for use in humans, I, in collaboration with the same research groups, showed that a more potent human anti-CHIKV monoclonal antibody significantly reduced CHIKV disease in rhesus macaques. For this study, twelve rhesus macaques were infected with CHIKV, and the antibody therapy was administered at days 1 and 3 post infection. At 7 days post infection, necropsies were performed to measure the efficacy of the therapeutic in reducing CHIKV disease. Together, we showed that the anti-CHIKV therapy eliminated viremia and reduced inflammation and cellular infiltration into the muscles and joints of infected tissues. This work suggests that anti-CHIKV monoclonal antibody therapy could reduce CHIKV-induced disease in humans.

In Chapter Four, I present data showing that a vaccine that stimulates anti-CHIKV T cells is protective during CHIKV infection. Current research has implicated anti-CHIKV CD4<sup>+</sup> T cells as a major contributor to joint swelling after CHIKV infection. CD8<sup>+</sup> T cells were suggested to not protect mice against CHIKV infection as they do for other viral infections. However, studies performed with other alphaviruses showed that T cells could have a tissue-specific effect that was not evaluated in the CHIKV models. To address this knowledge gap regarding the T cell responses during CHIKV infection, I generated murine cytomegalovirus (MCMV) and

adenovirus (AdV)-vectored vaccines that encoded immunodominant CHIKV T cell epitopes as tools to elicit T cell responses in mice. Mice vaccinated with the MCMV and AdV vectors developed CHIKV-specific T cell responses, but they were not protected from CHIKV challenge in the footpad. However, vaccinated mice that were challenged intramuscularly had a 2-3 log reduction in virus in the calf muscle. Depletion of CD8<sup>+</sup> and CD4<sup>+</sup> T cells in vaccinated mice showed that the protection in the calf was mediated by both CD4<sup>+</sup> and CD8<sup>+</sup> T cells. In this study, I showed that T cells make up an important part of anti-CHIKV immunity in the muscle tissue, and my results suggest the feasibility of a therapeutic T cell vaccine in eliminating viral burden in muscle tissue and thus eliminating CHIKV-induced muscle pain.

In conclusion, I showed that Src Family Kinase inhibitors reduced viral replication by targeting the translation step of viral replication. I showed that an antibody therapy reduced CHIKV disease in rhesus macaques. Lastly, I showed that a T cell-specific inducing vaccine reduced CHIKV viral burden in the muscle tissue. Together these studies provide unique insights into the development of antivirals, therapeutics, and vaccines directed against CHIKV with lessons that could be applied to other reemerging alphaviruses that cause human disease.

## ACKNOWLEDGEMENTS

I would like to first and foremost thank my mentor **Dr. Daniel Streblow** for his support throughout my graduate career. Dr. Streblow was a very forgiving and thoughtful mentor, and he introduced me to many different skills and techniques that I will utilize in my future postdoctoral position. I would also like to thank all the members of the Streblow Lab for their many hours of support and technical assistance. **Craig Kreklywich** helped develop protocols for the CHIKV RNA analysis. **Michael Denton** helped me develop skills in cloning, including BAC recombineering and virus reconstitution in cell culture. **Takeshi Ando** taught me skills in mouse handling and all procedures involving the mouse CHIKV model. **Takeshi Ando, Craig Kreklywich, Patsy Smith, Nicole Haese, Daniel Streblow, and Michael Denton** all assisted me during the very long mouse harvest and tissue titrating days in the ABSL3 and BSL3. Additionally, all members of the Streblow lab were involved in the CHIKV nonhuman primate studies.

I would like to acknowledge my thesis committee, **Dr. Victor DeFilippis, Dr. William Messer, Dr. Jonah Sacha, and Dr. Daniel Streblow**, for their suggestions and generous support during our committee meetings. I would especially like to thank **Dr. Daniel Streblow, Dr. Victor DeFilippis, Dr. William Messer, and Dr. Alec Hirsch**, who wrote letters of support for my postdoc applications. In addition, our collaborators in the laboratories of **Dr. Michael Diamond, Dr. Mark Heise, Dr. Thomas Morrison, and Dr. Nathaniel Moorman** were very generous with reagents and some of them performed experiments for these studies.

Lastly, and most importantly, I would like to thank my friends and family who supported me through five years of graduate school, especially my husband **Kyle Broeckel** and his unwavering support throughout my graduate career. He tolerated my long hours in the lab on evenings and weekends, and sometimes even came out to the VGTI to take me out to eat during 12 and 18 hour experiments.

## SELECTED ABBREVIATIONS

*Ae.:* *Aedes*

*An.:* *Anopheles*

BFV: Barmah Forest Virus

CHIKV: Chikungunya Virus

*Cs.:* *Culiseta*

*Cx.:* *Culex*

MAYV: Mayaro Virus

NHP: Nonhuman Primate

*Oc.:* *Ochlerotatus*

ONNV: O'nyong-nyong Virus

*Ps.:* *Psorophora*

RRV: Ross River Virus

SINV: Sindbis Virus

VEEV: Venezuelan Equine Encephalitis Virus

## TABLE OF FIGURES

### Figures- Chapter 1

Figure 1-2: Alphavirus models of capsid and envelope proteins E1 and E2.....	7
Figure 1-3: Canonical cap-dependent translation initiation.....	26
Figure 1-4: Predicted RNA folding by MC-Fold ( <a href="http://www.major.irc.ca/MC-Sym/">http://www.major.irc.ca/MC-Sym/</a> ).....	28
Figure 1-5: Urban and sylvatic transmission cycles of CHIKV.....	36
Figure 1-6: CHIKV symptoms in humans.....	39
Figure 1-7: mTORC1 and mTORC2 signaling.....	67

### Figures- Chapter 2

Figure 2-1: Dasatinib, Torin 1, and PP242 block CHIKV replication in human fibroblasts.....	75
Figure 2-2: CHIKV replication and spread is limited by dasatinib and PP2.....	78
Figure 2-3: Dasatinib inhibits CHIKV and VEEV replication in IRF3 <sup>-/-</sup> and STAT1 <sup>-/-</sup> fibroblasts.....	79
Figure 2-4: CHIKV replication is suppressed in the absence of Src.....	81
Figure 2-5: SFK inhibitors do not reduce CHIKV RNA synthesis and replication complex formation.....	82
Figure 2-6: Dasatinib blocks structural protein accumulation.....	84
Figure 2-7: Dasatinib decreases the translation efficiency of CHIKV RNA.....	86
Figure 2-8: Dasatinib blocks translation of sgmRNAs from replicon-containing cells.....	87
Figure 2-9: Spherule-derived CHIKV sgmRNA is blocked by dasatinib.....	89
Figure 2-10: Dasatinib inhibits MAYV, ONNV, RRV, and ZIKV replication in NHDFs.....	92
Figure 2-11: Dasatinib and Torin 1 block translation of CHIKV sgmRNA.....	95

### Figures- Chapter 3

Figure 3-1: Characterization of neutralization, escape, and therapeutic efficacy of SVIR001 in mice.....	109
Figure 3-2: Plasma antibody levels and viral load following CHIKV mAb therapy.....	114
Figure 3-3: Tissue viral load following CHIKV mAb therapy.....	115
Figure 3-4: Histological images of joint-associated tissue from CHIKV-infected animals at 7 dpi.....	118
Figure 3-5: CHIKV mAb therapy reduced plasma cytokines and chemokine activation at 2 dpi.....	120

Figure 3-6: CHIKV mAb therapy reduced activation of peripheral blood monocytes/macrophages, Myeloid DCs, and NK cells. ....	121
Figure 3-7: CHIKV mAb treatment did not cause significant changes in CD4+ or CD8+ T cell proliferation. ....	124
<b>Figures- Chapter 4</b>	
Figure 4-1: IFN $\gamma$ responses in C57BL/6 mice at 7 and 14 days post CHIKV infection. ....	141
Figure 4-2: MCMV and AdV vaccine vector expression of the CHKVf5 fusion gene. ....	144
Figure 4-3: CHKVf5 vaccines did not protect mice against a footpad CHIKV challenge. ....	145
Figure 4-4: C57BL/6 mice were infected with CHIKV by three different routes, and their footpad swelling and tissue viral distributions are compared. ....	147
Figure 4-5: CHKVf5-vaccinated mice do not develop neutralizing antibodies to CHIKV, but their splenocytes produce IFN $\gamma$ in response to CHIKV peptide stimulation. ....	149
Figure 4-6: CHKVf5 vaccine groups had reduced levels of CHIKV in the ipsilateral calf. ....	151
Figure 4-7: Combined CD8+ and CD4+ T cell depletion reverses the protective effect of the CHKVf5 vaccine. ....	153
<b>Figures- Chapter 5</b>	
Figure 5-1: Adenoviruses vaccines expressing CHIKV 18-mer peptides were tested for their ability to block CHIKV infection in the calf. ....	166
<b>Figures- Supplemental</b>	
Figure S-1: Cell viability in NHDFs after treatment with different inhibitors. ....	167
Figure S-2: Dasatinib and PP2 block viral spread from infected cells. ....	168
Figure S-3: Dasatinib and Torin 1 differentially affect autophagy. ....	169
Figure S-4: Dasatinib does not affect RNA levels and dsRNA complexes. ....	170
Figure S-5: Erk inhibitor U0126 does not block CHIKV infection. ....	171
Figure S-6: Dasatinib enhances viral replication in vivo. ....	172
Figure S-7: Sequence alignment of SVIR001 escape variant viruses. ....	173
Figure S-8: T cell gating strategy. ....	174
Figure S-9: Gating strategy for NK cells, macrophages, and DCs. ....	175
Figure S-10: Plasma cytokines and chemokine analysis. ....	176
Figure S-11: B cell proliferative responses were not affected by SVIR001 therapy. ....	177

<b>Figure S-12: T cell depletions were confirmed in mice receiving CD4+ and CD8+ T cell depleting antibodies. ....</b>	<b>181</b>
--	------------

### **Tables- Chapter 1**

<b>Table 1-1: Alphaviruses, their arthropod and vertebrate hosts, and the disease they cause in humans.....</b>	<b>2</b>
<b>Table 1-2: Translation initiation factors dispensable for translation of alphavirus sgmRNA.....</b>	<b>29</b>
<b>Table 1-3: Commonly used mouse models for CHIKV infection and their phenotypes .....</b>	<b>43</b>
<b>Table 1-4: CHIKV vaccines: design, immunogenicity, and animal testing. ....</b>	<b>58</b>

### **Tables- Chapter 2**

<b>Table 2-1: Drugs used in this study, their targets, and their toxicity.....</b>	<b>76</b>
--	-----------

### **Tables- Chapter 3**

<b>Table 3-1: CHIKV isolation from tissue homogenates. ....</b>	<b>112</b>
<b>Table 3-2: Histological Findings in Joint Tissues at 7 dpi.....</b>	<b>117</b>

### **Tables- Chapter 4**

<b>Table 4-1: CHIKV-Specific Immunoreactive Peptides. ....</b>	<b>142</b>
--	------------

### **Tables- Supplemental**

<b>Table S-1: Primers used for sequencing and amplifying the E2 and E1 genes of CHIKV-181/25 ...</b>	<b>178</b>
<b>Table S-2: Oligonucleotide primers for mutagenesis of CHIKV infectious clones.....</b>	<b>179</b>
<b>Table S-3: Detailed histological findings reported per animal.....</b>	<b>180</b>

## TABLE OF CONTENTS

<b>Abstract</b> .....	<b>i</b>
<b>Acknowledgements</b> .....	<b>iv</b>
<b>Selected Abbreviations</b> .....	<b>v</b>
<b>Table of Figures</b> .....	<b>vi</b>
<b>Chapter 1 INTRODUCTION</b> .....	<b>1</b>
<b>1.1 Togaviridae</b> .....	<b>1</b>
1.1.1 Classification .....	1
<b>1.2 Alphaviruses</b> .....	<b>1</b>
1.2.1 Introduction.....	1
1.2.2 Arthritogenic Alphaviruses .....	9
1.2.3 Ross River Virus (RRV).....	11
1.2.4 Sindbis Virus (SINV) .....	12
1.2.5 O'nyong-nyong Virus (ONNV) .....	13
1.2.6 Mayaro Virus (MAYV).....	14
1.2.7 Chikungunya Virus (CHIKV) .....	15
1.2.8 Encephalitic alphaviruses.....	15
1.2.9 Venezuelan Equine Encephalitis Virus (VEEV) .....	16
<b>1.3 Alphavirus Replication Cycle</b> .....	<b>17</b>
1.3.1 Entry .....	17
1.3.2 Replication Complex Formation and RNA Replication .....	19
1.3.4 Translation of viral subgenomic mRNA.....	24
1.3.5 Assembly and release .....	31
1.3.6 Host transcription and translation shutoff .....	31
<b>1.4 Chikungunya Virus (CHIKV)</b> .....	<b>33</b>
1.4.1 Introduction and classification of CHIKV .....	33
1.4.2 CHIKV epidemiology.....	34
1.4.3 CHIKV transmission and replication in mosquitoes.....	35
1.4.4 CHIKV symptoms in humans.....	38
1.4.5 CHIKV persistence and long-term symptoms in humans.....	39
1.4.6 Severe symptoms of CHIKV in humans.....	40
1.4.7 Mouse models of CHIKV .....	41
1.4.8 Nonhuman Primate models of CHIKV .....	44
<b>1.5 CHIKV Immunity</b> .....	<b>45</b>
1.5.1 Innate Immunity to CHIKV.....	45
1.5.2 Anti-CHIKV antibodies .....	48
1.5.3 Anti-CHIKV T cells.....	50
<b>1.6 CHIKV Vaccines and Therapeutics</b> .....	<b>54</b>
1.6.1 Current treatment options for CHIKV patients.....	54

1.6.2 Vaccines in development for CHIKV .....	55
1.6.3 Therapies in development to treat CHIKV infections .....	60
<b>1.7 Signaling pathways involved in viral replication.....</b>	<b>62</b>
1.7.1 Kinase pathways and viral replication .....	62
1.7.2 Src Family Kinase signaling.....	62
1.7.3 PI3K-AKT axis.....	65
1.7.4 Signaling through mTOR.....	66
<b>CHAPTER 2 DASATINIB IS AN ANTIVIRAL COMPOUND EFFECTIVE AGAINST CHIKV REPLICATION .....</b>	<b>69</b>
2.1 Abstract.....	69
2.2 Introduction .....	70
2.3 Results .....	73
2.4 Discussion.....	94
2.5 Materials and Methods .....	99
<b>CHAPTER 3 HUMANIZED MONOCLONAL ANTIBODY THERAPY IS EFFECTIVE AGAINST VIRAL SPREAD AND JOINT PATHOLOGY IN RHESUS MACAQUES ...</b>	<b>104</b>
3.1 Abstract.....	104
3.2 Introduction .....	105
3.3 Results .....	108
3.4 Discussion.....	123
3.5 Materials and Methods .....	127
<b>CHAPTER 4 A T-CELL BASED VACCINE PROTECTS AGAINST CHIKV INFECTION IN MICE .....</b>	<b>136</b>
4.1 Abstract.....	136
4.2 Introduction .....	137
4.3 Results .....	140
4.4 Discussion.....	154
4.5 Materials and Methods .....	157
<b>CHAPTER 5 DISCUSSION AND FUTURE DIRECTIONS .....</b>	<b>162</b>
5.1 Small molecule kinase inhibitors and CHIKV .....	162
5.2 Monoclonal antibodies as therapies or prophylactics .....	163
5.3 Vaccine options for CHIKV .....	163
<b>APPENDIX I .....</b>	<b>167</b>
Supplemental Data: Dasatinib project.....	167
Supplemental Data: Monoclonal antibody therapy project.....	173
Supplemental Data: T cell Vaccine project.....	181
<b>REFERENCES.....</b>	<b>182</b>

## CHAPTER 1 INTRODUCTION

### 1.1 TOGAVIRIDAE

#### 1.1.1 CLASSIFICATION

Togaviruses are enveloped, positive-sense, single-stranded RNA viruses. The word *Toga* is derived from Latin for “cloak” referring to the viral envelope (10). The *Togaviridae* family consists of two genera: *Alphavirus* and *Rubivirus*. Rubella virus (RV), the sole member of the *Rubivirus* genus, is transmitted by respiratory secretions and is genetically distinct from other togaviruses. The *Alphavirus* genus has 31 recognized species (10), and most species are transmitted via bite by infected arthropods. Many alphaviruses, including o’nyong-nyong virus (ONNV), mayaro virus (MAYV), sindbis virus (SINV), and chikungunya virus (CHIKV) cause arthritic disease in humans (11-13). Other alphaviruses such as Venezuelan equine encephalitis virus (VEEV), western equine encephalitis virus (WEEV), and eastern equine encephalitis virus (EEEV) can cause encephalitis in humans which can be fatal or cause long-term neurological sequelae (14-16). Some alphaviruses are not known to infect humans, such as eilat virus (EILV), salmonid alphavirus (SAV), and southern elephant seal virus (SESV). The *Togaviridae* family encompasses a diverse group of viruses that have a very broad host range including insects, fish, birds, and mammals. Of all the alphaviruses that infect humans, CHIKV became a major threat to public health because of its ability to rapidly spread through urban areas and cause debilitating disease in humans.

### 1.2 ALPHAVIRUSES

#### 1.2.1 INTRODUCTION

The alphaviruses have broad host range and geographic distribution. Alphaviruses have been isolated from every continent except Antarctica. New World alphavirus species are

routinely isolated from mosquitoes in North and South America. Similarly, Old World alphaviruses are frequently isolated from mosquito pools in Southeast Asia, Australia, Africa, and Europe. It is possible that alphaviruses may even be found in the Antarctic. Southern elephant seal virus (SESV) has been isolated from elephant seal louse in a sub-Antarctic island (17). Southern elephant seals and their louse hitchhikers travel from this island into Antarctica, suggesting alphaviruses inhabit all seven continents.

Phylogenetic analysis of all the known alphavirus genomes demonstrated that there are three major groups of viruses: the Old World, New World, and aquatic alphavirus groups (18). One evolutionary theory is that the current day alphaviruses originated from an aquatic ancestor that was introduced to the New and Old Worlds (18). These introductions resulted in the present day Old and New World alphaviruses, with the Old World alphaviruses causing arthritic symptoms and the New World alphaviruses causing encephalitis. Though this is the general trend, there are examples of Old World alphaviruses in the New World and vice versa. Based on this information, there may have been subsequent introductions of Old World alphaviruses into the New World and New World alphaviruses into the Old World. The 31 alphavirus species are grouped into nine antigenic complexes that correlate with genetic similarity (**Table 1-1**) (10, 19-21).

**Table 1-1: Alphaviruses, their arthropod and vertebrate hosts, and the disease they cause in humans.**

Antigenic Complex	Virus (abbreviation)	Known Arthropod Hosts	Known Vertebrate Hosts	Disease in Humans	Geographic Distribution	Refs
BF	Barmah Forest (BF)	<i>Cx. annulirostris</i> , <i>Ae. camptohynchus</i> , <i>Ae. vigilax</i> , <i>Ae. procax</i> , <i>Ae. notoscriptus</i>	Humans, horses, brushtail possums	Fever, rash, arthritis	Australia, Southeast Asia	(22-24)
EEE	Eastern Equine Encephalitis (EEE)	<i>Cs. melanura</i> , <i>Ae. vexans</i> , <i>Coquillettidia perturbans</i> , <i>Oc. Canadensis</i> , <i>Oc. sollicitans</i>	Humans, birds, equines, swine, dogs	Fever, encephalitis	North America, Central America, South America	(25, 26)
	Madariaga (MAD)	<i>Cx.</i>	Humans,	Fever,	South and Central	(26,

Antigenic Complex	Virus (abbreviation)	Known Arthropod Hosts	Known Vertebrate Hosts	Disease in Humans	Geographic Distribution	Refs
		( <i>Melanoconion</i> ) spp.	birds, rodents, marsupials, reptiles	encephalitis	America	(27)
EILV	Eilat (EIL)	<i>An. coustani</i>	None known	Not Known	Israel	(20, 28, 29)
MID	Middelburg (MID)	<i>Ae caballus</i> ,	Humans, equines, livestock	Not Known	Africa	(30)
NDU	Ndumu (NDU)	<i>Mansonia uniformis</i> , <i>Ae. circumluteolus</i> , <i>Cx. pipiens</i>	Pigs, others not known	Not Known	Africa	(31-33)
SF	Bebaru (BEB)	Not Known	Not Known	Not Known	Australia	(34)
	Chikungunya (CHIK)	<i>Ae. albopictus</i> , <i>Ae. aegypti</i> , <i>Ae. furcifer</i> , <i>Ae. taylori</i> , <i>Ae. luteocephalus</i> , <i>Ae. africanus</i> , <i>Ae. neoafricanus</i> , <i>Ae. cordellieri</i>	Humans, primates, rodents	Fever, arthritis, rash	Africa, Southeast Asia, North America, Central America, South America, Europe	(35-38)
	Getah (GET)	<i>Cx. spp</i>	Humans, equines, pigs	Fever	Asia, Australia, Europe	(39, 40)
	Mayaro (MAY)	<i>Haemagogus janthinomys</i>	Humans, primates	Fever, arthritis, rash	South America	(41, 42)
	O'nyong-nyong (ONN)	<i>An. funestus</i> , <i>An. gambiae</i>	Humans	Fever, arthritis, rash	Africa	(43, 44)
	Ross River (RR)	<i>Cx. annulirostris</i> , <i>Ae. camptorhynchus</i> , <i>Ae. vigilax</i>	Humans, dogs, horses, flying foxes, brushtail possums, grey kangaroo	Fever, arthritis, rash	Australia, Southeast Asia	(22, 23, 45)
	Semliki Forest (SF)	<i>Ae. africanus</i> , <i>Ae. aegypti</i>	Humans, primates	Fever, arthritis,	Africa	(46)
	Una (UNA)	<i>Ps. ferox</i> , <i>Ps. albipes</i>	Humans, birds, horses	Not known	South America	(47)
VEE	Cabassou (CAB)	<i>Cx. portesi</i>	Not known	Not known	South America	(48)
	Everglades (EVE)	<i>Cx. (Melanoconion) spp.</i>	Birds, Humans, Dogs	Fever, encephalitis	North America	(49, 50)
	Mosso das Pedras	<i>Cx. (Melanoconion) spp.</i>	Not known	Not known	South America	(48)
	Mucambo (MUC)	<i>Cx. portesi</i>	Humans, primates	Fever, encephalitis	South America	(51, 52)
	Pixuna (PIX)	<i>An. nimbus</i> , <i>Trichoprosopon digitatum</i>	Rodents,	Not known	South America	(51)
	Rio Negro (RN)	<i>Cx. delpontei</i> , <i>Cx. maxi</i> , <i>Ps. cingulata</i>	Humans	Acute febrile illness	South America	(53, 54)
	Tonate (TON)	<i>Cx. portesi</i> , <i>Oeciacus vicarious</i> (cimicids)	Humans, birds	Fever, encephalitis	North America, South America	(55)
	Venezuelan Equine Encephalitis (VEE)	<i>Oc. taeniorhynchus</i> , <i>Ps. confinnis</i> , <i>An. aquasalis</i>	Humans, equines, rodents	Fever, encephalitis	North America, South America	(56-58)
WEE	Western Equine Encephalitis (WEE)	<i>Oc. melanimon</i> , <i>Ae. dorsalis</i> , <i>Cx. tarsalis</i>	Humans, equines, birds	Fever, encephalitis	North America, South America	(16)
	Aura (AURA)	<i>Ae serratus</i>	Not Known	Not Known	South America	(59)

Antigenic Complex	Virus (abbreviation)	Known Arthropod Hosts	Known Vertebrate Hosts	Disease in Humans	Geographic Distribution	Refs
	Fort Morgan (FM)	<i>Oeciacus vicarius</i> (cimicids)	Birds	Not Known	North America	(60)
	Highlands J (HJ)	<i>Cs. melanura</i>	equines, birds, potentially humans	Unclear, potentially encephalitis	North America	(61, 62)
	Sindbis (SIN) *Type Species	<i>Cx. pipiens</i> , <i>Cx. univittatus</i> , <i>Cs. Spp.</i> , <i>Hyaloma Marginatum</i> (ticks)	Humans, birds, bats	Fever, arthritis, rash	Europe, Asia, Australia, Africa	(63-65)
	Trocará (TRO)	<i>Ae. serratus</i>	Not Known	Not Known	South America	(66)
	Whataroa (WHA)	<i>Cs. Tonnoiri</i> , <i>Cx. pervigilans</i>	Birds, possibly humans	Possibly flu-like illness	New Zealand	(67)
Unclassified/ Aquatic Viruses	Salmon pancreas disease (SPD)	Not known	Atlantic salmon, rainbow trout	Not known	Western Europe, North America	(68)
	Southern Elephant Seal (SES)	<i>Lepidophthrus macrorhini</i> (louse)	Southern Elephant Seal	Not Known	Australia, Sub-Antarctica	(17)

## ALPHAVIRUS GENOME

Alphaviruses have positive sense RNA genomes of 11 - 12 kb. During replication, a full-length minus-strand RNA species is transcribed from the incoming positive-sense genomic RNA (gRNA), and the minus-strand RNA serves as a template for synthesis of positive-sense gRNA and subgenomic RNA (sgRNA). Both gRNA and sgRNAs are capped and poly-adenylated (69, 70). In contrast to most cellular mRNAs, these RNAs have a type 0 cap structure ( $m^7GpppN_1pN_2p$ ) that lacks methylation of the  $N_1$  or  $N_2$  position (70-72). Translation of the gRNA produces the nonstructural polyprotein (nsp), which consists of 4 processed components (nsp1-4). Translation of the sgRNA produces the structural polyprotein that consists of 5 structural proteins (C, E3, E2, 6K/TF, and E1) (**Figure 1-1**). These structural polyproteins are cleaved by viral and cellular proteases during replication.

The viral 5' and 3' untranslated regions (UTRs) are essential for replication. The lengths of the 5'UTR and 3'UTRs vary significantly among alphaviruses (ie. 5'UTRs 27-85 nt; 3'UTRs 87-723 nt) (73). The alphavirus 5'UTR contains a hairpin that is critical for replication. As proof,

mutagenesis of nucleotides that form the hairpin that disrupt the secondary structure abolish viral replication (74). The 5'UTR plays an important role in the synthesis of positive and negative RNAs. The 5'UTR and 3'UTR interact for initiation of minus-stranded RNA synthesis, and the complement of the 5'UTR on the minus-stranded RNA contains a promoter element for positive-stranded RNA synthesis (74, 75). The 3'UTR has a variable number of repeated sequence elements (RSEs) followed by a U-rich element, a conserved sequence element (CSE), and poly(A) tail (76). Importantly, the 3'UTR CSE and poly(A) tail sequences contain the promoter for synthesis of the minus-stranded RNA (77, 78). Viruses of the same antigenic complex may have RSEs that are similar in sequence to each other, but the number of RSEs appears to be unique to each alphavirus species (76). The 3'UTR also functions in RNA stability; it protects the viral RNA from deadenylation and degradation. One proposed mechanism for this process is that the virus recruits the cellular protein Human antigen R (HuR) from the nucleus to the cytoplasm, promoting interaction between the viral 3'UTR and HuR, which prevents viral RNA degradation and promotes viral replication (79, 80).

The viral genome contains two other conserved sequence elements (CSEs) that are shared among alphaviruses. One 51-nt CSE is located in the coding region of nsp1 (81). This CSE is predicted to form two RNA hairpins. Introduction of silent mutations that disrupt the CSE hairpins in SINV resulted in normal replication in mammalian cells, but attenuated replication in mosquito cells, suggesting that the CSE has a species-specific function (81). This CSE has also been implicated as a packaging signal for capsid to recognize the viral gRNA during assembly of the nucleocapsid (82). Another CSE, located at -19 to +5 nt relative to the start of the sgRNA, is the essential promoter for the sgRNA present on the complementary minus-sense RNA (83-85).

## ALPHAVIRUS PARTICLE STRUCTURE

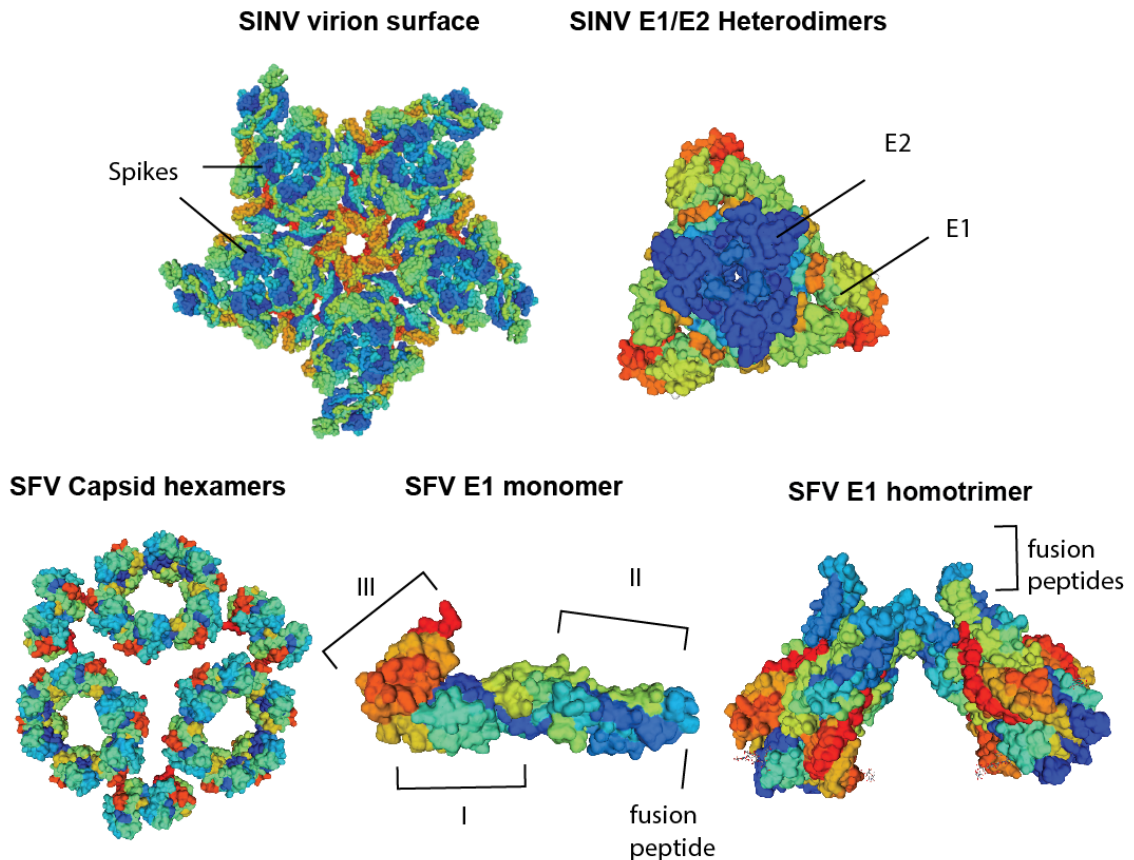
Alphavirus particles are about 700 Å in diameter. Alphavirus particles are coated with a host cell-derived lipid bilayer envelope that is studded with 240 copies of E1 and E2 glycoproteins arranged in an icosahedral lattice with T = 4 quasi-symmetry (86, 87). E1 and E2 form heterodimers that are arranged in trimers (**Figure 1-2**) (86). The virion envelope surrounds an icosahedral nucleocapsid core that is 400 Å in diameter and contains the viral gRNA (87, 88). The icosahedral capsid shell consists of 240 copies of capsid protein, and each capsid protein interacts with one E1/E2 dimer (88). Some alphavirus virions, like those of SINV and CHIKV, are associated with low levels of transframe (TF), a ribosomal frameshift product of 6K (89, 90). However, TF has never shown to be incorporated into the cryo-EM models.

In the mature virion, 240 copies of capsid proteins form hexamer and pentamer rings also called capsomeres. The capsomeres form an icosahedral shell around the viral gRNA during encapsidation (87). The number of capsid proteins was initially determined by mass predictions using scanning transmission electron microscopy (88). The mass was predicted by integrating the density of the nucleocapsid contours calculated relative to tobacco mosaic virus in the same field as a mass standard. In this study, the weight of the SINV nucleocapsid was determined to be 10,700 to 10,900 kDa, which is the weight of 240 copies of capsid protein (29.4 kDa) with one copy of the genome (3,790 kDa) (88). Early studies showed that purified nucleocapsids (isolated from virions treated with NP40 detergent and fractioned over a sucrose gradient) were sensitive to RNase treatment causing the nucleocapsid structure to lose integrity (91). These two findings suggest that the vRNA is exposed in the capsid shell and that capsid requires interaction with gRNA to maintain structural integrity. There are two main structural functions for capsid proteins: they interact with E2 and encapsulate the genomic RNA. The N-terminal domain of capsid is involved in assembling the capsid scaffold and in binding the genomic RNA. The C-terminal capsid domain points outwards towards the virion envelope

where it interacts with E2 (7). The specific interaction of capsid and E2 involves a capsid hydrophobic pocket that binds an E2 tyrosine residue present in the cytoplasmic tail (92, 93). The E2 tail is modified by palmitoylation, which has been suggested to fasten the E2 cytoplasmic tail to the plasma membrane in a manner that promotes correct conformational interaction with capsid (94).

For capsid to form a nucleocapsid shell, it requires single-stranded nucleic acid, as shown in *in vitro* capsid assembly assays (95, 96). Although capsid assembly does not

**Figure 1-1: Alphavirus models of capsid and envelope proteins E1 and E2.** Structures were modeled with the SWISS-MODEL server (1-4). Protein Data Bank (PDB) codes for the different structures are as follows: SINV virion surface PDB 3JOF (5); SINV E1/E2 heterodimer at low pH PDB 3MUU (6); SFV capsid PDB 1DYL (7); SFV E1 monomer PDB 2ALA (8); SFV E1 homotrimer PDB 1RER (9). The models were not modified from the original structures except the black labels. SWISS-MODEL specified that images generated from the server are free to redistribute according to the Creative Commons license <https://creativecommons.org/licenses/by/4.0/>.



necessarily require viral gRNA, capsid is preferential to incorporating gRNA, as shown with *in vitro* competition assays (97). The hypothesis that capsid selectively binds gRNA is supported by the idea that there are specific sites or “packaging sequences” in the genome that are potentially targeted by capsid. The putative gRNA: capsid binding sites have been identified by crosslinking immunoprecipitation followed by high-throughput sequencing (CLIP-seq): capsid was UV cross-linked onto the viral RNA in infected cells and the RNA was fragmented with RNAses. Capsid-RNA complexes were immunoprecipitated from the lysates, and cDNA libraries were generated from the RNA and deep-sequenced. The results of the deep sequencing showed that, when in the cytoplasm, capsid binds predominantly to two specific sites on the viral genome: the subgenomic promoter region and a small coding region of nsp1 (82).

In the mature virion, the envelope proteins E1 and E2 are single-pass transmembrane proteins that form heterodimers. E2 functions to: 1) bind the cellular entry receptor; 2) associate with E1 to shield the fusion peptide; and 3) interact with capsid to initiate viral budding. To accomplish these functions, E2 has a cytoplasmic tail, a transmembrane domain, and three domains (A, B, and C) within the ectodomain (6). The E2 cytoplasmic tail is 33 amino acids in length, and it interacts with a hydrophobic pocket in capsid (98). The transmembrane domain is a single helix. Structures of the ectodomain of E2 indicate that domain A and B locate to the tip of the E1/E2 heterodimer, with the fusion loop of E1 inserted in a pocket in domain B (99).

The function of E1 is to mediate membrane fusion during entry. E1 has three main domains within the ectodomain: the C-terminal tail (III), central domain (I), and dimerization domain (II) containing the fusion peptide (100). E1 has a single transmembrane helix and a short cytoplasmic tail (two arginine residues). The E1 protein, on its own, covers most of the surface of the virion, in a pattern similar to flavivirus E (98, 100). E2 penetrates the E1 layer to form the spikes, and each “spike” is a trimer of E1/E2 heterodimers (**Figure 1-2**). The E1 and E2 dimer is held together in the mature virion via domain C of E2 binding to E1 domain II. They

also interact at the tip of the dimer, with the fusion loop on domain II of E1 shielded by domain B of E2 (6). Three E2 proteins project out the central portion of the spike where they shield three E1 fusion domains; these three E2 proteins in the center of the spike interact with each other via domain A (98, 100). During fusion at low pH, E1 and E2 dissociate from each other, promoting E1 homotrimer formation, which exposes the fusion loop (**Figure 1-2**) (9, 100, 101). In SFV virions, E3 associates with the mature virion at the E2 domain A/B border to prevent premature fusion activity, but the structure modeling this interaction has not been solved (102, 103). This E3/E2 association has been described for SFV, but not in other alphaviruses thus far.

---

### 1.2.2 ARTHRITOGENIC ALPHAVIRUSES

All known alphaviruses are similar in structure and genomic organization. When comparing the whole genome sequences of all alphaviruses, three major genetic groups emerge: Old World, New World, and aquatic. The aquatic alphaviruses include SPD, found in Atlantic Salmon and rainbow trout, and SESV, which is transmitted by louse (18, 19). The remaining known alphaviruses form the Old and New World clades (18, 19). The Old World alphavirus group include the SF, MID, NDU, and BF antigenic complexes, and the New World alphavirus group includes WEE, EEE, VEE, and EILV (20). The Old World alphaviruses have predominantly been isolated in the Eastern Hemisphere, and the New World alphaviruses have routinely been isolated from the Western hemisphere. However, there is genetic evidence that some Old and New World alphavirus species spread into new continents and regions of the world. For example, the Old World alphaviruses MAYV and UNAV have only been found in the Americas, yet they are genetically placed in the Old World clade. The New World WEE antigenic complex is postulated to arise from a recombination event between ancestral SINV and EEEV, resulting in a WEEV complex ancestor with EEEV-like nonstructural and capsid genes and SINV-like envelope genes (21, 104). SINV, although genetically placed in the WEE antigenic complex, has only been found in the Eastern Hemisphere and causes symptoms

similar to other Old World alphaviruses. Therefore, a recombination with SINV and EEEV ancestors implies that SINV or EEEV ancestors were introduced into the Americas or eastern hemisphere. In addition, there are likely many other alphavirus species not yet identified. For example, Forrester et al. suggested that there may be a louse-borne branch of the alphavirus tree, of which only one species (SESV) has been discovered (18). Overall, the genetic analysis suggest that alphaviruses have an ability to spread and establish themselves in new areas and that they use a wide variety of invertebrate and vertebrate species to facilitate viral spread.

The arthritogenic alphaviruses cause acute febrile illness and rheumatic disease in humans, typically involving debilitating joint and muscle pain. The alphaviruses known to cause arthritic disease in humans are CHIKV, RRV, BFV, ONNV, MAYV, and SINV (**Table 1-1**). These viruses are historically referred to as “Old World” alphaviruses, but these viruses can be found in North America, South America, Australia, Asia, Africa, and Europe. All of the known arthritogenic alphaviruses are transmitted via the bite of infected mosquitoes.

The acute symptoms following infection with arthritic alphaviruses include fever, maculopapular rash, muscle pain, and arthralgia that commonly affects the peripheral joints: hands, wrists, knees, ankles, and feet (105, 106). The joint pain is believed to be caused by viral replication in and around the joint and by cellular infiltration into the affected area. This information is based on the detection of viral RNA and antigens in synovial and muscle biopsies from patients experiencing arthritic pain after infection with CHIKV and RRV (107-111). The arthralgia and myalgia following infection with these viruses can be recurring and last for several months to years following the acute phase of disease (112-114). Other viruses outside of *Togaviridae* that cause arthritis include parvovirus B19, hepatitis B, hepatitis C, human T-lymphotrophic virus type-1, and human immunodeficiency virus (115). However, the arthritis induced by alphaviruses differs from infections with these other viruses because alphaviruses specifically replicate in joint tissues and cause severe joint pain.

Arthritis caused by alphaviruses has been compared to rheumatoid arthritis (RA); however, there are several key differences between the diseases caused by alphavirus infection and RA. RA, unlike alphavirus-induced arthritis, is an autoimmune disease associated with the development of autoantibodies: rheumatoid factor (RF) and anti-citrullinated protein antibodies (ACPA) (116). RA is a progressive, destructive disease resulting in bone and cartilage damage (117). In contrast to RA, patients typically recover after alphavirus infection, although the recovery can take months to years. In addition, following alphavirus infection the T and B cell immunity is primarily directed against the virus, not against self-derived antigens. Despite these differences, the inflammatory environment induced by autoimmunity or virus may have some similarities. For example, two recent studies using mouse models for CHIKV and RRV suggested that viral infection leads to increased ratios of the receptor activator of NF- $\kappa$ B ligand to osteoprotegerin (RANKL:OPG), which could lead to generation of cells involved in bone resorption and bone loss, as observed with RA (118, 119). These studies also detected bone loss, but not bone erosion, following RRV and CHIKV infection in mice (118, 119). Drugs developed to treat RA symptoms and disease such as methotrexate and chloroquine, appear to have limited, and sometimes no effect, on reducing alphavirus-induced arthritis and joint swelling (120, 121). In fact, testing RA drugs in patients with CHIKV-induced joint disease could have detrimental effects because of the immunosuppressive nature of the drugs, which enhance virus replication (122). More studies are needed to fully compare the mechanisms of acute and chronic arthritis following alphavirus infection and RA in order to identify potential targets for therapeutic intervention.

---

### 1.2.3 ROSS RIVER VIRUS (RRV)

RRV commonly causes arthritic disease outbreaks in Australia, infecting several thousand people every year (123, 124). Like other arthritic alphaviruses, it causes an acute febrile illness, rash, fever, myalgia, and polyarthritis in humans, and the polyarthritis and myalgia

can be long-lasting (123). Viral RNA and antigens have been detected in synovial biopsies from patients experiencing RRV-induced arthralgia (107-109). RRV is spread by *Ae. vigilax*, *Ae. camptohynchus*, and *Cx. annulirostris* mosquitoes. Based on serosurveys, a number of small mammals native to Australia have been implicated as natural reservoirs for RRV (23, 106, 125).

Mice infected with RRV via footpad injection develop hind limb dragging and loss of hind limb gripping. Within 24-48 hours following RRV challenge, infectious virus can be recovered from ankles, muscle (quadriceps), serum, brain, and spleen (126). Utilization of a GFP reporter virus *in vivo* showed that the virus replicates in the periosteum lining the bone, in tendons of the joint, cells within the synovium, and in the skeletal muscle tissue (126). RRV also causes inflammation in the joint, bone, and muscle tissue. Similar to other arthritic alphaviruses, RRV is lethal in young mice (< 2 weeks old), but not in mice 3-weeks of age or older (126).

---

#### 1.2.4 SINDBIS VIRUS (SINV)

SINV was first isolated in 1952 in Sindbis, Egypt from a pool of *Cx. pipiens* and *Cx. univittatus* mosquitoes (64). SINV was later isolated from birds, ticks, bats, and humans (63, 65, 127). SINV infections are associated with mild fever, rash, and polyarthritits in humans (13). SINV has been identified as the causative agent of Pogosta disease, also known as Ockelbo disease or Karelian Fever (128, 129). SINV causes Pogosta disease outbreaks of rash and arthralgia about every seven years in the months of August and September in Finland (65, 130). SINV has been isolated from skin biopsies from patients experiencing a rash following SINV infection, demonstrating that SINV replicates locally in the skin (65). Grouse are implicated as an amplifying reservoir for SINV. Interestingly, grouse populations decline every 6-7 years coinciding with SINV outbreaks, and SINV antibodies were detectable in blood isolates from grouse after a SINV outbreak (131).

For many years, SINV was used as the prototypic alphavirus for experimental studies. SINV grows to high titers in baby hamster kidney cells (BHKs), chick embryo fibroblasts (CEFs), and Vero cells, which made SINV an easy and attractive model alphavirus to study viral replication in culture. In addition, SINV infection in mice has been used as a model for alphavirus induced encephalitis because SINV is neurotropic in mice. Initial studies in mice showed that a subcutaneous inoculation of 1,000 PFU SINV into the footpad of BALB/c mice resulted in an age-dependent lethality due to encephalitis (132). There are also neuroadapted strains available that cause encephalitis in older mice (133, 134). In general, SINV, despite being an Old World virus, represents a highly tractable model for studying virus-induced encephalitis in mice (135).

---

#### 1.2.5 O'NYONG-NYONG VIRUS (ONNV)

ONNV causes debilitating joint pain, rash, lymphadenitis, fever, and headache in humans (136). Currently, there are no other vertebrate hosts known. ONNV was first isolated in 1959 from a patient with acute febrile illness in Kenya. ONNV was first described as an alphavirus similar to, but distinct from, CHIKV (11, 137). *An. funestus* and *An. gambiae* mosquitoes are the principle vectors for transmission of ONNV (43). These vectors are unique to ONNV because no other alphaviruses are known to replicate in these night-feeding *Anopheles* mosquitoes. Nsp3 is implicated in this vector specificity because replacement of the CHIKV nsp3 gene with ONNV nsp3 allowed CHIKV to infect (but not disseminate in) *Anopheles* mosquitoes (138). ONNV caused a massive outbreak in eastern Africa in the 1960s, spreading from Uganda to the nearby countries of Kenya, Tanzania, Mozambique, Nyasaland, Zaire, and Senegal, resulting in over 2 million human infections (44). A second outbreak occurred in 1996-1997 in south-central Uganda (136). Other outbreaks may have occurred since 1997, but the cases are underreported, and/or patients may have been misdiagnosed with CHIKV (139).

Similar to other alphaviruses, the innate interferon signaling pathway appears to be important for controlling ONNV *in vivo*. Initial mouse experiments showed that adult and neonatal wild type mice (C57BL/6), mice lacking B and T cells (Rag1<sup>-/-</sup> mice), and mice lacking the interferon  $\gamma$  receptor (IFN $\gamma$ R<sup>-/-</sup>) did not develop any signs of disease. In addition, these mice do not become viremic following ONNV infection (137, 140). However, mice deficient in Type 1 interferon signaling (mice lacking the type I interferon receptor (A129) or Stat 1) are partially sensitive to s.c. infection with ONNV (140), but, in contrast with other arthritic alphaviruses (ie. CHIKV), ONNV is not 100% lethal in A129 or Stat1<sup>-/-</sup> mice. Early studies with ONNV in rhesus macaques showed that animals infected with ONNV did not develop viremia or neutralizing antibodies to ONNV, suggesting that the animals were not successfully infected (141). Overall, the animal models for ONNV appear more limited compared to the other arthritic alphaviruses and further studies are warranted to determine the reasons why this occurs.

---

#### 1.2.6 MAYARO VIRUS (MAYV)

MAYV was first isolated from a febrile patient in Mayaro County in Trinidad (12). MAYV causes acute febrile illness and joint pain in humans (41). It is transmitted by canopy-dwelling *Haemagogus janthinomys* mosquitoes. Serosurveys of mammals in the rainforest of French Guiana showed that primates within the rainforest canopy layer had neutralizing antibodies directed against MAYV, suggesting that MAYV has a sylvatic cycle involving *Haemagogus* mosquitoes and New World nonhuman primates (42). Additional studies are needed to determine whether these sylvatic cycles are maintained over time.

Currently, few studies describe MAYV infection of mouse and nonhuman primate animal models. MAYV infection in C57BL/6 mice was only recently described (142). Similar to the outcomes observed following CHIKV infection, mice infected with MAYV develop footpad swelling, viremia at 3 dpi, and detectable viral load in spleen, muscle, and ankle tissues (142).

Rhesus macaques infected with MAYV develop viremia and transient fever (141). While these animal studies with MAYV are limited, they clearly show that mouse and nonhuman primates are feasible animal models to study MAYV pathogenesis.

---

### 1.2.7 CHIKUNGUNYA VIRUS (CHIKV)

CHIKV was first isolated in the early 1950s during an epidemic of acute febrile illness and polyarthritis in present-day Tanzania (143). The first descriptions of CHIKV infections in humans indicated that patients experienced a sudden onset of high fever, polyarthritis, and rash (143). CHIKV is transmitted by the anthropophilic *Ae. albopictus* and *Ae. aegypti* mosquitoes. The virus can establish urban transmission cycles involving humans and mosquitoes as well as sylvatic cycles, between forest-dwelling mosquitoes and primates (144). CHIKV outbreaks occur periodically in sub-Saharan Africa and Southeast Asia (145). In 2013-2015, CHIKV caused a large outbreak in Central America that spread to South America and to the United States (146). These incidents highlight the ability of CHIKV to rapidly spread and establish outbreaks in new geographical areas.

The mouse and nonhuman primate models for CHIKV infection and disease are well established (147-150). C57BL/6 mice develop footpad swelling, viremia, and detectable virus in muscle and ankle tissues following CHIKV infection. Similarly, rhesus macaques develop a transient viremia, rash, joint redness and swelling, and virus is detectable in several tissues following CHIKV infection. More details will be discussed regarding CHIKV transmission, epidemiology, and animal models in Section 1.4.

---

### 1.2.8 ENCEPHALITIC ALPHAVIRUSES

The encephalitic alphaviruses including VEEV, WEEV, and EEEV can cause encephalitis and neurological disease in humans. Other alphaviruses, such as CHIKV, RRV, and HJV, can cause neurological symptoms and encephalitis, although these symptoms occur

less frequently compared to patients infected with VEEV, WEEV and EEEV (16). Currently, the encephalitic alphaviruses are almost exclusively found in North and South America. The symptoms observed following infection with the encephalitic alphaviruses are very similar to those infected with arthritic alphaviruses and include fever, headache, nausea, and myalgia. Those with severe disease can experience seizures, coma, encephalitis, and death. Surviving patients infected with the encephalitic alphaviruses often experience long-term neurological symptoms. While VEEV and WEEV infections have low case-fatality rates in humans (approximately 1% and 3-4%, respectively) (15, 151), the case-fatality rate for EEEV is an astounding 35-70% (16). In equines, VEEV has a case fatality rate of 20-80%, the WEEV case-fatality rate is 3-50%, and the case fatality rate for EEEV is 70-90% (16). The encephalitic alphaviruses pose a serious threat to public and veterinary health during outbreaks.

---

#### 1.2.9 VENEZUELAN EQUINE ENCEPHALITIS VIRUS (VEEV)

VEEV is an encephalitic alphavirus that causes a sudden onset of fever, severe headache, myalgia, and chills. VEEV can also cause long-term neurological sequela, including seizures, paralysis, headaches, and depression, and these symptoms are more commonly observed in children (151, 152). Encephalitis and death also occur after VEEV infection in humans, although this is relatively uncommon. VEEV infection is associated with spontaneous abortions in pregnant women. Virus is detectable in the brains of the aborted fetuses indicating that the virus can cross the placenta (15, 151, 153). VEEV also causes fatal encephalitis in equines; the virus was first isolated in Venezuela in 1938 from the brains of equines who had succumbed to infection (56). Two major transmission cycles have been identified for VEEV including: the enzootic cycle between *Cx.(Melanoconion)* mosquitoes and rodents (58); and the epizootic/epidemic cycle involving equines, humans, and *Ochlerotatus taeniorhynchus* and *Psorophora confinnis* mosquitoes (56). Interestingly, infection of horses with the enzootic isolates results in an attenuated infection, with no detectable viremia; but horses infected with

the epizootic VEEV isolates developed viremia and disease (154). The enzootic strain could establish viremia in horses after introducing epizootic E2 into the enzootic VEEV background (154). Further comparison of the enzootic and epizootic VEEV isolates by phylogenetic analysis suggested that the epizootic strains are derived from the enzootic strains (155, 156). Together, this leads to the hypothesis that the enzootic viruses can establish epizootic transmission cycles by acquiring specific point mutations that allow for efficient replication in epizootic vectors and equids (57).

VEEV replicates very efficiently in mouse and nonhuman primate models. Inoculation of mice in the footpad with VEEV results in viremia, viral replication in lymphoid tissue, and viral spread to the CNS via the olfactory neuroepithelium and the trigeminal nerve (157). The virus replicates locally in variable regions of the brain, which induces inflammation and encephalitis and death (158). Rhesus macaques and cynomolgus macaques are susceptible to VEEV infection, and they typically develop viremia and fever (159, 160). Both macaque species develop varying degrees of neurological pathology depending on the strain of virus, macaque species, and the route of infection (161, 162). Both mouse and nonhuman primate models are valuable tools to study VEEV-induced acute febrile illness and encephalitis.

## 1.3 ALPHAVIRUS REPLICATION CYCLE

### 1.3.1 ENTRY

The overall process of alphavirus entry is initiated when E2 binds to an unknown cellular receptor. The virion is taken up by the cell in a process that involves receptor-mediated endocytosis that results in endosomal localization of the particles. E1, the fusion protein, promotes fusion with the endosomal membrane, releasing the ribonucleocapsid (RNP) into the cytoplasm. The RNP disassembles releasing the positive-sense genomic RNA into the cytoplasm. Most alphaviruses infect both insect and mammalian species and replicate in these

very different cellular and biochemical environments (**Table 1-1**), which demonstrates the versatility and adaptability of these viruses. After engagement with the cellular receptor, the virus can be internalized via receptor-mediated endocytosis in clathrin-coated vesicles (163, 164). The low pH in the endosomal compartment triggers a molecular rearrangement of E1 and E2 so that E1 homotrimerizes exposing the hydrophobic fusion peptide at the tip of E1, which inserts into the cellular membrane (101, 165). Endosomal acidification to pH 5.85 was shown to be important for the dissociation of E1 and E2 to promote successful fusion (166). An alternative mechanism has been proposed with SINV, wherein the virus fuses directly with the plasma membrane at neutral pH (167, 168). These studies open possibilities that there may be more than one mechanism for viral entry.

During the entry process, the virus binds to attachment factors present in the extracellular matrix. Glycosaminoglycans (GAGs), which make up an important component of the extracellular matrix on the surface of mammalian cells, are negatively charged, and they interact with alphavirus E2 (169-172). When alphaviruses are passaged repeatedly in mammalian cells, the viruses that develop positively charged residues in E2 gain a growth advantage because the adapted virus can preferentially interact with the negatively charged GAGs. These tissue-culture adapted viruses often have an attenuated phenotype *in vivo* when compared to the founding virus (169). For example, the CHIKV vaccine strain was generated by repeated passaging of the Asian isolate AF15561 at total of 18 times in human fibroblasts (MRC-5 cells). The adapted strain 181-25 is attenuated *in vivo* (173) after acquiring 10 nucleotide point mutations, resulting in 5 amino acid changes (174). One of the mutations present in 181-25 E2, G82R, was responsible for its attenuation *in vivo* and reduced its ability to infect insect cells (C6/36 cells) (174, 175). Together, these studies demonstrate that GAGs are an important attachment factor for alphaviruses in cell culture systems, but that the natural

cycles between arthropods and mammals prevents GAG-adapted viruses from naturally emerging.

Alphaviruses enter both insect and mammalian cells infecting several different types of tissues during natural transmission cycles. One possible explanation for this remarkable ability is that the virus has one cellular receptor that is shared among many species and tissues. Alternatively, alphaviruses can utilize multiple receptors, which are used differently depending on the cell type and species of the target cell (176). Several host proteins have been proposed as cellular receptors for alphaviruses, including the laminin receptor, heparin sulfate, DC-SIGN, and L-SIGN. However, these proteins are likely attachment factors rather than a bona fide cellular receptor (reviewed in (176, 177)). Natural resistance-associated macrophage protein (NRAMP), was proposed as a receptor for SINV because the deletion of NRAMP in drosophila cells or its mammalian homolog reduced replication (178). These studies are not entirely convincing because while the reduction in virus replication was consistently observed as a 10-fold reduction, replication was never abolished in the absence of NRAMP. This indicates that alternative receptors and/or mechanisms of entry exist for the alphaviruses. Clearly, more experiments are needed to identify the cellular receptors for the alphaviruses. One helpful technique to identify virus receptors is clustered regularly interspaced short palindromic repeats (CRISPR)-Cas9. CRISPR-Cas9 was recently employed for the identification of the murine norovirus receptor (179), and this technique could be used to identify alphavirus receptors as well.

---

### 1.3.2 REPLICATION COMPLEX FORMATION AND RNA REPLICATION

The nonstructural proteins form replication complexes where the viral RNA replication occurs. These complexes form invaginations called spherules that localize to the plasma membrane and/or they are associated with endosomal compartments called type I cytopathic vacuoles (CPV1) depending on the cell type and the alphavirus species (180-183). The

spherules are 50 nm in diameter and are separated from the cytoplasm by a narrow opening or neck. Early observations by electron microscopy described the spherules as having an “electron-dense plug” around the neck and “thread-like” electron-dense material spewing from the neck, referring to the viral RNA (184). These spherules are detectable with antibodies to individual nonstructural proteins as well as dsRNA antibodies.

All four nonstructural proteins are essential for productive replication of alphavirus genomes. The incoming viral RNA is positive polarity, but the early generation of a minus-sense genomic RNA is required for RNA amplification. Using the minus-strand RNA as a template, additional positive stranded gRNA and sgmRNA are synthesized by the nonstructural protein complex. Early studies showed that the 5' sequences of the two RNA species were different, suggesting that while the gRNA transcription is initiated on the 3' end of the minus-stranded RNA, there is an internal promoter on the minus-stranded RNA that initiates transcription of the sgmRNA (72, 185). This internal promoter region is located at positions -19 to +5 relative to the start of the sgmRNA (83).

The incoming gRNA is translated to produce the nonstructural polyprotein nsp1-4 (annotated P1234). There is a leaky opal codon (UGA) between nsp3 and nsp4, so that 80-90% of the time, the polyprotein P123 is produced, and P1234 is made by read-through of the opal codon only 10-20% of the time (186). Some alphavirus species (ie. ONNV and SFV) lack the opal codon, and they synthesize P1234 100% of the time, but the specific consequences of this on viral replication are still unknown (187). Early during replication, P1234 is cleaved by nsp2 into P123 + nsp4 (188). The processed P123 + nsp4 form the replication complex that preferentially synthesizes minus-stranded genomic RNA within the first 2-4 hrs of infection (189). At later times, P123 is cleaved by the nsp2 into the mature forms of nsp1, nsp2, and nsp3. (190). This process shuts off synthesis of the negative stranded RNA, and initiates positive stranded gRNA and sgmRNA synthesis, which are very efficiently produced from the

negative strand (191). RNA replication is proposed to be linked to cleavage of the individual structural proteins due to conformational changes in the nonstructural proteins such that the complex can no longer initiate minus-stranded RNA synthesis (191, 192).

All the nonstructural proteins are essential for replication of vRNA, and each nonstructural protein has specific functions within the replication complex as well as auxiliary functions to promote an antiviral state in the cell. **Nsp1** is the viral methyltransferase (MTase) and guanylyltransferase (GTase). Viral nsp1 adds a cap to the viral gRNA and sgRNA during replication in a reaction distinct from cellular mRNA capping (193, 194). The capping reaction in higher eukaryotes is as follows (193):

- (1)  $\text{pppN}_1\text{pN}_2\text{pN}_3\dots \rightarrow \text{ppN}_1\text{pN}_2\text{pN}_3\dots + \text{P}_i$  (mediated by RNA triphosphatase)
- (2)  $\text{GTP} + \text{guanylyltransferase} \rightarrow \text{guanylyltransferase-GMP} + \text{PP}_i$
- (3)  $\text{Guanylyltransferase-GMP} + \text{ppN}_1\text{pN}_2\text{pN}_3\dots \rightarrow \text{GpppN}_1\text{pN}_2\text{pN}_3\dots + \text{guanylyltransferase}$
- (4)  $\text{GpppN}_1\text{pN}_2\text{pN}_3\dots + \text{S-adenosylmethionine} \rightarrow \text{m}^7\text{GpppN}_1\text{pN}_2\text{pN}_3\dots + \text{S-adenosylhomocysteine}$
- (5)  $\text{m}^7\text{GpppN}_1\text{pN}_2\text{pN}_3\dots + (\text{nucleoside-2'-O})\text{-methyltransferase} \rightarrow \text{m}^7\text{GpppmN}_1\text{pmN}_2\text{pN}_3\dots$

The capping reaction facilitated by nsp1 is as follows (73, 193):

- (1)  $\text{pppN}_1\text{pN}_2\text{pN}_3\dots \rightarrow \text{ppN}_1\text{pN}_2\text{pN}_3\dots + \text{P}_i$  (mediated by nsp2 (195))
- (2)  $\text{GTP} + \text{S-adenosylmethionine} \rightarrow \text{m}^7\text{GTP} + \text{adenosylhomocysteine}$
- (3)  $\text{m}^7\text{GTP} + \text{nsp1} \rightarrow \text{m}^7\text{GMP-nsp1} + \text{PP}_i$
- (4)  $\text{m}^7\text{GMP-nsp1} + \text{ppN}_1\text{pN}_2\text{pN}_3\dots \rightarrow \text{m}^7\text{GpppN}_1\text{pN}_2\text{pN}_3\dots$

The result of the first reaction, present in higher eukaryotes, is a type 1 cap structure, while the product of the nsp1 reaction is a type 0 cap, with no 2'-O-methylation at the N<sub>1</sub> or N<sub>2</sub>

position. Notably, the nsp1 reaction requires the RNA triphosphatase activity of nsp2 to prepare the viral RNA for capping by nsp1 (195).

When expressed in cells, nsp1 localizes to the inner leaflet of the plasma membrane, and the protein is anchored to the membrane by an amphipathic helix and by palmitoylation of conserved cysteine residues present at the C-terminus of nsp1 (193, 196, 197). Mutation of the residues within the amphipathic helix that prevent nsp1 membrane association is lethal to the virus (198).

**Nsp2** is the viral protease, helicase, and NTPase. Overexpression of nsp2 is toxic to mammalian cells and *E. coli* (199). On its N-terminus, Nsp2 possesses a helicase and NTP-binding domain, which binds to and unwinds the RNA secondary structure during RNA replication (199). The NTPase domain possesses RNA triphosphatase activity that is required for preparing the viral mRNA for the nsp1-mediated capping reaction (195, 200). The protease activity domain is localized to the center of nsp2, and it is essential for cleavage of the nonstructural polyprotein, as discussed above (201). The C-terminal methyltransferase-like domain of nsp-2 is implicated in degradation of the catalytic subunit of host RNA polymerase II in the nucleus to shut off host transcription (202). This specific function of nsp2 will be discussed below in section 1.3.6.

The precise functions of **nsp3** are still not well resolved. However, we have learned much about nsp3 through structural and binding partner identification analyses. The domains of nsp3 include: 1) an N-terminal macrodomain, 2) an alphavirus-specific unique domain with a zinc coordination site, and 3) a C-terminal hypervariable domain. The macrodomain is a domain that binds adenosine diphosphoribose (ADP-ribose). The macrodomain is conserved across alphaviruses, coronaviruses, toroviruses, and hepatitis E, but its specific role in viral replication is unknown (203). The CHIKV and VEEV nsp3 macrodomain crystal structures have been

solved with ADP-ribose bound. The macrodomain contains adenosine 1'-phosphate phosphatase activity, but it is unclear what role this plays in replication (204). Nsp3 is an essential component of the replication complex, and it associates with other nonstructural proteins during viral RNA replication. An additional crystal structure was solved of the precleaved P23 complex, that showed the nsp2 protease and MT-like domains in contact with the nsp3 macro and zinc-binding domain (205). Based on this structure, a P23 RNA binding site was predicted. This site has implications for the early stages of replication, when negative stranded RNA is preferentially made, because after P2/3 cleavage, positive sense RNA is preferentially generated.

The nsp3 hypervariable domain is heavily phosphorylated, and mutagenesis of the phosphorylation sites results in an attenuated infection *in vivo*, as shown with SFV (206). Nsp3 is present in cytoplasmic foci in infected cells, which co-localize with other nonstructural proteins, indicating that these foci are replication complexes (183). Nsp3 interacts with several cellular proteins during infection, including RasGAP SH3-domain binding protein (G3BP) (207). Immunoprecipitation experiments with mutant nsp3 proteins showed that the interaction between nsp3 and G3BP occurs through binding of the nsp3 hypervariable domain. This important interaction prevents an antiviral stress response during infection by blocking stress granule formation (207, 208). However, it is unknown whether the proteins associated with nsp3 also function in the replication complexes to promote RNA replication.

**Nsp4** is the alphavirus RNA-dependent RNA polymerase. As one might predict, Nsp4 localizes to replication complexes in infected cells (183). Alphavirus nsp4 proteins have the characteristic RNA polymerase GDD motif (209), which is essential for viral RNA synthesis (210, 211). Early observations showed that nsp4 protein expression levels are very low relative to the nonstructural polyprotein P1234 (212). Nsp4 possesses a conserved tyrosine residue on its N-terminus, which promotes its degradation by the N-end rule. By the N-end rule, the N-

terminal residue can destabilize a protein by targeting it for proteolysis. Mutagenesis of this Tyr residue was capable of stabilizing nsp4 (213). However, an infectious clone containing this Tyr mutation had reduced viral replication kinetics demonstrating that the tyrosine and protein degradation is important for efficient replication in cell culture (214). During replication, nsp4 protein levels are regulated at least two ways: nsp4 is produced only by read-through of the opal codon, occurring 10-20% relative to P123; and it is also degraded during replication by the N-end rule. The molecular importance of this tight regulation of nsp4 protein levels remains to be determined.

---

#### 1.3.4 TRANSLATION OF VIRAL SUBGENOMIC MRNA

The sgRNA is transcribed from an internal promoter of the minus strand genomic RNA located within the nsp4 gene and the subgenomic 5'UTR (83, 185). The sgRNA possesses a 5' cap and is polyadenylated at its 3' end. The translation product of the sgRNA forms the structural polyprotein that includes the proteins C, E3, E2, 6K, E1, and TF. sgRNA translation initiation occurs in the cytoplasm, and the capsid protein cleaves itself from the nascent chain, exposing an endoplasmic reticulum (ER) localization sequence on E3 that promotes translocation of the viral glycoproteins to the ER membrane (215-218). The polyprotein E3-E2-6K-E1 is cleaved between E2/6K and 6K/E1 by ER-localized signalase (218). In the trans-Golgi network, furin cleaves between E3/E2 (219, 220). Transframe protein (TF) was recently recognized as a protein produced from a -1 ribosomal frame-shift during synthesis of 6K; this results in a protein with the identical N-terminal region as 6K but with a unique C-terminal sequence (221). Interestingly, TF, but not 6K, is incorporated into virions (222). Viruses deleted of 6K/TF are still viable, although 6K/TF deletion mutants have defects in assembly and budding (221, 223). Two cysteine residues are palmitoylated only in TF, not in 6K, even though both proteins have the cysteines. Mutagenesis of two of the cysteines in 6K/TF resulted in defective

viral particle formation, with some particles incorporating more than one nucleocapsid into the envelope (89). This further confirms the importance of 6K/TF in viral assembly.

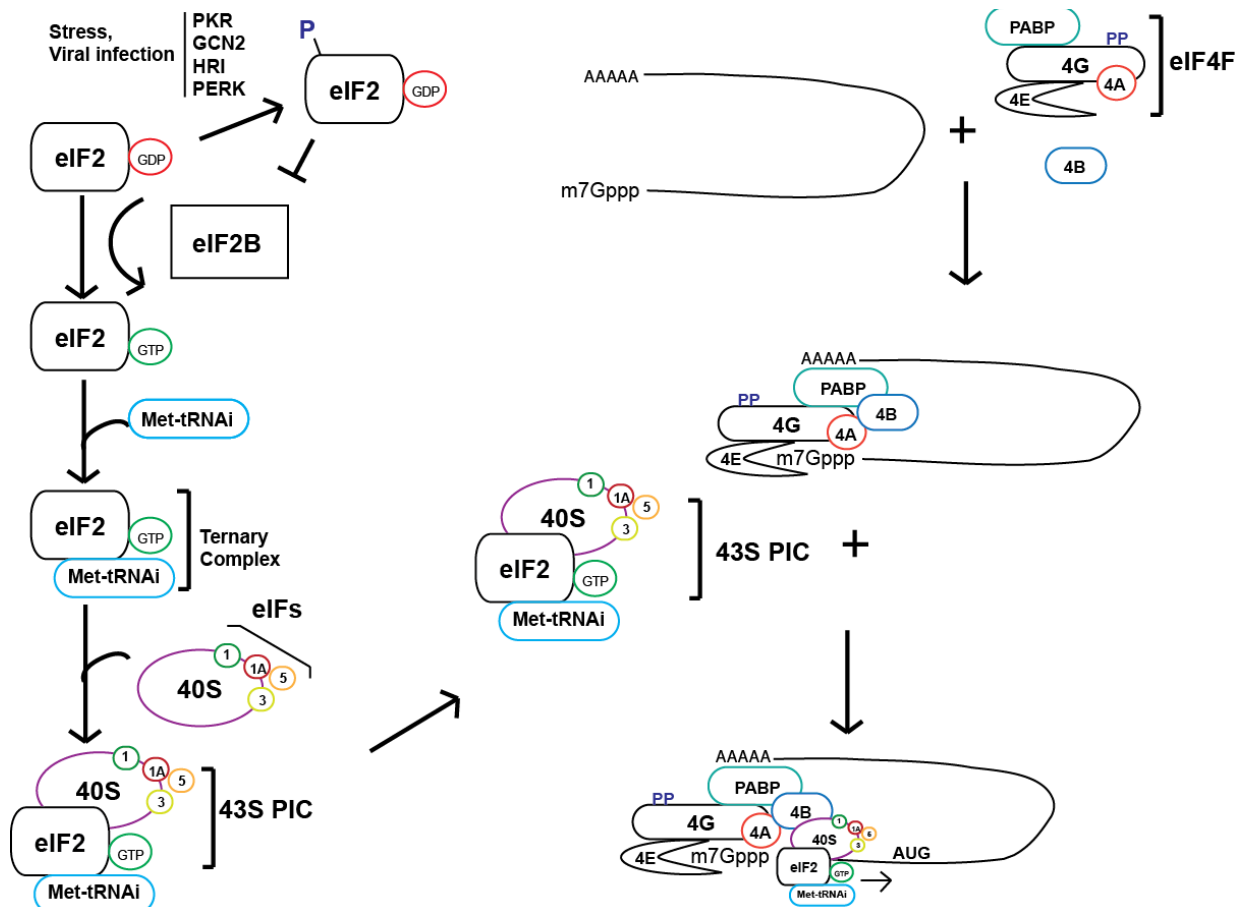
The process of canonical cap-dependent translation initiation involves multiple eukaryotic translation initiation factors (eIFs) as well as ribosomal subunits (**Figure 1-3**) (Reviewed in (224)). The 5'UTR is recognized by the ternary complex, consisting of a GTP-bound eIF2 with an initiator methionyl-tRNA (Met-tRNA<sub>i</sub>), and the small (40S) subunit of the ribosome, together making the 43S preinitiation complex (PIC). The 40S ribosomal subunit interaction with the ternary complex is facilitated by eIFs 1, 1A, 3, and 5. The 43S PIC interaction with the mRNA is facilitated by eIF3, the cap-binding complex eIF4F (consisting of eIF4E, eIF4G, and eIF4A), and the poly(A)-binding protein (PABP). Once bound, the 43S PIC scans the mRNA and identifies the AUG, and the PIC stops, eIF1 is released, and the eIF2-GTP complex is converted to eIF2-GDP.

One interesting feature of the translation of the sgRNA is that it efficiently occurs during host translational shutoff (225, 226). Alphavirus sgRNA does not follow classical translation initiation rules because it does not require many of the translation initiation factors. Notably, translation of the sgRNA can proceed when the eIF2 $\alpha$  subunit is phosphorylated/inactivated (227-229). Normally eIF2-GDP is converted to eIF2-GTP by the guanine exchange factor eIF2B, but the phosphorylation of the eIF2 $\alpha$  subunit inhibits the function of eIF2B and stops translation initiation. There are four kinases that activate eIF2 $\alpha$  phosphorylation in response to cellular stress: PKR (dsRNA sensor), PERK (ER stress), HRI (heme deprivation), and GCN2 (nutrient starvation) (230). eIF2 $\alpha$  phosphorylation/inactivation is sufficient to shut off translation of host mRNAs. Though some viruses prevent the inactivation of eIF2, alphaviruses *induce* eIF2 phosphorylation via PKR and are still able to translate their sgRNA in this state (228, 231). Consistent with this idea, treatment of cells with sodium arsenite, which induces eIF2 $\alpha$  phosphorylation and ER stress, will not block translation of the

sgmRNA, but it will impair maturation of the envelope proteins in the ER (232). Though eIF2 $\alpha$  phosphorylation/inactivation occurs during alphavirus replication by the kinase PKR, alphaviruses still induce host translation shutoff in PKR $^{-/-}$  cells, suggesting that there are other means of shutting off host transcription and translation in alphavirus-infected cells, and this is discussed further in section 1.3.6 (228).

To facilitate translation of viral sgmRNA in the presence of eIF2 alpha phosphorylation, many alphaviruses possess a stable CG-rich stem loop positioned downstream of the capsid AUG that allows for translation to proceed when eIF2 $\alpha$  is phosphorylated (225, 227, 233). This structure, called a downstream loop (DLP), was first identified as a translational enhancer with a predicted hairpin structure (234). Mutations introduced into the SINV DLP that disrupt the

**Figure 1-2: Canonical cap-dependent translation initiation.**

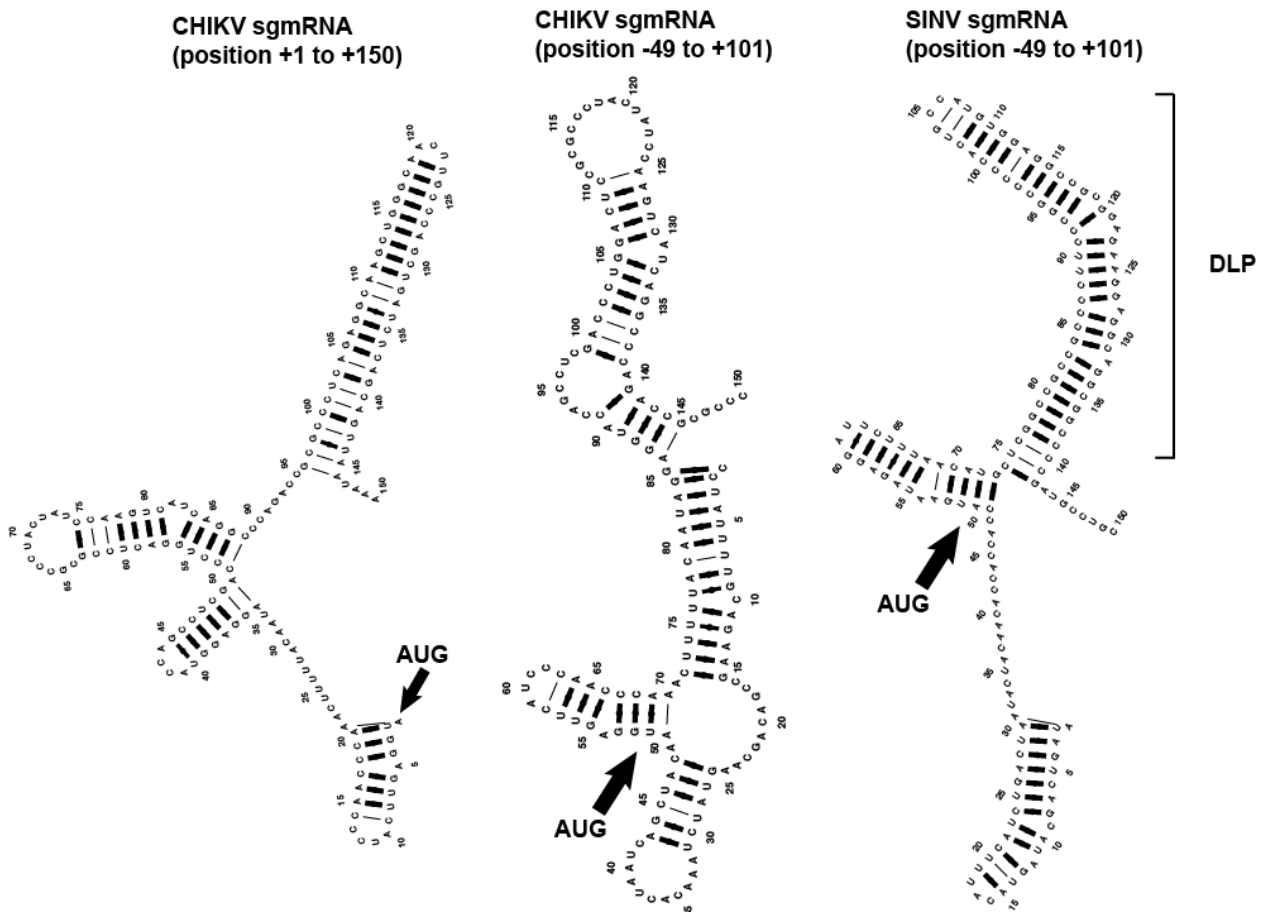


predicted DLP structure, with only one amino acid change in the coding sequence, displayed a 3-log growth defect in PKR<sup>+/+</sup> MEF cells, but only a 2 or 3-fold growth defect in PKR<sup>-/-</sup> MEF cells (227). The same trend was observed in mice with defects in PKR. Infection with either the DLP mutant or the wild type SINV resulted in equal levels of virus in the brain. However, infection of mice with a functional PKR gene with DLP mutant SINV had significantly reduced viral titers in the brain relative to the parental virus (235). Recent evidence suggests that the DLP may function by trapping the 40S ribosomal subunit in an ideal position for translation initiation at the sgRNA AUG (236). Many alphaviruses possess these DLP structures but they can have different stabilities and stem lengths relative to SINV (235). Interestingly, several medically relevant alphaviruses are not predicted to possess a DLP, including CHIKV, VEEV, WEEV, and ONNV (235). It is possible that these viruses possess an alternative RNA structure that performs the same function as a DLP, or other viral proteins could manipulate the infection state in the cell in another way to ensure that the virus translates the viral sgRNA efficiently. Currently, the mechanism for translation in the presence of inactive eIF2 $\alpha$  for these viruses remains unknown. Below is shown a diagram where I have used the RNA folding program MC-Sym and MC-fold (237) to predict the secondary structure of the SINV sgRNA using the sequence -49 to +101 nt relative to the start of capsid. The DLP stem loop for SINV is very stable, and I consistently mapped the DLP structure. For CHIKV, I ran two different structural predictions using nucleotides +1 to +150 or -49 to +101 (**Figure 1-4**). The CHIKV sequence was not predicted to form a large DLP but it is predicted to have a stem loop at about 100 nt downstream of the AUG. This stem loop does not appear to be as stable as the SINV DLP, but it may indicate that there is a secondary structure in that region that has not been initially defined.

The viral sgRNA was shown to not require many of the canonical translation initiation factors for its translation (**Table 1-2**). One of the essential members of the eIF4F cap binding

complex, eIF4G, was disposable for capsid production from viral replicons (238). To demonstrate this phenomenon, either the HIV-1 protease PR or the poliovirus 2A<sup>pro</sup>, viral proteins that cleave eIF4G, were cloned into the SINV replicon downstream of capsid. With this system, the eIF4G cleavage proteinases are translated with the same kinetics as the structural proteins. Capsid was still translated, although reduced, when BHKs were transfected with the replicons containing PR or 2A<sup>pro</sup> (238). To determine whether the replicon sgRNAs could still initiate translation in the absence of eIF4G, the cells were transfected with the replicons, and then a hypertonic solution was added to the cells to block translation initiation while allowing the polysomes to run off the mRNA (238, 239). When the hypertonic solution was removed, new translation initiation events would have to occur in the presence of the cleaved eIF4G to synthesize capsid. Capsid was still produced in the presence of cleaved eIF4G indicating that

**Figure 1-3: Predicted RNA folding by MC-Fold (<http://www.major.irc.ca/MC-Sym/>).**



translation initiation of sgRNAs does not require eIF4G (238). In contrast to the sgRNA, translation of the gmRNA requires intact eIF4G, and cleavage of eIF4G prior to infection reduces levels of nonstructural and structural proteins because of incomplete production of nonstructural proteins (238). Another member of the eIF4F cap-binding complex, eIF4A, was shown to have reduced requirements for alphavirus sgRNA. Treatment of cells with hippuristanol, an inhibitor of eIF4A, did not inhibit SINV structural protein synthesis, while other mRNAs were inhibited (240). Therefore the SINV sgRNA was shown to have decreased requirements for members of the cap binding complex eIF4F.

A proposed mechanism for translation initiation of alphavirus sgRNA is through the use of noncanonical translation initiation factors such as eIF2A or eIF2D, which potentially replaces the function of eIF2 during stress conditions when eIF2 is not available. However, SINV sgRNA was translated efficiently in cell lines that lack eIF2A and eIF2D, suggesting that translation of viral sgRNA does not require eIF2A or eIF2D (232).

**Table 1-2: Translation initiation factors dispensable for translation of alphavirus sgRNA.**

Translation initiation factor	Function of eIF	Representative experiments that suggest the sgRNA does not require the eIF	References
eIF2	Interacts with the Met-tRNA <sup>Met</sup> to form the ternary complex	Many alphaviruses have a DLP structure that stalls the ribosome and negates the need for eIF2.	(227, 235)
eIF4G	Member of the eIF4F cap-binding complex, interacts with eIF3 and PABP	Translation can still occur when eIF4G is cleaved by poliovirus 2A <sup>Pro</sup> or HIV-1 PR.	(238)
eIF4A	Member of the eIF4F cap-binding complex, acts as a helicase	SINV sgRNA translation is not sensitive to eIF4A inhibitor hippuristanol.	(240)
eIF2A	Non-canonical translation initiation, proposed to substitute for eIF2	eIF2A <sup>-/-</sup> cells were still able to support SINV replication to the same extent as the parental cells.	(232)
eIF2D	Suggested to substitute for eIF2	eIF2D <sup>-/-</sup> cells were still able to support SINV replication to the same extent as the parental cells.	(232)

Several groups used *in vitro* synthesized mRNAs to study the translational requirements of alphavirus sgRNA. One major takeaway is that the translational requirements of transfected mRNAs generated *in vitro* is not equivalent to the translation of mRNAs produced from replication complexes during infection. During infection, the virus induces cellular stress by engaging pattern recognition receptors and inactivates eukaryotic translation initiation factor eIF2 $\alpha$ , both of which induce an antiviral state in the cell. Exogenous transfection of viral sgRNA to uninfected cells does not accurately mimic an infection state in the cell; instead, many groups have studied sgRNA translation in the context of replicon systems. The replicon RNA possesses the nonstructural protein genes, but the structural protein genes are replaced with the genes for capsid and/or a fluorescent reporter. Transfection of replicon mRNA results in synthesis of the nonstructural proteins and formation of the replication complex. The replication complex will generate sgRNA, but only capsid and the fluorescent reporter are synthesized.

Translation of *in vitro* generated sgRNAs that were transfected into infected cells or replicon-containing cells was inhibited compared to uninfected cells (241). One reason for this finding is that the virus induces shutoff of cellular translation via nsP2 (242). Translation of transfected mRNA in infected cells was restored when a P726G mutation was introduced into nsP2, which also restored cellular translation (241). This supports the idea that translation of exogenous mRNAs in infected cells, even mRNAs that possess identical UTRs and capsid sequences as the native sgRNA, occurs “canonically” and is blocked by infection like other host mRNAs. In agreement with this hypothesis, translation of transfected sgRNAs was blocked by cleavage of canonical translation initiation factor eIF4G and by arsenite treatment, while translation of sgRNAs generated in replicon-containing cells was not affected (229). This suggests that the sgRNA generated from replication complexes is “privileged” because of its proximity to factors that facilitate its translation efficiently when host mRNAs and exogenously introduced mRNAs are blocked.

---

### 1.3.5 ASSEMBLY AND RELEASE

Capsid proteins assemble around the gRNA to form the nucleocapsid. The nucleocapsid then interacts with the mature E1/E2 dimer present on the plasma membrane and buds from the cell. The positive-sense viral gRNA is preferentially recognized by capsid at discrete sites: predominantly the coding region after nsp1 and the subgenomic promoter region (82). *In vitro* synthesized capsid proteins self-assemble around nucleic acid to form the nucleocapsid (95). The capsid protein has three major domains: the N-terminal domain contains the RNA-binding domain and a coiled-coil formation; the central domain binds RNA and is responsible for capsid-capsid homotypic interactions; and the C-terminal domain forms the capsomeres on the surface of nucleocapsid, contains the protease domain, and interacts with the cytoplasmic tail of E2. The coiled-coil region present in the N-terminal domain and the central domain appear to be the most important in mediating nucleocapsid formation (243). Specifically, capsid residues 108-111 are conserved among alphaviruses, and they are crucial for capsid oligomerization (92).

Once formed, the nucleocapsid binds to the cytoplasmic domain of E2, and this interaction is sufficient to mediate budding from the infected cell. Budding requires both envelope and capsid, because no particles are produced in the absence of capsid or E1/E2 (244). The specific interaction of the nucleocapsid and E2 occurs via a hydrophobic pocket in capsid that is eventually occupied by a conserved tyrosine residue in E2 (245). The capsid binding to E2 is believed to occur via a two-step process, where a tryptophan in capsid shifts its position to accommodate the tyrosine in E2 and stabilizes the particle (92).

---

### 1.3.6 HOST TRANSCRIPTION AND TRANSLATION SHUTOFF

Alphaviruses combat the innate antiviral response by inhibiting host transcription and translation. Eventually, blocking host transcription and translation will lead to cytopathic effects and cell death. As stated in the previous section, alphaviruses induce eIF2 $\alpha$  phosphorylation by

the dsRNA sensor PKR, and their own sgRNAs are efficiently translated in the absence of eIF2. However, host shutoff still occurs efficiently in the absence of PKR, and any PKR-dependent effects on host mRNA translation by eIF2 $\alpha$  phosphorylation are minimal during alphavirus infection (228, 231).

For Old World alphaviruses, the viral factor responsible for host transcription and translation shutoff is **nsp2**. Nsp2 colocalizes to the replication complexes as well as the nucleus during infection. A mutation of nsp2 was identified in an attenuated SINV mutant virus that persistently infected cells rather than causing cytotoxicity. This mutation was located in the nsp2 C-terminal MTase-like domain (P726S) (246). Another group separately identified that a mutation in SINV nsp2 (P726G) also persisted demonstrating less cytopathic infection (247). The P726G virus could establish a persistent infection in cells lacking type I IFN responses (ie. Veros, BHKs, IFN- $\alpha$ / $\beta$ R-/- MEFs), but it would not persist in cells with intact type I IFN signaling (226). The P726G virus induced higher levels of IFN responses compared to the parental viruses, suggesting that the P726G mutant infection was efficiently controlled by the innate immune response. The P726G virus did not shut off global host translation to the levels of the parent SINV. Together, these data provide evidence that P726 is important for the function of nsp2 to counter innate immunity by shutting off host translation (226).

Additional experiments with SFV showed that mutation of the nuclear localization signal at R649D partially inhibited nsp2 localization to the nucleus, and host transcription was moderately restored (248). Later it was identified that nsp2 enters the nucleus and degrades Rpb1, the catalytic subunit of RNA polymerase II (202). Introduction of mutations in the MTase-like and the helicase domains, but not the protease domain, prevented degradation of Rpb1, suggesting that there are multiple sites in nsp2 responsible for degradation of Rpb1 (202). These data determined that mutations in nsp2 that blocked the ability of the protein to degrade Rpb1, also restored host transcription. Mutations that abolished nsp2/3 cleavage events are

completely devoid of nuclear localization (242). In this context, nsp2 is unable to enter the nucleus, and cellular transcription was weakly affected. However, host translation was still inhibited to the same extent as observed with wild type virus. This suggests that while nsp2 contributes to transcriptional shutoff via degradation of Rpb1 nucleus, nsp2 and/or other viral proteins may contribute to translational shutoff in the cytoplasm by a yet to be defined mechanism.

New World alphavirus capsid protein is responsible for host shutoff. During replication, capsid is involved in encapsulating the viral gRNA, but the New World capsid has an additional role: it localizes to the nucleus and inhibits cellular transcription (249). Unlike Old World alphavirus replicons, New World replicons are not nearly as toxic when introduced into cells. However, addition of New World capsid protein to these replicon constructs blocked RNA synthesis (250). Capsid's role in host transcriptional shutoff was attributed to a short peptide in the capsid N-terminus, and expression of this peptide was sufficient to shut off transcription (249). Capsid also associates with the nuclear envelope, but the significance of this localization is unknown.

## 1.4 CHIKUNGUNYA VIRUS (CHIKV)

### 1.4.1 INTRODUCTION AND CLASSIFICATION OF CHIKV

Chikungunya virus (CHIKV) is in the *Alphavirus* genus of the *Togaviridae*. CHIKV is a member of the Semliki Forest Virus antigenic complex, along with ONNV, SFV, MAYV, UNA, BEB, GET, and RRV. The characteristic symptom of CHIKV is severe joint pain that causes hunched posture. For this reason, the disease was named in the Makonde language *chikungunya*, which translates to “that which bends up” (251). CHIKV was first described during an outbreak in the Southern Province of Tanganyika (present day Tanzania) in the 1950s by Dr. Marion Robinson. The disease caused a sudden-onset of severe joint pain, high fever, and

maculopapular rash (251). CHIKV was later isolated from human sera by R. W. Ross, and he performed the first CHIKV experiments in mice and mosquitoes (143). CHIKV has caused two major outbreaks in the last 15 years, one in the Indian Ocean region and the second in the Americas. Each outbreak affected millions of people. The ability of CHIKV to cause long-lasting arthritic symptoms and its ability to rapidly spread to new areas necessitates the need to study CHIKV to develop antivirals and vaccines.

---

#### 1.4.2 CHIKV EPIDEMIOLOGY

CHIKV has likely caused outbreaks in Africa, Asia, and potentially the Americas, for centuries, but it was routinely mistaken for dengue or dengue-like illness (252, 253). CHIKV, as with other mosquito-borne viruses, causes sporadic outbreaks accompanied by years to decades of relative silence (145, 254). After a lag period, when populations lose herd immunity to CHIKV, the overall population becomes susceptible to another introduction and spread of the virus. Since its isolation and characterization in 1953, CHIKV has caused outbreaks in Africa, Asia, Europe, Australia, and the Americas. Only one CHIKV serotype has been identified because sera from individuals infected with one genotype can cross neutralize isolates of different CHIKV genotypes (255). Genetic comparison of CHIKV sequences from a panel of CHIKV isolates show that there are three major CHIKV clades: West African (Waf), East/Central/South African (ECSA), and Asian (145). The Waf lineage is genetically more distinct from the ECSA and Asian lineages, and typically causes more isolated outbreaks in rural areas, with documented outbreaks in Senegal, Nigeria, and Guinea from 1960-1992 (145).

The ECSA and Asian lineages have initiated large urban outbreaks, typically in Africa and Asia, but more recently in the Americas. The ECSA lineage initiated a large outbreak in Kenya in 2004, spreading to several countries in the Indian Ocean region until 2011. Another ECSA outbreak was initiated during this time in India and Southeast Asia in 2005 until 2015 (256). This outbreak was unprecedented in scale, affecting millions of people. During this

outbreak, CHIKV acquired a point mutation in E1 (A226V), which allowed for increased vector competence of *Ae. albopictus* mosquitoes (257). Since these mosquitoes can be found in more temperate climates such as the United States and Europe, there was increased risk of CHIKV spreading to new areas. During this outbreak, autochthonous transmission of CHIKV was initiated in Europe for the first time, with *Ae. albopictus* as the principle vector (258, 259). See section 1.4.3 for more details about the A226V mutation.

The Asian lineage is spread predominantly by *Ae. aegypti* mosquitoes, and it has caused periodic outbreaks in India, Sri Lanka, Philippines, Thailand, and other Southeast Asian countries in the 1960's, 1980's, 1990s, and early 2000's (145). Until this point, no documented cases of local transmission had occurred in the Americas, for at least one hundred years. In December of 2013, local CHIKV transmission occurred in St. Martin, a small island in the Caribbean. CHIKV subsequently spread throughout the Caribbean, Central America, Mexico, northern South America, and the United States (Florida) (260, 261). According to the Pan American Health Organization, approximately 2 million people were infected with the virus during this outbreak (262). Sequencing confirmed that it was the Asian lineage, rather than ECSA, that initiated the Caribbean outbreak (263-265). A second introduction of CHIKV occurred in Feira de Santana, Brazil, but this introduction was with an ECSA genotype virus, rather than the Asian lineage (266).

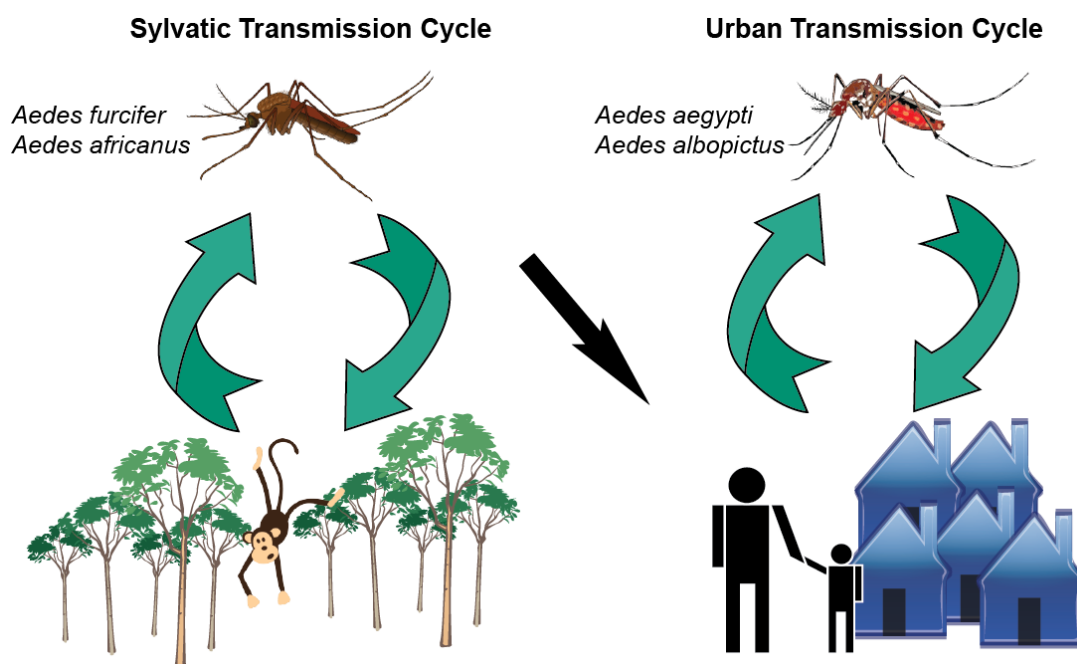
---

### 1.4.3 CHIKV TRANSMISSION AND REPLICATION IN MOSQUITOES

Experiments performed by R. W. Ross provided the first evidence that CHIKV was transmitted by mosquitoes. He allowed febrile patients to be fed upon by laboratory-bred *Ae. aegypti*, and he then inoculated mice with virus derived from the mosquitoes. Some of the mice developed disease after inoculation. Oddly, he was unable to successfully transmit CHIKV to the mice via mosquito bite, however, since then researchers have been able to experimentally infect mice through the bite of infected mosquitoes (143).

Since the early experiments of Dr. Ross and others, a number of epidemiological studies have identified two main transmission cycles for CHIKV: the sylvatic cycle and the urban cycle. The **sylvatic cycle**, best characterized for the WAf and ECSA CHIKV lineages, involves transmission between nonhuman primates (NHPs) and forest-dwelling *Ae. mosquitoes* (*Ae. furcifer*, *Ae. luteocephalus*, *Ae. taylori*) (**Figure 1-5**) (35, 36, 267) although, other wild vertebrates may be involved in the transmission cycle (e.g. squirrels, bats, and galagos, etc.) (36). *Ae. furcifer* has been implicated most consistently with the sylvatic cycles, and increases in the *Ae. furcifer* populations correlate with human outbreaks of CHIKV in isolated rural areas (35). While evidence for the existence of sylvatic cycles is most compelling in Africa, sylvatic cycles could be initiated in Asia and the Americas. Sylvatic cycling may already occur in Asia as CHIKV was isolated from NHPs in Malaysia (268), and antibodies were detected in Asian NHPs (269, 270). Whether this represents the initiation of sylvatic cycle in Asia or whether it is spillover from the urban outbreak is still unclear. In the Americas, there are competent canopy-dwelling *Aedes* spp. mosquitoes, which could potentially establish a sylvatic cycle with New World nonhuman primates (271).

**Figure 1-4: Urban and sylvatic transmission cycles of CHIKV.**



The **urban cycle** involves transmission between humans and mosquitoes, wherein a NHP intermediate is not required. The principle vectors responsible for CHIKV transmission in humans are *Ae. aegypti* and *Ae. albopictus*. CHIKV readily replicates in *Aedes* mosquitoes in laboratory settings (272, 273). Once infected by blood meal, CHIKV can rapidly disseminate from the midgut of the mosquito by 1 day post infection (dpi) and be detected in saliva by 2 dpi (257, 274, 275). While *Ae. aegypti* is the principle vector involved in most large-scale urban CHIKV outbreaks, CHIKV also adapted to replicate in *Ae. albopictus* mosquitoes during the Indian Ocean outbreak in 2005-2007 (276). This adaptation to *Ae. albopictus* was concerning because these mosquitoes have a wider distribution in temperate regions such as Europe and the United States. CHIKV could rapidly spread to Europe and the United States because there are large populations of CHIKV-naïve individuals. The ability of CHIKV to replicate in *Ae. albopictus* mosquitoes was attributed to a point mutation in E1 (A226V), and CHIKV strains with the A226V mutation disseminated better in *Ae. albopictus* compared to A226 viruses (257, 277). Additionally, virus isolates during the Indian Ocean outbreak obtained prior to the A226V mutation did not replicate in either *Aedes* species as well as the A226V mutant (257). There may be additional factors that contributed to the outgrowth of the A226V mutant strains, but these have yet to be discovered. *Ae. aegypti* and *Ae. albopictus* are highly competent for CHIKV replication under both laboratory settings and during large urban outbreaks. The A226V mutation demonstrates that CHIKV has the potential to accommodate mutations that allow for more efficient growth in different mosquito species allowing for quick adaptation and survival of the virus species.

Evidence suggests that transovarial and venereal transmission of CHIKV may occur in *Ae.* mosquitoes. Vertical or transovarial transmission of CHIKV in mosquitoes has been documented in regions experiencing CHIKV outbreaks because mosquitoes from larva collected in the field that emerged in a controlled laboratory environment were found to be positive for

CHIKV (278, 279). In addition, CHIKV was detected in male mosquitoes (280), which are not hematophagous. Transovarial transmission of CHIKV has been difficult to prove in the laboratory; some groups were unable to demonstrate transovarial transmission of CHIKV (281, 282). A recent report provided some explanation to this discrepancy, showing that transovarial transmission of CHIKV does not occur in the first egg-batch after an infectious blood meal, but rather CHIKV was detected in subsequent egg-batches at high rates (roughly 20%) (283). This is consistent with histological examination of mosquito ovaries at 6 dpi, which revealed CHIKV-positive staining of the eggs by 6 dpi (257). Additional studies suggested that venereal transmission could occur because CHIKV could be transferred from male to female mosquitoes during mating (284). These findings raise questions about the extent that these transmission patterns occur in natural environments and how much they contribute to the maintenance of CHIKV during and between epidemics.

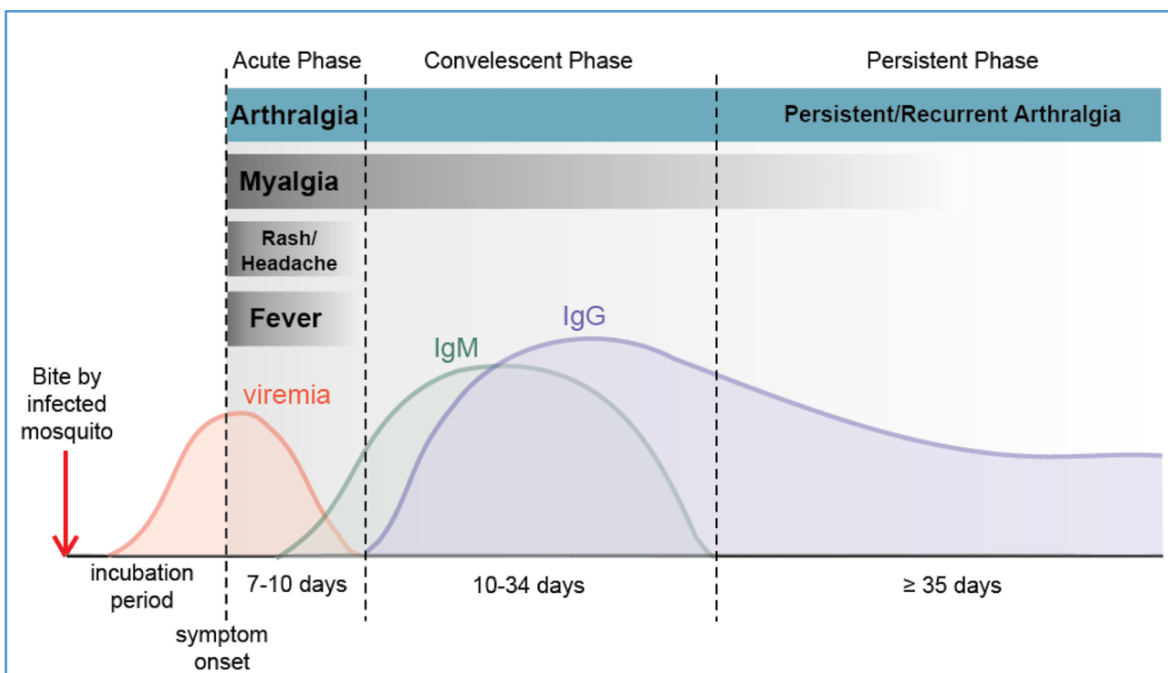
---

#### 1.4.4 CHIKV SYMPTOMS IN HUMANS

CHIKV is transmitted to humans via bite of an infected mosquito. Symptoms typically appear between 3-12 days later (251). Following the incubation period, most patients experience a sudden onset of high fever, rash, and an incapacitating arthralgia and myalgia (**Figure 1-6**) (285-287). The fever is typically high (102-104 °F) (251), and some patients may experience a biphasic fever, although this is less common (251). Skin lesions are typically morbilliform and can locate to arms, legs, trunk, neck, and face (288). The lesions typically appear 2-4 days after fever onset and resolve without sequelae. Arthralgia is the hallmark symptom of CHIKV infection, and it occurs most frequently in the peripheral joints: wrists, hands, ankles, and feet (251, 286, 287).

While many people recover following CHIKV infection, the duration of the arthralgia can vary from 1 week to several years post infection (105). Individuals over 60 years of age are at increased risk for developing chronic joint pain, neurological involvement, and cardiovascular issues (110, 289, 290). CHIKV infection in newborns can result in severe disease that can lead to encephalitis and death (291).

**Figure 1-5: CHIKV symptoms in humans.**



#### 1.4.5 CHIKV PERSISTENCE AND LONG-TERM SYMPTOMS IN HUMANS

Prolonged arthritic pain is a common symptom following the acute phase of CHIKV disease in humans, with as many as 43-75% of patients experiencing long-term symptoms (105, 110, 112, 292). Patients with long-term symptoms experience joint swelling, joint pain, and myalgia (293). Some patients develop a serious arthritic condition that involves joint swelling, bone erosion, synovitis, and tenosynovitis, while negative for rheumatoid factor and anti-cyclic citrullinated peptide antibodies (294, 295). It is not known whether the long-lasting arthralgia

occurs because of persistent viral infection or if it is an auto-inflammatory condition. However, patients experiencing chronic arthritic symptoms after CHIKV infection are typically negative for common autoimmunity markers in their serum (293).

Two studies provided evidence for persistent CHIKV infection in patients experiencing long-term arthritis. The first study (Ozden, et al., 2007 (111)) examined muscle biopsies for the presence of CHIKV antigen. The first biopsy was from a patient in the acute phase of the disease, and the second biopsy was from a patient roughly three months following acute symptoms. In both cases, the muscle biopsies stained positive for CHIKV antigen using mouse antisera. The second group (Hoarau, et al., 2010 (110)) examined synovial tissue and fluid from a patient experiencing severe chronic arthritic pain, and discovered that the patient's synovial macrophages stained positive for CHIKV E1. This finding suggested that macrophages are a site of viral persistence in joints. Similarly, RT-PCR performed on synovial tissue biopsy samples detected CHIKV RNA (both E1 and nsp2) as well as IFN $\alpha$  expression. As controls, two healthy patients who had recovered from CHIKV infection volunteered to have joint biopsies performed, and their tissues were negative for CHIKV. Though these studies are suggestive of CHIKV persistence, infectious virus has not yet been isolated from the joint or muscle tissue from patients experiencing chronic CHIKV-induced joint pain. However, it may be that CHIKV is persisting at a low level that is below the limit of detection by plaque assay. Alternatively, the viral genome is maintained in the absence of viral turnover, which can be tested by measuring viral genomes by qRT-PCR specific for the nonstructural genes in different tissues.

---

#### 1.4.6 SEVERE SYMPTOMS OF CHIKV IN HUMANS

Though people typically recover following CHIKV infection, some patients develop severe disease, which is more common in people with preexisting conditions, the elderly, and newborns (289, 296). The severe symptoms may fall into one of these categories: severe

chronic arthritic disease, cardiovascular disorders, neurological disorders, renal failure, ocular manifestations, skin manifestations, respiratory failure, and death (289, 290, 296-298).

There is no evidence that CHIKV can be transmitted across the placenta. However, if the infected mother is viremic during childbirth, CHIKV can be transmitted to the neonate, which can be very serious. Infected neonates experience seizures, brain swelling, cerebral hemorrhages, which is often associated with death of the neonate (291, 299). Infants infected with CHIKV experience fever, excessive crying, bullous lesions, and rash, but severe neurological symptoms are not as common as in neonates (300, 301).

---

#### 1.4.7 MOUSE MODELS OF CHIKV

R. W. Ross performed the first mouse and NHP experiments with CHIKV during the Newala epidemic in the 1950s (143). He found that Albino Swiss mice died following intracerebral inoculation with sera from patients experiencing febrile illness. He also found that the newborn mice were more susceptible to death compared to adult mice. Similar trends have been documented in the current literature on CHIKV mouse models. Neonatal mice, when inoculated with CHIKV intradermally in the ventral thorax, will die in an age-dependent manner. Infection of 6-day old mice results in 100% lethality, while infection of 12-day old mice results in 0% lethality (302).

The classic model for CHIKV infection is the immunocompetent C57BL/6 mouse. Subcutaneous (s.c.) inoculation of CHIKV into the footpad results in foot and ankle swelling and edema (in the ipsilateral foot), transient viremia, and infectious virus recoverable in ankle, muscle, lymph nodes, liver, and spleen tissue 1-7 dpi (147, 148). Very low levels of CHIKV RNA are detectable in the brain and spinal cord at 3 dpi (303). Persistent CHIKV RNA is detectable by qRT-PCR for up to 16 weeks following infection in both ipsilateral and contralateral ankles (303). Histological examination of ankle joints at 7 dpi shows massive infiltration of leukocytes.

These cells were identified as natural killer cells, neutrophils, CD4+ and CD8+ T cells, and macrophages (148). There is histological evidence that mice develop arthritis and tenosynovitis in the ankle, as well as necrotic myositis in the gastrocnemius and quadriceps muscle tissues (148).

In addition to the C57BL/6 model, there are also immunocompromised mouse models for CHIKV infection. CHIKV is lethal in *Ifnar*<sup>-/-</sup> mice (mice lacking the type I IFN receptor). Infection of these mice is typically lethal within 3-5 dpi (302). Infected *Ifnar*<sup>-/-</sup> mice have detectable levels of virus in the brain, mainly present in the meninges and choroid plexus. Other studies have shown that additional modulators of type I IFN signaling are important for viral replication *in vivo*. Mice lacking two key transcription factors for interferon induction (IRF3 and IRF7) also succumb to lethal infection (304). These studies show the importance of the type I IFN response in controlling acute CHIKV replication and limiting disease.

CHIKV infection of mice lacking components of the adaptive immune system indicates an important role for antibodies and T cells in CHIKV pathogenesis. For example, mice lacking B cells developed persistent viremia following CHIKV infection. In these mice, infectious virus can be isolated from the serum for the lifetime of the animal (303, 305). Mice lacking either CD4+ or CD8+ T cells had no change in viral load in the blood, and levels of virus in the ankles were identical to controls (306). However, the CD4+ T cells appear to contribute to the footpad swelling phenotype because the CD4<sup>-/-</sup> mice had reduced footpad swelling, especially at 4-8 dpi. CD4<sup>-/-</sup> mice also had reduced tissue damage, which suggests that CD4+ T cells contribute to the joint pathology in wild type mice (306). In contrast, CD8<sup>-/-</sup> mice had no differences in joint swelling or joint pathology compared to wild type mice. See **Table 1-3** for a list of mouse models commonly used for understanding various aspects of CHIKV infection and disease.

**Table 1-3: Commonly used mouse models for CHIKV infection and their phenotypes**

<b>Mouse Strain</b>	<b>CHIKV infection phenotype</b>	<b>Viral distribution</b>	<b>Model Importance</b>	<b>Reference</b>
C57BL/6, footpad infection	Not lethal, footpad swelling in ipsilateral foot, viremia, evidence of arthritis and tenosynovitis, persistent RNA in ankles detectable for weeks coinciding with chronic synovitis	Ankles, muscle, spleen; viral detection in liver, brain, spleen, spinal cord, and blood is transient	Vaccine and therapeutic testing, modeling arthritis, modeling chronic synovitis, testing antiviral drugs	(147, 148, 303)
Suckling or neonatal mice	Lethal within 6-12 days depending on strain, dose and route of infection; mice develop hind limb dragging, flaccid paralysis, hair loss	Virus present in blood, muscle, brain	Testing attenuation of live-attenuated vaccines, modeling acute CHIKV disease, modeling immature immunity	(143, 302, 307)
<i>Ifnar</i> <sup>-/-</sup> , lack type I IFN receptor	Lethal within 3-5 days, develop muscle weakness, become lethargic	Blood, liver, spleen, stomach, muscle, joint, skin, brain (meninges)	Understanding innate immunity during acute infection, testing attenuation of live-attenuated vaccines, anti-CHIKV antibody testing, modeling acute CHIKV disease, testing antiviral drugs	(302)
CD4 <sup>-/-</sup> , lack CD4 <sup>+</sup> T cells	Not lethal, little footpad swelling, RNA persistence in ankle	Ankles, muscle, spleen; viral detection in liver, brain, spleen, spinal cord, and blood is transient	Modeling factors driving CHIKV-induced arthritis, modeling adaptive immunity during CHIKV infection	(306)
CD8 <sup>-/-</sup> , lack CD8 <sup>+</sup> T cells	Not lethal, resembles C57BL/6 immunocompetent mice	Ankles, muscle, spleen; viral detection in liver, brain, spleen, spinal cord, and blood is transient	Modeling the adaptive immune response following infection	(306)
$\mu$ MT, lack B cells	Not lethal, footpad swelling in ipsilateral foot, persistent viremia, persistent virus in tissues	Persistent virus in blood, ankles, muscles	Modeling viral persistence, understanding B cells during CHIKV infection	(305, 308)
Rag1 <sup>-/-</sup> , lack T and B cells,	Not lethal, persistent viremia, persistent virus in tissues	Persistent infectious virus in blood, ankles, muscles for lifetime of mouse; levels in brain, liver, spleen are transient	Modeling viral persistence, understanding adaptive immunity during CHIKV infection	(303, 308)
Aged C57BL/6 mice (18-20 months old)	Not lethal, increased footpad swelling compared to 12-week old mice	Higher levels of CHIKV in tissues, CHIKV persistence is longer	Understanding the impact of aging on CHIKV infection and disease	(309)

---

#### 1.4.8 NONHUMAN PRIMATE MODELS OF CHIKV

While mouse models for CHIKV are beneficial for discerning immune mechanisms that control viral replication and disease, the NHP model more accurately recapitulates CHIKV disease in humans. NHPs have been used for modeling acute CHIKV disease, CHIKV persistence, and for preclinical testing of vaccines and therapeutics (310).

Acute disease in humans involves development of viremia, rash, fever, and arthritis. Similarly, rhesus macaques (*Macaca mulatta*), after a subcutaneous injection of CHIKV, develop transient viremia, rash on the chest and arms, fever, and joint swelling on the wrists and fingers that is warm to the touch (311-313). During the first few days of the disease, high levels of infectious virus are detectable in the blood. There is also a strong inflammatory response to infection, involving induction of inflammatory cytokines and chemokines in the blood as well as activated monocytes/macrophages, dendritic cells, and natural killer cells (311). By 7 dpi, viral RNA is detectable in joints and muscles of legs and arms, various draining lymph nodes, spleen, heart, and kidney (314). In addition, there is extensive cellular infiltration into the joints detectable at 7 dpi (311). Rhesus macaques develop B and T cell responses to CHIKV, and ultimately clear virus in most tissues (149, 315). While rhesus macaques represent a very accurate acute infection model, viral persistence, measured by vRNA detection, is limited to the spleen at late time points in aged rhesus macaques (> 17 yrs old) (149). A study performed with pregnant rhesus macaques showed that CHIKV was unable to infect the placenta or the fetus, which correlates with reports describing human CHIKV infections during pregnancy (312, 316); however, it may be worthwhile to study CHIKV infection of the pregnant mother and fetus during the intrapartum stage of pregnancy.

Cynomolgus macaques (*Macaca fascicularis*) have been used as a model for studying acute and persistent CHIKV disease. Similar to rhesus macaques, cynomolgus macaques develop viremia, fever, rash, and joint swelling following CHIKV infection during the acute stage

of disease (150). There is also evidence that CHIKV can replicate persistently in cynomolgus macaques, with infectious virus recovered from spleen, liver, and muscle at 44 dpi (150). Both rhesus and cynomolgus models closely mimic many aspects of acute and persistent CHIKV disease in humans, which makes them tractable models for testing vaccines, therapeutics, and learning about CHIKV pathogenesis.

## 1.5 CHIKV IMMUNITY

### 1.5.1 INNATE IMMUNITY TO CHIKV

During replication, CHIKV produces pathogen associated molecular patterns (PAMPs) recognized by host pattern recognition receptors (PRRs), which induce signal transduction pathways that lead to the production of type I interferon (IFN). Binding of type I IFN to the IFN- $\alpha\beta$  receptor and signaling through the JAK-STAT pathway results in the expression of hundreds of IFN-stimulated genes (ISGs) that promote a cellular antiviral state. The innate immune response to CHIKV is critical for controlling viral replication in mouse models (302, 317). Mice lacking the IFN- $\alpha\beta$  receptor (*Ifnar*<sup>-/-</sup> mice) or STAT1 (*Stat1*<sup>-/-</sup>) succumb to infection within 3-5 days (302). Mice lacking interferon signaling have higher viral titers in blood and tissues and viral infection in the CNS. In humans and animal models, CHIKV induces IFN during infection that is detectable in the plasma, and the production of IFN is very important for controlling viral replication (317). CHIKV is still able to replicate and spread, despite a strong interferon response, probably due to its ability to shutoff host transcription and translation during infection.

During CHIKV replication, the viral RNA genome and replication intermediates trigger cytoplasmic and endosomal PRRs, which induce expression of type I IFNs and cytokines and chemokines (318). The relevant cytoplasmic PRRs include: retinoic acid inducible gene I (RIG-I) and melanoma differentiation-associated gene 5 (MDA5). The relevant endosomal PRRs include: Toll-like receptor 3 (TLR3) and TLR7 that recognize the viral RNA genome (319).

These PRRs engage signaling pathways that culminate in IRF3 translocation to the nucleus to activate transcription of type I IFN. Mice lacking the cytoplasmic PRRs RIG-I and MDA5 do not have strong phenotypic differences in viral loads, tissue distribution, or pathogenesis compared to wild type mice (317). Similarly, mice lacking the downstream signaling adaptor of RIG-I and MDA5, CARD adaptor inducing IFN $\beta$  (Cardif), had higher levels of virus in the blood, but overall had a more mild phenotype when compared to *Ifnar*<sup>-/-</sup> mice (317). This suggests that signaling via other PRRs (such as PKR and the TLRs) may act in combination with RIG-I and MDA5 to mount an effective innate immune response to CHIKV. Similarly, mice lacking the TLR adaptor molecule MyD88 had increased viral loads in blood and tissues relative to wild type control mice (317); however, these mice also did not recapitulate the pathogenic phenotype observed in *Ifnar*<sup>-/-</sup> mice. In addition, mice lacking TLR3 or its adaptor TIR domain-containing adaptor-inducing interferon- $\beta$  (TRIF) did not succumb to infection but had increased tissue viral titers compared to controls (319). Together these findings suggest that signaling by these three (and possibly additional) PRR pathways mediate an effective interferon response: 1) MAVS (via RIG-I and MDA5), 2) MyD88 (via TLRs and IL-1R), and 3) TRIF (via TLR3).

Dendritic cells (DCs) are an important player in the immune response and IFN-producing cell type that are involved in many arbovirus infections including alphaviruses (320-322). Skin resident DCs are one of the initial cell types infected, and these cells can direct the rest of the innate immune response. Immature DCs are permissible to infection with many types of alphaviruses (322-324). However, CHIKV stands out among the alphaviruses in that it does *not* infect DCs (human, mouse, and NHP DCs), nor does it induce IFN production from DCs (150, 317, 325). Using bone marrow chimeras, it was shown that wild type mice were protected from lethal CHIKV infection, even if reconstituted with *Ifnar*<sup>-/-</sup> bone marrow (317). This suggests that the control of viral replication by interferon is largely dependent on the response from the non-

hematopoietic cells. This protective IFN response may be produced predominantly by fibroblasts, which are readily infected *in vivo* and *in vitro* (228, 317).

Unlike DCs, macrophages are an important target for CHIKV replication. Macrophages infiltrate infected tissues in mouse, NHP, and human patient samples (110, 148, 150). Monocyte chemoattractant protein-1 (MCP-1) is a potent chemokine that is found in the blood during the early viremic phase that is believed to be associated with recruitment of macrophages to the site of infection. Treatment of CHIKV infected mice with an MCP-1 inhibitor, bindarit, reduced joint inflammation (119). However, mice lacking the MCP-1 receptor, CCR2, had increased neutrophil recruitment to the joints, with more severe arthritic disease and cartilage damage (326). The group that performed the CCR2 mouse studies showed that reduced monocyte/macrophage recruitment to the joints was associated with a more destructive neutrophil infiltration and damage to the joint in these animals. Depletion of macrophages by clodronate liposomes in mice resulted in decreased footpad swelling relative to the controls, but these animals also experienced higher levels of virus in the blood (147). It has been proposed that the infiltrating macrophages in CHIKV and RRV-infected joints and muscle tissues are M2 subtype macrophages, which are associated with a wound-healing anti-inflammatory response and express Arginase 1. Specific deletion of Arginase 1 in macrophages and neutrophils in mice resulted in decreased viral load after RRV infection (327). These studies suggest that macrophages work to control virus replication and control recruitment of neutrophils, but that they also infiltrate the joint and cause inflammation and contribute to arthritis. During the chronic arthritic phase of CHIKV infection, macrophages are implicated as a reservoir for persistent viral replication because macrophages stained positive for CHIKV antigen from patient and NHP samples obtained during this late phase of disease (110, 150). These studies provide evidence that macrophages play a complex role during viral replication, and more studies will be needed

to clarify the precise functions these cells have during acute and persistent phases of CHIKV disease.

Natural killer (NK) cells are another tissue infiltrating cell type that became activated in the blood during CHIKV infection in both mouse and NHP models (148, 311). Similarly, CHIKV-infected patients have activated NK cells in their blood during the acute phase of disease (110), and patients with higher viral loads had increased percentages of circulating NK cells compared to patients with lower viral loads (328). Depletion of NK cells in mice using anti-asialo antibody prior to CHIKV infection resulted in decreased footpad swelling (329). These studies are consistent with the theory that NK cells are mobilized in response to CHIKV infection and that they partially mediate joint inflammation during the acute phase of the disease.

CHIKV infection is associated with a robust inflammatory response during the acute phase. In mouse models, cytokine and chemokine levels of  $\text{TNF}\alpha$ , MCP-1,  $\text{IFN}\gamma$ , IL-6, and  $\text{IFN}\alpha/\beta$  peak at 2 dpi, correlating with the peak of viremia (147). Similarly, NHPs infected with CHIKV had inflammatory cytokines and chemokines in the blood, with levels peaking at 2 dpi (IL-1 $\beta$ , G-CSF, IL-6, Eotaxin, MIP-1 $\alpha$ , MCP-1, HGF,  $\text{IFN}\gamma$ , I-TAC, IL-1RA, MIF, IP-10, and MIG) (150, 311). In CHIKV patients, certain cytokines tend to correlate with higher viral burdens such as MCP-1,  $\text{IFN}\alpha$ , IL-15, IP-10, IL-12, and IL-6 (328). Many of these cytokines and chemokines promote macrophage recruitment to the infected tissues as well as their differentiation and activation.

---

### 1.5.2 ANTI-CHIKV ANTIBODIES

The adaptive immune response, comprised of both humoral and cellular responses, is very important for alphaviral control and clearance from the blood and tissues. The most compelling evidence that both of these responses are critical for control of virus is derived from experiments wherein mice lacking B and T cells (Rag1 $^{-/-}$  or Rag2 $^{-/-}$ ) infected with CHIKV

develop chronic viremia and high levels of viral replication in joint and tissues (303, 306). Passive transfer of CHIKV neutralizing antibodies to Rag1<sup>-/-</sup> mice prior to challenge is protective, and these mice will not develop chronic viremia or detectable tissue viral loads. However, Rag1<sup>-/-</sup> mice given antiviral antibodies in a therapeutic context control serum viremia but this treatment has little effect on reducing tissue viral burden (303). This suggests that neutralizing antibodies can provide an important level of control of viral infection and are responsible for clearing virus in the blood, but they have limited efficacy in clearing CHIKV in the tissues once infection is established. This finding argues that prophylactic vaccination and/or passive immunotherapeutic treatments designed to create robust antibody responses may be able to protect against initial challenge but unable to clear persistent infections that are associated with chronic disease. Similarly,  $\mu$ MT mice, which have functional T cells responses but lack mature B cells and antibody responses, develop chronic serum viremia after CHIKV infection (305, 308). However, these mice have an approximately 2-log decrease in their serum viremia relative to Rag1<sup>-/-</sup> mice, suggesting that T cells may also promote viral clearance in the absence of antibodies (308). Thus, both humoral and cellular immunity against CHIKV appears to be required for proper control of viral replication to reduce viral loads and chronic disease.

B cells are antibody-producing cells derived from the bone marrow, and they make up the humoral arm of adaptive immunity. Antiviral antibodies can block infection by neutralizing virus directly, recognizing infected cells, activating complement, and opsonizing virus. Analysis of serum in mice, NHP, and humans infected with CHIKV shows that IgM antibodies predominate the early antiviral antibody response, which then matures into IgG antibodies within 2-3 weeks post infection (305, 315, 330). B cell epitopes have been mapped in mice, NHPs, and humans in order to identify the CHIKV antigens that are recognized by B cells during CHIKV infection (305, 315, 331). In most cases, the B cell response was primarily directed against the CHIKV receptor-binding protein E2. One epitope that mapped to the N-terminus of E2, called

E2EP3, is a major epitope recognized in most species including mice, NHPs, and humans (305). In general, antibodies that neutralize CHIKV recognize the exposed outward-facing region of the E1/E2 dimer. Antibodies directed against the fusion loop and the inner face of the E1/E2 dimer are typically not neutralizing (332). Some antibodies that neutralize CHIKV may also cross-neutralize other closely related alphaviruses. One study identified a panel of mouse and human monoclonal antibodies that cross-neutralized several alphaviruses by binding domain B of E2 (142). This suggests that a vaccine that induces neutralizing antibody responses against the B domain of E2 could potentially protect against multiple alphaviruses.

Importantly, anti-CHIKV neutralizing antibodies can prevent CHIKV acquisition. Passive transfer of anti-CHIKV neutralizing monoclonal antibodies protects susceptible *Ifnar*<sup>-/-</sup> mice from lethal CHIKV challenge (333, 334). Passive transfer of neutralizing antibodies can also be effective as a therapeutic; administration of neutralizing antibodies up to 60 hours post CHIKV infection could protect a majority of the *Ifnar*<sup>-/-</sup> mice. Similarly, neutralizing antibody therapy has been shown to be effective against CHIKV in NHPs when administered at 1 dpi (311, 314). Because antibodies play a protective role during CHIKV infection, the most effective vaccines will elicit strong neutralizing antibody responses to protect individuals from CHIKV acquisition. Natural infection with CHIKV is believed to confer sterilizing immunity due to the presence of long-lasting neutralizing antibodies (335, 336).

---

### 1.5.3 ANTI-CHIKV T CELLS

T cells mature in the thymus, and they make up the cellular arm of adaptive immunity. There are two types of T cells: CD4<sup>+</sup> and CD8<sup>+</sup> T cells. CD8<sup>+</sup> T cells can directly kill infected cells, while CD4<sup>+</sup> T cells provide costimulation to B and T cells during infection. CHIKV infection in humans is associated with the activation of CD4<sup>+</sup> T cells and CD8<sup>+</sup> T cells during the first few days of symptom onset (337). CHIKV-specific IFN $\gamma$ -producing T cells are detectable in

peripheral blood from patients infected with CHIKV (338). These CHIKV-specific T cells develop during the acute phase, but they may become chronically activated during the persistent/chronic phase of CHIKV disease. Patients experiencing the chronic phase tend to have higher levels of circulating NK cells and activated CD8<sup>+</sup> T cells compared to healthy patients, although the significance of this is unclear (339). NHPs and mice infected with CHIKV also develop CHIKV-specific T cells (148, 149, 306). CD4<sup>+</sup> and CD8<sup>+</sup> T cells have been isolated from infected mouse joints, and they are capable of producing IFN $\gamma$  in response to CHIKV whole virus particles (306).

While the protective role for anti-CHIKV antibodies in NHPs and mice and promotion of viral clearance from the blood are well defined, there is little evidence for protective effects of T cells. Mice that lack CD8<sup>+</sup> T cells have no known phenotypic differences in joint swelling, joint inflammatory infiltration, or viral burden compared to wild type controls (306). In contrast, CD4<sup>+</sup> T cells have been implicated in promoting severe joint disease and arthritis in the mouse model. The evidence for this is that CD4<sup>-/-</sup> mice are protected from some of the joint pathology observed in C57BL/6 mice. CD4<sup>-/-</sup> mice had equal levels of virus in their blood and ankles compared to controls (306). These findings suggest that CD4<sup>+</sup> T cells play no role in controlling viral burden and that they enhance joint inflammation. Consistent with this hypothesis, Teo et al. performed adoptive transfers of CHIKV-specific CD4<sup>+</sup> T cells from CHIKV-infected mice into mice lacking the T cell receptor (TCR<sup>-/-</sup>), and the recipients were infected with CHIKV. TCR<sup>-/-</sup> mice that received CHIKV<sup>+</sup> CD4<sup>+</sup> T cells had increased edema, synovitis, and inflammation in the muscle tissue relative to TCR<sup>-/-</sup> mice receiving naïve CD4<sup>+</sup> T cells after CHIKV infection (340).

Recent reports suggest that blocking CD4<sup>+</sup> T cell activation or preventing their ability to traffic to infected tissues could alleviate joint inflammation. One study showed that expansion of regulatory T cells, using an IL-2/anti-IL-2 antibody complex, successfully blocked CHIKV-

specific CD4<sup>+</sup> T cell recruitment to the infected footpad (341). This treatment had no effect on viral load in the ankle, but the treatment greatly diminished CHIKV footpad swelling and inflammation. Another group showed that treatment of CHIKV-infected mice with an inhibitor of T cell trafficking from the lymph node, fingolimod, resulted in diminished footpad swelling relative to controls (340). Fingolimod binds to the sphingosine-1-phosphate receptor on T cells and prevents them from leaving the lymph node. Use of this drug has many unwanted side effects such as herpesvirus reactivation (342), which may prohibit its wide usage in CHIKV-infected patients. Miner et al. showed that treatment of mice with CTLA4-Ig, an inhibitor of T cell co-stimulation, at 3 dpi resulted in a slight decrease in peak footpad swelling, but there were no differences in viral loads in the joints at 7 dpi and at 28 dpi relative to vehicle-treated controls (122). Collectively, these results show that inhibition of CD4<sup>+</sup> T cell trafficking or T cell activation reduces joint inflammation, but these treatments had no effect on tissue viral burden.

Most of the evidence points to the idea that T cells have a pathogenic role (CD4<sup>+</sup> T cells) or a neutral role (CD8<sup>+</sup> T cells) during CHIKV infection in mice. Importantly, the results from another study showed that T cells may have a protective role but this was teased out in the absence of B cells and antibody responses. As stated previously,  $\mu$ MT mice develop persistent viremia following CHIKV infection, but these mice have a lower persistent serum viremia compared to Rag1<sup>-/-</sup> mice (308). When these mice were vaccinated with inactivated whole virus and challenged with CHIKV, they had a 1 to 1.5 log reduction in serum viremia during the first 6 days compared to control-vaccinated groups. Interestingly, the vaccinated mice had increased footpad swelling during the first 4 days of CHIKV infection compared to control vaccinated mice (308). This group did not deplete T cells or perform T-cell adoptive transfer experiments to ensure that T cells were responsible for the reduction in serum viremia elicited by the vaccine. However, the study provided some evidence that T cells could be antiviral in the absence of B cells, despite the enhanced footpad swelling.

Similarly, T cells have been shown to be protective in the context of infection with other alphaviruses. One study provided evidence that CD8<sup>+</sup> T cells may be responsible for clearing RRV in the musculoskeletal tissues (343). RRV causes similar joint and musculoskeletal disease in mice as CHIKV and infection in the footpad results in detectable viral levels in the muscle and ankle tissue. Infection of CD8 $\alpha$ <sup>-/-</sup> mice resulted in equal levels of virus in the quadriceps and ankle that was detectable at 7 dpi, but the viral levels in the quadriceps were increased by about 1 log in CD8 $\alpha$ <sup>-/-</sup> mice at 14 and 21 dpi compared to wild type controls. Depletion of CD8 $\alpha$ <sup>+</sup> T cells in wild type mice at 7 and 12 dpi resulted in increased levels of RRV in the quadriceps at 14 dpi while there was no difference in RRV levels in the ankle in these mice. As further proof that CD8<sup>+</sup> T cells could protect mice from RRV, T cells from wild type mice or CD8<sup>+</sup> T cells alone from wild type mice were adoptively transferred into Rag1<sup>-/-</sup> mice. Compared to the media controls, Rag1<sup>-/-</sup> mice receiving the T cells had a 1 log reduction in RRV in the quadriceps, and a slight decrease in serum viremia, while the ankles were still unaffected by the treatment. Though the T cells provided some protection in Rag1<sup>-/-</sup> mice against RRV challenge, CD8<sup>+</sup> T cells alone had no effect. This suggests that CD4<sup>+</sup> T cell help may be required for protection from RRV in the muscle tissue.

In addition to RRV, protective roles of T cells have been shown in the context of SINV and VEEV mouse models. In the case of SINV, T cells were shown to be important mediators of viral clearance in the brain and spinal cord (344). Rag1<sup>-/-</sup> mice develop a persistent infection in the brain and spinal cord with SINV, but after adoptive transfer of SINV-specific T cells, the virus was cleared in the spinal cord, and SINV levels were reduced by 1.5 logs in the brain. Testing of a live-attenuated vaccine for VEEV showed that CD4<sup>+</sup> T cells were an important mediator of protection elicited by the vaccine (345). This was demonstrated by adoptively transferring CD4<sup>+</sup> T cells from vaccinated mice into mice lacking T cells, and the recipient mice were protected from lethal VEEV challenge compared to controls. Together, these data show that B cells and

antibodies are important mediators of protection, but that T cells may also mediate protection from alphavirus infection, although the protection is subtle compared to the effects of antibodies. Data will be presented in Chapter 4 that further explores the role of T cells in CHIKV infection and defines the protective effects of a T-cell specific vaccine in mice.

## 1.6 CHIKV VACCINES AND THERAPEUTICS

### 1.6.1 CURRENT TREATMENT OPTIONS FOR CHIKV PATIENTS

No vaccines or anti-viral therapeutics are currently approved for preventing or treating CHIKV infection. Thus, the current standard of care for CHIKV patients is to treat Chikungunya disease with non-steroidal anti-inflammatory drugs (NSAIDs).

Many anti-rheumatic drugs were developed for the treatment of rheumatoid arthritis, and some of these have been proposed as possible therapies to treat chronic CHIKV-induced arthritis. DMARDs or disease-modifying anti-rheumatic drugs that prevent damage to the joint by controlling joint inflammation (346). DMARDs can be immunosuppressive, which should be considered with caution when trying to use it to treat disease caused by a viral infection since they may interfere with natural immunity against the pathogen. Importantly, most patients with chronic CHIKV-induced arthritis are negative for RF or anti-CCP, and thus do not meet the criteria for RA (339). A small trial with the anti-rheumatic drug chloroquine was performed in 70 patients that had chronic joint pain after CHIKV infection (121). The trial found that patients treated with chloroquine had no improvements over meloxicam, an NSAID. Another DMARD, methotrexate, was originally developed as a cancer drug by preventing thymidine and purine synthesis and thus blocks cell cycle progression (347). However, the anti-rheumatic mechanisms of methotrexate are unknown. There has been some efficacy reported with methotrexate treatments in CHIKV-infected patients, with one study reporting 75% of patients having improvements after methotrexate therapy (348). One methotrexate and chloroquine

combination study showed that 50% of patients had improvements in the disease score after 16 weeks. A triple combination therapy of chloroquine, methotrexate, and sulfasalazine showed improvement in disease score after 24 weeks compared to chloroquine alone (120). These studies show that there might be limited efficacy with these drugs, but none of these groups include placebo controls. In addition, many people recover from CHIKV-induced arthritic pain over time, so it is difficult to assess if the recovery occurs as an effect of the treatment or natural recovery. Further studies are required to assess the role of current anti-inflammatory agents and for the development of new therapeutic approaches to treat Chikungunya arthritic disease.

---

### 1.6.2 VACCINES IN DEVELOPMENT FOR CHIKV

Typically, vaccines against viruses fall into one of the following categories: live-attenuated, inactivated, DNA, virus-like particles (VLPs), subunit, and viral-vectored. Live-attenuated vaccines (LAV) are generated by passaging the virus in tissue culture, which causes genetic mutations that can increase infectivity in cultured cells but decrease viral fitness *in vivo*. LAVs, because they infect their host, promote immunity that would be generated following natural infection. LAV-induced immune efficacy is usually long lasting (349). Whole inactivated vaccines are created by treating virus preparations with chemical modifiers that prevent the virus from infecting cells. While these virus preparations elicit antibody responses the inactivated viruses do not infect cells, which can reduce their ability to induce potent T cell responses and immune responses tend to be short lived. Virus like particles are similar to inactivated vaccines and share many of the same properties but are not chemically modified, which reduces the level of tertiary epitope destruction promoting neutralizing antibody responses. VLPs tend to elicit short-lived protection and are dramatically enhanced with adjuvants to stimulate the immune response during vaccination. DNA vaccines incorporate viral gene antigens into plasmid constructs for delivery. This type of vaccine platform tends to have a lower safety concern, but they typically require multiple immunizations to achieve protective

immunity, and the duration of protective immunity may be shorter than other vaccine platforms. The last category of vaccines currently used in humans are subunit vaccines, which are usually derived from an antigenically active portion of the viral proteome. Subunit vaccines require adjuvants to enhance immunogenicity and to increase longevity of the response. **Table 1-4** contains a list of the vaccine platforms and adjuvants that are currently under investigation for use against CHIKV.

The first vaccine developed against CHIKV was a live-attenuated strain of the Asian isolate AF15561, which was generated by passaging the virus 18 times in human fibroblasts (MRC-5 cells) (173). This vaccine, called 181-25, induced protective neutralizing antibodies to CHIKV in mice and NHPs, but the vaccine was halted in Phase II clinical trials because approximately 8% of patients experienced arthritic pain after vaccination (350). Additional unique live-attenuated vaccines for CHIKV were attenuated *in vivo* compared to the wild type virus, but most of them were not tested in susceptible *Ifnar*<sup>-/-</sup> or neonatal mice (351, 352). This is an important test to determine the degree of attenuation relative to the standard live-attenuated vaccine 181-25, and it may predict whether certain immunocompromised groups will be susceptible to disease after vaccination. The CHIKV/IRES vaccine, which incorporates the encephalomyocarditis virus internal ribosome entry site in place of the native CHIKV subgenomic 5'UTR, was shown to be more attenuated in neonatal and A129 mice in comparison to 181-25 (353). It also protected cynomolgus macaques from CHIKV challenge, demonstrating that the CHIKV/IRES vaccine is a realistic candidate (354).

One CHIKV plasmid DNA study involved the insertion of E1, E2, and E3 into a plasmid and that was used to vaccinate mice and NHPs (355). One downside to using DNA vaccines is that they require multiple immunizations, with three immunizations performed in mice and five immunizations reported in NHPs to achieve significant antibody and T cell responses. To show vaccine efficacy, they performed a stringent i.n. challenge with 10<sup>7</sup> PFU CHIKV, which is lethal

in BALB/c mice, and the vaccinated mice did not succumb to CHIKV challenge, but they still had detectable virus in their blood. The researchers showed that the vaccine induced anti-CHIKV antibodies and T cell responses in NHPs, but they did not show if the immunogenicity correlated with protection against CHIKV challenge. Another group had a novel approach to vaccinate mice with a plasmid that had the cDNA sequence of the live-attenuated CHIKV strain (356). Vaccination with this plasmid resulted in higher neutralizing titers compared to the live attenuated vaccine and demonstrates the advantages of combining and/or merging various vaccine platforms to achieve increased efficacy.

Virus-like particle (VLP) vaccines for CHIKV required multiple immunizations in mice even when administered with a vaccine adjuvant (357). The CHIKV VLP vaccine elicited higher neutralizing antibody titers compared to the DNA vaccine equivalent, and it was effective in blocking the induction of viremia in rhesus macaques and mice. In addition, it protected *Ifnar*<sup>-/-</sup> mice from lethal challenge. Despite requiring multiple vaccinations and an adjuvant, the VLP seems like a safe alternative to the live-attenuated vaccines.

Compared to other vaccine options, viral-vectored vaccines can elicit very strong antibody and T cell responses. Alphavirus chimeric genome vaccines contain the nonstructural genes of either EEEV, SINV, or VEEV along with the CHIKV structural genes in place of the native structural genes. These chimeric viruses could replicate in cell cultures. As vaccines, these chimeras were highly attenuated in neonatal mice, and they elicited very strong neutralizing antibody titers by 3 weeks post infection (358). The chimeric viruses did not require multiple immunizations or adjuvants to elicit protective immunity. Similarly, the Eilat-vectored CHIKV vaccine is an alphavirus chimera platform. Eilat virus is unique in that it is naturally replication-defective in mammalian cells, but it grows efficiently in insect cells. A recombinant EILV expressing the CHIKV structural genes in place of the EILV structural genes is completely attenuated in A129 mice (359). In addition, the EILV vaccine protected A129 mice and

cynomolgus macaques from CHIKV challenge. In general, this particular vaccine appears to be both highly immunogenic and highly attenuated in mice, and it represents an ideal vaccine candidate.

Recombinant replication-defective vaccines have also shown efficacy against CHIKV. A replication-defective adenovirus expressing the CHIKV structural gene was highly immunogenic in mice after one vaccination, and the vaccination protected mice from CHIKV challenge, even 6.5 weeks post vaccination (360). Several modified vaccinia virus ankara (MVA) vectored vaccines were developed for CHIKV by inserting the structural genes or just the E3 and E2 genes into the MVA backbone. One group that described the MVA-E3E2 vaccine provided evidence that CD4+ T cells, rather than antibodies, were providing protection mediated by the vaccine because depletion of CD4+ T cells resulted in lethality following CHIKV challenge (361). Mice vaccinated with MVA-E3E2 showed very little neutralizing antibody responses and passive transfer of vaccinated mouse serum did not protect naïve mice from CHIKV challenge. Although this is suggestive that the vaccine-mediated protection was not via neutralizing antibodies, the CD4+ T cells may be providing costimulation to the B cells to mount a more effective antibody response against CHIKV during challenge. Therefore, the group could test their vaccine in  $\mu$ MT mice (lacking B cells) to clarify if this is the case.

**Table 1-4: CHIKV vaccines: design, immunogenicity, and animal testing.**

Vaccine type		Vaccine design	Immunity demonstrated	Testing in mice, NHPs, and/or humans	References
Live-attenuated	CHIKV 181-25	Passage isolate AF15561 plaque-to-plaque in MRC-5 cells, look for small plaque phenotype	Neutralizing antibodies	Mice, NHPs, humans (phase II)	(173, 350)
	CHIKV/IRES	ECMV IRES inserted in place of the subgenomic promoter	Neutralizing antibodies	Mice, NHPs	(353, 354)

Vaccine type		Vaccine design	Immunity demonstrated	Testing in mice, NHPs, and/or humans	References
	Transmembrane mutants	Transmembrane domain	Neutralizing antibodies	Mice	(352)
	Heparan sulfate-adapted	CHIKV La Reunion (LR) strain with mutation of E2 at E79K	Neutralizing antibodies	Mice	(362)
	6K-deleted	CHIKV LR with 6K deleted	Neutralizing antibodies, T cells	Mice	(351)
	Nsp3 hypervariable domain-deleted	CHIKV LR with deletion in nsp3 hypervariable domain	Neutralizing antibodies, T cells	Mice, NHPs	(351, 363)
Inactivated	Formalin-killed Thailand isolate	Inactivate live virus (isolate from a patient in Thailand) with formalin	Neutralizing antibodies	Mice, NHPs (safety testing), humans	(364)
	Binary ethyleneimine-inactivated	Inactivated Asian isolate	Neutralizing antibodies, antibodies boosted with adjuvant	Mice	(147)
	UV-inactivated	Virus was treated with UV irradiation for 5 minutes.	Antibodies	NHPs, no challenge data	(365)
	Betapropiolactone (BPL)-inactivated	Virus was inactivated with BPL	Neutralizing antibodies	Mice	(366)
DNA	Plasmid	Plasmids encoding E1, E2, or capsid	Antibodies, T cells	Mice, no challenge data	(367)
	Plasmid	One plasmid encoding E3, E2, and E1	Neutralizing antibodies, T cells	Mice, challenged i.n., NHPs	(355)
	iDNA	One plasmid, encoding the entire infectious clone for CHIKV 181-25	Neutralizing antibodies	Mice, challenged i.n.	(356)
VLP	VLP from expression plasmid	Cloned the structural genes into an expression vector and isolated VLPs from the supernatants	Neutralizing antibodies	Mice, NHPs, humans	(357, 368)
	VLP from baculovirus expression system	A recombinant baculovirus expressed the CHIKV structural gene in insect cells,	Neutralizing antibodies	Mice	(369, 370)

Vaccine type		Vaccine design	Immunity demonstrated	Testing in mice, NHPs, and/or humans	References
		VLPs were purified from supernatants			
Subunit	Recombinant E1 protein	Recombinant E1 protein was vaccinated with different adjuvant combinations	Neutralizing antibodies	Mice	(371)
	Recombinant E2 protein	Recombinant E2 protein was vaccinated alone or with different adjuvant combinations	Neutralizing antibodies	Mice	(366)
Viral Vectors	EILV vector	EILV backbone with the CHIKV structural genes	Neutralizing antibodies	Mice	(359)
	Modified vaccinia virus Ankara (MVA) vector	1) MVA expressing the CHIKV structural genes, 2) MVA expressing E3-E2	1) Neutralizing antibodies, T cells 2) antibodies, CD4+ T cells	1) Mice, NHPs 2) mice	(361, 363, 372, 373)
	Replication-defective adenovirus vector	Adenovirus with deletions in E1, E3, and E4 expressed the CHIKV structural genes	Neutralizing antibodies	Mice	(360)
	Vesicular stomatitis virus (VSV) vector	VSV lacking G, expressing the CHIKV envelope genes, the virions have the CHIKV envelope proteins on their surface	Neutralizing antibodies, T cells	Mice	(374)
	Chimeric alphavirus backbones	Chimeric viruses were generated that express the CHIKV structural genes along with nonstructural genes from VEEV, EEEV, or SINV	Neutralizing antibodies	Mice	(358)

### 1.6.3 THERAPIES IN DEVELOPMENT TO TREAT CHIKV INFECTIONS

Some anti-rheumatic DMARD therapies have been tested in the CHIKV mouse model, including naproxen, etanercept, CTLA-4, methotrexate, tofacitinib, and methylprednisolone (122). When these therapies were administered at 3 dpi, only CTLA-4 and tofacitinib treatment resulted in a reduction in footpad swelling, while none of the treatments had any effect on viral

load. As discussed previously, CTLA-4 therapy may act by preventing T cell-mediated inflammation in the infected joints. Tofacitinib blocks JAK signaling at a point downstream of the type I IFN receptor, but interestingly the drug had no effect on viral load. However, it could be risky to pursue an inhibitor of type I IFN signaling for treating disease caused by a virus that has a strong lethal phenotype in *Ifnar*<sup>-/-</sup> mice. Bindarit, which is a CCR2 inhibitor (119), also had the dual advantage of not increasing viral load while reducing joint inflammation, presumably by blocking macrophage recruitment to the infected joint. Fingolimod, an inhibitor of T cell egress from the lymphoid organs, was able to block CHIKV-induced joint swelling without affecting viral load in the joint (340). The main trend with the therapies tested in the mouse model is that the drugs appeared to block T cell or macrophage migration or infiltration into the infected tissue. In addition, these therapies blocked CHIKV-induced inflammation in the footpad, but none of the drugs were inhibitory to CHIKV replication in the joint or muscle tissue. Clearly more testing is needed to find drugs that block CHIKV replication in blood and tissues, and consequently reduce CHIKV-induced inflammation.

The most effective therapeutics undergoing preclinical testing are anti-CHIKV neutralizing antibodies. Passive transfer of antibodies was effective in preventing lethal infection in *Ifnar*<sup>-/-</sup> mice when used up to 60 hpi (375). Similarly, two studies have shown efficacy of antibody therapies in rhesus macaques (311, 314). The most important benefit to neutralizing antibodies as therapeutic treatments is that they are directly antiviral, which effectively reduces CHIKV-induced joint inflammation. In addition, the antiviral immunotherapeutic antibody treatment could be delivered to either reduce viremia in infected patients or to prevent viremia in travelers to CHIKV-endemic regions of the world. The major drawbacks for this type of therapy are that the antibody may not be effective after the viremic phase, and that more testing is needed in NHPs to determine the how long the therapy can be effective against preventing

CHIKV-induced disease. Chapter 3 details our findings with an anti-CHIKV monoclonal antibody that was tested in mice and rhesus macaques.

## 1.7 SIGNALING PATHWAYS INVOLVED IN VIRAL REPLICATION

### 1.7.1 KINASE PATHWAYS AND VIRAL REPLICATION

The human kinome consists of 518 kinases that range in expression and activity (376). Kinases catalyze the biochemical reaction of transferring ATP terminal phosphate groups onto serine, threonine, or tyrosine residues located on the substrate proteins. Kinases play a significant role during viral infection because they can modulate major cellular processes that the virus requires, including: protein synthesis, cytoskeletal rearrangements, stress responses, cell cycle control, metabolism, apoptosis etc. Identifying changes in the cellular kinome after viral infection may reveal important details about the virus-host interactions that are previously unknown. Knowledge about the kinome-virus dynamic allows for the use of kinase inhibitors or kinase specific knockdown/knockout as novel tools to show whether specific cellular pathways are essential for viral replication *in vitro* and *in vivo*.

### 1.7.2 SRC FAMILY KINASE SIGNALING

The Src Family Kinases (SFKs) are an important group of non-receptor tyrosine kinases. The SFK members include the ubiquitously expressed Src, Yes and Fyn. Other members are Blk, Fgr, Hck, Lck, Yrk, and Lyn; and these kinases have a more limited expression profile. SFKs mediate signaling through integrins, receptor tyrosine kinases (RTKs), G-protein-coupled receptors (GPCRs), and signal transducers and activators of transcription (STATs) (377, 378). They facilitate the transfer of a phosphoryl group from ATP to a tyrosine in their protein substrate. The overall structure of SFKs is highly conserved except for the first 50 amino acids at the N-terminal portion of the protein. The N-terminus contains a palmitoylation and/or myristoylation motif that anchors the protein to the membrane and a Src homology 4 domain

(SH4) that is unique to each family member. Centrally located within the protein are the Src homology domains SH2 and SH3 that are involved in docking with other target proteins. For example, SH2 domains mediate interactions with FAK, CAS, paxillin and growth factor receptors; whereas the SH3 domains promote interactions with PI3K and Shc. The kinase domain (SH1) mediates the transfer of the phosphate group to the target protein (379). There are two crucial regulatory tyrosines located in the C-terminal portion of SFKs at residues Y416 and Y527. SFK activation occurs when phosphorylated at Y416, and inactivation occurs when Y527 is phosphorylated and Y416 is dephosphorylated.

Given that SFKs mediate a wide range of signaling pathways, it is not surprising that some viruses have evolved to utilize them for replication and pathogenesis. The first group to be explored were the SFKs encoded by cancer promoting avian retroviruses that include vSrc, vYes and vFgr. Other viruses utilize SFKs by directly binding them via viral proteins and/or modulating SFK expression and signaling during replication (reviewed in (380)). For example, the herpes simplex virus 1 (HSV-1) tegument protein VP11/12 recruits and binds Lck, which phosphorylates VP11/12 and promotes AKT activation in a process required for virus replication (381). Hepatitis C Virus (HCV) protein NS5A co-immunoprecipitated with several SFK family members and reduced or enhanced their kinase activities (382). Human Immunodeficiency virus (HIV) protein Nef was shown to bind Lck and reduces its enzymatic activity (383). Clearly SFKs are commonly utilized during virus replication.

Dasatinib is a Src family kinase inhibitor that was generated as a backup treatment of imatinib-resistant chronic myelogenous leukemia (CML). CML is a myeloproliferative disorder associated with the Philadelphia chromosome, which is a translocation of the ABL tyrosine kinase gene on chromosome 9 with the BCR gene on chromosome 22, generating a BCR-ABL oncogene (384). BCR-ABL has overactive tyrosine kinase activity, and several inhibitors were developed to block BCR-ABL signaling including imatinib and dasatinib. Imatinib is an ATP-

competitive inhibitor that binds to the active site of BCR-ABL, and it also blocks signaling through platelet derived growth factor receptor (PDGFR), Arg, and c-kit (385). Dasatinib is slightly more promiscuous than imatinib because it can also block signaling through Src and Ephrin receptors (386).

In mice, dasatinib exhibits the best pharmacokinetics when administered orally compared to i.v. (387). After a 5 mg/kg loading dose of dasatinib, plasma concentration in mice is in the range of 100 to 10 ng/ml for the first 12 hrs. The concentration of dasatinib drops between 1 and 10 ng/ml from 12-24 hrs. It was also demonstrated that mice administered human CML tumors s.c. had reduced BCR-ABL phosphorylation for the first 12 hrs after 2.5 mg/kg treatment with dasatinib, and the phosphorylation returned to normal after 24 hrs. Dasatinib treatment may inhibit adaptive immunity by blocking signaling through B and T cell receptors. Thus, dasatinib blocks antigen-specific T cell responses and NK cell cytotoxicity in mice (388). The authors also suggested that dasatinib may block B cell activation. Therefore, dasatinib may be immunosuppressive at high doses *in vivo*. CML patients in the chronic disease phase are prescribed 100 mg dasatinib daily, but imatinib-resistant CML patients in the accelerated phase are typically prescribed 70 mg twice daily or 140 mg once daily (389).

In tissue culture systems, dasatinib and other SFK inhibitors are implicated in inhibiting many different stages of viral replication. West Nile virus, a Flavivirus, was sensitive to the Src inhibitor PP2 but not at the level of viral RNA or protein production. PP2 blocked viral egress and prevented the production of infectious virus particles (390). Dasatinib also blocked Dengue, a related Flavivirus, but this occurred at the step of virus RNA replication and assembly (391, 392). It also blocked HIV-1 replication in CD4+ T cells by inhibiting reverse transcription (393). Dasatinib and imatinib had efficacy against variola virus and monkeypox virus, presumably by blocking viral release (394). In addition, dasatinib inhibited the coronaviruses MERS and SARS (395). Overall, these studies demonstrate the ability to use SFK inhibitors to learn about

pathways important for viral replication *in vitro*. The role of SFKs in alphavirus replication is explored in Chapter 2.

---

### 1.7.3 PI3K-AKT AXIS

Viruses may modulate PI3K-AKT signaling upon entry and/or during replication to modulate the cellular environment to promote viral replication (396). Alphaviruses are known modulators of the PI3K-AKT axis. Signaling mediated by PI3K and AKT affect the activation of mTOR to influence autophagy and translation processes. However, AKT can directly modulate pathways leading to translation, apoptosis, and cell growth. Two alphaviruses, SFV and CHIKV, localize their replication complexes to different cellular membranes in a process that is mediated by the PI3K-AKT axis (397). CHIKV replication complexes are primarily localized to the plasma membrane whereas SFV complexes are internalized and present on endosomal membranes. The ability of SFV to enhance AKT phosphorylation is attributed to the replication complex internalization, which remain at the plasma membrane after treatment with an inhibitor that blocks AKT phosphorylation, such as the PI3K inhibitor wortmannin. However, CHIKV also induces AKT phosphorylation, but not to the same degree as SFV. Together, this suggests that the PI3K-AKT pathway promotes alphavirus replication complex internalization but that this process may be fine-tuned to each member of the *Alphavirus* genus. As such alphaviruses have differing levels of sensitivity to pharmacological inhibitors of the PI3K-AKT pathway. CHIKV replication is sensitive to the PI3K inhibitor wortmannin in HeLa cells (398). Interestingly, SFV and SINV are not sensitive to wortmannin, despite the block in replication complex internalization from the plasma membrane (181). This indicates that the replication complexes function for SINV and SFV despite their localization, showing that their localization may affect a different process.

---

#### 1.7.4 SIGNALING THROUGH MTOR

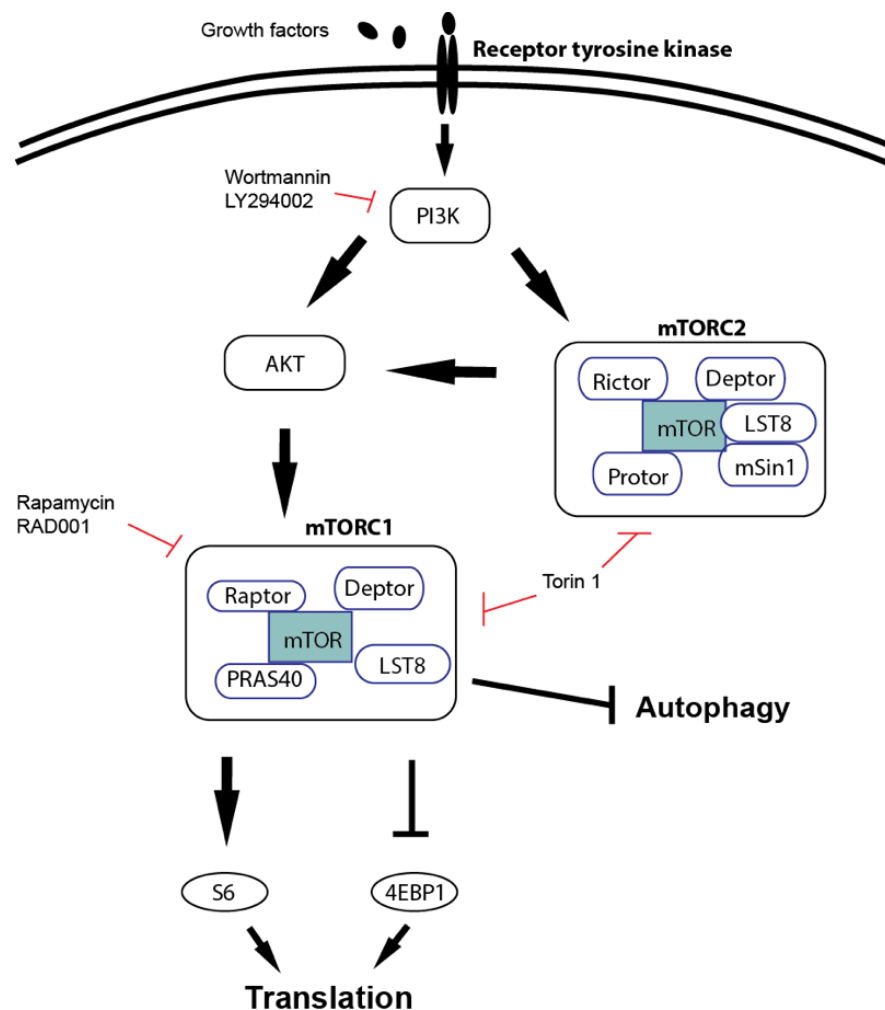
There are two major signaling complexes associated with mammalian target of Rapamycin (mTOR) named mTORC1 and mTORC2 (**Figure 1-7**) that are comprised of different base proteins with unique functionality. mTORC1 consists of mTOR, Raptor, Deptor, and PRAS40. Signaling by mTORC1 influences protein synthesis via S6K and 4E-BP1, affects lipid metabolism and blocks autophagic pathways. mTORC2 consists of mTOR, Rictor, Deptor, mSin1, and Protor, and it influences cell survival, proliferation, and cytoskeleton changes. mTOR signaling through either complex has direct effects on translation (399). Pharmacological inhibitors have been developed to block mTOR (ie. Rapamycin inhibits mTORC1; Torin 1 and PP242 efficiently block both mTORC1 and mTORC2).

Several reports have demonstrated that blocking mTORC1 with rapamycin *enhances* CHIKV replication by about 2 or 3-fold in both mouse and human cells (400, 401). One study proposed that the inhibition of mTORC1 promotes CHIKV infection by enhancing eIF4E phosphorylation via an mTORC1-alternative MNK-dependent pathway (400). This was suggested because a MNK inhibitor reversed the replication-enhancing effect of the mTORC1 inhibitor. Since the levels of nonstructural proteins as well as CHIKV RNA levels were enhanced in the presence of the mTORC1 inhibitor, eIF4E may be necessary for the translation of the incoming genomic mRNA. The enhancement of eIF4E phosphorylation after rapamycin treatment may seem counterintuitive because eIF4E is downstream of mTORC1. However, there are other signaling pathways, such as the MNK pathway, that intersect the mTORC1 pathway that can activate eIF4E when mTORC1 is inhibited (402, 403).

Another effect of blocking mTORC1 is the induction of autophagy (404). Macroautophagy is the cellular process of sequestering cytosolic components into vesicles, called autophagosomes that fuse with a lysosome for degradation. Autophagy involves the activation of several autophagy-related proteins (Atgs), promoting the recruitment of light chain

protein 3 (LC3) to the autophagosome membrane (405). There are controversial reports about whether autophagy enhances CHIKV replication or if it is antiviral. Joubert, et al. showed that CHIKV infection caused the accumulation of punctate lipid-associated LC3 vesicles, indicating that autophagy was induced after CHIKV infection (406). The authors claimed that autophagy was antiviral, and they showed that infection of mouse fibroblast cells that cannot undergo autophagy (Atg5<sup>-/-</sup> MEF cells) with CHIKV resulted in only 2 to 3-fold increase in viral replication. They also showed that mice that have reduced ability to undergo autophagy (lack Atg16L) had a slight decrease in survival compared to wild type mice (using 9-day old mice). However, the role of autophagy on interferon signaling or other immunological pathways are

**Figure 1-6: mTORC1 and mTORC2 signaling.**



unknown, as is their role in controlling CHIKV replication. A conflicting report from Krejbich-Trotot, et al. showed that autophagy inhibitor 3-methyladenin (3-MA) reduced viral replication in HEK 293 cells, and treatment with rapamycin (which induces autophagy via blocking mTORC1) resulted in a 2-fold increase in replication (401). The authors concluded that autophagy increases viral replication. A third study (Judith, et al.) demonstrated that deletion of autophagy components using siRNAs in HeLa cells resulted in slight decreases viral replication (398). They also demonstrated that nsp2 interacts with the autophagy receptor NDP52 in human cells, but nsp2 did not interact with the mouse homologue NDP52. Therefore, they concluded that autophagy was proviral in human cells, and antiviral in mouse cells due to these differences in nsp2 interactions. Overall, the key interpretation from these studies is that modulating autophagy components has minimal phenotypic effects on viral replication. Most of these studies measured CHIKV replication using GFP fluorescence, and they only reported a 2 or 3-fold increase or decrease on viral replication when the autophagy pathways were modulated. Overall, more studies are needed to clarify the role of autophagy during CHIKV replication. The effect of modulating mTOR is explored in more detail as described in Chapter 2.

## CHAPTER 2 DASATINIB IS AN ANTIVIRAL COMPOUND EFFECTIVE AGAINST CHIKV REPLICATION

Most data and experiments were generated and analyzed by Rebecca Broeckel with assistance from Craig Kreklywich, Patricia Smith, and Daniel Streblov. Some data was contributed from our collaborators in the laboratories of Dr. Thomas Morrison and Dr. Nathaniel Moorman as indicated. In addition, Dr. Victor DeFilippis and Dr. Michael Diamond provided useful reagents for this study.

### 2.1 ABSTRACT

Alphaviruses are arthropod-transmitted RNA viruses that can cause arthralgia, myalgia, and encephalitis in humans. No FDA approved vaccines or antiviral therapeutics are available to prevent alphavirus infection or treat disease. Rather than targeting viral components for development of therapeutics, we explored the utility of blocking cellular kinases to inhibit alphavirus infection. Treatment of cells with SFK inhibitors blocked replication of multiple alphaviruses including Chikungunya virus (CHIKV), Mayaro virus (MAYV), O'nyong-nyong virus (ONNV), Ross River virus (RRV), and Venezuelan equine encephalitis virus (VEEV). Dissecting the effect of Src inhibition on alphavirus replication, we found that structural protein levels were significantly reduced, but synthesis of both genomic and subgenomic RNA was unaffected. Fractionation of translation complexes by velocity sedimentation through linear sucrose gradients followed by RNA analysis revealed that dasatinib treatment shifts CHIKV vRNA into monosomal fractions, suggesting that translation is blocked at the level of polysome formation. Our results demonstrate a role for SFK signaling in alphavirus subgenomic RNA translation and replication. Targeting host factors involved in alphavirus replication represents an innovative, perhaps paradigm-shifting strategy for exploring CHIKV replication and antiviral therapeutic development.

## 2.2 INTRODUCTION

Alphaviruses are positive-sense, single-stranded RNA viruses in the *Togaviridae* family, and many are transmitted via bite by infected mosquitoes. Some alphaviruses cause acute febrile illness and arthritic disease in humans, including O'nyong-nyong virus (ONNV), Mayaro virus (MAYV), Sindbis virus (SINV), and Chikungunya virus (CHIKV) (11-13). The joint and muscle pain caused by CHIKV can be severe (145, 407), and the arthritic pain may last for several months up to years after acute symptoms resolve (105, 292). Alphaviruses causes widespread outbreaks in areas of serologically naïve individuals. In 2013, a CHIKV outbreak occurred in the Caribbean islands, and CHIKV subsequently spread to several Central and South American countries (263), infecting an estimated 1.9 million people (262). Other alphaviruses such as Venezuelan Equine Encephalitis Virus (VEEV) cause acute febrile illness and neurological disease, including fatal encephalitis (56, 408). In 1995, a VEEV epidemic in Colombia and Venezuela resulted in 75,000-100,000 human cases, with a small proportion of those developing encephalitis (15, 151). Treatment of all alphavirus infections, including CHIKV and VEEV, is currently limited to supportive care. New knowledge of the cellular requirements for alphavirus replication will facilitate development of effective antiviral therapies to treat individuals suffering from alphavirus infections.

Alphavirus virions are internalized into host cells by clathrin-mediated endocytosis (409, 410), and the glycoproteins initiate viral fusion in endosomal compartments releasing the viral genome into the cytoplasm. The nonstructural proteins nsP123 and nsP1234 nonstructural protein precursors are efficiently translated from the incoming capped and polyadenylated genomic RNA (70, 71). The nsP1234 proteins form an RNA replication complex that synthesizes the full-length negative and positive strands of viral genomic RNA as well as the subgenomic RNA (sgmRNA) (411). Replication complexes form host membrane invaginations, called spherules, which encompass the RNA replication compartment (182, 184, 412, 413).

Depending on the alphavirus species, there are two fates for these spherules: 1) they are internalized in a phosphatidylinositol-3-kinase (PI3K) dependent manner as shown for Semliki forest virus (SFV) and SINV, or 2) they remain near the cell periphery as with CHIKV (397). During the late phase of infection, the sgmRNA is translated into the structural proteins capsid (C), E3, E2, 6k, and E1 as a single polyprotein that is autocatalytically cleaved in the cytoplasm (215-217). Translation of the sgmRNA is efficient even during phosphorylation and inactivation of eukaryotic translation initiation factor 2 (eIF2) that blocks canonical, cap-dependent translation (227). In addition to eIF2, translation of the SINV sgmRNA does not appear to require eIF4G, eIF2D, or eIF2A (232, 238). Translation of SINV sgmRNA is facilitated by a GC-rich structural element in the sgmRNA called a downstream loop (DLP), which allows for efficient translation in the absence of eIF2 (227, 235, 236). However, CHIKV and VEEV have no predicted DLP structure (235), but rather they may have an alternative mechanism for efficient sgmRNA translation in the absence of active eIF2.

Capsid protein is autocatalytically cleaved from the nascent polyprotein chain, exposing an N-terminal ER localization signal sequence on pE2 (414, 415). The pE2-6K-E1 polyprotein is processed by the ER-localized signalase, which cleaves the polyprotein between pE2 and 6K and between 6K and E1, promoting pE2 and E1 heterodimerization (176). Furin cleaves the N-terminal E3 domain away from E2 in the trans-Golgi network (219). Late in the assembly process, E2 is phosphorylated near the C-terminus, causing a translocation of the C-terminus to the cytoplasmic side of the membrane (416) in an event that promotes nucleocapsid association with the C-terminus of E2 (92). Virions bud at plasma membrane where they obtain their envelope and are released as infectious particles (417). Each of these virus replication steps is carried out by a highly complex and organized combination of host and viral factors.

Viruses utilize and modulate cellular signaling pathways to promote an intracellular environment suitable for viral replication (418, 419) by influencing major cellular processes such

as metabolism, growth, differentiation, transcription, translation, and cytoskeletal rearrangement (420, 421). Src family kinases (SFKs) are ubiquitous, non-receptor tyrosine kinases involved in cell survival, migration, and proliferation (379, 422-425). There are 9 Src Family Kinase members: Src, Fyn, Yes, Blk, Fgr, Hck, Lck, Yrk, and Lyn. SFKs are myristoylated and sometimes palmitoylated (426) membrane-associated molecules that mediate signal transduction of many receptors, including G-Protein-Coupled Receptors (427), receptor tyrosine kinases (428), and integrins (377). Many viruses encode proteins that directly interact and modulate SFK activity (382, 429-431). SFK inhibitors have been employed to study the role of SFKs in the virus replication cycle. For example, SFK inhibitors effectively block West Nile Virus (WNV) envelope protein trafficking and maturation (390). The SFK inhibitor dasatinib inhibits replication of dengue virus (DENV) (391, 392), human immunodeficiency virus (HIV) (432), and Hepatitis C virus (HCV) (433). Dasatinib affected multiple stages of DENV replication by reducing DENV RNA accumulation (391) and preventing virion assembly in the ER (392). Dasatinib suppressed HIV production from CD4+ T cells by blocking reverse transcription and integration (393, 432). In addition, dasatinib was shown to inhibit Ephrin2A kinase signaling necessary for CD81-CLDN1 cofactor complex formation thus blocking HCV fusion during entry (433, 434). Therefore, there is a precedent for utilizing SFK inhibitors to identify steps in viral replication that require Src-related kinase activity.

Identification of the specific kinases and signaling pathways that promote alphavirus replication will aid development of anti-alphavirus compounds. In order to identify which kinase pathways are important for alphavirus replication, we treated CHIKV-infected cells with a panel of inhibitors that target the SFK-PI3K-AkT-mTOR pathway. Herein, we demonstrate that SFK inhibitors including dasatinib as well as the mTORC1/2 inhibitors, such as PP242 and Torin 1, block alphavirus replication in human fibroblasts. Though dasatinib and Torin 1 had minimal effects on viral RNA synthesis, both treatments decreased structural protein accumulation for

both CHIKV and VEEV. Furthermore, dasatinib decreased CHIKV RNA association with polysomes indicating that CHIKV relies on SFKs and mTORC1/2 for structural protein synthesis or a step occurring after viral RNA transcription but prior to synthesis of the structural protein. Our novel findings provide insight into the CHIKV replication cycle and the requirement of SFK activity in alphavirus replication.

## 2.3 RESULTS

**Src family kinase inhibitor dasatinib blocks CHIKV replication and prevents CHIKV-induced cell death.** To validate the requirement of the SFK pathway during CHIKV replication, inhibitors of the SFK/PI3K/Akt/mTOR pathways were tested for their ability to block CHIKV replication (**Table 2-1**). To ensure that the inhibitors were used at concentrations that were not toxic to the cells, cell viability assays were performed in uninfected normal human dermal fibroblasts (NHDFs) at 24 hrs post drug treatment (**Fig S1**). Drug concentrations that reduced cellular viability by more than 20% were considered toxic. For example, PP242 concentrations greater than 1  $\mu$ M and GSK690693 concentrations greater than or equal to 20  $\mu$ M were toxic to NHDFs and were not included in subsequent experiments. To assess the effects of the SFK/PI3K inhibitors on CHIKV replication, NHDFs were pretreated for 2 hrs with inhibitor and infected with CHIKV SL15649 (MOI = 1) in the presence of drug. At 2 hpi, the inoculum was removed and cells were washed with PBS, and new drug and media was added back to the cells. Supernatants were collected at 20 hpi and titered by limiting dilution plaque assay on Vero cells. Dasatinib and Torin 1 treatment blocked CHIKV replication over 10-fold, and PP242 and LY294002 treatment mildly reduced CHIKV replication. In contrast, treatment with GSK 690693, GSK 650394, CGP 57380 had no effect on CHIKV replication, and treatments with RAD001 and Rapamycin slightly increased CHIKV replication in NHDFs (**Fig 2-1A**).

Of the inhibitors tested, dasatinib treatment resulted in strongest inhibition of CHIKV replication. To determine whether dasatinib could block CHIKV-mediated cell death, a cell viability assay was performed in CHIKV-infected cells in the presence of increasing doses of dasatinib at 24 hpi. As expected, dasatinib increased cell viability during CHIKV infection in a dose-dependent manner (**Fig 2-1B**). The activity of many of the SFK/PI3K/Akt/mTOR inhibitors were confirmed by testing inhibitor-treated infected cell lysates for the presence of phospho-S6; S6 is a ribosomal protein that becomes phosphorylated after mTOR activation (435, 436). A phospho-S6 western blot confirmed that the inhibitors specific for the PI3K/Akt/mTOR axis successfully blocked S6 phosphorylation (**Fig 2-1C**). Dasatinib is a potent inhibitor of Src Family Kinases (SFKs) (386, 437). As confirmation of this activity in NHDFs, the activating phosphorylation of Src at Tyr416 was analyzed in cell lysates at 6, 8, and 18 hpi (438). In the absence of dasatinib, there was an increase of Src Tyr416 phosphorylation in CHIKV-infected cells compared to uninfected cells at 18 hpi. Phosphorylation of Src at Tyr416 was reduced in cells treated with dasatinib when compared to untreated in both infected and uninfected lysates (**Fig 2-1D**), demonstrating that dasatinib inhibited Src activation. Together these data suggested that dasatinib blocks CHIKV replication and CHIKV-mediated cell death in NHDFs.

To validate the inhibition of CHIKV by dasatinib, immunofluorescence staining was performed on CHIKV infected cells. NHDFs were infected with CHIKV (MOI = 1) and treated with dasatinib or another SFK inhibitor PP2. Cells were fixed at 24 hpi and stained with antibodies directed against CHIKV glycoprotein and actin as well as the DNA stain DAPI. Foci of CHIKV infected cells were observed in non-treated cells, whereas dasatinib and PP2 treatments resulted in the presence of single infected cells (**Fig 2-2**). Similar findings were observed in VEEV infected cells wherein SFK inhibitors blocked the ability of the virus to spread through the culture (**Fig S-2**). Combined this data indicates that SFK inhibitors reduce virus spread by reducing infectious virus production from infected cells.

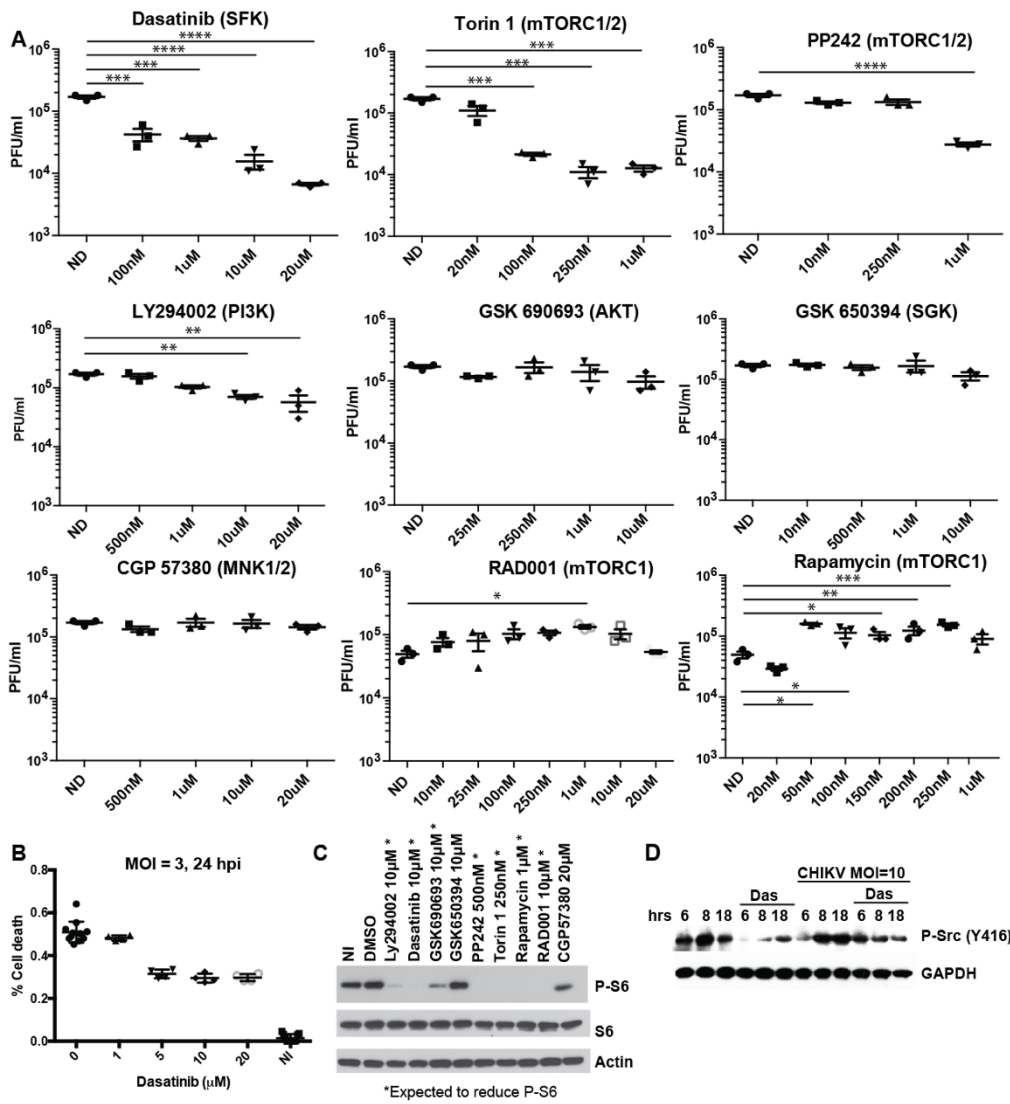


**Figure 2-1: Dasatinib, Torin 1, and PP242 block CHIKV replication in human fibroblasts.**

NHDFs were pretreated for 2 hrs with drug and infected with CHIKV pMH56 MOI = 1. Cells were washed twice with PBS at 2 hpi, and inhibitor-containing media was added to the cells. **(A)** Supernatants from infected cells were collected at 20 hpi and titered on vero cells by limiting dilution plaque assay. **(B)** NHDFs were infected with CHIKV MOI = 3, and treated with dasatinib at 2 hpi. At 24 hpi, cells were analyzed for viability using the CellTiter-Glo Viability Assay Kit (NI is uninfected). **(C)** NHDFs were treated as in **(A)** and cell lysates were analyzed by western blotting for p-S6, S6, and Actin. **(D)** NHDFs were infected with CHIKV 181/25 MOI = 10 or left uninfected. At 2 hpi, cells were washed twice with PBS and media was replaced with or without drug. Cell lysates were collected at the indicated times. Western membranes were probed with anti-p-SFK (Tyr416) and GAPDH antibodies. Statistics were performed on log-transformed data and multiple comparisons were performed using Dunn's multiple comparison test, and multiplicity adjusted *P* values are reported. (*n* = 3, \* *P* < 0.05, \*\* *P* < 0.005, \*\*\* *P* < 0.0005, \*\*\*\* *P* < 0.00005)

Data produced and analyzed by Rebecca Broeckel.

<b>Drug</b>	<b>Targets</b>	<b>Cell Viability after 24 hr treatment in NHDFs</b>
Dasatinib	SFKs, Bcr-Abl, Arg, c-kit, signaling through PDGFR and Ephrin	90% viability 100 nM to 50 $\mu$ M
Torin 1	mTORC1/mTORC2	>80% viability 20 nM to 1 $\mu$ M
PP242	mTORC1/mTORC2	>80% viability 10 nM to 1 $\mu$ M
LY294002	PI3K	>80% viability 100 nM to 50 $\mu$ M
GSK 690693	AKT	>80% viability 10 nM to 10 $\mu$ M
GSK 650394	SGK	>90% viability 10 nM to 20 $\mu$ M
CGP 57380	Mnk1/2	>85% viability 10 nM to 20 $\mu$ M
RAD001	mTORC1	>90% viability 10 nM to 20 $\mu$ M
Rapamycin	mTORC1	>90% viability 20 nM to 1 $\mu$ M

**Table 2-1: Drugs used in this study, their targets, and their toxicity.**

**Dasatinib and Torin 1 reduce alphavirus infection in an interferon-independent manner.** Since alphaviruses are highly sensitive to interferon (325, 439, 440), We tested whether dasatinib treatment could still inhibit CHIKV in cells lacking a functional interferon response. CHIKV infection activates interferon regulatory factor 3 (IRF3), resulting in transcription of type I interferon, which can potently block CHIKV replication (228). Further, Src was shown to phosphorylate TANK binding kinase 1 (TBK1), which activates IRF3 and promotes type I IFN production (441). Therefore, dasatinib, an inhibitor of Src, would block the type I IFN production via TBK1. By this rationale, inhibiting TBK1 phosphorylation with dasatinib might promote viral infection because activation of IRF3 will be inhibited. However, this rationale is contrary to what was observed in that dasatinib blocks CHIKV infection. To test whether dasatinib-mediated inhibition of CHIKV replication was dependent on IRF3, human fibroblasts deficient in IRF3 (IRF3<sup>-/-</sup>) (442) were infected with CHIKV or VEEV and treated at 0 hpi or 2 hpi with dasatinib. Supernatants were collected at 24 hpi and titered by limiting dilution plaque assays. Viral replication for both CHIKV and VEEV was inhibited by dasatinib treatment in IRF3<sup>-/-</sup> cells (**Fig 2-3A**). Another component of the interferon response is the protein signal transducer and activator of transcription 1 (STAT1), which acts downstream of the type I interferon receptor and activates transcription of interferon stimulated genes. STAT1 deleted telomerized human fibroblasts (STAT1<sup>-/-</sup>) (442) were infected with CHIKV or VEEV and treated with dasatinib or Torin 1 at 2 hpi. At 24 hpi, supernatants were titered revealing that CHIKV and VEEV maintained sensitivity to dasatinib in STAT1<sup>-/-</sup> THFs (**Fig 2-3B**). Together, these data indicate that the mechanism of dasatinib and Torin inhibition of CHIKV and VEEV replication is independent of STAT1- and IRF3-mediated innate immunity.

**Torin 1 and dasatinib differentially regulate autophagy.** Torin 1 and dasatinib both block mTOR signaling. One common downstream pathway of mTOR is autophagy, which is induced when mTOR is inhibited (404). There have been conflicting reports regarding whether

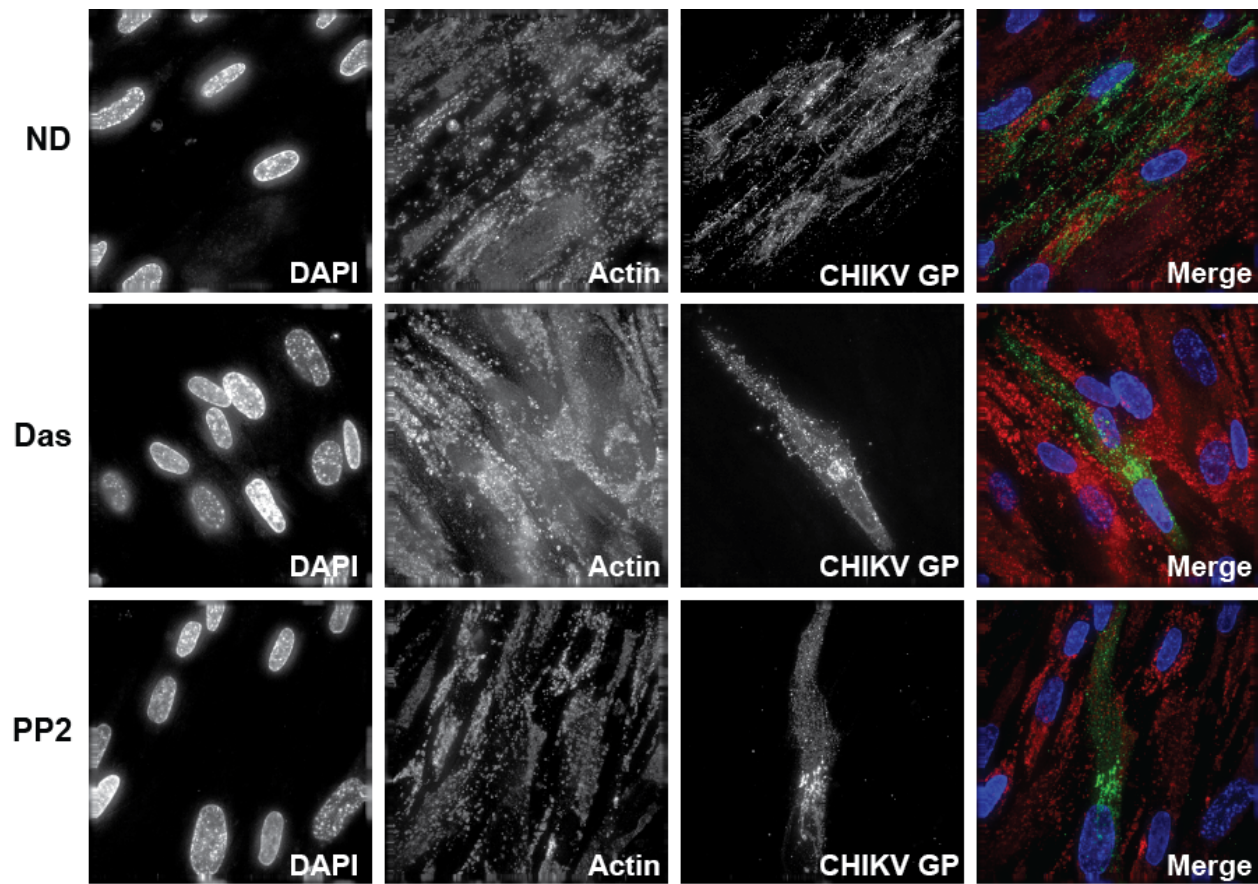


**Figure 2-2: CHIKV replication and spread is limited by dasatinib and PP2.**

NHDF cells were infected with CHIKV 181/25 (MOI = 1) and treated with dasatinib or PP2 at 2 hpi. At 24 hpi, cells were fixed and stained for virus-specific envelope glycoproteins and counterstained with DAPI and Phalloidin to highlight host DNA and Actin filaments.

Data produced by Rebecca Broeckel and Patricia Smith and analyzed by Rebecca Broeckel.

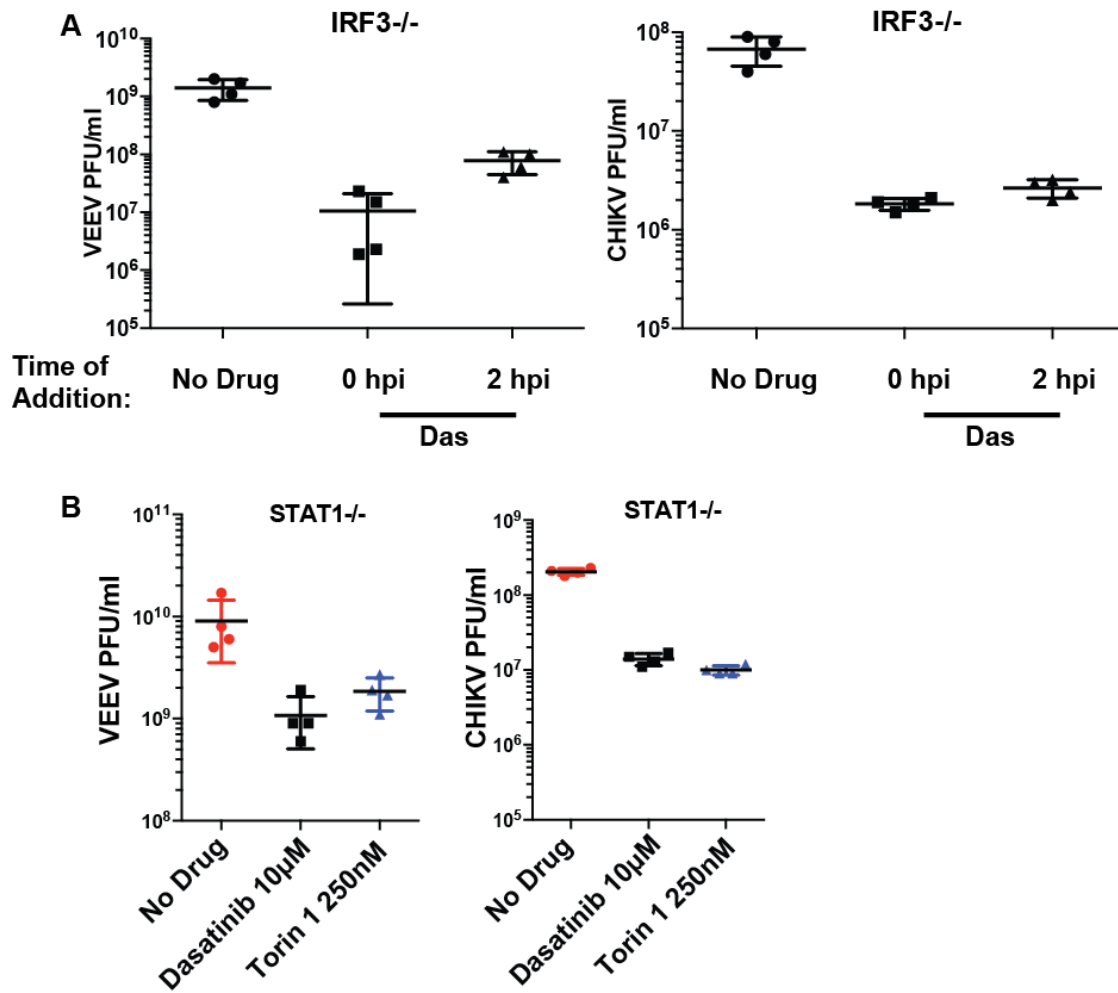


**Figure 2-3: Dasatinib inhibits CHIKV and VEEV replication in IRF3<sup>-/-</sup> and STAT1<sup>-/-</sup> fibroblasts.**

(A) IRF3<sup>-/-</sup> telomerized human fibroblasts were infected with CHIKV and VEEV MOI = 1 and treated with dasatinib at 0 or 2 hpi. Supernatants were taken at 24hpi from infected cells and titered on Veros by limiting dilution. (B) STAT1<sup>-/-</sup> telomerized human fibroblasts were infected with CHIKV or VEEV (MOI = 1) and treated with inhibitor at 2 hpi. Supernatants were collected at 24 hpi and titered on Veros.

Cells provided by Dr. Victor DeFilippis. Data produced and analyzed by Rebecca Broeckel.

autophagy is pro or antiviral for CHIKV (398, 401, 406). Therefore, to address whether Torin 1 and dasatinib induced autophagy in NHDFs and whether this was involved in blocking alphavirus replication, CHIKV infected cells were treated with dasatinib, Torin 1, or the autophagy inhibitor 3-MA (1mM). At 7 hpi, cell lysates were harvested and evaluated by western blotting for LC3-I and LC3-II. The shift of LC3-I to LC3-II indicates formation of the autophagosome and the induction of autophagy (405). Western blotting analysis revealed that while Torin 1 induced LC3-II accumulation, dasatinib and 3-MA did not alter the LC3 status compared untreated infected cells (**Fig S-3A**). Blotting cellular lysates for E2 indicated that while dasatinib and Torin 1 reduced E2 levels, 3-MA induced CHIKV E2 accumulation compared to the untreated control (**Fig S-3B**). Our data indicate that autophagy may be inhibitory to CHIKV replication in NHDFs, because E2 levels were enhanced in the presence of the autophagy inhibitor 3-MA. Together, these data suggest that dasatinib does not influence autophagy, but Torin 1 induces autophagy. However, both Torin 1 and dasatinib block E2 accumulation, indicating that these two inhibitors may be inhibiting CHIKV ultimately by different mechanisms but affecting similar steps in the virus replication cycle.

**CHIKV requires c-Src for replication.** Dasatinib has many cellular targets, including Src, Lck, Lyn, Yes, Fyn, Ephrin receptors, and Bcr/Abl (443). To confirm the importance of Src in CHIKV replication, CHIKV growth was measured in SYF<sup>-/-</sup> MEFs (mouse fibroblasts lacking Src, Yes, and Fyn) and Src<sup>+</sup> SYF<sup>-/-</sup> MEFs, in which Src was stably reintroduced. CHIKV titers in Src<sup>+</sup> SYF<sup>-/-</sup> MEFs were consistently higher than titers in SYF<sup>-/-</sup> MEFs at both a high and low MOI (**Fig 2-4**). This data is consistent with the hypothesis that Src is important for efficient CHIKV replication.

**Dasatinib does not block CHIKV RNA replication.** To identify the mechanism of SFK inhibition on CHIKV replication, viral RNA (vRNA) accumulation was monitored in the presence of inhibitor. Dasatinib likely has multiple effects on viral replication. To circumvent any effects of

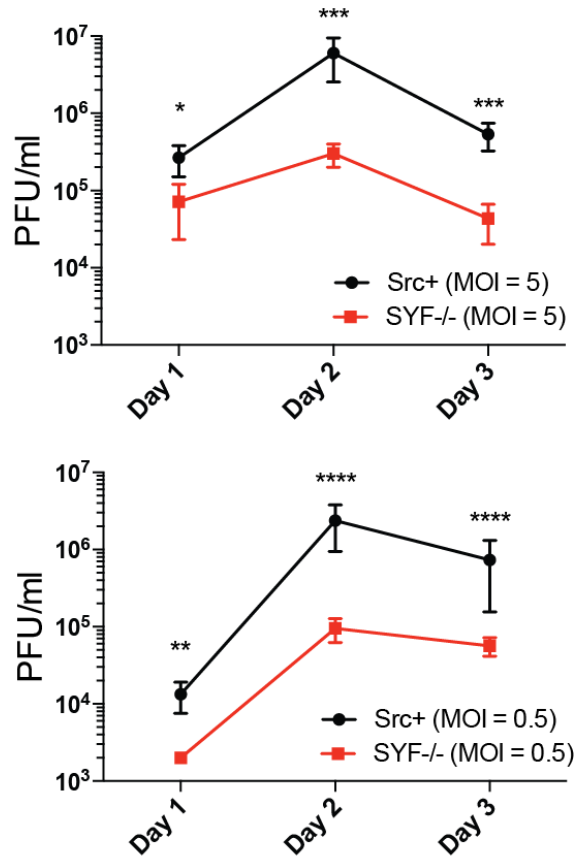


**Figure 2-4: CHIKV replication is suppressed in the absence of Src.**

SYF -/- (MEF K/O Src, Yes, and Fyn) and Src+ cells (SYF -/- stably transfected with Src) were infected at MOI = 5 (top) or MOI = 0.5 (bottom), and supernatants were collected at 1, 2, and 3 dpi and titered by plaque assay on confluent monolayers of vero cells. Statistics were performed on log-transformed data using Sidak's multiple comparisons test, and multiplicity-adjusted *P* values are reported (*n* = 3, \* *P* < 0.05, \*\* *P* < 0.005, \*\*\* *P* < 0.0005, \*\*\*\* *P* < 0.0001).

Data produced and analyzed by Daniel Streblow.

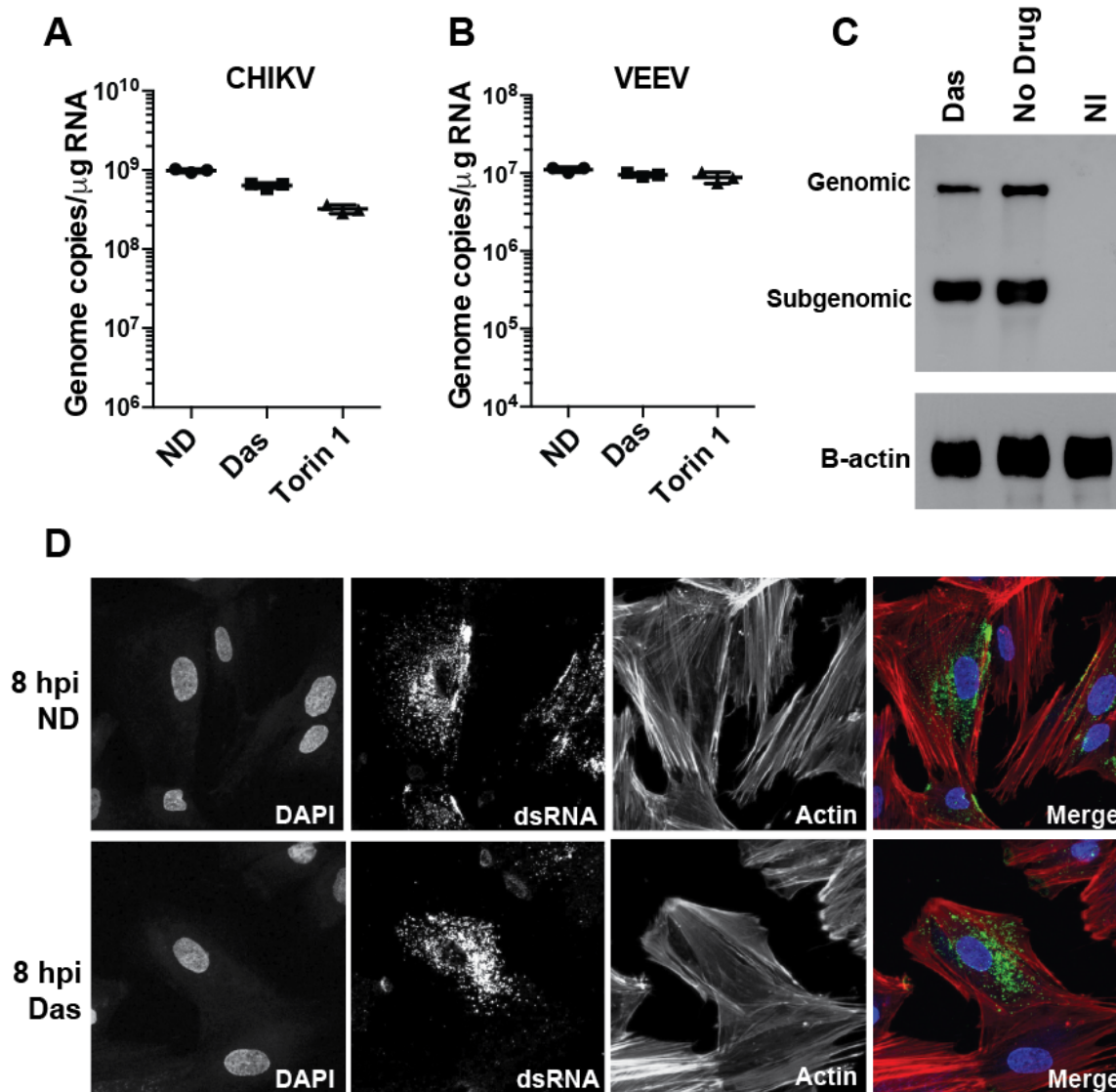


**Figure 2-5: SFK inhibitors do not reduce CHIKV RNA synthesis and replication complex formation.**

NHDFs were infected with CHIKV 181-25 (**A**) or VEEV (**B**) (MOI = 3). At 2 hpi, cells were washed twice with PBS, and cells were treated with 10  $\mu$ M dasatinib. At 12 hpi, cells were washed extensively in PBS and cells were lysed with Trizol reagent for total RNA isolation. Relative levels of vRNA was analyzed by qRT-PCR using gene-specific primers and probes. (**C**) RNA from uninfected and infected cells treated with and without dasatinib were analyzed by Northern blotting for genomic and subgenomic RNA levels. (**D**) NHDFs were infected with CHIKV 181-25 (MOI = 25) and treated with dasatinib at 2 hpi or left untreated (ND). At 8 hpi, cells were fixed and stained for dsRNA (J2), Actin (Phalloidin), and DNA (DAPI).

Data produced and analyzed by Rebecca Broeckel.

dasatinib or Torin 1 on viral entry, NHDFs were infected with CHIKV or VEEV (MOI = 3), and dasatinib and Torin 1 was added to the media at 2 hpi. CHIKV and VEEV vRNA levels were measured by qRT-PCR at 12 hpi. Dasatinib treatments slightly decreased CHIKV RNA, while Torin 1 had a slightly larger effect on CHIKV RNA accumulation (**Fig 2-5A**). Dasatinib and Torin 1 had very little effects on VEEV RNA accumulation (**Fig 2-5B**). To further analyze the effects of dasatinib on vRNA production, I performed a northern blot on RNA isolated from NHDFs infected with CHIKV MOI = 3 for 12 hrs and treated with or without dasatinib at 2 hpi. A dsDNA digoxigenin-labeled probe recognizing E2-6K-E1 was generated to distinguish between genomic vRNA and subgenomic vRNA. Dasatinib treatment had relatively little effect on the levels of genomic or subgenomic CHIKV RNA (**Fig 2-5C**). Similarly, qRT-PCR results demonstrate that the ratio of CHIKV nsP2 and E2 RNA levels were unaffected by dasatinib treatment (**Fig S-4A-B**). Combined these data indicate that CHIKV RNA amplification in the presence of dasatinib is largely unaffected and the minimal effects on RNA levels could be attributed to a block in subsequent rounds of replication due to the block in the production of infectious virus. Thus, these data suggest that dasatinib is blocking a subsequent step in the virus replication cycle.

Next we determined whether dasatinib disrupts CHIKV replication complex formation. At 8 hpi, replication complexes were identified by immunofluorescence staining with an antibody specific for double-stranded RNA (dsRNA) (207, 397). The presence of viral replication complexes appeared unchanged in dasatinib-treated cells when compared to untreated cells (**Fig 2-5D**). Additionally, there were no visual differences in the amount of dsRNA staining at 8 hpi (**Fig S4C**), which is consistent with data demonstrating that dasatinib blocks a step post vRNA synthesis.

**Dasatinib blocks CHIKV and VEEV structural protein synthesis.** We hypothesized that dasatinib does not influence synthesis of viral nonstructural proteins since viral RNA levels and replication complex formation appeared normal in treated cells. To test this hypothesis,

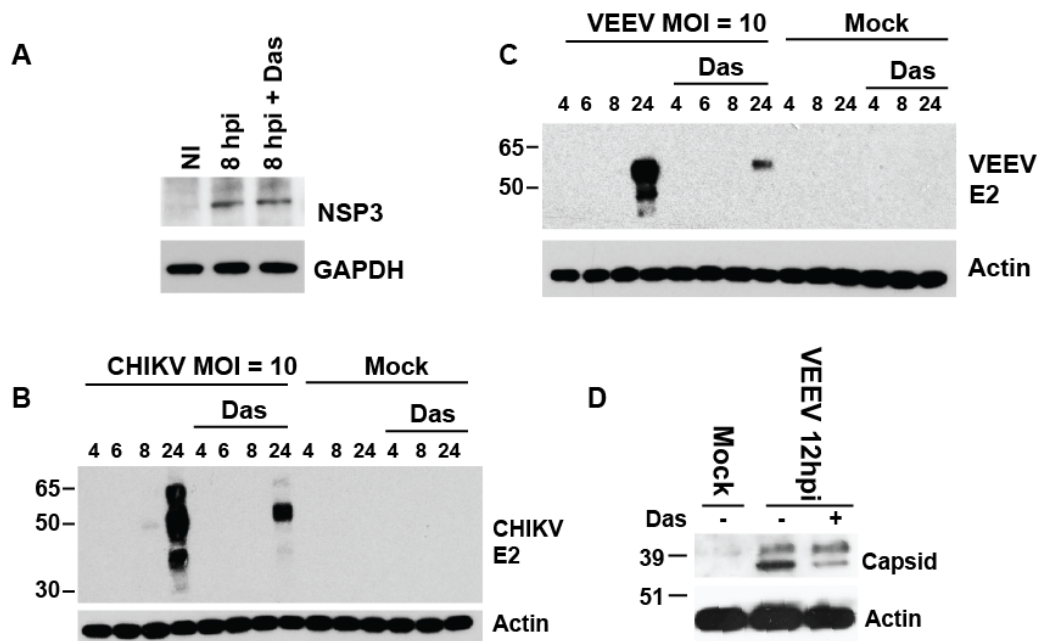


**Figure 2-6: Dasatinib blocks structural protein accumulation.**

(A) NHDFs were infected with CHIKV 181-25 (MOI = 10), treated with dasatinib at 2 hpi, and cell lysates were analyzed for nsP3 protein levels at 8 hpi by western blot. NHDFs were infected with CHIKV 181-25 (B) or VEEV (C) (MOI = 10), and E2 protein levels were analyzed at the indicated times by western blot. (D) For comparison with another structural protein, NHDFs were infected with VEEV (MOI = 1) and treated with dasatinib at 2 hpi and analyzed for VEEV capsid levels by western blotting.

Data produced and analyzed by Rebecca Broeckel.

western blot analysis for nsp3 was performed on lysates from CHIKV infected cells with or without dasatinib at 8 hpi. We observed no difference in nsP3 levels with dasatinib treatment (**Fig 2-6A**). In contrast to the nonstructural protein levels, immunoblotting cell lysates for envelope protein E2 revealed a strong reduction in E2 protein accumulation upon dasatinib treatment (**Fig 2-6B**). Similarly, levels of VEEV capsid and glycoprotein were also dramatically reduced in the presence of the drug (**Fig 2-6C-D**). Together these data suggest that dasatinib blocks synthesis of the structural proteins, but it has very minimal effects on the production of vRNA or nonstructural proteins.

Next, we sought to determine the mechanism by which dasatinib blocks CHIKV structural protein accumulation. To accomplish this goal, ribosomal profiling was performed on lysates from CHIKV-infected, inhibitor treated NHDFs at 12 hpi. Lysates were fractionated by centrifugation over a linear sucrose gradient, and 17 fractions were collected and analyzed for optical density at 264 nm ( $OD_{264}$ ) as well as for the level of vRNA by qRT-PCR. Absorbance readings of the fractions revealed that dasatinib caused an increase of absorbance in the 80S monosomal peak and a decrease in absorbance in polysome fractions (fractions 9-15) (**Fig 2-7A**). In dasatinib-treated cells, the vRNA was shifted towards fractions containing monosomes (**Fig 2-7B**). The translation efficiency, which is equated as a ratio of viral RNA levels in the monosome fractions compared to the polysome fractions, was reduced by approximately 80% in dasatinib treated samples (**Fig 2-7C**). These results suggest that dasatinib treatment disrupted CHIKV protein synthesis by preventing the translation machinery from associating with viral RNA. In this experiment, we quantified viral RNA by measuring E1, which is present on both sgRNA and gmRNA. To determine if dasatinib affects the gmRNA specifically, we could quantify the gmRNA in the fractionated samples using an nsp2 primer and probe set. While we did not quantify the translation efficiency of the sgRNA and gmRNA separately, the translation efficiency calculated in **Fig 2-7** is most likely representative of the translation efficiency of the

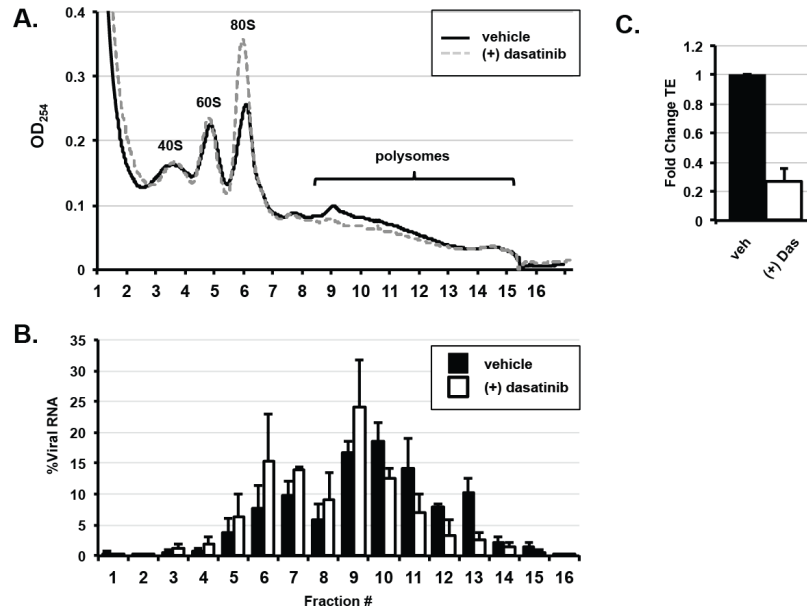


**Figure 2-7: Dasatinib decreases the translation efficiency of CHIKV RNA.**

**(A)** NHDFs infected with CHIKV (MOI = 3) were untreated or treated with 10  $\mu$ M dasatinib. Cytoplasmic lysates of infected cells were collected at 12 hpi and resolved through 10-50% linear sucrose gradients. The presence of ribosomal subunits (40S, 60S), monosomes (80s) and polysomes was monitored by continuous measurement of absorbance (OD<sub>254</sub>) during fractionation. **B.** Total RNA was prepared from each fraction, and the percent of CHIKV RNA per fraction was determined by qRT-PCR as a percentage of the total cytoplasmic viral RNA. **C.** The translation efficiency of CHIKV RNA in each condition was determined by qRT-PCR. The fold change in translation efficiency for CHIKV RNA in the presence of dasatinib is reported. The translation efficiency of the vehicle treated control cells is set to one (n = 2).

Data produced and analyzed by Dr. Nathaniel Moorman's group.

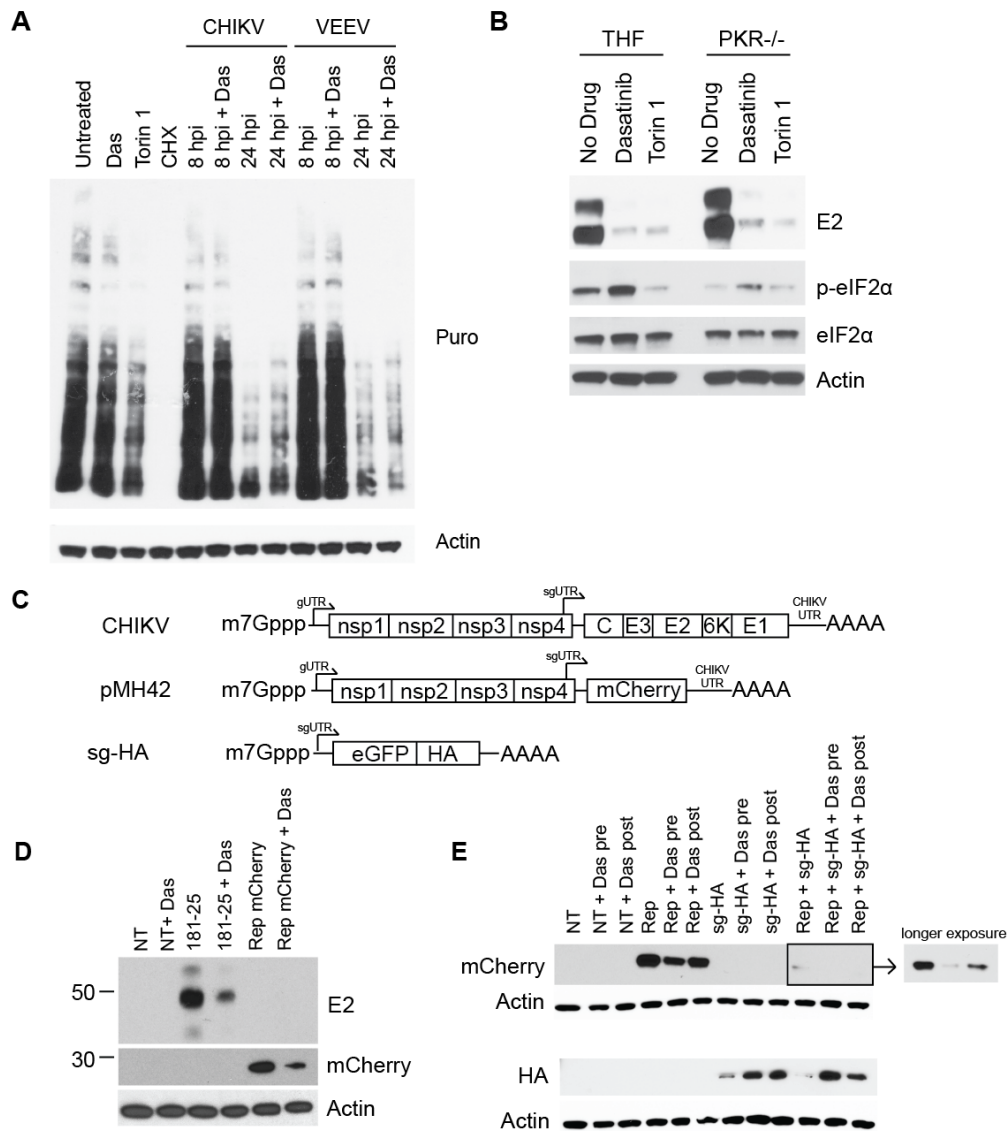


**Figure 2-8: Dasatinib blocks translation of sgRNAs from replicon-containing cells.**

**(A)** NHDFs were infected with CHIKV or VEEV (MOI = 10) or left uninfected. At 2 hpi, cells were treated with 10  $\mu$ M dasatinib, 250 nM Torin 1, or 200  $\mu$ g/ml cycloheximide (CHX) as indicated. At 8 hpi or 24 hpi, cells were pulsed with 10  $\mu$ g/ml puromycin for 15 min. Following treatment, puromycin-free media was added to the cells for 1 hr and lysates were collected and analyzed by western blotting for puromycin incorporation and actin. **(B)** PKR<sup>-/-</sup> THFs or parental THFs were infected with CHIKV SL15649 (MOI = 3). At 8 hpi, lysates were analyzed by western blotting for E2, p-eIF2 $\alpha$ , eIF2 $\alpha$ , and actin. **(C)** Schematic of *in vitro* synthesized mRNAs. **(D)** 2  $\mu$ g of CHIKV 181-25 mRNA or pMH42 mRNA was transfected into NHDFs and treated with 10  $\mu$ M dasatinib 45 min post transfection. At 20 hrs post transfection, cell lysates were analyzed for CHIKV E2, mCherry, or actin by western blotting. **(E)** NHDFs were pretreated with 10  $\mu$ M dasatinib for 30 min prior to transfection or posttreated 30 minutes after transfection as indicated. mRNAs were transfected with 2  $\mu$ g pMH42, sg-HA, or a combination of both mRNAs. Lysates were collected 20 hrs post transfection and analyzed by western blotting for mCherry, HA, and actin.

Data produced and analyzed by Rebecca Broeckel. PKR<sup>-/-</sup> cells provided by Dr. Victor DeFilippis.

sgmRNA because 1) the sgmRNA is synthesized in excess relative to gmRNA at 12 hpi (see northern blot in **Fig 2-5C**), and 2) the translation product of the gmRNA was not affected by dasatinib while the translation product of the sgmRNA was significantly affected (see **Fig 2-6**).

**Dasatinib does not inhibit alphavirus-mediated translation shutoff.** The precise mechanism of translation of CHIKV and VEEV sgmRNA is not known, but the translation of the sgmRNA is very efficient during host transcription and translation shutoff (242). Translation of the sgmRNA may not require many of the canonical translation initiation factors, as has been previously documented for SINV (232, 238, 240). To determine if dasatinib affects the virus-induced shutoff process, we performed a puromycin pulse-chase assay in dasatinib treated or untreated NHDFs infected with CHIKV or VEEV. Interestingly, the addition of dasatinib, despite having a significant effect on viral E2 accumulation, did not interfere with virally-induced host shutoff at 24 hpi (**Fig 2-8A**). Additionally, in uninfected cells, dasatinib did not affect puromycin incorporation into newly synthesized protein, whereas cycloheximide (CHX) treatment abolished protein production and Torin 1 reduced global protein production.

A marker for shutoff of cellular translation during viral infection is the phosphorylation status of the alpha subunit of eukaryotic initiation factor 2 (eIF2 $\alpha$ ). eIF2 is a translation initiation factor essential for translation of capped mRNAs. Phosphorylation inactivates eIF2 $\alpha$ , which prevents cap-dependent cellular translation. Translation of CHIKV sgmRNA may not require eIF2 because the sgmRNA is still translated efficiently when eIF2 $\alpha$  is phosphorylated (228). The kinase responsible for eIF2 $\alpha$  phosphorylation during CHIKV replication is the cytoplasmic dsRNA sensor protein kinase R (PKR) (228). Therefore, we determined the effects of dasatinib and Torin 1 treatment on CHIKV replication in PKR $^{-/-}$  cells. Compared to the parental cell line, dasatinib and Torin 1 still reduced E2 levels in PKR $^{-/-}$  THFs (**Fig 2-8B**). Western blotting was used to assess the phosphorylation status of eIF2 $\alpha$  in infected PKR $^{-/-}$  cells following dasatinib

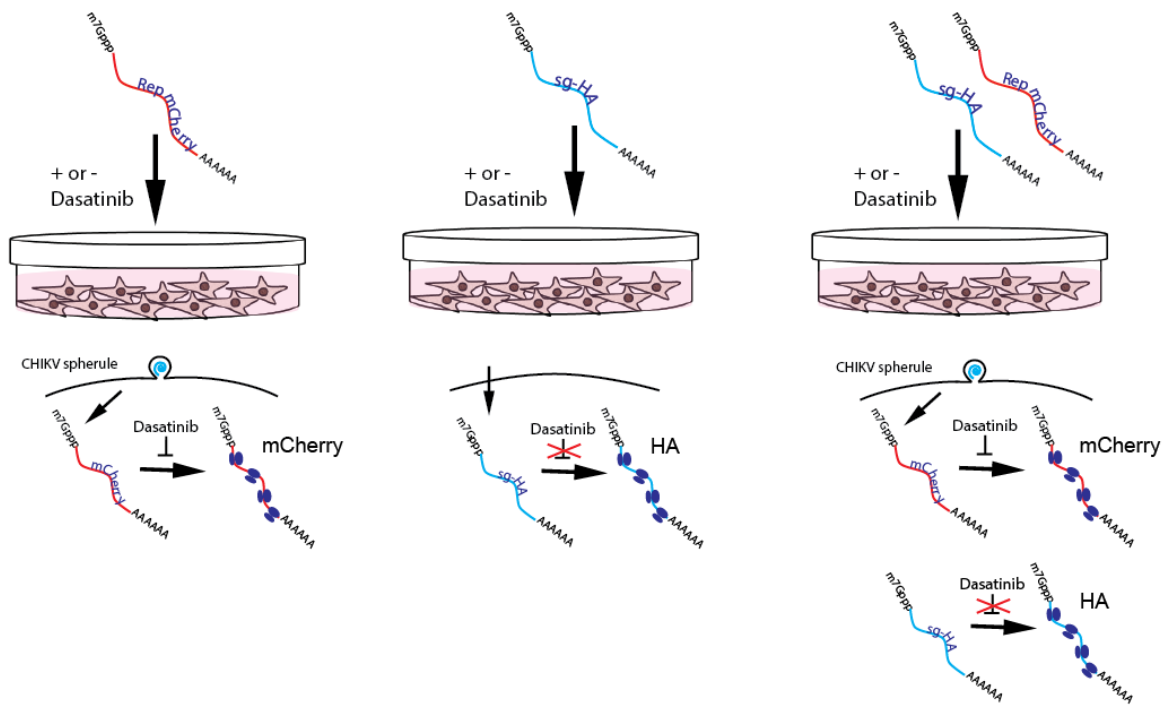


**Figure 2-9: Spherule-derived CHIKV sgRNA is blocked by dasatinib.**

NHDFs were transfected with *in vitro* capped mRNAs with lipofectamine. Left: Transfection of the mCherry replicon in the presence of dasatinib resulted in reduced mCherry levels. Center: An eGFP-HA mRNA containing the CHIKV 5'UTR was transfected into cells, but HA levels were not inhibited in the presence of dasatinib. Right: The mCherry replicon and the eGFP HA mRNA were co-transfected into NHDFs. In the presence of dasatinib, only the mCherry was reduced, while HA levels were not inhibited.

Figure generated by Rebecca Broeckel.

treatment. Consistent with previously published data, we found that CHIKV infection resulted in the induction of eIF2 $\alpha$  phosphorylation in a PKR-dependent manner. In addition, dasatinib treatment increased eIF2 $\alpha$  phosphorylation in both the parent THF cell line and PKR $^{-/-}$  THFs, suggesting that dasatinib induces eIF2 $\alpha$  phosphorylation in a PKR-independent manner. However, eIF2 $\alpha$  phosphorylation may not be relevant to the effects of dasatinib on CHIKV infection because the sgRNA does not require active eIF2. Future experiments will include important controls that confirm that these cells are deleted of PKR, show the effects of dasatinib in uninfected cells, show the relative levels of nsp3 in these cells during CHIKV infection.

Since we observed a decrease in structural protein accumulation after dasatinib treatment, we tested whether dasatinib could block translation from *in vitro* transcribed and capped mRNAs transfected into NHDFs (experiments graphically represented in **Fig 2-9**). mRNA was generated from the CHIKV 181-25 infectious clone or a CHIKV replicon (pMH42) wherein mCherry replaces the CHIKV structural gene (**Fig 2-8C**). Transfection of these mRNAs into cells results in nonstructural polyprotein production and replication complex formation, and subgenomic mRNA (sgmRNA) encoding either mCherry (replicon derived) or the viral structural proteins (infectious clones derived) are produced. mRNA-transfected NHDFs were treated with dasatinib and the production of E2 or mCherry was quantified at 20 hours post transfection (hpt) by western blotting. The levels of E2 were reduced following dasatinib treatment (**Fig 2-8D**). Similarly, a reduction in mCherry was observed in dasatinib treated cells, indicating that dasatinib efficiently blocks translation of the sgmRNA, which confirms our findings following treatment of infected cells with dasatinib described above.

To determine whether dasatinib could block sgmRNA outside of the context of the replicon, another mRNA was generated that contained the CHIKV 5' sgUTR followed by an HA-tagged version of eGFP (constructs are depicted in **Fig 2-8C**). mRNA derived from the pMH42 mCherry expressing replicon, sg-HA, or a combination of both were transfected into NHDFs with

and without dasatinib treatment. Consistent with our previous data, mCherry generated from the replicon was reduced after treatment with dasatinib (**Fig 2-8E**). In contrast, samples transfected with sg-HA mRNA demonstrated increased HA levels in the presence of dasatinib. When both mRNAs were transfected together, mCherry levels were reduced relative to replicon transfection alone, but expression of mCherry was blocked in the presence of dasatinib while HA levels were increased relative to untreated cells. These data suggest that dasatinib blocks the translation of sgRNAs generated from replicon-complexes, but does not block translation of mRNAs outside the context of a replicon or viral replication machinery (modeled in **Figure 2-9**). Though we did not specifically test the transcription of the sgRNAs in this experiment, we have confirmed previously that dasatinib does not affect transcription in a normal infection context (**Fig 5**). To test whether transcription of sgRNA was affected in the context of the transfected replicon, we could generate a qRT-PCR primer and probe set to look at mCherry expression with and without dasatinib treatment.

**Dasatinib and Torin 1 block eIF4E phosphorylation, but Rapamycin does not.**

SFKs modulate a complex array of signaling pathways, and the two major signaling pathways affected by dasatinib treatment include the Raf/MEK/Erk pathway and the Akt/mTOR pathway (444-446). The Raf/MEK/Erk pathway and the p38 MAP kinases contribute to activation of eIF4E, which is a rate-limiting factor in the translation initiation complex of capped mRNAs (447). **Fig S5A** demonstrates that Erk1/2 phosphorylation was blocked by dasatinib treatment. To test whether signaling through the Raf/MEK/Erk/MNK cascade was responsible for the reduction in viral structural protein synthesis, NHDFs were CHIKV infected and treated with U0126, a specific inhibitor of MEK1/2 (448). U0126 reduced phosphorylation of Erk1/2, but the treatment failed to affect viral titers or CHIKV E2 protein levels (**Fig S5B**). Similarly, the MNK inhibitor CGP 57380, which blocks eIF4E phosphorylation, did not block CHIKV replication (**Fig**

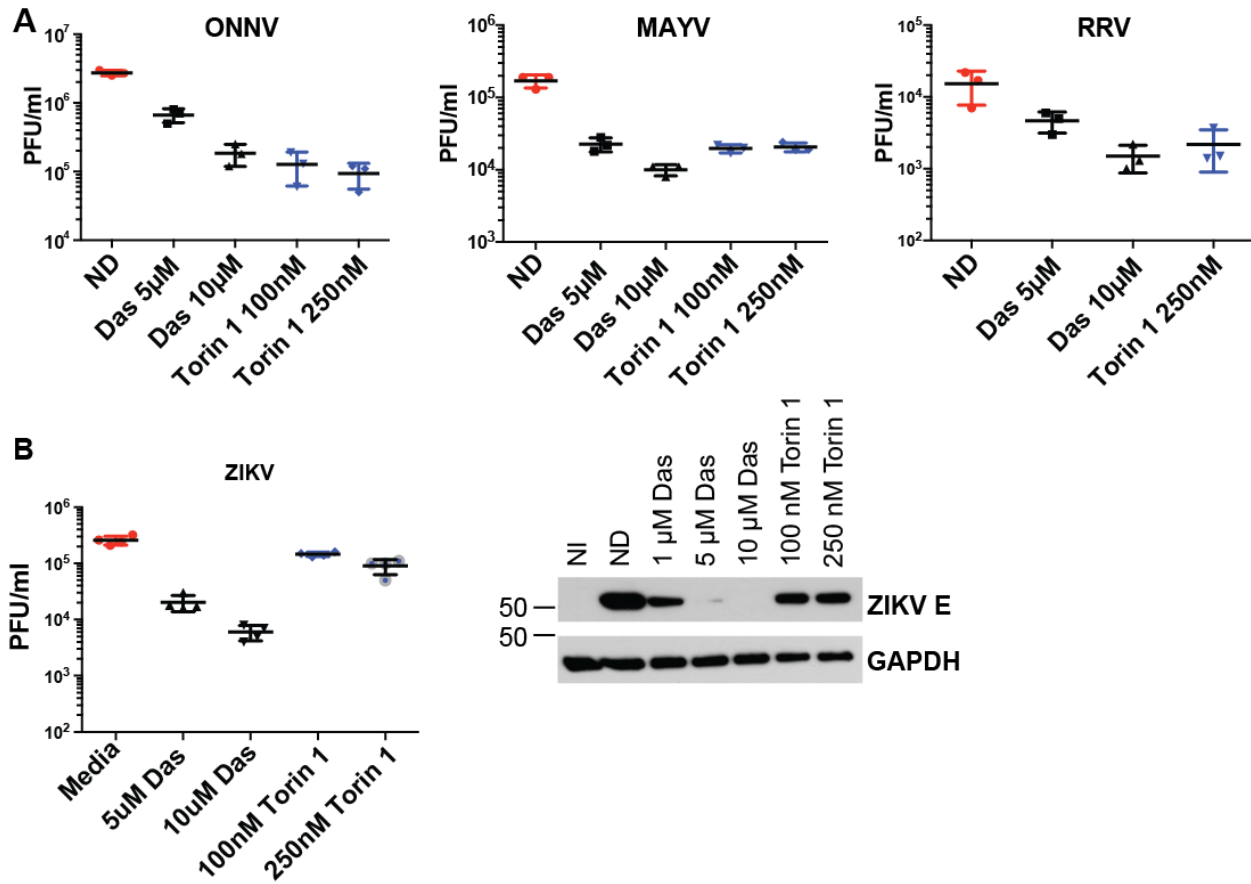


**Figure 2-10: Dasatinib inhibits MAYV, ONNV, RRV, and ZIKV replication in NHDFs.**

(A) NHDFs were infected with ONNV, MAYV, or RRV (MOI = 3) and treated with inhibitor at 2 hpi. Supernatants were collected at 24 hpi and titered on Veros (B) NHDFs were infected with ZIKV (MOI = 3) and treated with dasatinib at 2 hpi. Supernatants were collected at 48 hpi and titered on Veros. Lysates from infected cells were analyzed for ZIKV E and GAPDH by western blotting.

Data produced and generated by Rebecca Broeckel.

**2-1A)** or E2 accumulation (data not shown). This indicates that the dasatinib-mediated decrease in viral protein synthesis is most likely not related to its effects on Raf/MEK/Erk signaling.

**ONNV, MAYV, and RRV are sensitive to dasatinib and Torin 1.** We next determined the antiviral breadth of dasatinib and Torin 1. For this experiment, NHDFs infected with ONNV, MAYV, or RRV and treated with dasatinib or Torin 1. At 20 hpi, supernatants from infected cells were titered on confluent monolayers of vero cells by limiting dilution plaque assays (**Fig 2-10A**). Viral titers revealed that ONNV, MAYV, and RRV were all sensitive to dasatinib and Torin 1, suggesting that the inhibition mediated by dasatinib and Torin 1 is a broad anti-alphavirus effect. To determine if another mosquito-transmitted virus from the family *Flaviviridae* was also sensitive to both dasatinib and Torin 1, I tested the ability of these inhibitors to block Zika virus (ZIKV) replication. Dasatinib treatment of ZIKV-infected NHDFs blocked viral replication; however, Torin 1 treatment did not block ZIKV infection to the same extent as dasatinib (**Fig 2-10B**). Consistent with the viral titers, ZIKV E levels were reduced in dasatinib treated cells but only moderately decreased by Torin 1. Together these data indicate that CHIKV, VEEV, ONNV, RRV, and MAYV are sensitive to both dasatinib and Torin 1, and ZIKV likely has differential requirements of the Akt/mTOR pathways compared to the alphaviruses tested because it was sensitive to dasatinib but not Torin 1.

**Dasatinib enhances infection *in vivo*.** To determine whether dasatinib had effects on CHIKV dissemination and disease *in vivo*, we treated C57BL/6 mice with increasing doses of dasatinib (5 mg/kg, 25 mg/kg, 50 mg/kg, or 100 mg/kg) by oral gavage 1 day prior to infection and twice daily after infection (**Fig S6A**). At 5 dpi, mice were sacrificed and their tissue viral titers were measured by plaque assay. CHIKV levels increased in a dose-dependent manner in most tissues (**Fig S6B-F**). Clearly, the immunosuppressive side effects of dasatinib may preclude the ability of the drug to be used to treat CHIKV infection *in vivo*.

## 2.4 DISCUSSION

Alphaviruses are positive sense, single-stranded RNA viruses that cause persistent infection in arthropod vectors, which can be transmitted to their vertebrate hosts. Since there is no FDA-approved antiviral therapy or vaccine, treatment for alphaviruses is limited to supportive care, and there is imminent need for antiviral research. In this study, we sought to understand the importance of SFK signal transduction during alphavirus infection. We found that the SFK inhibitor dasatinib and the mTORC1/2 inhibitor Torin 1 were effective in inhibiting virus replication at the level of structural protein synthesis (summarized in **Fig 2-11**). We pursued a mechanism of SFK involvement in CHIKV replication. Our RNA analysis demonstrated that both dasatinib and Torin 1 had very minimal effects on the formation of the replication complexes or vRNA levels in CHIKV and VEEV infected cells. However, both drugs dramatically inhibited viral structural protein synthesis. Polysome profiling revealed that there were fewer CHIKV viral mRNA transcripts associated with translation-active ribosomal complexes in dasatinib treated cells relative to controls. Therefore, these results demonstrate that dasatinib-mediated inhibition of alphaviruses occurs at a step between RNA transcription and viral structural protein synthesis. We envision that the inhibition mediated by dasatinib could occur at one of the following events: 1) blocking viral sgRNA from physically transporting to translation components from the replication complex, 2) inhibiting a unique translation initiation event of the sgRNA during infection, or 3) inhibiting translation elongation factors in the context of viral infection.

Dasatinib is a broadly acting SFK inhibitor that affects several cellular processes, and many of these may be required for effective replication of CHIKV and other alphaviruses. We showed that SFK inhibition could block infection in the absence of functional interferon signaling by demonstrating that dasatinib could block CHIKV and VEEV replication in IRF3<sup>-/-</sup> and STAT1-

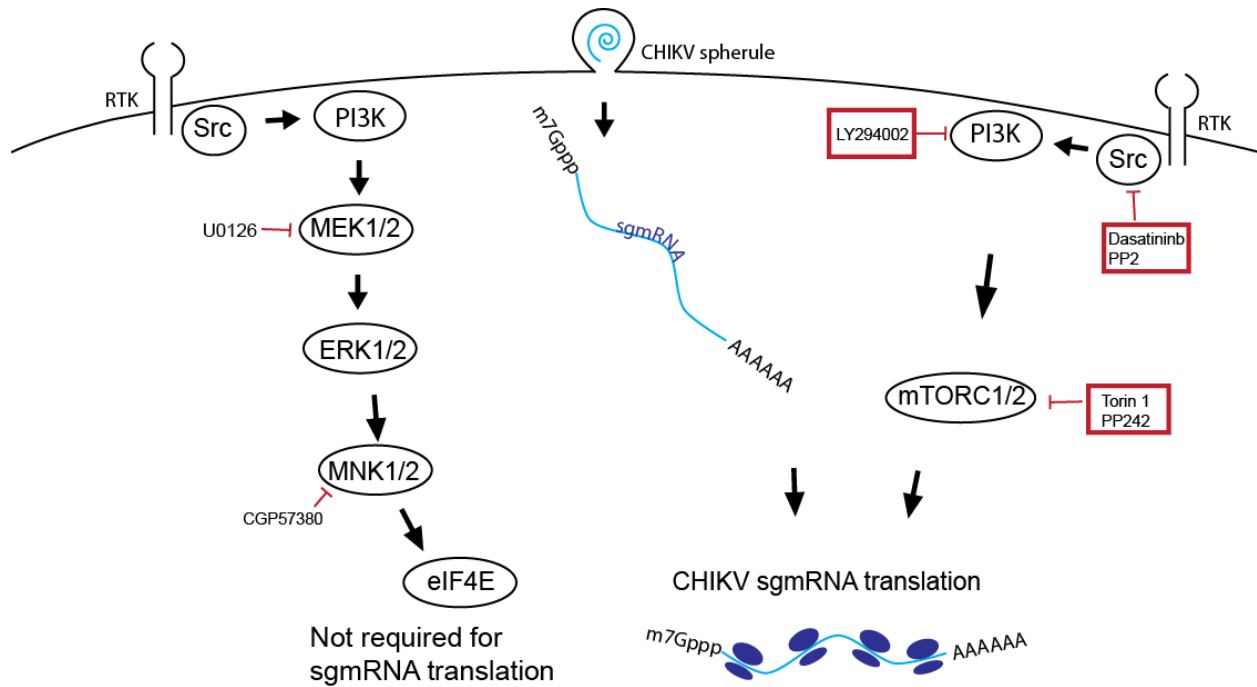


**Figure 2-11: Dasatinib and Torin 1 block translation of CHIKV sgmRNA.**

In this study, we found that CHIKV is sensitive to SFK inhibitor dasatinib, the PI3K inhibitor LY294002, and the mTORC1/2 inhibitors Torin 1 and PP242. We showed that dasatinib and Torin 1 block CHIKV sgmRNA translation. In contrast, inhibitors of the Ras/Raf/MEK/ERK pathway did not block CHIKV sgmRNA translation.

Figure generated by Rebecca Broeckel.

/- cell lines. We also demonstrated that dasatinib, unlike Torin 1, does not induce LC3-II accumulation and thus does not induce autophagy. Interestingly, we found that inhibition of autophagy by 3-MA increased E2 accumulation, suggesting that autophagy has a negative effect on viral replication, which may mean one of the mechanisms of Torin 1 inhibition of alphavirus translation and replication may involve the promotion of autophagy. However, our conclusions may contradict other reports using HEK293 cells (401), but these differences could reflect differences in cell type. Thus, our results demonstrate that dasatinib-mediated inhibition of alphaviruses is independent of IRF3- and STAT1-dependent interferon signaling and autophagy processes.

Based upon our data showing a reduction in alphavirus structural protein translation, we hypothesized that SFK signaling events were responsible for reduced translation of viral sgmRNAs. In addition to inhibiting structural protein translation during infection, dasatinib treatment also blocked replicon-derived sgmRNAs. Importantly, the replicon experiments showed that dasatinib did not block host mRNAs or *in vitro* transcribed and capped sgmRNAs in the absence of host shut off (**Fig 2-9**). These results are reminiscent of previous studies with SINV replicons showing that the translational behavior of exogenously transfected subgenomic mRNAs is different from that of subgenomic mRNAs derived from replicons (229, 241). SINV replicon-derived sgmRNAs were reported to be translated efficiently in the presence of arsenite, and that the replicon-derived sgmRNA had reduced requirements for eukaryotic initiation factor 2 (eIF2 $\alpha$ ), eIF4A, and eIF4G (238, 240). In contrast, the exogenously transfected sgmRNA was sensitive to arsenite and required eIF4G.

During alphavirus infection, translation of host mRNAs is strongly inhibited while translation of viral sgmRNAs is very efficient (225, 226, 228). Though host translation inhibition has been attributed to inactivation of eukaryotic initiation factor 2 $\alpha$  (eIF2 $\alpha$ ) by the dsRNA sensing protein kinase R (PKR), host translation is still inhibited in PKR $^{-/-}$  cells, where eIF2 is

still active, suggesting an alternative mechanism to host shutoff (228, 231). Consistent with previous findings, we showed that CHIKV induced eIF2 $\alpha$  phosphorylation in a PKR-dependent manner. In addition, dasatinib enhanced eIF2 $\alpha$  phosphorylation in PKR<sup>+/+</sup> and PKR<sup>-/-</sup> cells. eIF2 $\alpha$  is phosphorylated by one of four kinases: heme-regulated inhibitor (HRI), PKR-like endoplasmic reticulum kinase (PERK), general control non-depressible 2 (GCN2), or protein kinase R (PKR) (230). Therefore, dasatinib may induce eIF2 $\alpha$  phosphorylation through HRI, PERK, or GCN2. One hypothesis based on our results is that the virus requires eIF2 for its replication and that dasatinib tips the balance of active vs. inactive eIF2 available for the viral sgRNA. Alternatively, the virus does not require active eIF2 for translation of its sgRNA, and dasatinib is mediating another effect on the cell that blocks synthesis of viral structural proteins.

Current literature regarding translation of alphavirus sgRNA supports the theory that alphaviruses do not require active eIF2 (227, 233, 236). Sindbis virus (SINV) possesses a structural component in the 5' end of the sgRNA called a downstream loop (DLP), a G/C rich loop downstream of the capsid AUG, that promotes stalling of the ribosome and negates the need for an activated eIF2 (227, 235, 236). Other alphaviruses either possess similar DLP structures with different stabilities and stem lengths, or they have no predicted DLP-like structure (235). CHIKV, VEEV, and ONNV, for example, do not possess a predicted DLP structure, and may have a different structural feature that serves the same function as a DLP, or these alphaviruses have differential requirements for translation initiation. MAYV, however, has a predicted DLP structure, but it was still sensitive to dasatinib treatment. To further address whether the absence of a DLP contributed to inhibitory effects of dasatinib on CHIKV, we generated mutant CHIKV viruses that contain the SINV DLP, but my initial experiments showed that CHIKV E2 levels were still reduced after dasatinib treatment in the DLP mutants to the same extent as the CHIKV parent. Therefore, the effect of dasatinib on eIF2 $\alpha$  phosphorylation is probably not relevant to its inhibitory effect on CHIKV replication.

To identify an SFK-dependent signaling pathway that modulates CHIKV replication, we utilized a panel of inhibitors specific for downstream molecules of the Ras/Raf/MEK/ERK and PI3K/Akt/mTORC1 signaling pathways. We showed that treatment with U0126, an inhibitor of MEK1/2, did not affect viral protein synthesis or levels of infectious virus. This indicated that the effect of dasatinib on viral protein synthesis was mediated by another signaling event such as the PI3K/Akt/mTOR pathway. Previous studies found that mTORC1 inhibition by rapamycin and other rapalogs could enhance CHIKV replication, presumably by enhancing phosphorylation of eIF4E (400). Rapamycin inhibition of mTOR may result in feedback activation of Akt and increase eIF4E phosphorylation, while PI3K inhibitors and dual mTORC1 and mTORC2 inhibitors decrease eIF4E phosphorylation (403, 449, 450). This feedback loop could explain the discordant effects of Torin 1 and rapamycin treatments on alphavirus replication. We found, however, that CGP 57380, a MNK1/2 inhibitor that blocks eIF4E phosphorylation, did not block CHIKV replication, suggesting that eIF4E may not be necessary for translation of the CHIKV sgRNA.

Our data indicate that SFKs play a crucial role during alphavirus replication step of structural protein translation but not at the level of RNA synthesis. While a high dosage of dasatinib enhanced viral replication *in vivo*, this could be attributed to the fact that the drug is immunosuppressive since it blocks B, T and NK cell signaling (388). However, identification of the specific host factor(s) that dasatinib targets *in vitro* for activity against alphavirus structural protein translation may facilitate the development of an effective antiviral *in vivo*. Therefore, further research on these pathways will facilitate development of novel therapeutics against alphaviruses and provide insight into the replication cycle and signaling pathways in which the virus relies on in the cell.

## 2.5 MATERIALS AND METHODS

**Cells.** Normal human dermal fibroblasts (NHDF; ATCC PCS-201-012), Veros (CCL-81), Src/Yes/Fyn knockout mouse fibroblasts (451) (SYF<sup>-/-</sup>; ATCC CRL-2459), and SYF<sup>-/-</sup> reconstituted with Src (SYF + c-Src; ATCC CRL-2498) mouse fibroblasts were grown at 37°C in complete Dulbecco's modified eagle medium (DMEM; Corning) containing 5% or 10% fetal calf serum (ThermoScientific) and supplemented with 1x penicillin-streptomycin-glutamine (Life Technologies). *Aedes albopictus* C6/36 cells (452) (ATCC CRL-1660) were grown at 28°C in complete DMEM-10. STAT1<sup>-/-</sup> telomerized human fibroblasts, IRF3<sup>-/-</sup> telomerized human fibroblasts, and PKR<sup>-/-</sup> telomerized human fibroblasts were generated as previously described and grown under antibiotic selection (442). Cell viability was assessed using the CellTiter-Glo Luminescent Cell Viability Assay Kit (Promega) according to the manufacturer's instructions.

**Viruses.** Experiments with VEEV were performed with VEEV-TC83 (453). O'nyong-nyong virus (ONNV), Mayaro virus (MAYV), Ross River virus (RRV) were obtained from Dr. Robert Tesh (University of Texas Medical Branch-Galveston) and the infectious clones of Chikungunya virus (CHIKV SL15649-pMH56 and CHIKV 181/25) as well as the CHIKV replicon pMH42 were provided from Dr. Mark Heise (University of North Carolina at Chapel Hill). Virus stocks were propagated in C6/36-insect cells by infecting with a low multiplicity of infection. At 48-72 hpi (CHIKV, VEEV, MAYV, ONNV, RRV), stocks were produced by pelleting clarified supernatants through a 15% sucrose cushion by ultracentrifugation (25,000 rpm, 76,618 x g, 1.5 hrs, SW 32 Ti Rotor). Plaque forming units for all viral stocks were determined by serial dilution plaque assays on Vero cells using a carboxy-methylcellulose overlay. At 48 hpi, cells were fixed with 3.7% formaldehyde and stained with methylene blue and the plaques were enumerated to determine virus titers.

**Kinase Inhibitors.** Dasatinib, Torin 1, and Rapamycin were obtained from LC Laboratories (Boston, MA). PP242 and RAD001 were obtained from Selleckchem (Houston,

TX). PP2, U0126, and GSK 690693 were obtained from Sigma-Aldrich (St. Louis, MO). GSK 650394 was obtained from Santa Cruz Biotechnology, Inc. (Santa Cruz, CA). LY294002 was obtained from Cell Signaling (Danvers, MA). CGP 57380 was obtained from abcam (Cambridge, MA). Kinase inhibitors were diluted in dimethyl sulfoxide (DMSO) prior to use.

**Quantitative RT-PCR analysis.** Viral RNA was quantified in infected NHDFs using real-time RT-PCR. Primers and probes include: CHIKV-LR E1 fwd: GAGGTGTGGGACTGGTTGTTG, rev: CAAGTTAGTGCCTGCTGAACGA, probe: AATCGTGGTGCTATGCGT; CHIKV E1 (#2) fwd: CGGCGTCTACCCATTTATGT, rev: CCCTGTATGCTGATGCAAATTC, probe: AAACACGCAGTTGAGCGAAGCAC; CHIKV nsP2 fwd: AGAGACCAGTCGACGTGTTGTAC, rev: GTGCGCATTTTGCCTTCGTA, probe: ATCTGCACCCAAGTGTACCA; VEEV-TC83 E2 fwd: TCCCGACGCCTTGTTTAC; rev: CGCCAAAGTCGGATGAATACA; and probe: CACCGACACTTTCAGCGG. Total RNA was prepared from infected NHDFs by the Trizol method at 0, 2, 4, 6, 8, 12 and 24 hpi. The isolated RNA was quantified using a Nanodrop 2000 spectrophotometer (Thermo Scientific). RNA was treated with RNase-free DNase and then single stranded cDNA was generated using random hexamers and Superscript III RT (Invitrogen). Gene amplicons served as quantification standards (limit of detection is 10-100 copies). Quantitative RT-PCR results were analyzed using ABI StepOne Plus Real-Time PCR system (Applied Biosystems).

**RNA analysis by northern blotting.** NHDFs with and without kinase inhibitors were infected with CHIKV 181/25, and total RNA was collected at 12 hpi by the Trizol method. RNA was electrophoretically separated on a formaldehyde agarose gel and transferred onto a Hybond-N+ positively charged nylon membrane (Amersham). Probes were labeled with Digoxigenin (DIG) using the DIG DNA labeling kit (Roche). CHIKV RNA was detected using an E2-6k-E1 specific DIG probe constructed by polymerase chain reaction using the forward primer: 5'-CGCAGTTATCTACAAACGGTA-3', and reverse primer: 5'-

TTTACTCTCAGGTGTGCGA-3'. Human  $\beta$ -actin RNA was detected using a DIG probe constructed using forward primer: 5'-ACCCTGAAGTACCCCATCGA-3' and reverse primer: 5'-CGGACTCGTCATACTCCTGC-3'. Detection was performed using the DIG-High Prime DNA Labeling and Detection Starter Kit II (Roche). DIG-labeled membranes were incubated with a CSPD alkaline phosphatase chemiluminescent substrate and visualized on CL-XPosure Film (Thermo).

***In vitro* mRNA synthesis and mRNA transfections.** A CHIKV subgenomic mRNA construct expressing an eGFP-HA tag fusion protein (sg-HA) was generated as follows: the CHIKV subgenomic 5'UTR was amplified from pMH56 using the forward primer (5'-ATATAAGCTTCGTCATAACTTTGTACGGCGG-3') and reverse primer (5'-CTCCTCGCCCTTGCTCACCATTGTAGCTGATTAGTGTTTAG-3'). The eGFP-HA fragment was amplified using the forward primer 5'-CTAAACACTAATCAGCTACAATGGTGAGCAAGGGCGAGGAG-3' and reverse primer 5'-ATATGGATCCTTAGGCGTAGTCGGGCACATCGTACGGGTACTTGTACAGCTCGTCCATGC-3'. The fusion gene sg-HA was synthesized by overlapping PCR, and cloned into the pSP64 Poly(A) Vector. The 181-25 infectious clone and pMH42 were linearized with NotI (NEB), and pSP64 was digested with EcoRI (NEB). Capped and polyadenylated mRNA transcripts were generated from the linearized plasmids using the SP6 mMMESSAGE mMACHINE SP6 Transcription Kit (Thermo Fisher). Samples were digested with TURBO DNase I, and mRNAs were purified using the RNeasy Plus Mini Kit (Qiagen). mRNAs were transfected into fibroblasts using Lipofectamine MessengerMAX (Invitrogen) according to the manufacturer's instructions.

**Protein analysis.** Cells were washed with ice cold PBS and lysed with Cell Lysis Buffer (Cell Signaling) supplemented with 1 mM Phenylmethylsulfonyl fluoride (PMSF; Fisher) on ice for 15 min. Lysates were centrifuged at 4°C for 10 minutes at 13,200 rpm and the supernatant was transferred to a clean tube. The sample was boiled in Laemmli's sample buffer and

analyzed by SDS-PAGE using 4-12% Bis-Tris polyacrylamide gels (Life Technologies). Proteins were transferred onto PVDF membranes by semi-dry transfer and the blots were blocked with 5% milk or 5% Bovine Serum Albumin (BSA; Fisher) in Tris Buffered Saline with 0.1% Tween (TBST). Immunoblots were incubated with primary antibodies directed against CHIKV E2 (provided by Dr. Michael Diamond (WUSTL)), NSP3 (provided by Dr. Mark Heise (UNC)),  $\beta$ -actin-HRP conjugate (13E5), GAPDH-HRP (14C10), pS6 Ribosomal Protein (Ser235/236), S6 (5G10), p-Src Family (Y416), p44/42 Erk1/2 (Thr202/Tyr204), p-4EBP1 (236B4), 4EBP1, p-eIF4E (S209), eIF4E (C46H6) (Cell Signaling); LC3B (Sigma-Aldrich); Anti-Erk 1 (C-16), anti-LC3B, and c-Src (Src 2) (Santa Cruz); and VEEV gp and VEEV capsid (AlphaVax, Inc). Primary antibodies were diluted 1:1000 in 5% milk in TBST or 5% BSA and incubated for 1 hour at room temperature. The blots were washed with 10 volumes of TBST and then incubated for 30 minutes with horseradish peroxidase-linked secondary antibodies diluted 1:10,000 in milk/TBST or BSA/TBST. After washing, the positive bands were detected after addition of chemiluminescence reagents and visualized on CL-XPosure Film (Thermo).

**Immunofluorescence.** Cells were plated onto 4-well Lab-Tek chambered coverglass slides (Fisher) and infected as indicated. Cells were fixed with 4% paraformaldehyde for 15 minutes and washed 3 times with PBS. Cells were incubated for least 1 hour with a permeabilization buffer containing 0.2% saponin and 1% BSA. Cells were incubated overnight as indicated with anti-CHIKV E2, -VEEV gp, or -dsRNA (J2, Scicons) diluted 1:1000 in the presence of saponin and BSA. Cells were washed 3 times and incubated with goat anti-mouse Alexa Fluor 488 (abcam), DAPI, and anti-mouse Texas Red-X Phalloidin for 1 hour. Cells were washed several times visualized using a confocal fluorescent microscope.

**Translation Complex Analysis.** NHDFs were mock-infected or infected with CHIKV 181-25 (MOI = 3). At 2 hpi, media was removed and cells were washed twice with PBS. The media was replaced with or without 10 $\mu$ M Dasatinib. At 12 hpi, 0.1 mg/ml cycloheximide

(Sigma-Aldrich) was added to the media, and cells were incubated for 10 minutes. Following incubation, cells were washed twice with ice-cold PBS containing 0.1 mg/ml cycloheximide. The cells were scraped and pelleted for 10 minutes at 2,200 rpm and frozen at -80°C. Samples were loaded into ultracentrifuge tubes containing a 10-50% linear sucrose gradient cushion and spun at 35,000 x *g* for 3 hours at 4°C. The gradient was separated into 17 fractions, and RNA was isolated from each fraction and quantified by RT-PCR. The translation efficiency was calculated as the sum of CHIKV RNA in the polysome containing fractions (9 to 15) divided by the sum of CHIKV RNA in the fractions containing ribosomal subunits and monosomes (fractions 4-7) (n = 2).

**Mice.** CHIKV mouse experiments were performed in compliance with Institutional Animal Care and Use Committee (IACUC) protocols in an ABSL3 facility accredited by the Assessment and Accreditation of Laboratory Animal Care (AAALAC) International at Oregon Health and Science University. Dasatinib was prepared in a propylene glycol/water (1:1) emulsion and administered by oral gavage. C57BL/6J mice were dosed with dasatinib (5, 25, 50, or 100 mg/kg) or with the diluent 1 day prior to infection and the morning of infection (n = 7/group). Mice were challenged with 1000 pfu CHIKV SL15649 subcutaneously in the right footpad. Mice were treated with dasatinib or diluent twice daily until 5 dpi, when the experiment was terminated and tissues were collected and homogenized with Silica beads (Biospec) in RPMI. An aliquot of tissue homogenate was titered directly on Veros.

## CHAPTER 3 HUMANIZED MONOCLONAL ANTIBODY THERAPY IS EFFECTIVE AGAINST VIRAL SPREAD AND JOINT PATHOLOGY IN RHESUS MACAQUES

This chapter was completed by the following authors:

Rebecca Broeckel, Julie M. Fox, Nicole Haese, Craig N. Kreklywich, Soila Sukulpovi-Petty, Alfred Legasse, Patricia P. Smith, Michael Denton, Carsten Corvey, Shiv Krishnan, Lois M. A. Colgin, Rebecca M. Ducore, Anne D. Lewis, Michael K. Axthelm, Marie Mandron, Pierre Cortez, Jonathan Rothblatt, Ercole Rao, Ingo Focken, Kara Carter, Gopal Sapparapau, James E. Crowe Jr., Michael S. Diamond, Daniel N. Streblow.

This manuscript was published online in June, 2017. doi: [10.1371/journal.pntd.0005637](https://doi.org/10.1371/journal.pntd.0005637)

### 3.1 ABSTRACT

Chikungunya virus (CHIKV) is a mosquito-borne virus that causes a febrile syndrome in humans associated with acute and chronic debilitating joint and muscle pain. Currently no licensed vaccines or therapeutics are available to prevent or treat CHIKV infections. We recently isolated a panel of potentially neutralizing human monoclonal antibodies (mAbs), one (4N12) of which exhibited prophylactic and post-exposure therapeutic activity against CHIKV in immunocompromised mice. Here, we describe the development of an engineered CHIKV mAb, designated SVIR001, that has similar antigen binding and neutralization profiles to its parent, 4N12. Because therapeutic administration of SVIR001 in immunocompetent mice significantly reduced viral load in joint tissues, we evaluated its efficacy in a rhesus macaque model of CHIKV infection. Rhesus macaques that were treated after infection with SVIR001 showed rapid elimination of viremia and less severe joint infiltration and disease compared to animals treated with SVIR002, an isotype control mAb. SVIR001 reduced viral burden at the site of infection and at distant sites and also diminished the numbers of activated innate immune cells and levels of pro-inflammatory cytokines and chemokines. SVIR001 therapy; however, did not substantively reduce the induction of CHIKV-specific B or T cell responses. Collectively, these results show promising therapeutic activity of a human anti-CHIKV mAb in rhesus macaques and provide proof-of-principle for its possible use in humans to treat active CHIKV infections.

## 3.2 INTRODUCTION

Chikungunya virus (CHIKV) is a mosquito-transmitted, positive-sense, enveloped RNA virus. The mature virion has an icosahedral surface studded with viral glycoproteins E1 and E2 and a central capsid core, which encapsulates viral RNA (99). CHIKV causes severe, debilitating joint and musculoskeletal disease that may persist for months to years following acute infection (110, 112, 293). Over the past decade, CHIKV has caused several large-scale epidemics and expanded its geographic range to five continents. During the 2004-2007 Indian Ocean Island outbreak, CHIKV emerged from Kenya to several islands in the Indian Ocean, where infection attack rates reached as high as 75% of the population (454-456), and to India, where a suspected 1.3 million people were infected during 2006 (457). From India, the virus spread to China and Southeast Asia (264). At the end of 2013, local transmission of CHIKV occurred in the Caribbean island of Saint Martin (265). CHIKV disseminated rapidly throughout the Caribbean and to neighboring countries in Central and South America, infecting an estimated 1.8 million people in more than 40 countries (262). The recent outbreak of CHIKV in the Americas raises concern about its continued spread in this region and its introduction into new areas with large naïve populations.

In humans, CHIKV infection symptoms appear within 3 to 12 days after the bite of an infected mosquito (251). During the acute phase, humans experience arthralgias, high-grade fever, skin rash, and headaches. CHIKV-induced polyarthralgia can be debilitating, affecting many peripheral joints including the ankles, knees, wrists, and fingers (287). The elderly (>60 years) and newborns typically sustain higher viral loads (458) and are at increased risk for severe disease manifestations such as encephalitis, seizures, cardiovascular complications, and death (289, 290). During the convalescent phase of the disease, viremia, fever and rash resolve although joint and muscle pain may linger for months to years (110, 292). Continued long-term arthralgias is a common symptom, with one population-based survey reporting that

43-75% of patients experienced long-term joint pain for at least two years following CHIKV infection (105). Although infectious virus has not been recovered from joints of patients experiencing chronic pain, CHIKV RNA and antigen were detected in muscle and synovial biopsies months after the resolution of the acute symptoms (110, 459). These results suggest that CHIKV may establish a persistent infection in musculoskeletal tissue, which results in chronic joint and muscle pain. Currently there are no approved vaccines or therapies for the prevention or treatment of CHIKV.

Many of the candidate CHIKV vaccines under development rely on the induction of neutralizing antibodies for protection against challenge (353, 357, 460). In humans, prior infection and development of anti-CHIKV neutralizing antibodies have been associated with protection from reinfection, further supporting the development of antibody-based vaccines and therapeutics (335, 461, 462). CHIKV-specific IgM can be detected by day 4 of illness and CHIKV-specific IgG antibodies can be detected by day 10 (462, 463). The antibody response following CHIKV infection is directed primarily against viral glycoprotein E2 and is long-lived (464). Anti-CHIKV antibodies generated following CHIKV infection possess broad neutralizing activity against viruses belonging to different CHIKV genotypes (375, 464), and antibodies generated following infection with closely related non-CHIKV alphaviruses could have cross-neutralizing activity against CHIKV (465). Since CHIKV naturally infects nonhuman primates (NHPs) during sylvatic transmission cycles, NHPs are a relevant animal model for testing CHIKV vaccines and therapeutics and studying immunity. NHPs also develop antibodies directed against CHIKV following infection; mapping of the linear B cell epitopes showed that these antibodies were directed against several CHIKV proteins, including E2 (315, 463).

Antibody-mediated protection against CHIKV infection has been reported in animal models. Passive transfer of immune sera into susceptible neonatal mice as well as *Ifnar-/-* and AG129 mice protects against lethal CHIKV challenge (333, 334, 466, 467). Mice deficient in B

cells ( $\mu$ MT) develop a nonlethal infection with persistent viremia (303, 305), which can be prevented by passive transfer of serum-derived anti-CHIKV polyclonal antibodies (308). Neutralizing mouse monoclonal antibodies (mAbs) have protective efficacy in animal models when administered as post-exposure therapy (333, 334). Our group previously established the utility of mAb therapy for CHIKV in *Ifnar*<sup>-/-</sup> mice and in rhesus macaques (*Macaca mulatta*) (314, 334). In *Ifnar*<sup>-/-</sup> mice, passive transfer of a combination of two mouse mAbs (CHK-152 and CHK-166) against E2 and E1 proteins increased survival when given up to 60 hours post-infection. In rhesus macaques, CHK-152 and CHK-166 combination therapy at days 1 and 3 of CHIKV infection resulted in elimination of viremia and reduction of viral spread to joints and muscles of the legs. However, the viral load at the site of infection and in the draining lymph nodes were unchanged relative to controls at 7 days post infection (dpi). These results suggested that a CHIKV mAb therapeutic required further optimization to control acute infection, minimize viral persistence, and prevent long-term joint disease.

To this end, we recently isolated 4N12, a highly neutralizing human mAb, from a subject who had a history of CHIKV infection 5.5 years prior to blood donation (375). This mAb exhibited high levels of protection in *Ifnar*<sup>-/-</sup> mice, even when administered as monotherapy up to 60 hours after CHIKV infection (375). In this current study, we (Sanofi) engineered the mAb SVIR001, which was derived from the parent mAb 4N12, and characterized its therapeutic potential. SVIR001 was as effective in neutralizing CHIKV as the parent 4N12, and therapeutic administration of SVIR001 reduced viral burden in joint tissues of wild-type (WT) immunocompetent mice (experiments performed by Dr. Michael Diamond's group). In rhesus macaques, SVIR001 treatment at days 1 and 3 after infection eliminated viremia and infectious virus from tissues. SVIR001 reduced CHIKV infection at the inoculating site and blocked spread to and inflammation within distant tissue sites including joints and muscles (experiments performed by Rebecca Broeckel and Dr. Dainel Streblov's laboratory). These results in rhesus

macaques suggest the potential for SVIR001 mAb therapy to reduce CHIKV-associated inflammatory disease in humans.

### 3.3 RESULTS

**SVIR001 neutralizes infection in cell culture and in mice.** Our previous study demonstrated that combination therapy in NHPs with two mouse mAbs directed against CHIKV E1 and E2 proteins reduced spread but had limited efficacy at reducing viral burden in tissues that were infected prior to treatment (*i.e.*, arm and finger joints and muscle) (314). Our goal is to develop therapies against CHIKV that could be used during infection to reduce both viral load in tissues and clinical disease. In the current studies, we modified a previously described human mAb (4N12) that demonstrated therapeutic efficacy in immunocompromised mice (375). We (Sanofi) generated a synthetic human IgG1 kappa antibody, SVIR001, that had identical complementarity determining region amino acid sequences to mAb 4N12. The purpose of generating the synthetic antibody was to control the antibody glycosylation, which can affect the antibody effector function, and to control the plasma half-life of the antibody. To confirm that SVIR001 was functionally equivalent to 4N12, we compared their neutralization capacities directly. Both mAbs showed similar inhibitory activity to CHIKV-181/25 in Vero cells (**Fig 3-1A**); the concentration required to inhibit 50% of infection ( $EC_{50}$ ) was similar (SVIR001  $EC_{50}$  = 4.1 ng/ml (95%CI 3.2-5.1); 4N12  $EC_{50}$  = 5.0 ng/ml (95%CI: 4.3-5.9)), with no statistically significant differences.

4N12 was previously shown to bind E2, and mutagenesis of the arch domain of E2 at position D250A prevented 4N12 binding (375). To determine if the targeting epitope of SVIR001 resembles that of 4N12, CHIKV-181/25 was passaged serially six times in the presence of 10  $\mu$ g/ml of SVIR001 to obtain a virus that was resistant to SVIR001 inhibition. The escape variant was no longer sensitive to neutralization by SVIR001, whereas infection with the parent virus

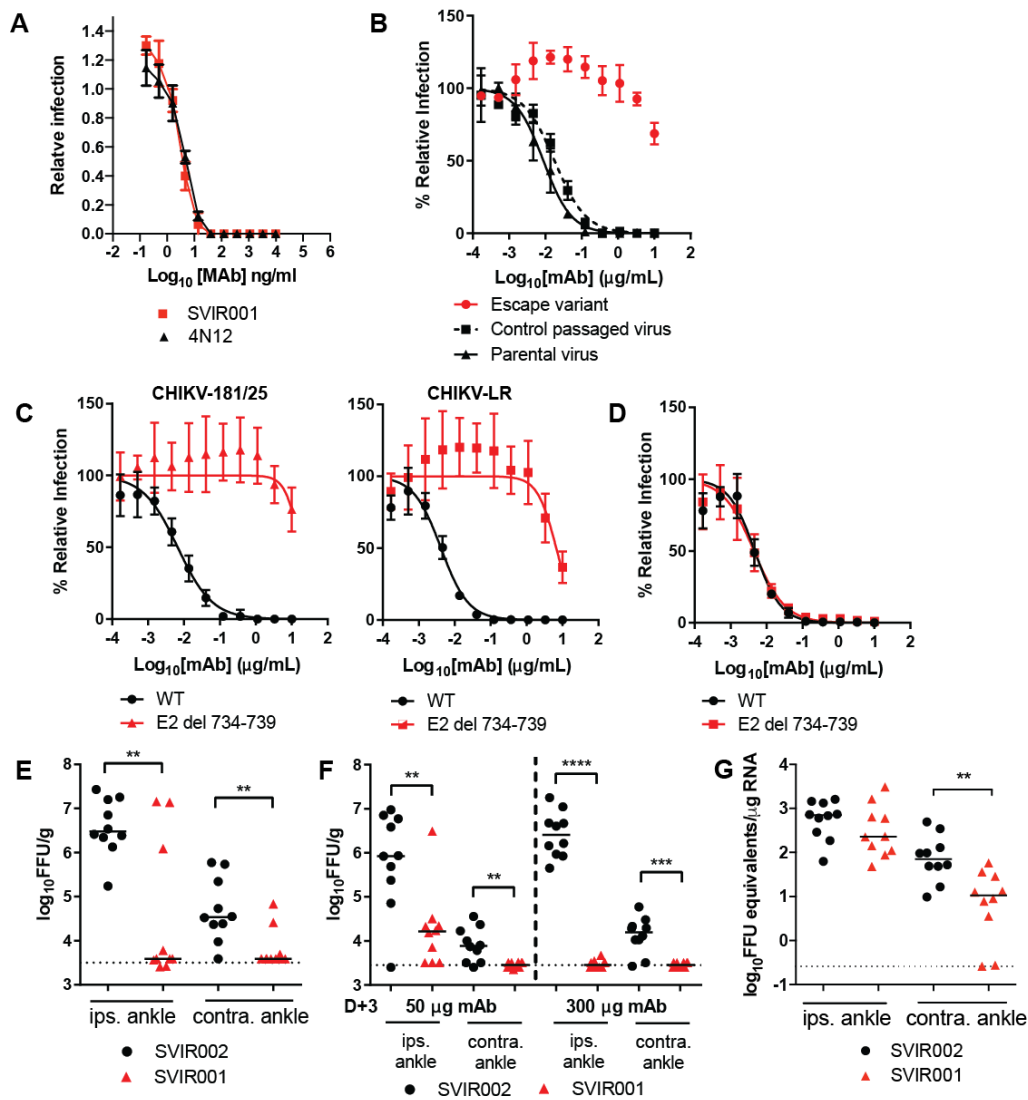


**Figure 3-1: Characterization of neutralization, escape, and therapeutic efficacy of SVIR001 in mice.**

(A) SVIR001 and parent 4N12 mAbs were evaluated by neutralization assay in Vero cells. Virus was pre-incubated with indicated concentrations of mAb for 1 h and used to inoculate Vero cells. Data are reported as the relative infection normalized to a no mAb control. Results are representative of one of three independent experiments performed in duplicate. (B) The escape variant virus, which was generated by serial passage in the presence of SVIR001, was subjected to neutralization with SVIR001 and compared to a virus passaged in the absence of SVIR001 (control passaged virus). Results are representative of one of three independent experiments performed in duplicate. (C-D) Confirmation of SVIR001 escape phenotype with engineered six nucleotide deletion (E2 del 734-739). WT or deletion CHIKV-181/25 or CHIKV-LR viruses were incubated with indicated mAb for 1 h. Virus-mAb mixture was added to Vero cells. Data was normalized to a no mAb control. Each graph is two independent experiments done in triplicate and the mean  $\pm$  SD are shown. (E-G) WT mice were inoculated subcutaneously with 10<sup>3</sup> FFU of CHIKV-LR in the footpad and treated with 50  $\mu$ g (E-F) or 300  $\mu$ g (F-G) of anti-CHIKV mAb SVIR001 or control mAb SVIR002 at 1 (E), 3 (F), or 3 and 10 (G) dpi. At 3 (E), 5 (F), or 28 (G) dpi, virus was quantified by infectious focus (E-F) or qRT-PCR (G) assays from the ipsilateral and contralateral ankle to determine therapeutic efficacy. The median value is shown with the limit of detection indicated by the dotted line. Statistics were calculated on log-transformed data using the Mann-Whitney test (\*\*,  $P < 0.01$ , \*\*\*,  $P < 0.001$ , \*\*\*\*,  $P < 0.0001$ ). Each data point represents an individual animal. The data (E-G) were pooled from 2 independent experiments.

This figure was produced by Julie Fox in the laboratory of Michael Diamond.

was neutralized by SVIR001 (**Fig 3-1B**). Sequencing of the gene encoding E2 of the SVIR001 escape variant virus revealed a six nucleotide deletion in E2 (nucleotides 734-739). The deletion resulted in substitution of amino acids 245-247 with a single lysine residue (NAE → K) (**Fig S-7A**). This deletion is adjacent to Asp250, which is important for 4N12 binding to E2, suggesting that SVIR001 has a similar antigen binding site to 4N12. This six nucleotide deletion has not been noted to occur naturally, as determined by an alignment of 300 complete genome sequences of CHIKV (<http://www.viprbrc.org>). To confirm the escape mutation, the deletion was engineered into the CHIKV-181/25 and CHIKV-LR infectious clones (E2 del 734-739) (**Fig S-7B-C**). The 181/25 and LR E2 del 734-739 viruses were resistant to SVIR001, whereas the WT viruses were neutralized by SVIR001 (**Fig 3-1C**). The LR E2 del 734-739 and WT viruses however, were neutralized equivalently by a different human anti-CHIKV mAb (1H12), which bound domain A, B, and arch domain of E2 (**Fig 3-1D**) (375). This result suggested that the six-nucleotide deletion did not cause widespread effects on E2 folding, and that possible changes in particle-to-plaque forming unit (PFU) ratio between the WT and mutant virus did not influence neutralization efficiency. These data suggest that SVIR001 and 4N12 bind to the same region of E2 and possess similar neutralizing profiles *in vitro*.

Prior studies suggest that the parent mAb 4N12 was effective at mitigating CHIKV-induced morbidity and mortality in infected *Ifnar*<sup>-/-</sup> mice (375). To assess the *in vivo* therapeutic efficacy of SVIR001, we used a 4 week-old WT mouse model of CHIKV infection in which animals are inoculated subcutaneously in the foot and virus replicates preferentially in musculoskeletal tissues (303), as seen in humans. In initial therapeutic studies, we treated CHIKV-infected WT mice one day post-inoculation (1 dpi) with 50 µg (~3.3 mg/kg) of SVIR001 or control SVIR002 via an intraperitoneal route and measured infectious viral burden in the ipsilateral and contralateral ankles at 3 dpi. Treatment with SVIR001 resulted in significantly lower viral titers in both tissues (**Fig 3-1E**). We extended the window of treatment and

administered a single dose of either 50 or 300  $\mu\text{g}$  (3.3 to 20 mg/kg) at 3 dpi and analyzed viral burden at 5 dpi. SVIR001 treatment significantly reduced viral load in the ipsilateral and contralateral ankles at 5 dpi (**Fig 3-1F**). Moreover, treatment with 300  $\mu\text{g}$  (20 mg/kg) of SVIR001 at 3 and 10 dpi also resulted in lower levels of CHIKV RNA in the contralateral ankle in the chronic phase, at 28 dpi (**Fig 3-1G**). Collectively, the protective activity of SVIR001 in WT mice demonstrates its feasibility as a post-exposure therapeutic for CHIKV (375).

**SVIR001 reduces viral burden in CHIKV-infected rhesus macaques.** To further characterize the efficacy of SVIR001, we used a rhesus macaque model of CHIKV infection (149, 314). Animals were inoculated subcutaneously with a total of  $10^7$  PFU of CHIKV-LR divided over 10 injection sites (5 per arm). Following infection, animals displayed erythema and swelling of arm joints (especially the wrist) beginning at 1 to 2 dpi that lasted until 5 dpi. The affected joints were warm to the touch compared to unaffected areas, indicating active inflammation. Most animals developed a maculopapular rash, and upper extremity edema that was consistent with previous experiments in NHPs (149, 312). This effect occurred irrespective of treatment group and the degree of the rash and swelling appeared different for each individual monkey. At day 1 and 3 of infection, animals received CHIKV mAb SVIR001 (5 or 15 mg/kg) or isotype control antibody SVIR002 (15 mg/kg) diluted in saline by intravenous infusion (**Table 3-1**).

Rhesus macaque infection with CHIKV results in viremia that is detectable at day 1 and lasts for about 3 to 4 days (149, 314). To determine the effects of SVIR001 on viremia, blood was collected on 0, 1, 2, 3, 4, 5, and 7 dpi. The blood drawn on day 1 and 3 after infection occurred prior to antibody administration. Human antibody levels were measured at all time points by ELISA; all animals were positive for human anti-CHIKV (SVIR001) or anti-lysozyme antibodies (SVIR002) after the first i.v. treatment (**Fig 3-2A**). Antibody levels peaked at 2 and 4

mAb	Dose (mg/kg)	Animal	Tissue Virus Isolation
<b>SVIR002 (anti-lysozyme control)</b>	15	31559	Spleen, Finger Joints
		31055	Finger Joints
		31289	Wrist Joints
		31333	Elbow & Wrist Joints, Hamstring
<b>SVIR001 (anti-CHIKV)</b>	15	31078	Negative
		31296	Negative
		31312	Negative
		31302	Negative
	5	31088	Negative
		31335	Negative
		30430	Negative
		31651	Negative

**Table 3-1: CHIKV isolation from tissue homogenates.**

Three groups of four animals each were treated with control antibody SVIR002 at 15 mg/kg, SVIR001 at 15 mg/kg, or SVIR001 at 5 mg/kg. To isolate CHIKV from the infected joint and muscle tissues an aliquot of tissue homogenate was incubated in C6/36 cells for four days. Following incubation, infectious virus was recovered by plaque assay on Vero cells. Only the virus isolation-positive tissues are listed. The limit of detection was 1 PFU per ml of C6/36 supernatant.

Virus isolation and plaque assays performed by Rebecca Broeckel, table generated by Daniel Streblow and Rebecca Broeckel.

dpi after the first and second antibody administration, respectively. The SVIR001 and SVIR002 15 mg/kg dose groups had similar peak plasma human antibody levels at 2 dpi ( $208 \pm 26 \mu\text{g/ml}$  and  $269 \pm 88 \mu\text{g/ml}$ , respectively) and at 4 dpi ( $333 \pm 110 \mu\text{g/ml}$  and  $420 \pm 114 \mu\text{g/ml}$ , respectively). As expected, the group receiving 5 mg/kg SVIR001 had lower plasma human antibody levels at 2 and 4 dpi compared to the 15 mg/kg groups ( $52 \pm 33 \mu\text{g/ml}$  and  $100 \pm 68 \mu\text{g/ml}$ , respectively). Plasma viral load in the presence of the control antibody SVIR002 was high at 1 dpi and peaked at 2 dpi (**Fig 3-2B**). The levels began to drop at 3 dpi with little residual virus detected at 5 and 7 dpi. Plasma from the animals treated with SVIR001 had high levels of CHIKV at 1 dpi, and levels dropped to an undetectable range at 2 dpi following treatment and remained undetectable through day 7. Only one SVIR001-treated animal had any detectable virus at 5 dpi, and the level was near the detection limit of the assay.

In NHP, CHIKV rapidly disseminates (within 2 days) from the initial site of infection, and is present in many tissues at 7 dpi, including joint and musculoskeletal tissues, lymph nodes, spleen, heart, lung, and kidney (314). To demonstrate the efficacy of the mAb treatment on virus infection and dissemination, animals were euthanized at 7 dpi for tissue viral load analysis. In contrast to control-treated animals, where infectious virus was isolated from the tissue of at least one joint of all animals, infectious virus was not recovered from any tissue in animals receiving anti-CHIKV mAb (**Table 3-1**). Viral RNA levels in tissues were reduced in the SVIR001 anti-CHIKV mAb treated animals compared to controls in the arm joint tissues and muscles (**Fig 3-3A**). The reduction of viral RNA in the arms following SVIR001 therapy was superior to previous results with a combination of anti-CHIKV mAbs, which failed to lower viral loads in the arms of infected macaques (314). Animals treated with 15 mg/kg SVIR001 had reduced viral load in finger joints ( $1.1 \times 10^4 \pm 5.8 \times 10^3$  vs.  $4.8 \times 10^2 \pm 1.0 \times 10^2$  copies/ $\mu\text{g}$ ;  $P < 0.04$ ) and elbow joints ( $6.8 \times 10^4 \pm 1.1 \times 10^5$  vs.  $1.5 \times 10^3 \pm 2.8 \times 10^3$  copies/ $\mu\text{g}$ ;  $P < 0.002$ ). CHIKV infection in the

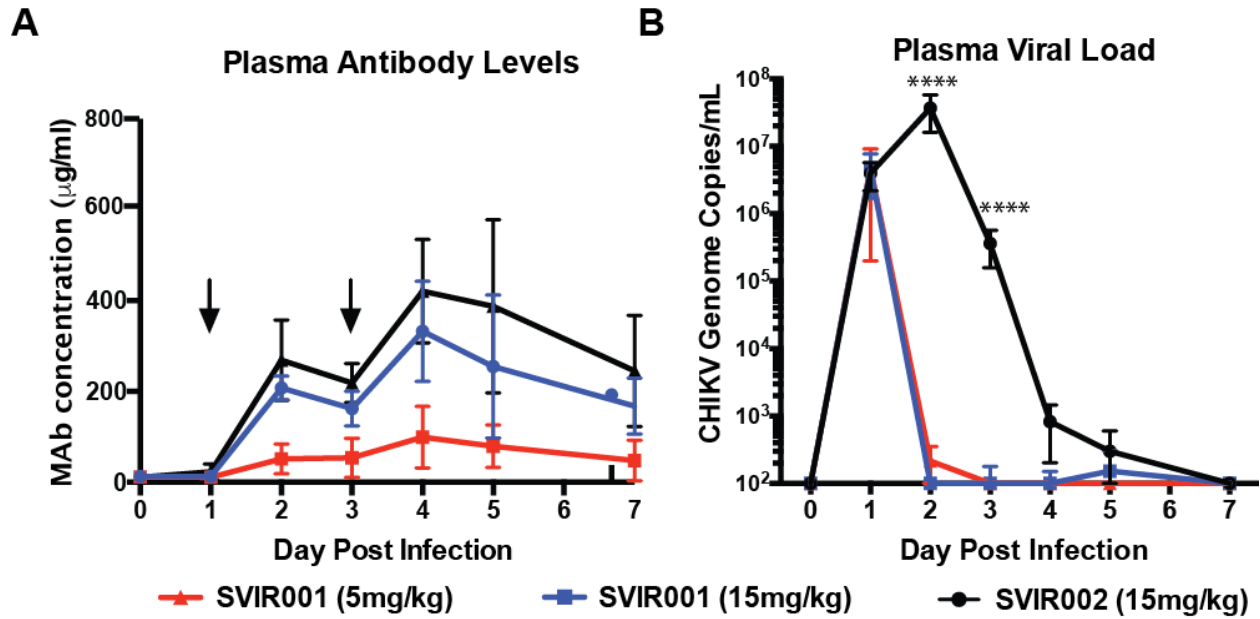
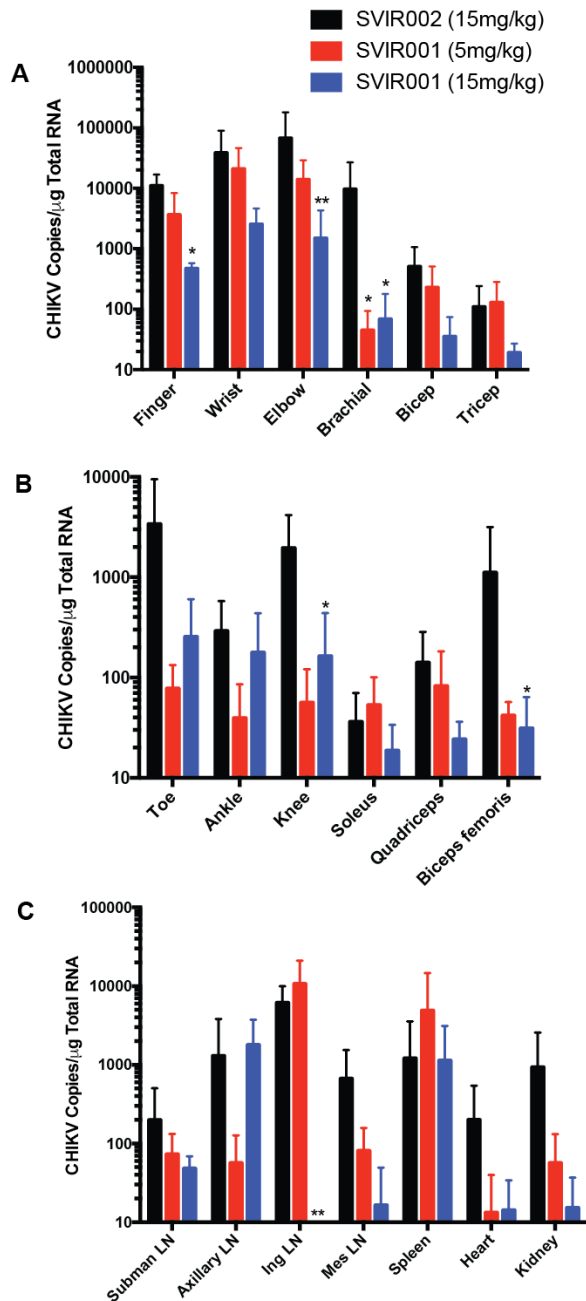


**Figure 3-2: Plasma antibody levels and viral load following CHIKV mAb therapy.**

Rhesus macaques were inoculated subcutaneously in both arms with  $1 \times 10^7$  PFU of CHIKV LR. On day 1 and 3 after infection, rhesus macaques were administered 5 or 15 mg/kg SVIR001 (human anti-CHIKV mAb) or 15 mg/kg SVIR002 (human anti-lysozyme mAb),  $n = 4$ /group. Blood was collected on 0, 1, 2, 3, 4, 5, and 7 dpi. **(A)** Human mAb concentration in the plasma was measured by ELISA with lysozyme or CHIKV virions, and mAb concentration was calculated using a standard curve. Statistical significance was calculated using Tukey's multiple comparison test ( $n = 4$ ; \*\*\*,  $P < 0.0005$ , \*\*,  $P < 0.01$ , \*,  $P < 0.05$ ). **(B)** Virus was quantified from plasma by qRT-PCR. Statistically significant differences are reported on the log-transformed data using Dunnett's multiple comparison test ( $n = 4$ ; \*\*\*\*,  $P < 0.0005$ ).

Panel A generated and analyzed by Rebecca Broeckel. Panel B was performed by Craig Kreklywich and data analyzed by Daniel Streblow.



brachial muscle was reduced in both SVIR001 treatment groups ( $9.7 \times 10^3 \pm 1.7 \times 10^4$  vs.  $45 \pm 49$  and  $69 \pm 1.1 \times 10^2$  copies/ $\mu$ g, respectively;  $P < 0.03$ ). Infection also was reduced at distant musculoskeletal sites by the anti-CHIKV mAb compared to control-treated animals. Viral load was decreased in the 15 mg/kg SVIR001 treatment group in the knee ( $2.0 \times 10^3 \pm 2.2 \times 10^3$  vs.  $1.6 \times 10^2 \pm 2.8 \times 10^2$  copies/ $\mu$ g;  $P < 0.03$ ) and biceps femoris muscle ( $1.1 \times 10^3 \pm 2.0 \times 10^3$  vs.  $31 \pm 33$  copies/ $\mu$ g;  $P < 0.03$ ) (**Fig 3-3B**). We also observed a reduction of viral load in submandibular lymph nodes, inguinal lymph nodes, mesenteric lymph nodes, heart, and kidney (**Fig 3-3C**). In some tissues there was an SVIR001 concentration-dependent decrease in viral loads with a greater impact seen with the higher 15 mg/kg dose. This effect was most evident in the joint tissues of the arms. Similarly, viral loads in the inguinal lymph nodes were undetected with high dose treatment of SVIR001, which is consistent with the overall reduction of infection in the legs ( $6.2 \times 10^3 \pm 3.8 \times 10^3$  vs.  $3.3 \pm 6.5$  copies/ $\mu$ g;  $P < 0.004$ ). No effect of treatment on CHIKV RNA levels was observed in the spleen, as was seen previously (314). These results establish the efficacy of SVIR001 therapy in reducing tissue viral load at the site of infection and spread to distant sites. Measuring virus by plaque assay is the ideal measurement because it is a measure of infectious, replicating virus. However, there are high levels of variability with the plaque assay that can be resolved by measuring viral burden by qRT-PCR.

**SVIR001 inhibited CHIKV-associated inflammation.** To evaluate the impact of anti-CHIKV mAb treatment on cellular infiltration into the joints, tissue sections were analyzed from animals in each treatment group at 7 dpi by pathologists blinded to treatment groups. Sections consisted of the soft tissue from the finger, wrist, elbow, toe, ankle, and knee joints bilaterally. The animals treated with the control mAb SVIR002 had a higher average cumulative score (average score 10.75) with more inflammation in affected joints and higher numbers of joints affected within individuals (**Table 3-2, S-3 Table**). Sections from animals treated with 5 mg/kg

mAb	SVIR002	SVIR001	SVIR001
	(15 mg/kg)	(15 mg/kg)	(5 mg/kg)
Right finger	1.5	1	0.25
Left finger	1.5	0.75	0.25
Right wrist	0.5	0.25	0.25
Left wrist	0.75	1.25	1
Right elbow	0.25	0.25	0.75
Left elbow	1.5	0.75	0.25
Right toe	0.5	0	0
Left toe	0.75	0	0
Right ankle	0.5	0	0
Left ankle	0.75	0.25	0
Right knee	1.25	0	0.25
Left knee	1	0.25	0.25
<b>Total score</b>	<b>10.75</b>	<b>4.75</b>	<b>3.25</b>
<b># joints affected</b>	<b>7.75</b>	<b>3.75</b>	<b>3</b>

**Table 3-2: Histological Findings in Joint Tissues at 7 dpi.**

Each joint was evaluated for the presence of perivascular infiltrates of lymphocytes, histiocytes and plasma cells in hematoxylin and eosin stained microscopic sections and assigned a score between 0-3. A score of 0 indicates no evidence of inflammation; 1 indicates few perivascular infiltrates forming one layer and affecting three vessels or less; 2 indicates perivascular infiltrates forming one to three layers and affecting more than three vessels; 3 indicates perivascular infiltrates forming four or more layers. The average score for each treatment group is reported (n = 4). See **S3 Table** for the scores for each animal.

Joint evaluations performed by Louis Colgin, Rebecca Ducore, and Anne Lewis. Table prepared by Rebecca Broeckel.

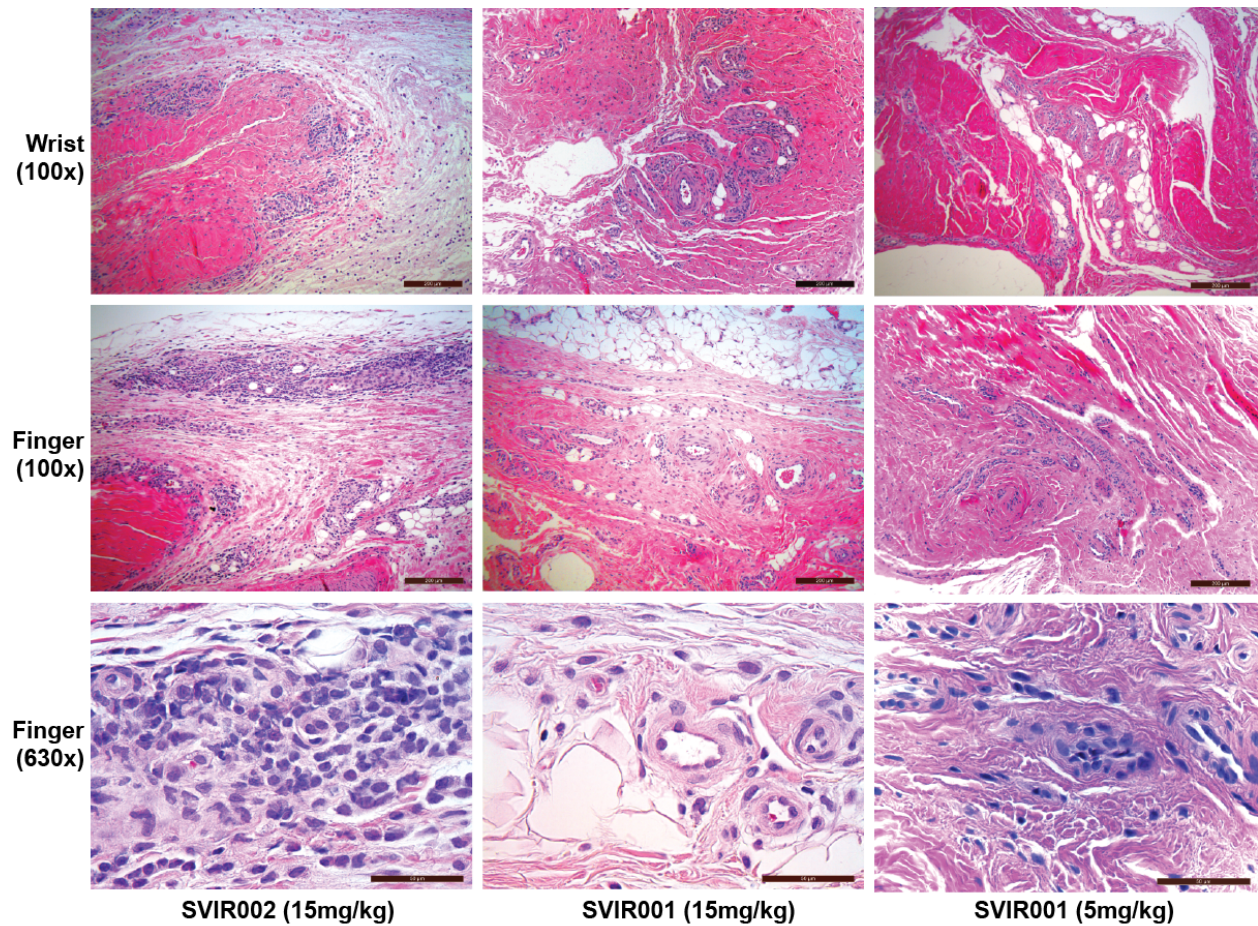


**Figure 3-4: Histological images of joint-associated tissue from CHIKV-infected animals at 7 dpi.**

At 7 dpi, joint-associated tissue from the wrist and finger of each animal were fixed, paraffin embedded, sectioned, and stained with hematoxylin and eosin. Shown are representative images of stained sections from joint-associated soft tissue of four animals treated with control antibody SVIR002 or CHIKV mAb SVIR001. In the SVIR002 treated animals, there was abundant inflammation surrounding multiple vessels. In the SVIR001 treated animals (5 or 15 mg/kg dose), there was limited or no perivascular inflammation.

Images generated by Anne Lewis. Figure assembled by Rebecca Broeckel.

(average score 3.25) and 15 mg/kg (average score 4.75) of SVIR001 had less inflammation within affected joints and fewer joints affected (**Fig 3-4**). Collectively, these results suggest that in rhesus macaques, SVIR001 therapy reduced viral load in the periphery and thereby prevented or diminished acute inflammation in musculoskeletal tissues infected with CHIKV.

To understand the basis for reduced cellular inflammation conferred by SVIR001 treatment, we measured chemokine and cytokine levels in plasma over time on days 0, 1, 2, 3, 5, and 7 following CHIKV infection using a quantitative 29-plex cytokine magnetic bead assay. In the control antibody treatment group, there was a significant increase in plasma levels of IL-1 $\beta$ , G-CSF, IL-6, Eotaxin, MIP-1 $\alpha$ , MCP-1, HGF, IFN $\gamma$ , I-TAC, MIF, IL-1RA, IP-10, and MIG at 2 dpi (**Fig 3-5 and Fig S-10**), which coincides with peak viremia. However, plasma from the groups that received CHIKV mAb therapy did not show increased levels of these cytokines and chemokines at 2 dpi. In comparison, plasma levels of FGF-basic, IL-10, IL-12, RANTES, IL-17, GM-CSF, MIP-1 $\beta$ , IL-15, EGF, IL-5, VEGF, MDC, TNF $\alpha$ , IL-2, IL-4, and IL-8 were either undetectable or without differences between the treatment groups (**Fig S-10**). The decrease of plasma cytokine/chemokine induction at 2 dpi in the SVIR001-treated animals could account in part for the reduction in joint tissue cell infiltration and inflammation. One way to test this is to administer general anti-inflammatory drugs such as tofacitinib and look for changes in cellular infiltration into the infected tissues. However, we did not test this directly in this study.

We next assessed whether there were differences in levels of activated monocyte/macrophages, DCs, or NK cells in blood associated with SVIR001 treatment. PBMCs were stained with antibodies against the cell surface markers HLA-DR, CD14, CD169, CD11c, CD20, CD3, CD8, and CD16, and subsets were defined (**Fig S-9**). In all treatment groups, we observed an increase in activation of monocyte/macrophages and myeloid DCs as reflected by CD169<sup>+</sup> staining peaking at 2-3 dpi followed by a steady decrease, returning to nearly baseline

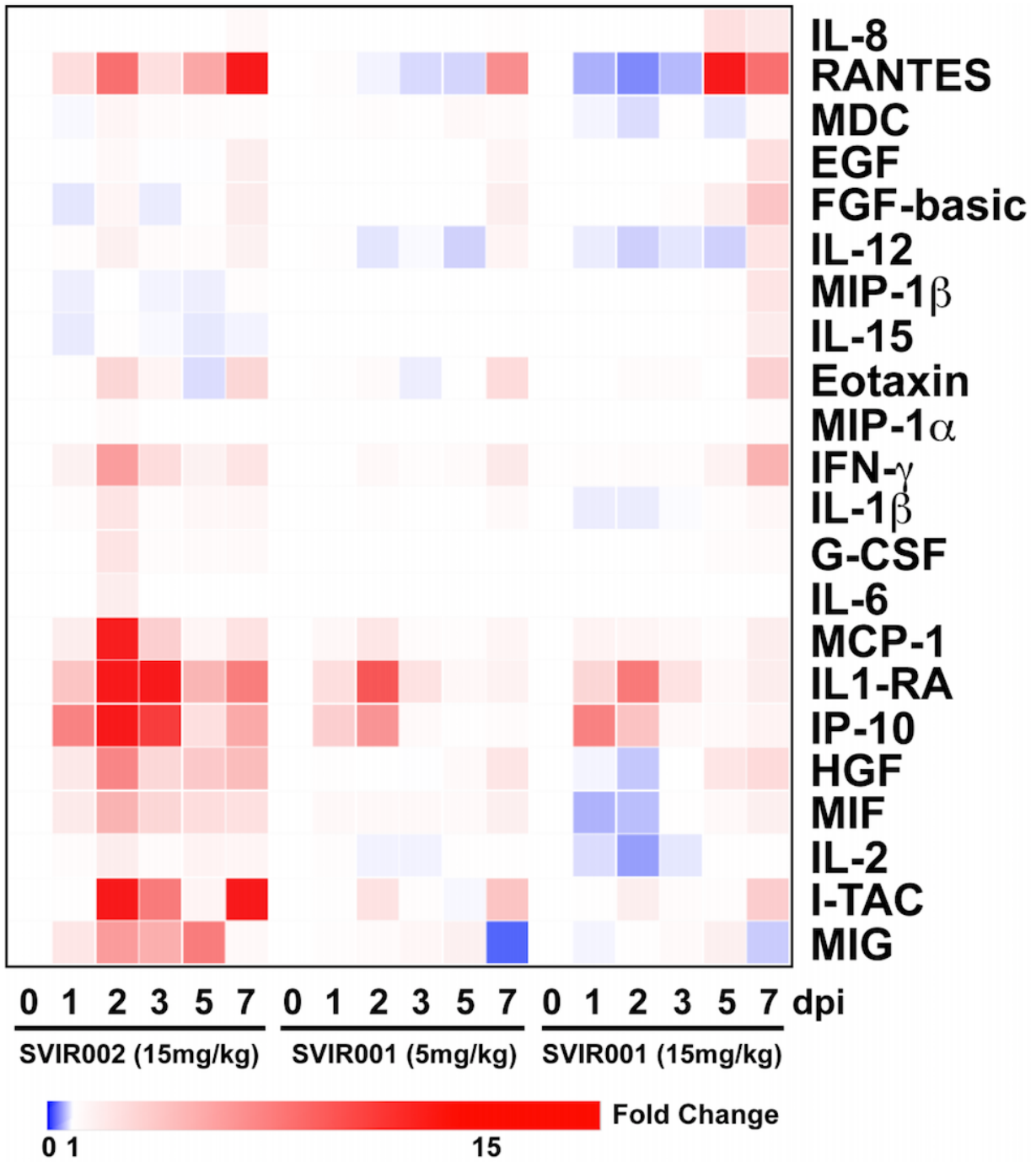


**Figure 3-5: CHIKV mAb therapy reduced plasma cytokines and chemokine activation at 2 dpi.**

Heat map comparing average fold-change in plasma cytokine profiles for NHP treated inoculated with CHIKV and treated with control antibody SVIR002 or CHIKV mAb SVIR001. Clustering was performed using the Broad Institute's webtool Morpheus. A 29-plex-cytokine magnetic bead assay was performed on plasma from rhesus macaques isolated at day 0, 1, 2, 3, 5, and 7 post-infection.

Data generated and analyzed by Rebecca Broeckel. Figure prepared by Rebecca Broeckel and Daniel Streblow.

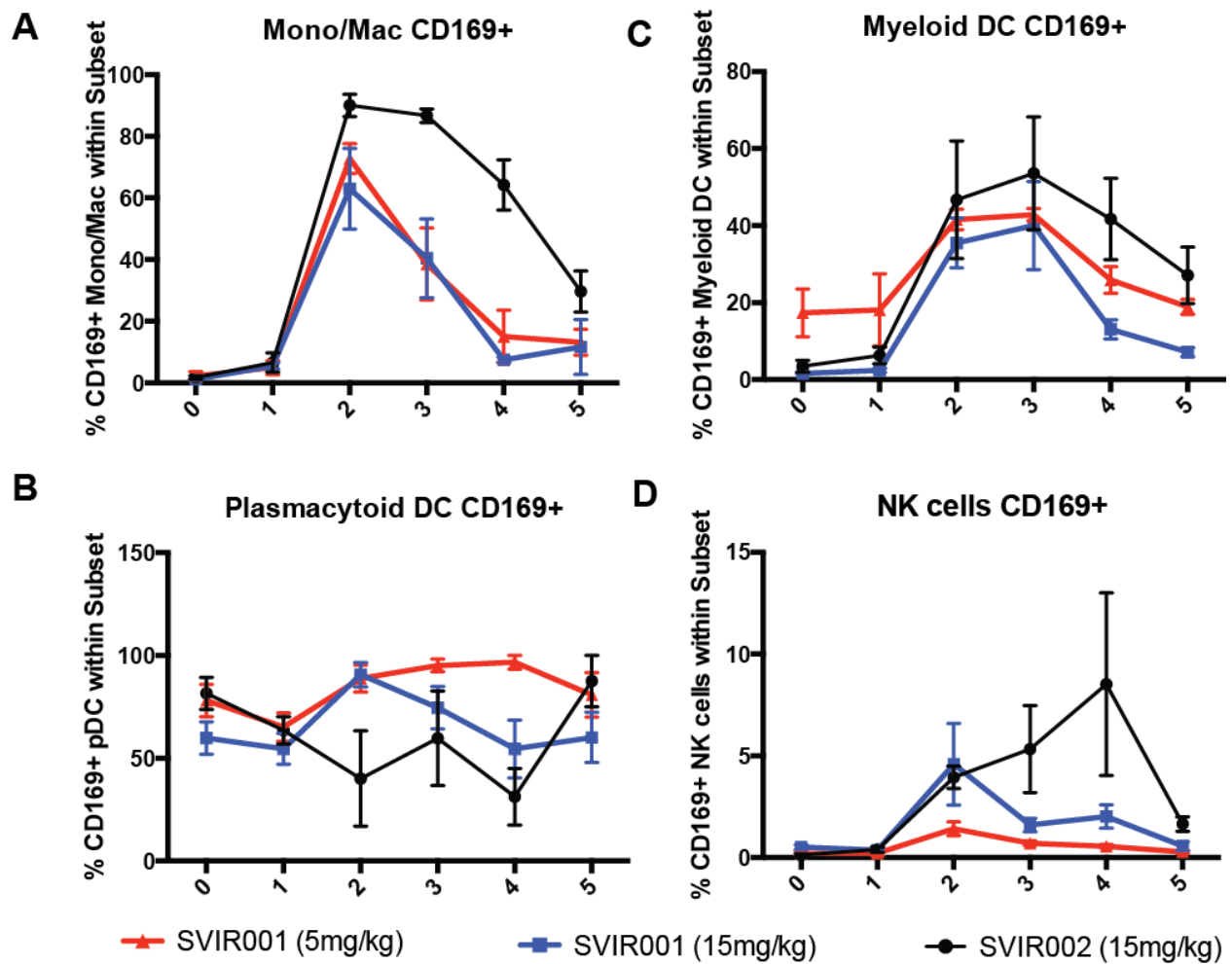


**Figure 3-6: CHIKV mAb therapy reduced activation of peripheral blood monocytes/macrophages, Myeloid DCs, and NK cells.**

Total peripheral blood mononuclear cells from 0, 1, 2, 3, 4 and 5 dpi were stained with antibodies directed against HLA-DR, CD14, CD169, CD11c, CD20, CD3, CD8, and CD16 to assess changes in the activation of macrophage/monocyte, DC, and NK cell subsets. The percent of activated, CD169<sup>+</sup> (A) monocyte/macrophages, (B) plasmacytoid DCs, (C) myeloid DCs, or (D) NK cells within the population are reported (n = 4).

Data generated by Nicole Haese.

levels (**Fig 3-6A**). However, the number of activated monocytes/macrophages and mDCs was higher and endured longer in the control mAb-treated (SVIR002) compared to SVIR001-treated animals (**Fig 3-6A-C**). Similarly, NK cell activation (CD169<sup>+</sup> staining) was sustained in the control-treated compared to anti-CHIKV antibody-treated animals (**Fig 3-6D**). These results, together with decreased plasma levels of inflammatory chemokines and cytokines and decreased cellular infiltration into the joints of SVIR001 treated animals, suggest that SVIR001 therapy reduced viral burden and consequently inhibited cellular and soluble mediators of inflammation.

**SVIR001 treatment did not diminish anti-CHIKV adaptive immunity.** We next determined whether anti-CHIKV mAb therapy altered lymphocyte mobilization and function. Flow cytometry was used to assess changes in frequency and phenotype of lymphocytes in blood during the course of infection. PBMCs were stained with CD4, CD8, CD95, and CD28 markers to differentiate naïve (NV), central memory (CM), and effector memory (EM) T cell subsets. Subsequently, the cells were stained with antibodies against Ki67 to determine the proportion of proliferating T cells. The gating strategies used to define the T cell subsets and phenotypes are shown in **Fig S-8**. Over the course of CHIKV infection, we observed an increase in proliferation of all CD4<sup>+</sup> T cells subsets (NV, CM, and EM) with the maximal level observed at 7 dpi (**Fig 3-7A-C**), as seen previously in NHPs (149). We did not observe a significant difference in T cell phenotype or proliferation status between the SVIR001 and SVIR002 treated animals. Similar to the CD4<sup>+</sup> T cell proliferative response, Ki67<sup>+</sup>CD8<sup>+</sup> T cell subsets from both SVIR001- and SVIR002-treated animals increased throughout infection and the maximal level was observed at 7 dpi (**Fig 3-7D-F**). Thus, treatment with SVIR001 did not negatively impact the generation of T cell proliferative responses despite reducing the viral antigen burden. We also did not observe differences in B cell proliferative responses between treatment groups (**Fig S11**).

The functionality and frequency of the CHIKV-specific T-cell responses in the peripheral blood was measured using an IFN $\gamma$  ELISpot. PBMCs isolated at 7 dpi were stimulated with overlapping peptide pools for the nine different CHIKV proteins (149), inactivated whole virus (iCHIKV), or PMA/ionomycin as a positive control. CHIKV-reactive T cells were present in animals from both the control mAb (SVIR002) and anti-CHIKV mAb (SVIR001) treatment groups (**Fig 3-7G**). We did not observe significant differences between the two groups, suggesting that the antibody treatment did not affect the breadth of the CHIKV-specific T cell response at 7 dpi. These results, along with the T cell proliferation profiles, suggest that SVIR001 treatment did not negatively impact the generation of anti-CHIKV specific T cell responses. Thus, an immunotherapeutic mAb against CHIKV can reduce viral loads and prevent CHIKV-induced joint disease without a detectable effect on the induction of antiviral adaptive immunity, which would prevent disease associated with a second infection.

### 3.4 DISCUSSION

CHIKV is a clinically relevant re-emerging alphavirus that causes chronic polyarthritis and even death in certain immunocompromised or elderly populations. In the current studies, we determined the efficacy of SVIR001, a fully human anti-CHIKV immunotherapeutic in mouse and rhesus macaque models. In WT mice, recombinant antibody substantially reduced levels of infectious virus from ankle tissues when given at 1 or 3 dpi, and reduced levels of persistent viral RNA in some joint tissues at 28 dpi. In NHPs, SVIR001 aborted CHIKV viremia, prevented its spread to distal joints and muscle, and reduced viral RNA loads in the hands and arms, the initial sites of infection. This feature of reducing viral loads in the joints of the arm was not observed in a previous study with two mouse anti-CHIKV mAbs (CHK-152 and CHK-166), suggesting that SVIR001 is more effective at clearing established infections (314). SVIR001 also reduced CHIKV-induced joint disease, an effect that likely was due to reductions in viral

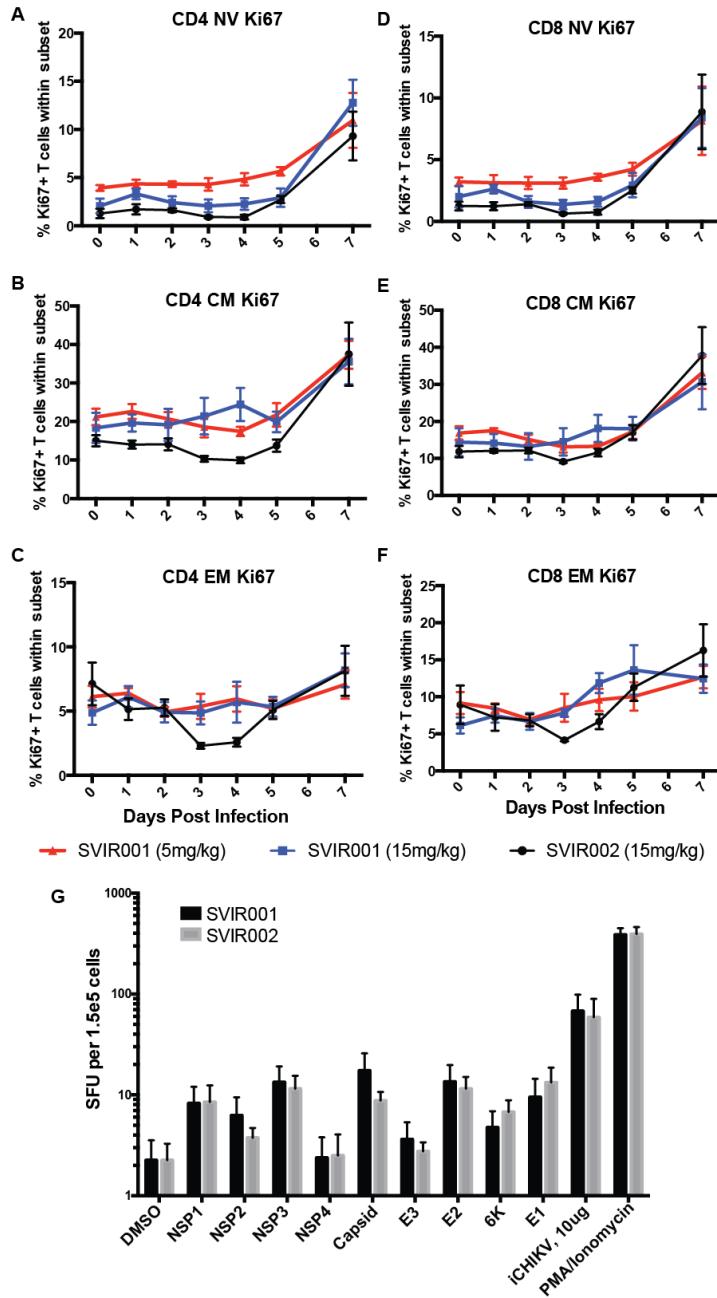


**Figure 3-7: CHIKV mAb treatment did not cause significant changes in CD4+ or CD8+ T cell proliferation.**

Rhesus macaques were inoculated with CHIKV and treated with control antibody SVIR002 or CHIKV mAb SVIR001. Blood was drawn daily 0-7 dpi, and PBMCs were examined for proliferative responses of different (A-C) CD4<sup>+</sup> and (D-F) CD8<sup>+</sup> T cell subsets. T cell subsets were defined in S2 Fig as Naïve (NV), Central Memory (CM), and Effector Memory (EM). The Ki67<sup>+</sup> proliferative status was plotted as a percentage of the total population. (G) IFN $\gamma$  ELISpot analysis was performed on PBMCs from rhesus macaques at 7 dpi. PBMCs from animals treated with SVIR001 (5 mg/kg or 15 mg/kg) or SVIR002 (15 mg/kg) were stimulated with CHIKV peptide pools (10  $\mu$ g/well), inactivated CHIKV (iCHIKV) (10  $\mu$ g/well), or PMA/Ionomycin as a positive control. DMSO was used as a negative control to establish the baseline number of IFN $\gamma$ -producing T cells for each animal. Spots were quantified on an AID ELISpot plate reader (n = 4/group).

Data generated by Nicole Hases (A-F), and Rebecca Broeckel (G). Figure prepared by Rebecca Broeckel.

burden and therefore reduced generalized inflammatory responses. However, this signature of reduced inflammation did not compromise induction of adaptive B or T cell immunity against the virus. These features make SVIR001 a candidate treatment for humans who are acutely infected by CHIKV or possibly those suffering from the long-term joint pain caused by persistent infection.

Acute CHIKV infection in rhesus macaques induces a viremia that lasts for approximately 3 to 4 days, with peak viral titers occurring around 2 to 3 dpi (141, 149, 150, 314). Virus in plasma was not detected in animals receiving anti-CHIKV antibody therapy after the first treatment dose. Anti-CHIKV antibody likely neutralizes virus in the blood rapidly, which reduces dissemination to distant sites of infection including the joints and muscles of the legs. Consistent with this idea, tissue viral loads at 7 dpi were decreased markedly in animals treated with SVIR001. The reduction in tissue viral loads included those of the joint and muscle tissue from the arms, the site of infection, which contrasts with our previous findings with mouse CHK-152 and CHK-166 (314). Although further studies are required, the marked improvement of this mAb therapy compared to our previous mAb combination therapy could be due to different specific mechanism of neutralization, a greater recognition of E2 on the surface of infected cells that augments effector-based clearance, or a longer relative half-life in plasma.

CHIKV disease is mediated by active replication in musculoskeletal tissues that promotes immune cell infiltration and production of inflammatory mediators, which causes synovitis, tenosynovitis, and bone effacement, and results in severe and acute joint pain (110, 286, 287, 294). High CHIKV levels in human patients have been associated with increased severity of illness during acute infection (328, 462), and analogously, higher peak viremia in cynomolgus macaques was associated with worse outcomes including arthritis, meningoencephalitis, and death (150). High tissue viral loads correlate with an increase in the duration of long-term arthralgia in patients (110). Thus, antiviral therapies that reduce viral loads

during the acute phase may limit joint and muscle disease and mitigate chronic CHIKV disease. Histological analysis of the joint tissues from the infected monkeys at 7 dpi revealed less severe acute disease in the SVIR001 treated compared to the control-treated animals. This observation included a reduction in the number of inflamed joints and a decreased severity of the disease. This finding was supported by a reduction in cellular infiltration and production of proinflammatory cytokines and chemokines in animals receiving SVIR001 therapy. Several of the cytokines that were diminished in plasma after SVIR001 treatment are elevated in human plasma during the symptomatic phase of CHIKV infection, including IFN $\gamma$ , IP-10, IL-1 $\beta$ , MCP-1, MIG and IL-6 (337, 468-470), with an increase in IL-1 $\beta$  and IL-6 being linked to more severe disease in humans (470).

SVIR001 and other effective anti-CHIKV therapeutics could serve as treatments for CHIKV infection. We previously showed the efficacy of 4N12 prophylaxis and acute therapy in *Ifnar*<sup>-/-</sup> mice (375). We also demonstrated that treatment of mice and monkeys with immunotherapeutics during the viremic phase reduces virus dissemination to the distal joints and tissues (314). An important, yet unanswered question, is what is the therapeutic window for antibody treatment against CHIKV? In humans the acute viremic phase following CHIKV infection lasts 4 to 12 days post symptom onset (458, 471, 472), making this window relatively narrow. The clinical utility of an antiviral that works solely by blocking viral dissemination may be limited due to delays in diagnosis of CHIKV infection during the viremic phase. Further studies are needed to determine whether SVIR001, alone or in combination with other antibodies or immunomodulatory agents, can reduce musculoskeletal disease, viral burden, or the transition to persistence when administered at later time points. The addition of a second antibody to the cocktail could limit the risk of emergence of resistance (314).

A theoretical concern of immunotherapeutic treatments for CHIKV and other viral infections is that by quickly eliminating antigen, they may interfere with the development of

adaptive immunity and render the host susceptible to reinfection. However, we did not observe any differences in T or B cell proliferation or activation in response to infection when the therapy was initiated at 1 dpi. Similarly, we did not detect any differences in CHIKV-specific IFN $\gamma$ -producing T cell responses at 7 dpi. These observations suggest that SVIR001 did not inhibit the induction of adaptive immunity and that long-term protection is most likely not compromised by an antiviral therapeutic antibody.

In summary, our results demonstrate that the anti-CHIKV mAb therapeutic SVIR001 reduced viremia and dissemination in infected animals and mitigated inflammation systemically and locally. Because SVIR001 promotes elimination of CHIKV from infected tissues, studies are warranted to determine its possible efficacy in preventing or treating viral persistence. Such studies will help to determine the potential clinical utility for prophylaxis or therapy for CHIKV disease.

### 3.5 MATERIALS AND METHODS

**Ethics Statement.** All experiments involving rhesus macaques and mice were performed in compliance with good animal practices as outlined in local and national animal welfare bodies. Rhesus macaque studies were performed in the ABSL-3 containment facility at the Oregon National Primate Research Center (ONPRC). Mouse experiments were performed at Washington University School of Medicine in an approved ABSL-3 facility (IACUC #20140199). Both facilities are accredited by the Assessment and Accreditation of Laboratory Animal Care (AAALAC) International. All experiments were performed in strict accordance to Institutional Animal Care and Use Committee (IACUC) protocols (IACUC #0993). Appropriate procedures were utilized in order to reduce potential distress, pain and discomfort. For example, ketamine (10 mg/kg) was used to sedate the Rhesus macaques during all procedures including routine blood draws performed by trained veterinary staff. The animals were fed standard monkey chow with routine food supplements for enrichment. The infected animals were caged

with partners or separately but within visual and auditory contact of other animals in order to promote social behavior. Animals were euthanized according to the recommendations of the American Veterinary Medical Association 2013 Panel on Euthanasia.

**Cells and viruses.** The infectious clone of CHIKV-LR (CHIKV LR2006 OPY1) was provided generously by Steven Higgs (Kansas State University, Manhattan, KS). Viral stocks were propagated in BHK21 cells and passaged in C6/36 *Aedes albopictus* cells. The infectious clone of CHIKV-181/25 was provided generously by Terence Dermody (University of Pittsburgh, Pittsburgh, PA). Stocks were propagated in BHK21 cells or Vero cells. CHIKV plaque or focus-forming assays were performed on Vero cell culture monolayers, as previously described (314, 334). All cells were cultured in Dulbecco's Modified Eagle Medium (DMEM) supplemented with 5-10% fetal bovine serum (FBS) and penicillin-streptomycin-glutamine. Vero and BHK21 cell monolayer cultures were grown at 37°C with 5% CO<sub>2</sub>, and C6/36 cells were grown at 28°C with 5% CO<sub>2</sub>.

**Neutralization assays.** Neutralization assays with CHIKV were performed as previously described (334). Approximately 100 focus-forming units (FFU) of CHIKV-LR were incubated with serial dilutions of mAbs for 1 h at 37°C and then plated onto Vero cells. Plates were incubated for 90 minutes at 37°C and overlaid with a carboxy methylcellulose-containing medium. At 18 h post-infection, plates were fixed with 1% paraformaldehyde in PBS, and infectious virus was measured by a FFU assay. Plates were incubated with a detection anti-CHIKV mouse mAb (CHK-11 (334)) diluted in permeabilization solution containing 0.1% saponin and 0.1% bovine serum albumin followed by an anti-mouse horseradish peroxidase-conjugated secondary antibody. Foci were visualized using the TrueBlue peroxidase substrate (KPL) and quantified with an ImmunoSpot 5.0.37 microanalyzer (Cellular Technologies Ltd).

**Human mAbs.** SVIR001 is a recombinant, fully human IgG1 antibody that recognizes the E2 protein of CHIKV. The complementarity determinant region sequence of the antibody was derived from the human hybridoma mAb 4N12 (375). SVIR002 is a recombinant isotype control human IgG1 mAb directed against chicken lysozyme. Recombinant mammalian cell-expressed SVIR001 and SVIR002 antibodies were produced at Evitria AG (Wagistrasse 27, 8952 Zurich-Schlieren, Switzerland). The antibody heavy-chain and light-chain cDNAs were cloned into Evitria's evi-5 mammalian gene expression vector. The antibodies were produced by CHO-evi cells, which are Chinese hamster ovary (CHO) K1 cells adapted to serum-free growth in suspension culture. The seed culture was grown in eviGrow medium, a chemically defined, animal component-free, serum-free cell culture medium. Transfection and antibody expression were performed in eviMake at 37°C and 5% CO<sub>2</sub> using eviFect as the transfection reagent. The cell culture supernatant was harvested by centrifugation eight days after transfection and sterile filtered (0.2 µm). The antibodies were purified by MabSelect SuRe affinity chromatography using Dulbecco's PBS as the wash buffer and 0.1 M glycine, pH 3.0-3.5 as the elution buffer. The purified antibodies were dialyzed against PBS, sterile filtered, and stored at 4°C. Antibody purity was assessed by polyacrylamide gel electrophoresis (Bio-Rad Experion system) under non-reducing and reducing conditions and determined to be greater than 95% for both SVIR001 and SVIR002. The percentage of the total antibody present in an aggregated form, determined by analytical gel filtration chromatography (SEC-HPLC), was less than 0.8% for SVIR001 and less than 0.1% for SVIR002. Endotoxin was determined with the Charles River Endosafe-PTS system and found to be less than 1 EU per milligram of antibody.

**Generation of SVIR001 escape mutant CHIKV.** A CHIKV-181/25 strain SVIR001 escape variant virus was generated by repeated passaging in the presence of mAb, as previously described (334). For the first passage,  $1.2 \times 10^5$  FFU of CHIKV-181/25 was incubated with 10 µg/ml of SVIR001 for 1 h at 37°C prior to inoculation in Vero cells. After 24 hrs, half of

the supernatant was removed and incubated with 10 µg/ml SVIR001 for 1 h, and these complexes were used to inoculate fresh Vero cell monolayer cultures. Following six passages with SVIR001, viral RNA was harvested using QIAamp viral RNA mini kit (Qiagen) and cDNA was generated with random hexamers and Superscript III RT (Invitrogen). The cDNA was amplified by PCR and the E2 and E1 genes were sequenced to identify the genetic change associated with the mAb resistant phenotype. A list of primers used for sequencing are provided in **S1 Table**. A deletion of E2 nucleotides 734-739 was identified and the deletion was engineered into the CHIKV-181/25 and CHIKV-LR infectious clones using Phusion high fidelity DNA polymerase (New England Biolabs). A list of mutagenesis primers are provided in **S2 Table**. The cycling times were 98°C for 30 sec, 18 cycles of 98°C for 30 sec, 50°C for 30 sec, 72°C 7 min with a final extension at 72°C for 10 min. The parental plasmid was digested with DpnI at 37°C for 3 h and the mutant plasmid was transformed into XL-Gold Ultracompetent cells (Agilent). Bacteria were plated onto LB agar supplemented with 100 µg/ml of carbenicillin. Deletion was confirmed by sequencing of the plasmid. WT and mutant CHIKV were produced after plasmid linearization with NotI (New England Biolabs) and *in vitro* transcription with SP6 RNA polymerase (Ambion) following the manufacturer's instructions. RNA was electroporated into BHK21 cells using a 2 mm cuvette with 2 pulses (850 V, 25 µF, and infinite resistance). Virus was collected from the supernatant of transfected cells 40 h later. To confirm stability of the mutation, RNA was isolated from virus stocks. cDNA was produced using Superscript III First Strand Synthesis system (Invitrogen) and amplified using primers listed in **Table S1** or previously described (334) and sequenced directly.

**Mouse experiments.** CHIKV infections were performed in 4 week-old C57BL/6J WT mice. For the infection studies, WT mice were inoculated with 10<sup>3</sup> FFU of CHIKV-LR subcutaneous (s.c.) in the footpad. At times indicated, the mice were administered 50 or 300 µg anti-CHIKV mAb SVIR001 or isotype control antibody SVIR002 via an intraperitoneal route. At

3, 5 or 28 dpi, animals were sacrificed and ankle tissues were homogenized. Ankle viral load was measured by focus forming unit assays on Vero cells or by a TaqMan-based quantitative real time reverse transcription PCR assay (qRT-PCR, see below).

**NHP experiments.** Each of twelve male rhesus macaques was inoculated subcutaneously with  $10^7$  PFU of CHIKV-LR diluted in 1 ml of PBS that was distributed over both hands and arms as ten 100  $\mu$ l injections as previously described (314). At 1 and 3 dpi monkeys were infused intravenously with either control mAb (SVIR002) at 15 mg/kg or anti-CHIKV mAb (SVIR001) at 5 or 15 mg/kg (see **Table 3-1** for specific animal groupings). The mAbs were diluted with saline into a total of 20 mls and infused at 1 ml/minute using a medical syringe pump delivery system. Peripheral blood samples were obtained at 0, 1, 2, 3, 4, 5 and 7 dpi. Whole blood was centrifuged over lymphocyte separation medium (Corning) for 45 min at 3,000 rpm ( $1,459 \times g$ ) to isolate peripheral blood mononuclear cells (PBMCs) and plasma. PBMCs were analyzed for lymphocyte phenotype and frequency by flow cytometry, and plasma was assessed for viral load by qRT-PCR and levels of cytokines by a Monkey Magnetic 29-plex Panel for Luminex Platform Kit (Invitrogen). Animals were euthanized at 7 dpi and complete necropsies were performed. Representative tissue samples from (joints, muscles, organs, brain, lymph nodes and bone marrow) were collected and stored in RNA*later*, Trizol (RNA isolation), medium (virus isolation), and 10% buffered formalin (microscopic evaluation).

**Pharmacokinetic analysis of mAb.** Plasma mAb levels were measured by enzyme-linked immunosorbent assay (ELISA). High-binding polystyrene ELISA plates (Corning) were coated with 100  $\mu$ l of  $10^7$  PFU/ml of CHIKV 181/25 to measure SVIR001 levels or 1  $\mu$ g/ml of lysozyme (Fisher) in PBS to measure SVIR002 levels. Plates were blocked with 2% milk in 0.05% Tween-PBS followed by incubation with plasma dilutions in milk/Tween buffer for 2 h. Plates were washed with 0.05% Tween-PBS and incubated with peroxidase-conjugated anti-human IgG gamma chain (Rockland). Bound antibody was detected using the o-

phenylenediamine dihydrochloride (OPD) substrate (Life Technologies), and the plates were read with a Synergy HTX Microplate Reader (BioTek) at 490 nm. A standard curve was generated using serial dilutions of SVIR001 or SVIR002. Plasma antibody concentrations were calculated using the standard curve and multiplied by the dilution factor.

**qRT-PCR analysis.** CHIKV RNA levels were measured using a published qRT-PCR assay (149, 314). Rhesus macaque tissues were homogenized in 1 ml of TRIzol reagent plus approximately 250  $\mu$ l of SiLiBeads, type S (1.7 to 2.1 mm), using a Precellys 24 homogenizer (Bertin Technologies). Total RNA from tissue samples was prepared using Trizol. Total RNA was prepared from 200  $\mu$ l of plasma using the Viral RNA kit (Zymo). The isolated RNA was quantified using a Nanodrop spectrophotometer. RNA was treated with RNase-free DNase, and then single-stranded cDNA was generated from 1  $\mu$ g of RNA using random hexamers and Superscript III RT (Invitrogen). Gene amplicons or viral RNA isolated from infectious virus served as quantification standards (sensitivity, 10 to 100 copies). Quantitative RT-PCR was performed and analyzed using ABI StepOne Plus real-time PCR system (Applied Biosystems). Relative CHIKV copy numbers of left and right joints and muscles were averaged for each animal. For the mouse studies, primer and probe sets, as previously described (473), were used in a one-step reverse transcription (RT)-qPCR assay. Perfused mouse ankles were homogenized in 1 ml of RLT buffer plus approximately 200  $\mu$ l of silica beads using a MagNA Lyser instrument (Roche). RNA was extracted using the RNeasy mini kit (Qiagen) following manufacturer's instructions and eluted in 50  $\mu$ l of RNase-free water. A one-step qRT-PCR assay (Applied Biosystems) was performed with 2  $\mu$ l of RNA using a 7500 Fast real-time PCR machine (Applied Biosystems). A standard curve was generated with serial dilutions of RNA extracted from virus stocks to determine CHIKV FFU equivalents. RNA was quantified using a Nanodrop spectrophotometer and total  $\mu$ g of RNA was determined.

**CHIKV isolation from tissues.** NHP tissues were homogenized in 1 ml of cell culture medium plus approximately 250  $\mu$ l of SiLiBeads using a bead beater (Precellys 24 homogenizer) (Bertin Technologies), and cellular debris was pelleted by centrifugation (5,000  $\times$  g for 2 min). Clarified samples were sterile-filtered (0.45  $\mu$ m filter), and a 400  $\mu$ l sample of the clarified lysate was applied to a T25 flask of C6/36 cells for three days. Supernatant titers from these cultures were determined by limiting dilution plaque assays on Vero cells. Mouse tissues were titered by focus forming assay. Perfused ankles were homogenized in 1 ml of cell culture medium plus approximately 200  $\mu$ l of silica beads using the MagNA Lyser. Clarified homogenate was serially diluted and added to a confluent Vero cells cultured in a 96-well plate. After 2 h, tissue inoculum was removed and cells were overlaid with a carboxy methylcellulose-containing medium. Cells were fixed 18 h later and processed as described above.

**Phenotypic analysis of PBMCs.** PBMCs were analyzed by flow cytometry for cellular differentiation markers as well as Ki67 (marker of active proliferation) or CD169 (activation marker for myeloid lineage cells and natural killer (NK) cells) as previously described (149). T cell panel analysis was performed at all time points, and dendritic cell (DC)/monocyte/macrophage/NK cell panel analysis was performed on PBMCs from 0-5 dpi. For T cell analysis, PBMCs were stained with fluorophore-conjugated antibodies directed against CD4, CD8 $\beta$ , CD28, CD95, CD127 and Ki67 (Biolegend). For DC/monocyte/macrophage/NK analysis, PBMCs were stained with fluorophore-conjugated antibodies against CD3, CD20, CD14, HLA-DR, CD11c, CD123, CD16, CD8, and CD169 (Biolegend). The T cell and DC/monocyte/macrophage/NK cell gating strategy is depicted in **Fig S-8** and **Fig S-9**, respectively. Stained samples were read using an LSRII instrument (BD Pharmingen) and the data were analyzed by FlowJo (TreeStar).

**CHIKV-specific T cell responses.** Monkey gamma interferon (IFN $\gamma$ ) enzyme linked immunospot assays (ELISpotPlus; Mabtech) were used to quantify CHIKV-specific T cell

responses in peripheral blood of infected NHP at 7 dpi. Assays were performed according to the manufacturer's instructions. Briefly, ELISpot plates were washed with PBS and blocked with RPMI containing 10% FBS, penicillin/streptomycin, and glutamine. Approximately,  $1.5 \times 10^5$  rhesus monkey PBMCs were stimulated with: (1) 1  $\mu$ l DMSO-negative control; (2) overlapping CHIKV peptide pools (10  $\mu$ g/well; ThermoScientific (149)) of nsP1, nsP2, nsP3, nsP4, capsid, E3, E2, 6K, or E1; (3) 10  $\mu$ g of inactivated CHIKV; or (4) 1  $\mu$ l each of phorbol 12-myristate 13-acetate (PMA; 40  $\mu$ M stock) and ionomycin (7 mM stock)-positive control. The inactivated whole virus was prepared using 3 mM binary ethylenimine (BEI) treatment overnight followed by clarification through a 20% sucrose cushion at 22,000 rpm (68,128 x g) for 3 hrs; BEI treatment is an established inactivation technique for a number of viruses (474-476). Successful inactivation of the virus was confirmed by plaque assay. The ELISpot plates were incubated at 37°C for 18 h and then washed with PBS. Detection of IFN $\gamma$  was performed by incubating the plates for 2 h with a biotin-conjugated anti-IFN $\gamma$  antibody (7-B6-1, Mabtech) diluted in PBS with 0.5% FCS. Following this incubation, the plates were washed with PBS and then incubated with streptavidin-alkaline phosphatase in PBS plus 0.5% FBS for 1 h. Plates were washed and then developed with filtered 5-bromo-4-chloro-3-indolyl-phosphate/nitro blue tetrazolium (BCIP/NBT) substrate solution; flushing the wells with water stopped this reaction. The plates were air-dried and scanned using the AID EliSpot Reader Classic (AID). The average spot forming units per stimulus were calculated and graphed using Graph Pad Prism v6 software.

**Serum cytokine assays.** Macaque cytokine assays were performed using a Cytokine Monkey Magnetic 29-plex Panel for Luminex Platform Kit (Invitrogen) according to the manufacturer's instructions using a 7-point standard curve. Following a 2 h incubation with monkey plasma, beads were washed twice and then labeled with biotinylated detector antibody for 1 h. Following additional washes, beads were incubated with streptavidin conjugated to R-

Phycoerythrin for 30 min and washed. Cytokines were identified and quantified using a Luminex 200 Detection system (Luminex).

**Histological analysis.** Rhesus macaque joint tissue fixed in 10% buffered formalin was routinely processed, embedded in paraffin, sectioned at 5 microns, and stained with hematoxylin and eosin. Sections of twelve joints were examined by two pathologists (ADL; LMAC) blinded to group assignment. A semiquantitative scoring system was developed by assessing inflammation which occurred in periarticular fat, tendon, connective tissue and/or skeletal muscle. Each joint was scored individually and then cumulative scores were calculated for each animal.

**Statistical analysis.** All statistical analysis was performed in Prism v6 software (GraphPad Software, Inc). EC<sub>50</sub> values were determined by non-linear regression. For plasma viral load and tissue viral burden from monkeys, data was log-transformed and Dunnett's multiple comparison test was performed. For mouse viral burden experiments, data was log-transformed, and the Mann-Whitney test was used. For cytokine and chemokine analysis, a Sidak's multiple comparison test was used to determine significance.

## CHAPTER 4 A T-CELL BASED VACCINE PROTECTS AGAINST CHIKV INFECTION IN MICE

This chapter was written by Rebecca Broeckel. The experiments were performed by Rebecca Broeckel with assistance from Streblow Lab members Takeshi Ando, Craig Kreklywich, Patricia Smith, and Michael Denton. Useful reagents were provided by the laboratories of Dr. Ilhem Messaoudi, Dr. Thomas Morrison, and Dr. David Curiel.

### 4.1 ABSTRACT

Chikungunya virus (CHIKV) is a mosquito-transmitted RNA virus that causes severe and debilitating joint and muscular pain that can be long lasting. Currently, no FDA-approved vaccine exists for CHIKV. In addition, CHIKV vaccines under development rely on the generation of neutralizing antibodies for protection; however, the role of T cells in controlling CHIKV infection is still unclear. We performed an interferon gamma ELISpot screen of the entire CHIKV peptidome in order to identify CHIKV-specific T cell epitopes recognized in C57BL/6 infected mice at 7 and 14 days post infection. A total of 26 unique 18-mer peptides stimulated T cells from these infected mice. Based on this information, we generated both adenovirus and cytomegalovirus-vectored vaccines expressing a fusion protein containing five T cell epitopes (CHKVf5). Mice vaccinated with CHKVf5 elicited robust T cell responses to higher levels than normally observed following CHIKV infection. Vaccination with the CHKVf5 vaccine vectors did not elicit neutralizing antibodies. Intramuscular CHIKV challenge of CHKVf5-vaccinated mice had significantly reduced infectious viral load. Antibody-mediated depletion of both CD4<sup>+</sup> and CD8<sup>+</sup> T cells in vaccinated mice rendered them fully susceptible to CHIKV challenge. However, depletion of CD4<sup>+</sup> T cells did not reverse the protection by the vaccine, whereas depletion of CD8<sup>+</sup> T cells reduced the effectiveness of the protection. Our data demonstrated a protective role for CD8<sup>+</sup> T cells in CHIKV infection. These results also indicate that a T cell-biased prophylactic vaccination approach is effective against CHIKV challenge and reduces viral load. Further studies are currently underway to determine whether this approach would also be

effective as a therapeutic vaccine that could be utilized to treat patients with chronic infection and disease.

## 4.2 INTRODUCTION

Chikungunya virus (CHIKV) is a mosquito-transmitted virus that causes fever, rash, and debilitating joint and muscle pain in humans. Though the fever and rash resolve, joint and muscle pain can be long lasting. According to some studies, up to 75% of CHIKV-infected patients experience chronic arthritic and muscle pain for months to years following resolution of the acute disease (105, 110, 293). The consequences of chronic joint pain are significant, with patients reporting limited mobility, depression, and decreased quality of life (477). CHIKV can rapidly spread and cause disease in millions of people in a short period of time, as illustrated by recent epidemics in the Indian Ocean region (2004-2011) and the Americas (2013-2015) (144, 145, 478). Since no FDA-approved vaccines or antivirals exist for CHIKV, research into prophylactic and therapeutic interventions are highly warranted. The protective role for anti-CHIKV neutralizing antibodies has been well established in both mouse and nonhuman primate models (303, 311, 314, 333). Potent neutralizing antibodies can provide sterilizing immunity if administered prophylactically or if derived through vaccination. However, after the first few days of infection, neutralizing antibodies may have limited efficacy to clear virus from infected tissues (303), suggesting other immune components, such as T cells, could be involved in viral clearance of persistent joint-localized CHIKV.

Vaccine candidates currently under development for CHIKV include the live-attenuated CHIKV/IRES vaccine and the Eilat/CHIKV chimeric vaccine (353, 354, 359). The Eilat chimeric vaccine offers several advantages over other vaccines because the vaccine only requires a single dose, is attenuated in the susceptible *Ifnar*<sup>-/-</sup> mice, and induces potent and protective neutralizing antibodies against CHIKV (359). Similarly, the CHIKV/IRES vaccine elicited neutralizing antibody responses in A129 mice and passive transfer of serum from immunized

mice protected naïve mice from lethal CHIKV challenge (460). Both of these vaccines elicit humoral and cellular responses against CHIKV antigens. However, in the context of vaccine-induced neutralizing antibodies, the role of cellular immunity appears minimal. In fact, T cell depletion of CHIKV/IRES-vaccinated A129 mice or adoptive transfer of immune CD4<sup>+</sup> or CD8<sup>+</sup> T cells did not protect A129 mice from CHIKV challenge (460). However, a modified vaccinia virus ankara (MVA) vaccine vector that expresses E3/E2 was shown to require CD4<sup>+</sup> T cells for protection since CD4<sup>+</sup> T cell depletion increased susceptibility to CHIKV challenge (373). While low levels of E2 neutralizing antibodies were identified following vaccination that may have contributed to the protection seen in A129 mice, a role of direct cellular immunity or CD8<sup>+</sup> T cells was not shown.

CD4<sup>+</sup> T cells have been implicated as a major contributor to joint inflammation during CHIKV infection of mice. Footpad injection of C57BL/6 mice results in edema, arthritis, tenosynovitis in the ankle joint, as well as necrosis in the musculoskeletal tissues (148). Infiltrating cells in the ankle include CD4<sup>+</sup> and CD8<sup>+</sup> T cells, macrophages, neutrophils, and natural killer cells (148). Mice lacking CD4<sup>+</sup> T cells have reduced inflammation of the footpad after infection, but viral levels in the blood and ankle are similar to control mice (306). Adoptive transfer of CHIKV-specific CD4<sup>+</sup> T cells into TCR<sup>-/-</sup> mice also resulted in increased footpad swelling and joint vascular leakage compared to controls after CHIKV infection, while viral load in the blood remained the same as controls (340). In contrast, depletion of CD8<sup>+</sup> T cells fails to reduce footpad swelling or affect viral loads in the blood and ankle (306). This data supports a pathogenic role for CD4<sup>+</sup> T cells but the role for CD8<sup>+</sup> T cells is still unclear. However, recent reports suggest a role for T cells in viral clearance during CHIKV infection. Mice lacking B and T cells (Rag1<sup>-/-</sup> or Rag2<sup>-/-</sup>) develop persistent infections characterized by chronic viremia and tissue persistence (303, 308). Passive transfer of neutralizing antibodies into Rag1<sup>-/-</sup> mice fails to clear CHIKV in tissues of persistently infected animals (303). In addition, vaccinated mice

lacking mature B cells ( $\mu$ MT mice) have decreased levels of virus in the serum compared to control-vaccinated mice after CHIKV challenge, although the vaccinated mice also had increased footpad swelling (308). This suggests that T cells could be mediating the limited protection from vaccination, but this was not directly tested. Together, these data are suggestive of a role of cellular immunity in protection against CHIKV infection.

Antiviral CD8<sup>+</sup> T cells have been shown to be important for reducing viral loads and disease for other alphavirus infections. Depletion of CD8<sup>+</sup> T cells in Ross River virus (RRV) infected mice at 7 and 12 dpi increased levels of RRV RNA in the quadriceps at 14 dpi (343). Similarly, infection of CD8 $\alpha$ <sup>-/-</sup> mice with RRV results in increased levels of RRV RNA in the quadriceps at 14 and 21 dpi, but equal levels of virus is detected in the ankle, compared to wild type mice. Investigators who performed CD8<sup>+</sup> T cell depletions in CHIKV-infected mice did not report virus levels in the muscle tissue, so it is possible that CD8<sup>+</sup> T cells may be effective in the muscle in CHIKV-infected mice as with RRV. T cells have also been implicated in protection against Sindbis virus (SINV) infiltration into the CNS (344), and CD4<sup>+</sup> T cells may protect against Venezuelan Equine Encephalitis virus (VEEV) -induced encephalitis in mice (345).

In the current study, we utilized murine cytomegalovirus (MCMV) and adenovirus (AdV) vaccine vectors as tools to investigate the role for antiviral CD4<sup>+</sup> and CD8<sup>+</sup> T cells during CHIKV infection. We profiled T cell epitopes recognized in CHIKV mice using a complete CHIKV (306) overlapping peptide library. Based upon the results from this screen, we generated a CHIKV fusion gene called CHIKVf5 that encodes several peptides that elicited IFN $\gamma$  responses. The fusion gene was recombined into MCMV and AdV vaccine vectors to elicit T cell responses in mice. After vaccination, we found that the vaccine caused an earlier joint inflammation in mice challenged in the footpad, and significant reduction of viral loads in leg muscle tissue in mice challenged intramuscularly. T cell depletion experiments demonstrated that CD8<sup>+</sup> T cells were

essential for protection in the muscle tissue. This study describes a tissue-specific role for CD8+ T cells in protection against CHIKV infection.

### 4.3 RESULTS

**Identification of CHIKV T cell epitopes in C57BL/6 mice.** Few dominant CHIKV T cell epitopes have been experimentally described in C57BL/6 mice (340, 367). To identify T cell epitopes recognized during CHIKV infection in mice, we screened T cell responses by IFN $\gamma$  ELISpot using a CHIKV overlapping 18mer peptide library. For this assay, splenocytes were isolated and pooled from 3 mice infected with CHIKV for 7 or 14 days (**Fig 4-1A**). Splenocytes were cultured on 96-well ELISpot plates for 2 days in the presence peptides, negative control peptides, or PMA/ionomycin (positive control) and then fixed and stained for IFN $\gamma$ . The stained wells were scanned and spots were enumerated. We identified several CHIKV peptides that elicited an IFN $\gamma$  response that mapped to nsp1, E2 and E1. In addition, we observed a wider breadth of IFN $\gamma$  responses at 7 dpi (26 peptides) that became more refined at 14 dpi (15 peptides). To confirm responding peptides that elicited a strong IFN $\gamma$  response, the screen was repeated with the active peptides (**Fig 4-1B**). The peptides eliciting the strongest responses included peptides 47, 256, 350, 439, and 451. Peptides 451 (CAVHSMTNAVTIREAEIE) and 350 (DNFNVYKATRPYLAHCPD) were previously shown to elicit T cell responses, providing further validation of our assay (340, 367). **Table 4-1** depicts the full list of peptides and their amino acid sequences for those peptides that consistently elicited an IFN $\gamma$  response above background.

**Generation of MCMV and AdV-vectored vaccines for CHIKV.** In order to generate a novel T cell antigen CHIKV vaccine, we constructed a fusion polypeptide (CHIKVf5) containing two peptides that elicited strong IFN $\gamma$  responses (peptide 47 and 451) with a small region of nsp4 (aa 167 to 475) that was predicted *in silico* to contain several H2-Db restricted T cell

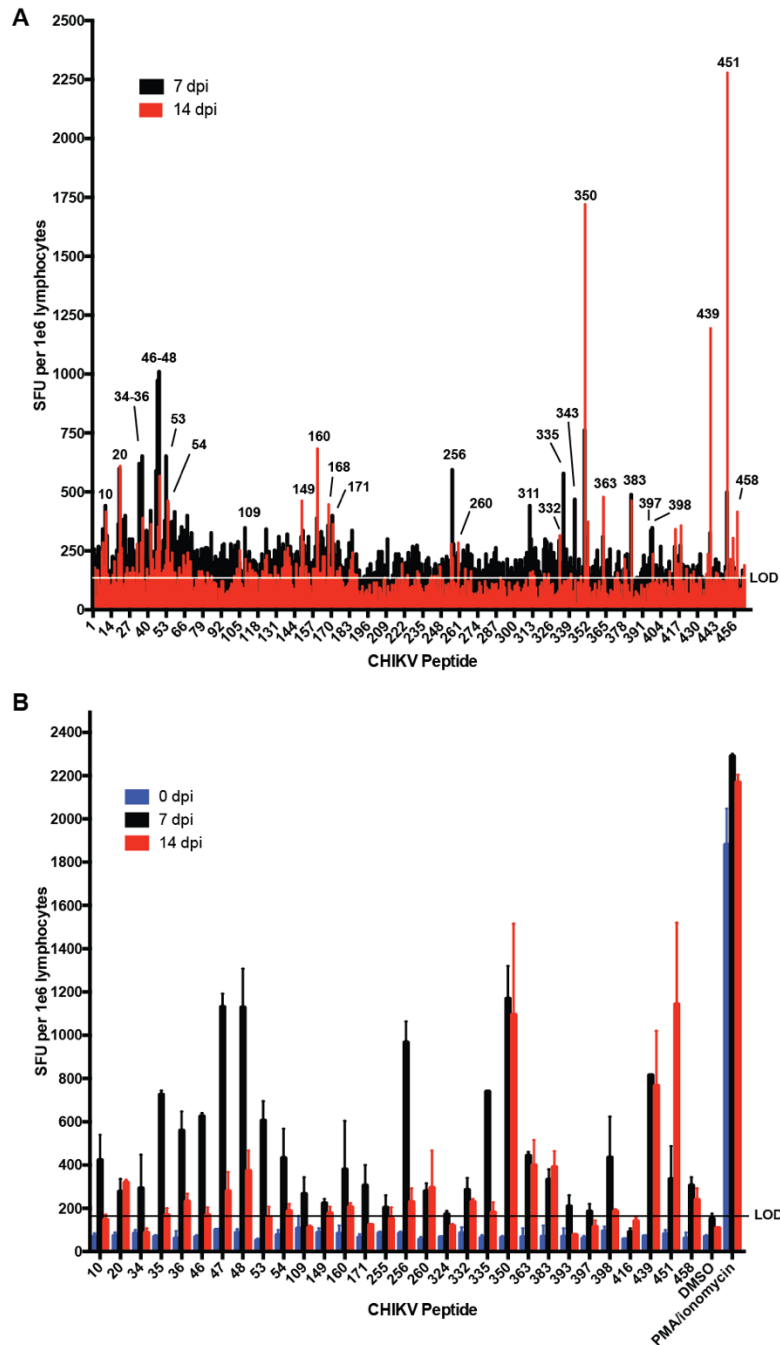


**Figure 4-1: IFN $\gamma$  responses in C57BL/6 mice at 7 and 14 days post CHIKV infection.**

Mice were infected with 1,000 PFU CHIKV SL15649 in the footpad. At 7 or 14 dpi, mouse splenocytes were isolated and incubated with individual CHIKV 18-mer peptides overlapping by 10 amino acids and 1e5 cells were incubated on IFN $\gamma$  ELISpot plates. At 48 hrs post incubation, ELISpot plates were washed and analyzed for spot formation. **(A)** Splenocytes from 3 mice were pooled and incubated with each individual CHIKV 18-mer in the CHIKV peptidome. Peptide numbers for reactive samples are indicated. **(B)** IFN $\gamma$ - eliciting peptides from **(A)** were repeated by ELISpot for two additional animals infected for 7 or 14 days. "LOD" indicates limit of detection.

Data produced and analyzed by Rebecca Broeckel.

<b>18-mer peptide sequence</b>	<b>Peptide #</b>	<b>CHIKV protein</b>
MSDRKYHCVCPMRSAEDP	10	nsP1
VYAVHAPTSLYHQAIKGV	20	nsP1
HLKGKLSFTCRCDTVVSC	34	nsP1
TCRCDTVVSCEGYVVKRI	35	nsP1
SCEGYVVKRITMSPGLYG	36	nsP1
LNQRIVVNGRTQRNTNTM	46	nsP1
<b>GRTQRNTNTMKNYLLPVV</b>	<b>47</b>	<b>nsP1</b>
<b>TMKNYLLPVVAQAFSKWA</b>	<b>48</b>	<b>nsP1</b>
CCLWAFKKQKHTVYKRP	53	nsP1
QKHTVYKRPDTQSIQKV	54	nsP1
RTTNEYNKPIVDDTTGST	109	nsP2
VTWVAPLGVRGADYTYNL	149	nsP2
CVLGRKFRSSRALKPPCV	160	nsP2
PGGVCKAVYKKWPESFKN	171	nsP3
KQHAYHAPSIRSAVPSPF	255	nsP4
<b>SIRSAVPSPFQNTLQNVL</b>	<b>256</b>	<b>nsP4</b>
ELPTLDSAVFNVECFKKF	260	nsP4
GYYNWHHGAVQYSGGRFT	332	Capsid
KPGDSGRPIFDNKGRVVA	335	Capsid
<b>DNFNVYKATRPYLAHCPD</b>	<b>350</b>	<b>E2</b>
GETLTVGFTDSRKISHSC	363	E2
VPKARNPTVTYGKNQVIM	383	E2
MCMCARRRCITPYELTPG	398	E2
<b>PYSQAPSGFKYWLERGA</b>	<b>439</b>	<b>E1</b>
<b>CAVHSMTNAVTIREAEIE</b>	<b>451</b>	<b>E1</b>
KDHIVNYPASHTTLGVQD	458	E1

**Table 4-1: CHIKV-Specific Immunoreactive Peptides.**

Splenocytes from mice infected with CHIKV were stimulated with the complete CHIKV 18-mer peptide library, and IFN $\gamma$  production was measured by IFN $\gamma$  ELISpot. Peptides that consistently induce IFN $\gamma$  above background are reported. Bolded peptides indicate those peptides that elicited the strongest IFN $\gamma$  responses.

Data produced and analyzed by Rebecca Broeckel.

epitopes (479). We identified a dominant epitope contained in peptide 256 in this region of nsp4. Peptide 416 (in E1) is a peptide that consistently failed to induce IFN $\gamma$  response by ELISPOT in splenocytes from CHIKV-infected mice, was included as a negative peptide control (**Fig 4-2A**). The CHIKVf5 fusion protein contained an in-frame C-terminal HA tag for detection. As described in the materials and methods, the fusion construct was generated by overlapping PCR, and cloned into shuttle plasmids that allowed recombineering into a MCMV Smith strain bacterial artificial chromosome and recombination into an E1A/E3 deleted AdV genome (**Fig 4-2B**). MCMV and AdV were reconstituted as previously described, and the vaccine vectors were sequenced to ensure successful incorporation of the fusion gene. Vaccine vectors were used to infect mouse fibroblasts, and at 24 hpi lysates were produced and analyzed by SDS-PAGE. Western blotting for the HA tag confirmed fusion protein expression from both constructs (**Fig 4-2C**).

**Immunogenicity and efficacy assessment of MCMV and AdV CHKVf5 vaccine vectors.** To test the vaccine immunogenicity, mice were vaccinated once with either MCMV CHKVf5, wild type MCMV lacking the CHKVf5 insert, or PBS by intraperitoneal injection (n = 10/group). Separate groups of 10 mice per group were vaccinated in the left quadriceps muscle with AdV CHKVf5 or AdV control. The vaccine groupings and schedule are depicted in **Fig 4-3A**. At eight weeks post MCMV vaccination or two weeks post AdV vaccination two mice per group were sacrificed and splenocytes were prepared for T cell analysis by ELISpot assays. The MCMV vaccine has been shown previously to elicit robust CD8<sup>+</sup> T cell responses by 8 weeks post vaccination (480, 481). Adenovirus vaccines typically elicit CD8<sup>+</sup> T cell responses that peak 10 to 14 days post vaccination (482). Splenocytes were incubated with peptides encoded by CHKVf5 (peptides 47, 255, 260, and 451), the immunodominant peptides for the MCMV proteins M45 and IE3, or stimulated with PMA/Ionomycin as a positive control (**Fig 4-3B**). Splenocytes from animals receiving MCMV CHKVf5 and AdV CHKVf5 developed high

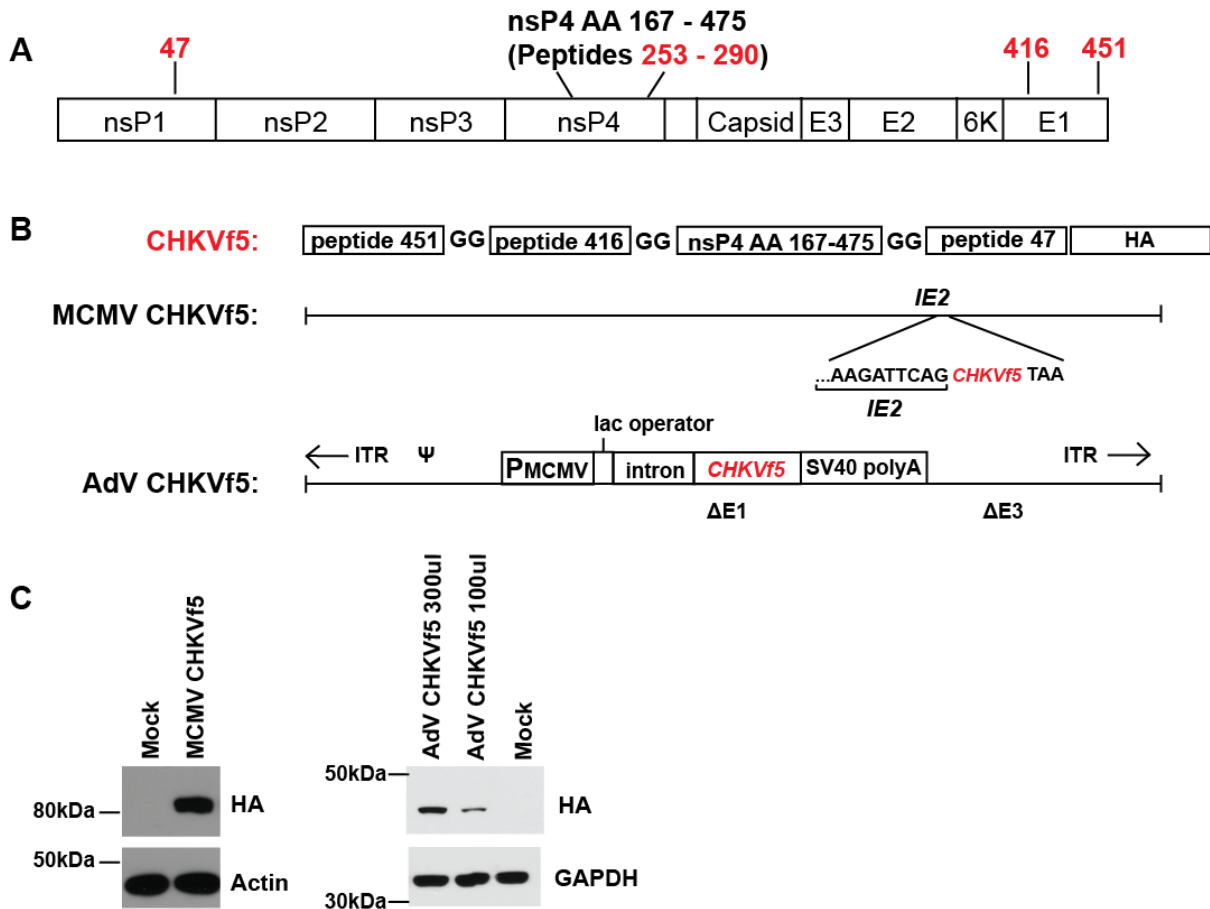


**Figure 4-2: MCMV and AdV vaccine vector expression of the CHKVf5 fusion gene.**

(A) Shown is the genomic position of the CHIKV peptides contained in CHIKVf5. (B) The CHIKVf5 fusion gene contains amino acid sequences for peptide 47, 416, and 451 as well as a 308 amino acid portion of nsp4 that are separated by two Gly residues. A C-terminal HA epitope (8 amino acids) was added for detection purposes. The CHKVf5 fusion gene was inserted into MCMV as a C-terminal fusion with IE2 and into a replication defective adenovirus 5 vector (deleted of E1 and E3). (C) Recombinant MCMV and AdV expressing CHKVf5 vectors were tested for HA expression in transduced NIH 3T3 cells. Cell lysates were analyzed at 1 dpi for HA and the loading controls actin or GAPDH.

Data produced and analyzed by Rebecca Broeckel.

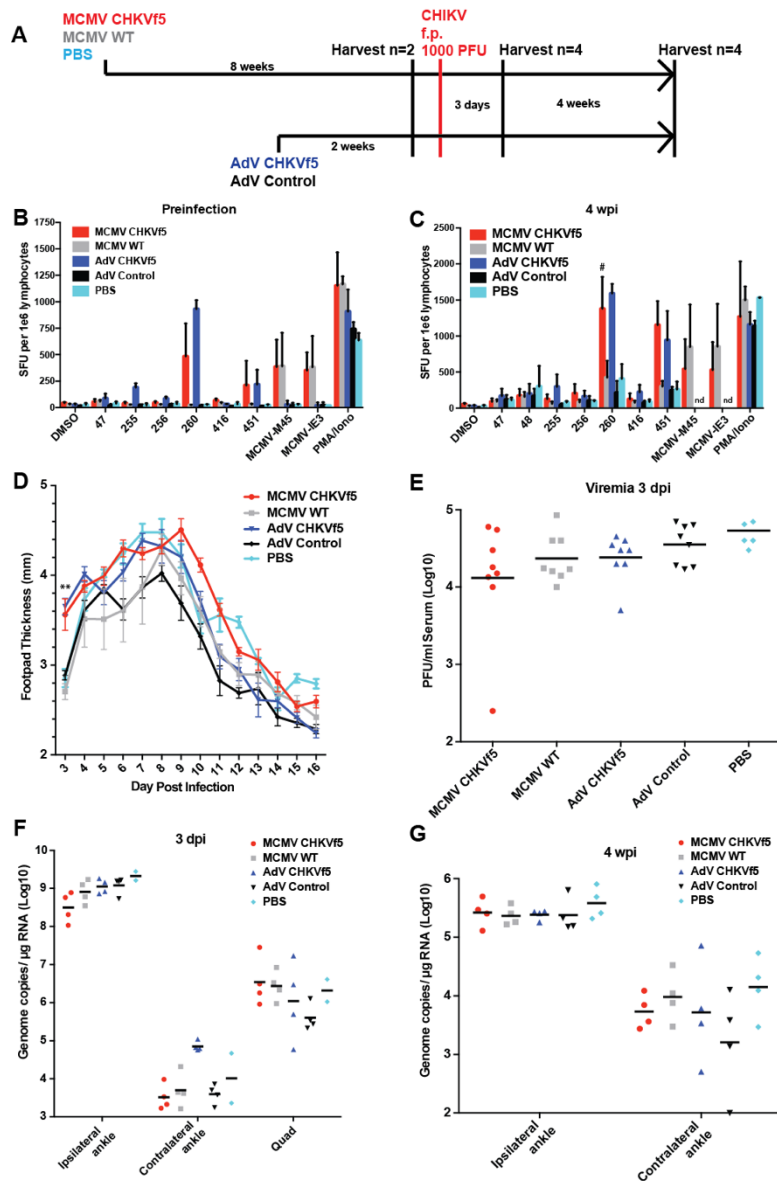


**Figure 4-3: CHKVf5 vaccines did not protect mice against a footpad CHIKV challenge.**

(A) Mice were administered MCMV CHKVf5, MCMV WT, or PBS i.p. for 8 weeks and then analyzed by ELISpot for the presence of T cell responses or challenged. Separate groups of mice were vaccinated with AdV CHKVf5 or AdV Control for 2 weeks prior to T cell response analysis or challenged. (B) Splenocytes from 2 mice per group were collected and IFN $\gamma$  ELISpot assays were performed by stimulating the splenocytes with CHIKV peptides incorporated in the CHKVf5 fusion gene. (C) IFN $\gamma$  ELISpot assay performed using splenocytes from mice vaccinated with the indicated vaccine and challenged with CHIKV SL15649 in the footpad (“#” indicates too numerous to count; “nd” indicates not done). (D) Footpad thickness was measured using calipers from 3 to 16 dpi. (E) At 3 dpi, mice were bled and their serum was titered by limiting dilution plaque assay on confluent monolayers of Vero cells. (F) At 3 dpi, viral RNA extracted from ipsilateral and contralateral ankles and ipsilateral quadriceps was quantified by qRT-PCR. (G) At 4 wpi, viral RNA was extracted from ipsilateral and contralateral ankles and viral RNA levels were measured by qRT-PCR.

Data produced and analyzed by Rebecca Broeckel.

levels of IFN $\gamma$  in response to stimulation with nsp4 peptide 260 and E1 peptide 451.

Splenocytes from mice receiving AdV CHKVf5 also developed moderate IFN $\gamma$  responses to stimulation with nsp4 peptide 255. As expected, MCMV vaccinated but not AdV vaccinated mice responded to peptides M45 and IE3. The animals were challenged with 1,000 PFU CHIKV SL15649 s.c. in the right footpad, and four mice per group were sacrificed at 3 dpi and the remainder were sacrificed at 4 weeks post infection (wpi) to measure tissue viral burden and splenocyte IFN $\gamma$  responses by ELISpot assay. The vaccinated mice produced an increased frequency of IFN $\gamma$  positive T cells to peptides 260 and 451 relative to non-challenged controls. Control-vaccinated mice also developed IFN $\gamma$  responses to the CHIKV peptides due to the CHIKV infection, although the frequency of IFN $\gamma$  responding cells was significantly lower relative to CHIKVf5-vaccinated mice. Together, this data suggests that the CHKVf5 vaccinated mice developed robust IFN $\gamma$  responses to CHIKV peptides pre-challenge, and these responses were boosted following CHIKV challenge.

After CHIKV challenge, footpad swelling was monitored from 3 to 16 dpi. Interestingly, the CHKVf5 vaccinated mice had significantly increased footpad swelling at 3 dpi compared to the control mice (**Fig 4-3D**). However, serum viremia and tissue viral loads were not affected by CHKVf5 vaccination (**Fig 4-3E and F**). Similarly, there were no differences in ankle tissue viral loads at 4 wpi (**Fig 4-3G**). CHIKV RNA in the quadriceps was undetectable at 4 wpi in both CHKVf5 vaccinated and control mice (data not shown). These data suggest that the vaccine-elicited T cell responses did not reduce viral load in the blood or tissues. However, the vaccine caused an increase in footpad swelling at 3 dpi compared to controls. These data are largely consistent with other studies showing that T cells do not contribute to viral control in the CHIKV footpad challenge model (306, 340).

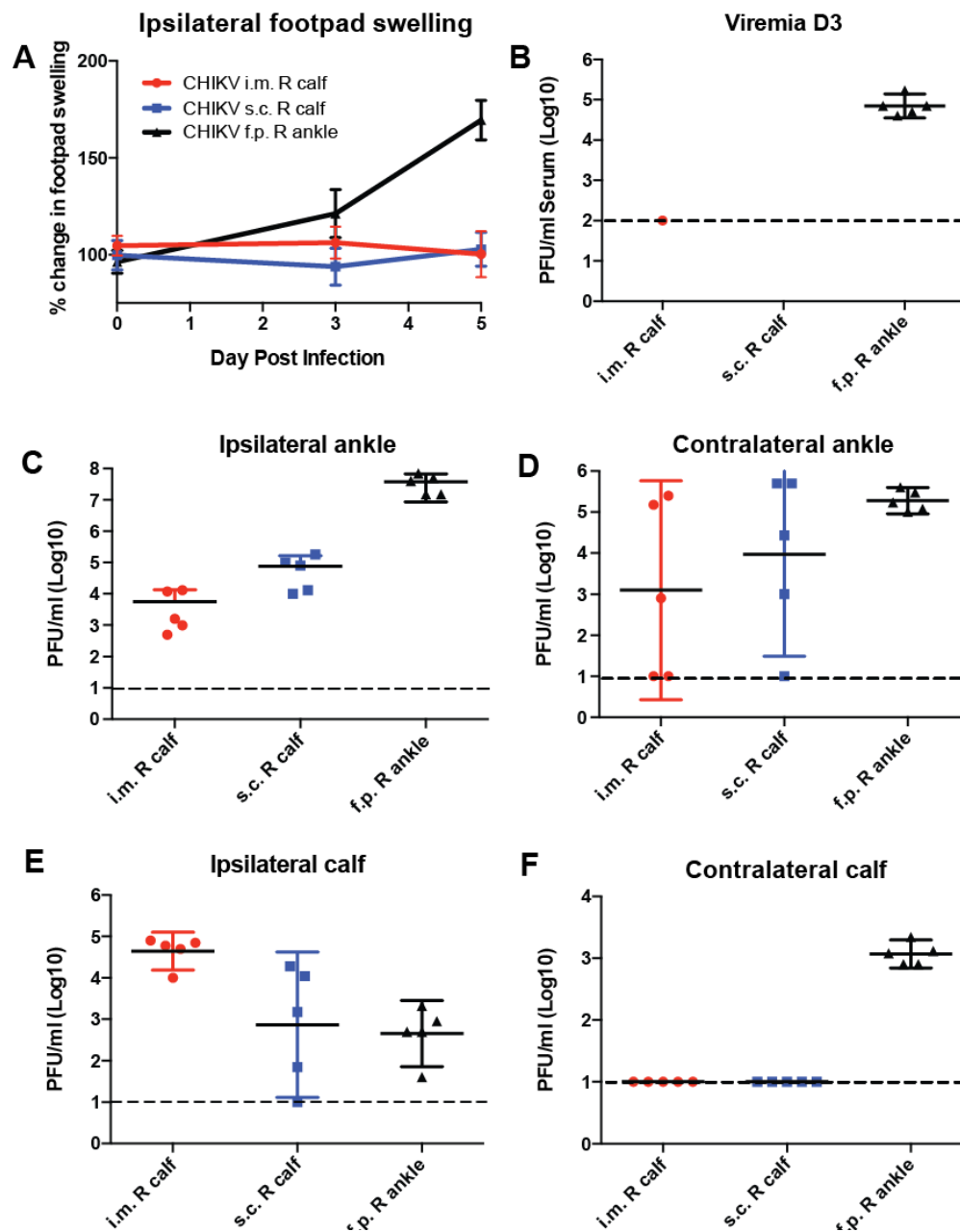


**Figure 4-4: C57BL/6 mice were infected with CHIKV by three different routes, and their footpad swelling and tissue viral distributions are compared.**

C57BL/6 mice were infected with 1,000 PFU CHIKV SL15649 intramuscularly in the right calf (i.m. R calf), subcutaneously in the skin of the right calf (s.c. right calf), or in the right leg footpad (f.p.). (A) Footpad swelling measurements were taken at 0, 3, and 5 dpi using calipers. (B) Serum from CHIKV-infected mice was isolated at 3 dpi, and viremia was measured by limiting dilution plaque assay on confluent monolayers of Vero cells. (C-F) At 5 dpi, mice were sacrificed and whole tissues were dissected and homogenized in 1 ml cell culture media. Infectious viral levels in the ankle and calf muscle tissue homogenate were measured by limiting dilution plaque assay on confluent monolayers of Vero cells (n = 5).

Data produced and analyzed by Rebecca Broeckel.

### **CHKVf5 vaccines induced protective responses in mice challenged**

**intramuscularly.** Following CHIKV challenge, the CHIKVf5 vaccine elicited earlier inflammatory responses at 3 dpi compared to control mice. In general, CHIKV replicates to high titers in the ankle, and infection by this route may promote viral replication and dissemination in a manner that T cells are unable to control. This lead us to the hypothesis that the route of CHIKV infection may influence the efficacy of the vaccine. To test this hypothesis, we compared three different infection routes (footpad, intramuscular into the calf muscle, vs. subcutaneous) in unvaccinated mice and monitored footpad swelling and viral tissue distribution (**Fig 4-4**). Only animals infected in the footpad developed swelling in the ipsilateral footpad and ankle but not in the contralateral ankle (**Fig 4-4A**). Similarly, only the animals infected via the footpad route developed viremia at 3 dpi (**Fig 4-4B**). Infectious virus was isolated from footpad-infected animals in both ipsilateral and contralateral ankles and calf muscles (**Fig 4-4C-F**). In contrast, animals infected intramuscularly had the highest levels of virus in the ipsilateral calf at 5 dpi and detectable virus in the ipsilateral ankle, while virus isolation from the contralateral calf was variable. Animals infected s.c. had detectable virus in the ipsilateral ankle, and levels in the ipsilateral calf and contralateral ankle were variable with no virus detectable in the contralateral calf muscle.

The footpad infection group had the best viral distribution. However, the i.m. group had consistent viral titers in the ipsilateral calf and ankle. Therefore, we vaccinated a second group of mice with MCMV and AdV CHIKVf5 or control vaccines as described above. In addition, we included a group of mice that received a primary MCMV-CHKVf5 or MCMV control vaccine followed at 8 weeks with a secondary boost vaccine using AdV CHIKVf5 or AdV control vaccine (**Fig 4-5A**). Prior to challenge with CHIKV, T cell responses were measured in splenocytes from two of the vaccinated animals per group by IFN $\gamma$  ELISpot assays. While splenocytes from AdV-CHKVf5 vaccinated mice produced higher levels of IFN $\gamma$  expressing T cells in response to

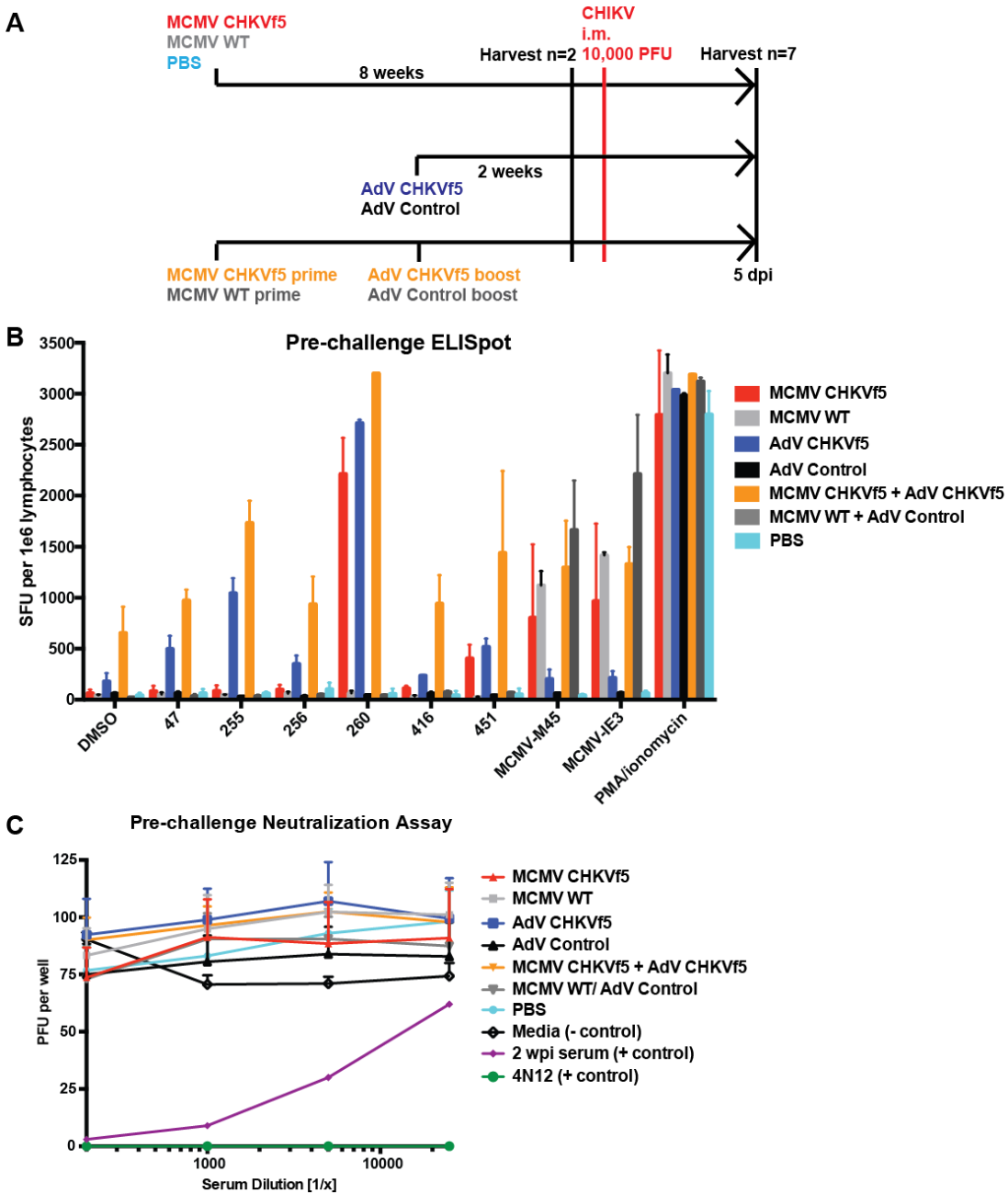


**Figure 4-5: CHKVf5-vaccinated mice do not develop neutralizing antibodies to CHIKV, but their splenocytes produce IFN $\gamma$  in response to CHIKV peptide stimulation.**

(A) Mice were vaccinated with the indicated vaccine, challenged with CHIKV i.m., and harvested at 5 dpi. (B) Prior to CHIKV challenge, IFN $\gamma$  ELISpot assays were performed on vaccinated mice (n = 2), and (C) sera from each of the mice were tested for neutralization potential via PRNT assays (n = 9). PRNT assay positive controls included convalescent mouse sera from a previously CHIKV infected mouse (shown in purple) as well as a potent neutralizing monoclonal antibody (4N12; shown in green).

Data produced and analyzed by Rebecca Broeckel.

CHIKV peptide stimulation compared to the MCMV vaccine platform, T cell responses were highest for the prime boost approach (**Fig 4-5B**). In fact, the prime boost approach induced reactive frequencies for some of the peptides to levels that were greater than an additive score. Since two of the peptides included in the CHIKVf5 are derived from E1, we measured neutralizing antibody levels in the serum from mice vaccinated by the different regimens outlined here. Standard plaque reduction neutralization titer (PRNT) assays were performed on 5-fold dilutions of serum. Positive control serum from an infected animal and a potent neutralizing monoclonal antibody (4N12) as well as negative control sera from uninfected non-vaccinated animals were used as controls for PRNT assays (311). Serum from all the CHIKVf5 vaccine groups failed to neutralize CHIKV, suggesting that the CHIKVf5 vaccine does not elicit neutralizing antibodies (**Fig 4-5C**).

A total of seven mice from each of these vaccine groups were challenged by intramuscular calf injection with  $10^4$  pfu of CHIKV. At 5 dpi, mice were euthanized and tissues were collected for virological and immunological assessments. Infectious viral titers in the ipsilateral ankle and calf muscle were determined by limiting dilution plaque assays from tissue homogenates (**Fig 4-6A-B**). Though there was no statistically significant reduction in virus load in the ipsilateral ankle, there was a significant reduction in infectious virus in the ipsilateral calf from all of the CHIKVf5 vaccine groups (MCMV, AdV and prime/boost) relative to the appropriate vaccine controls. This finding suggests that the vaccine dramatically reduces viral loads in the calf muscle, but not the ankle tissues.

**CD8+ T cells mediate protection by the CHIKVf5 vaccine in mice.** Since neutralizing antibodies were not detected in the vaccinated animals at the time of challenge, we hypothesized that the protection elicited by the CHIKVf5 vaccine is mediated by the induction of protective T cell responses. Therefore, to determine whether the CHIKVf5 vaccine-mediated protection was due to T cells, we performed T cell depletion experiments using CHIKVf5

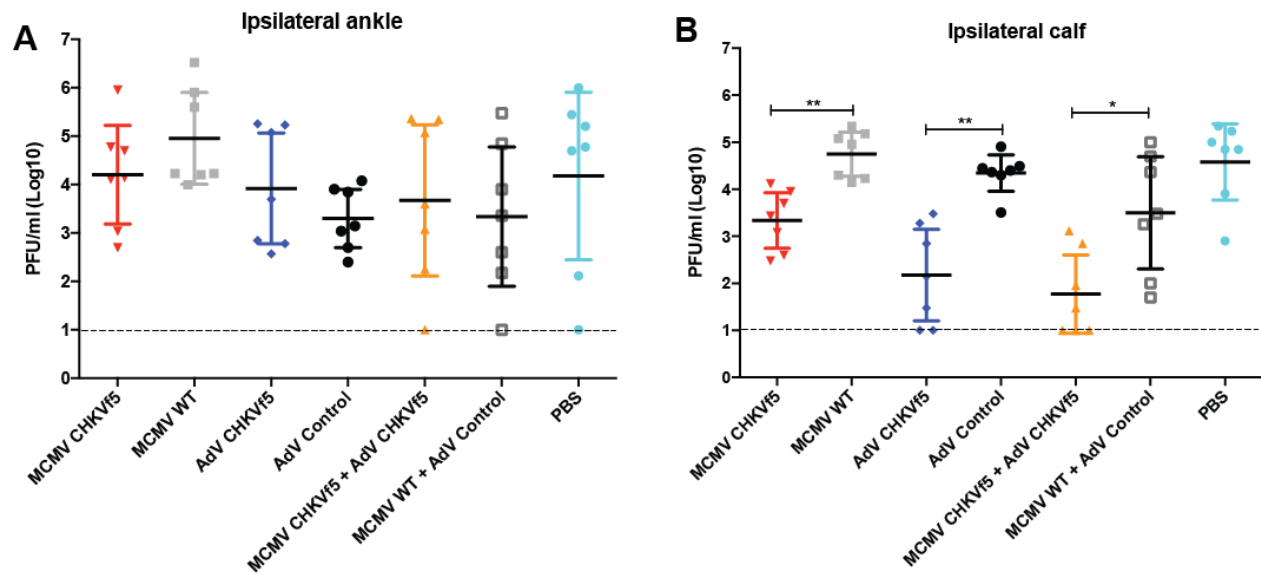


**Figure 4-6: CHKVf5 vaccine groups had reduced levels of CHIKV in the ipsilateral calf.**

Mice were vaccinated as outlined in **Figure 4-5**, and challenged i.m. with 10,000 PFU CHIKV SL15649. Whole tissues were collected in 1 ml media, and homogenates were titered by limiting dilution plaque assays on confluent monolayers of Vero cells. **(A)** Infectious virus levels detected in the ipsilateral ankle and **(B)** ipsilateral calf. Statistics were reported on log-transformed data using Holm-Sidak's multiple comparison test (\*  $p < 0.05$ ; \*\*  $p < 0.005$ ;  $n = 7$ ).

Data produced by Rebecca Broeckel, Takeshi Ando, Daniel Streblov, and Michael Denton and analyzed by Rebecca Broeckel.

prime/boost vaccinated animals. Animals were infused with depleting antibodies targeting CD4+, CD8+, or both CD4+ and CD8+ T cells (**Fig 4-7A**). To confirm effective and specific T cell subset depletion, at 5 dpi splenocytes isolated from three mice were collected and stained with fluorophore-conjugated antibodies to measure T cell depletion by flow cytometry. As shown in **Fig S-13**, depletion of specific T cell subpopulations (CD4 and/or CD8) were appropriately depleted to levels of greater than 95%. Similar to the experiments described in **Figure 4-6**, mice challenged after receiving the CHKVf5 vaccine that were untreated or those receiving a control rat IgG or CD4+ T cell depleting antibody had significantly reduced levels of infectious CHIKV present in the calf muscle relative to control groups but similar levels in the ankle (**Fig 4-7B**). These groups were not significantly different from each other suggesting that CD4+ T cells do not play a major role in CHIKVf5-mediated protection. However, depletion of CD8+ T cells increased levels of infectious CHIKV present in the calf, suggesting that CD8+ T cells play a role in the vaccine-mediated protection against CHIKV i.m. challenge. Interestingly, mice receiving depleting antibodies directed against both CD4+ and CD8+ T cells demonstrated a dramatic increase in CHIKV present in calf muscle to levels observed in the vaccine control groups. This finding suggests that the effects of CD4+ and CD8+ T cells synergize to mediate protection in the calf muscle. There were three mice that, when depleted of CD8+ T cells, did not have increased levels of virus in the ipsilateral calf. Future experiments are planned to measure viral burden in these samples by qRT-PCR because it has a lower limit of detection compared to plaque assay. **Fig 4-7C** show data to confirm that CHIKV neutralizing antibodies were not present in the vaccinated mice prior to CHIKV challenge. In addition, splenocytes from the various groups were analyzed by peptide ELISpot assays to determine whether the specific peptide responses were diminished appropriately by specific CD4 and CD8 depletion. As shown in **Fig 4-7D**, *in vivo* depletion of CD4+ T cells eliminated IFN $\gamma$  responses for peptide 255, but responses for peptides 260 and 451 were blocked by depletion of CD8+ T cells. These data indicate that muscle tissue protective immunity elicited by the CHKVf5 vaccine is mediated by

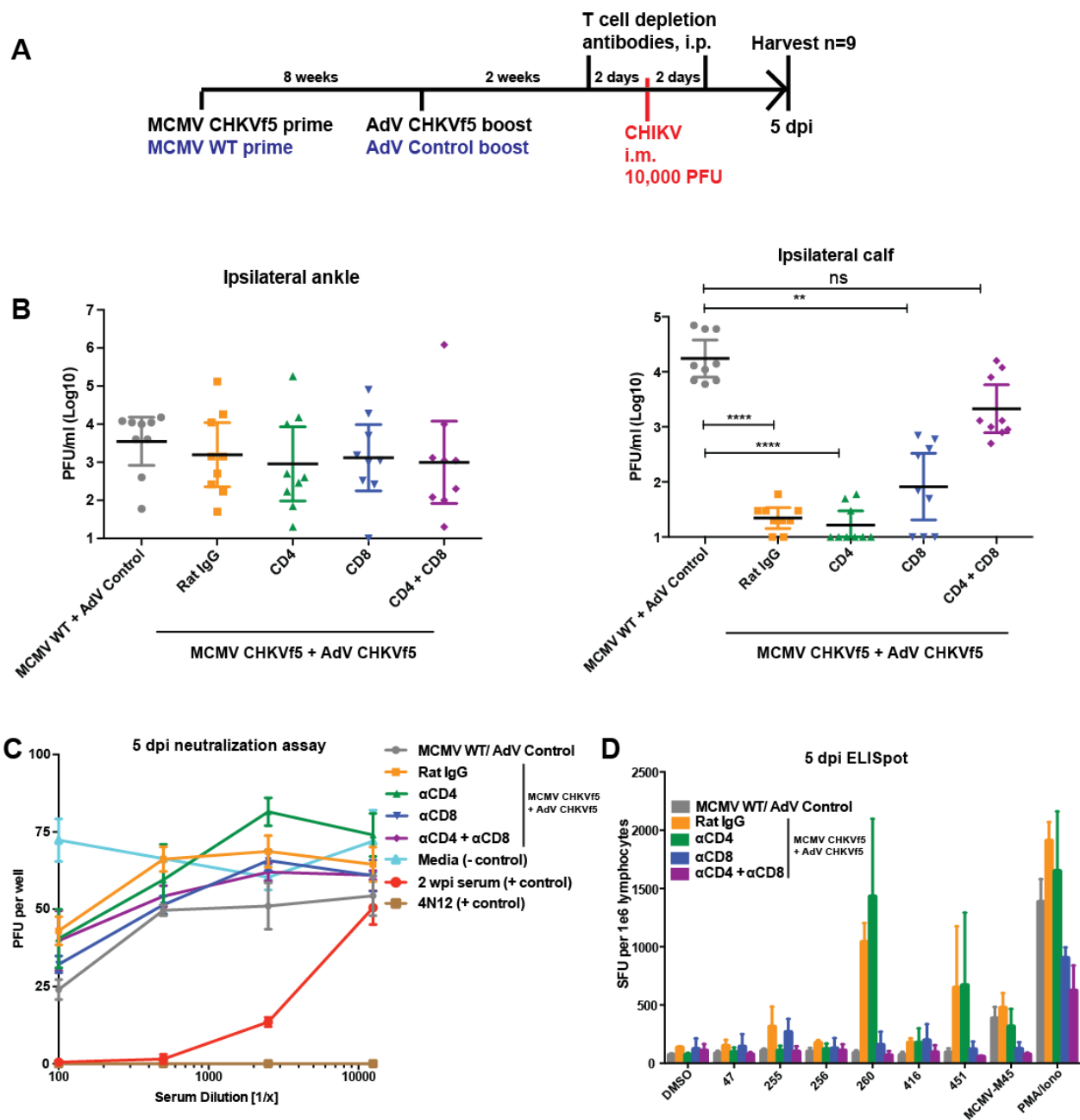


**Figure 4-7: Combined CD8+ and CD4+ T cell depletion reverses the protective effect of the CHKVf5 vaccine.**

(A) Mice vaccinated with MCMV CHKVf5 and boosted with AdV CHKVf5, or control vectors were treated with 300  $\mu$ g rat isotype control, anti-CD4, anti-CD8, or anti-CD4 plus anti-CD8 depleting antibodies at two days prior to challenge. Mice were infected i.m. with 10,000 PFU CHIKV SL15649, and (B) ankle and calf tissue viral loads were measured by limiting dilution plaque assays. Statistical analysis was performed on log-transformed data using Dunn's multiple comparison test (\*\*  $p < 0.005$ ; \*\*\*\*  $p < 0.0001$ ;  $n = 9$ ). (C) Neutralization assays were performed using mouse serum isolated at 5 dpi. (D) Splenocytes from vaccinated mice were collected and stimulated with CHIKV peptides on ELISpot plates. The results of the ELISpot assay are reported ( $n = 4$ ).

Data produced in panel B by Rebecca Broeckel, Craig Kreklywich, Daniel Streblov, and Patricia Smith and analyzed by Rebecca Broeckel. All other data produced and analyzed by Rebecca Broeckel.

the potent generation of both CD4<sup>+</sup> and CD8<sup>+</sup> T cell responses that act in a synergistic manner. Further experiments to measure levels of anti-CHIKV antibodies in CHIKVf5-vaccinated mice by ELISA are ongoing.

#### 4.4 DISCUSSION

While the development of neutralizing antibodies is a clear immunological correlate of protection for CHIKV, it was unknown what role T cells play in protection against CHIKV infection and disease. In the current study, we first mapped the complete T cell response to CHIKV using a CHIKV peptide library of 18-mers overlapping by 10 amino acids in order to identify potential CHIKV targets for development of a T cell vaccine. During this T cell profiling experiment, we identified 26 unique peptide sequences that elicited significant IFN $\gamma$  responses in splenocytes obtained from CHIKV-infected C57Bl/6 mice. Based upon this information, we constructed a fusion polyprotein that contained the amino acid sequence for a number of these positive CHIKV T cell peptides. This CHIKVf5 fusion gene was inserted into two different T cell promoting vaccine platforms including MCMV and AdV. Vaccinated mice developed robust T cell responses directed against the transgene construct that were amplified following challenge with CHIKV. While the vaccine did not protect against footpad challenge with CHIKV, the vaccine significantly reduced viral loads in the calf muscle when challenged by this route. Two crucial findings indicate that the CHIKVf5 vaccine elicits protection through T cells. First, depletion of CD4<sup>+</sup> and CD8<sup>+</sup> T cells at 2 days before challenge negated the protective efficacy of the vaccine by restoring viral loads to levels observed in vaccine controls and non-vaccinated mice. It appears that both T cell subtypes contribute to immune efficacy since depletion of either CD4<sup>+</sup> or CD8<sup>+</sup> T cells failed to restore CHIKV tissue load to control levels. However, depletion of CD8<sup>+</sup> T cells significantly reduced the ability of mice to control virus indicating a dominant role for these cells. We presume that CD4<sup>+</sup> T cell help is required for full efficacy. Second, the CHIKVf5 vaccine does not contain any known CHIKV neutralizing domains. As such, we did not

detect neutralizing antibodies against CHIKV in any of the vaccinated mice, and the generation of antibody responses against CHIKV following challenge developed with normal kinetics and amplitude when compared to controls. Together, these data demonstrate that the CHKVf5 vaccine constructs elicit robust T cell responses that protected against CHIKV in muscle tissues.

T cell responses directed against CHIKV have been reported in humans during both the acute and chronic phases of infection. During the acute phase, there is a mobilization and amplification of activated CD8<sup>+</sup> T cells, followed by CD4<sup>+</sup> T cells (337). Following the acute phase, both patients who recovered from CHIKV and patients with chronic CHIKV-induced arthritis had roughly equal frequencies of CHIKV-specific IFN $\gamma$ -producing T cells in the blood (338). There is also evidence that T cells can enter CHIKV infected joint tissues in humans. In a synovial biopsy of a patient with chronic CHIKV-induced arthritis, activated (HLA-DR<sup>+</sup>) CD4<sup>+</sup> T cells were identified as a major cellular infiltrate, but oddly, CD8<sup>+</sup> T cells were rarely found (110). CHIKV RNA and antigen have been detected in joint synovial biopsies and muscle tissue (110, 111), which is suggestive of viral persistence in the joints and muscle. Though it is not known whether T cells protect against CHIKV in humans, our data would suggest that antiviral CD8<sup>+</sup> T cells may promote viral clearance in the muscle tissue.

We showed that vaccinated animals had a significant reduction of CHIKV titers in the calf muscle. The tissue-specific protection is reminiscent of the study with RRV, where protection by CD8<sup>+</sup> T cells was observed in the muscle tissue during RRV infection (343). The authors of this study showed that CD8<sup>+</sup> T cell depletion resulted in higher levels of RRV in the quadriceps, that CD8<sup>-/-</sup> mice had higher levels of virus in the quadriceps compared to controls, and that T cell adoptive transfer into Rag1<sup>-/-</sup> mice reduced RRV levels in the quadriceps. However, none of these treatments affected the ankle tissue in the RRV model. Similarly, we found that CHKVf5-elicited T cells were unable to reduce viral burden in the ankles. In addition to RRV, T cells play a protective role in SINV and VEEV infections. For SINV, T cells were

shown to be important for viral clearance in the brain and spinal cord (344). Adoptive transfers of SINV-specific T cells into Rag1<sup>-/-</sup> mice resulted in viral clearance. For VEEV, CD4<sup>+</sup> T cells were important for protection mediated by a live-attenuated vaccine (345). Together these studies demonstrate the importance of T cells in viral clearance from alphavirus-infected tissues.

An interesting finding that became apparent through the results of our vaccine study was that T cell responses elicited by CHIKVf5 were more frequent and directed against different epitopes compared to those observed during CHIKV infection. For example, splenocytes from CHIKV infected mice had high frequencies of IFN $\gamma$  responses to peptides 47-48, 256, 350, 439, and 451. Since peptides 47, 256, and 451 were included in the CHKVf5 fusion gene, we expected that vaccinated mice would primarily induce responses to those epitopes. However, peptide 260 and 451 stimulated the highest frequency of IFN $\gamma$  responses in splenocytes from CHKVf5 vaccinated mice. Thus, the vaccine-induced cellular responses were skewed towards a different set of epitopes compared to those observed following CHIKV infection. This suggests that the protection elicited by the CHKVf5 vaccines may be because of the skewing of the immune response and the higher frequencies of responding cells to CHIKV epitopes.

Both MCMV and AdV CHKVf5 vaccines elicited strong T cell responses to the CHIKV peptides, but the breadth of responses was different depending on the vaccine vector. The AdV CHKVf5 vaccine induced a higher breadth of responses directed against peptides 47, 255, 256, 260, and 451, while MCMV CHKVf5 mainly induced responses directed against 260 and 451. Vaccination with both vaccines in a prime-boost approach dramatically increased the frequency of responses and elicited a full breadth of responses to CHKVf5. MCMV and AdV vectors can elicit different memory T cell populations after vaccination. Adenoviruses elicit potent effector and central memory CD8<sup>+</sup> T cells to a vaccine antigen inserted into the adenovirus genome (483). MCMV vaccine vectors uniquely elicit long-lasting effector memory T cells to vaccine

antigens fused to the C-terminus of the IE2 gene (480, 481, 484). Together, the MCMV prime/AdV boost may offer advantages in induction of a diverse T cell memory response to CHIKV epitopes. These responses were sufficient to control CHIKV replication in the muscle tissue following CHIKV exposure.

Neutralizing antibodies are an important correlate of protection for CHIKV, and it would be essential for a prophylactic CHIKV vaccine to induce neutralizing antibody responses to protect from CHIKV acquisition. The data presented here show that a T cell component in a prophylactic vaccine could also be beneficial. This type of vaccine could also be used to prophylactically boost existing immunity and/or skew the responses towards additional epitopes for increased protection against CHIKV acquisition. These data also suggest that T cell vaccine may be feasible in a therapeutic context. Though we did not specifically test whether the vaccine is effective as a therapy, our upcoming experiments will evaluate the therapeutic efficacy of the adenovirus-vectored CHKVf5 vaccine. This is because the AdV-CHKVf5 elicited robust T cell responses within 10-14 days post vaccination and this vaccine could boost the existing anti-CHIKV T cell responses to promote viral clearance in the muscle tissue. This approach could be effective for eliminating CHIKV-induced myalgia in infected patients because the vaccine was effective in eliminating virus in the muscle tissue. Therefore, future studies will examine the effects of the CHKVf5 vaccine as a therapy.

#### 4.5 MATERIALS AND METHODS

**Cells.** Veros, mouse embryonic fibroblasts (NIH/3T3), and 293-IQ cells (HEK293 cells expressing the lac repressor (485)) were propagated at 37°C with 5% CO<sub>2</sub> in Dulbecco's Modified Eagle Medium (DMEM) supplemented with 5 or 10% Fetal Bovine Serum (FBS) and Penicillin-Streptomycin-L-Glutamine (PSG). *Aedes albopictus* cells (C6/36s) were propagated at 28°C with 5% CO<sub>2</sub> in DMEM supplemented with 10% FBS and PSG.

**CHIKV.** CHIKV SL15649 and CHIKV 181/25 was generated from the infectious clones gifted from Dr. Mark Heise (UNC Chapel Hill). Briefly, the infectious clone was digested with NotI, and DNA was purified with the QIAquick PCR purification kit (Qiagen) according to the manufacturer's instructions. Viral mRNA was generated with the mMESSAGE mMACHINE SP6 Transcription Kit (ThermoFisher), and the mRNA was purified using the RNeasy Mini Kit (Qiagen). Roughly 3 µg RNA was transfected into Vero cells using Lipofectamine 2000 (ThermoFisher). CHIKV virus stocks were passaged once C6/36 cells for 72 hrs prior to ultracentrifugation. CHIKV stocks were prepared by ultracentrifugation over a 15% sucrose cushion (SW 32 Ti Rotor, 1 hr 10 min, 76,755 x g), and the virus pellets were resuspended in PBS. Virus aliquots were frozen at -80°C. For CHIKV plaque assays, 10-fold serial dilutions of tissue homogenates were plated on Vero cells. The cells were placed on a rocker in an incubator at 37°C with 5% CO<sub>2</sub> for 2 hrs, and DMEM containing 0.3% high viscosity carboxymethyl cellulose (CMC) (Sigma) and 0.3% low viscosity CMC (Sigma) was added to the cells. After two days, cells were fixed with 3.7% formaldehyde (Fisher), stained with 0.5% methylene blue (Fisher), and dried. Plaques were enumerated under a light microscope.

**MCMV vectors.** The Smith strain MCMV bacterial artificial chromosome (BAC) pSMfr3 (486) was utilized for generating infectious MCMV vaccines. The gene of interest was inserted in-frame onto the C-terminus of the MCMV *IE2* gene so that the insertion is co-expressed with *IE2* (480). Generation of the MCMV constructs was performed via a two-step galactokinase/kanamycin (GalK/Kan) cassette insertion and replacement (487, 488). The GalK/Kan cassette was generated by PCR with primers that overlapped *ie2* by 50 bp. The PCR product was electroporated into electrocompetent SW105 cells containing pSMfr3, and bacteria were selected on Kan-containing agarose plates. The fusion gene CHKVf5 was generated by overlapping PCR. A PCR product containing 50 bp homology with *ie2* was generated (F primer: GGTTCCTTCTCTTGACCAGAGACCTGGTGACCGTCAGGAAGAAGATTCAGTGTGCGGTGC

ATTCGATGAC, R primer:

AACCTCTTTATTTATTGATTA AAAACCATGACATACCTCGTGTCTCTCAGGCGTAGTCGGG  
CACATC) and electroporated into SW105 cells containing the IE2-GalK/Kan MCMV BAC.

Resulting bacteria were selected on 2-deoxy-galactose (DOG) minimal plates, and the presence of the insert was confirmed by PCR and sequencing. Virus was reconstituted by electroporation into NIH/3T3 cells, and passaged five times to eliminate the BAC cassette prior to ultracentrifugation. Constructs were screened by PCR and sequenced to confirm the presence of the insert. MCMVs were titered by plaque assays on NIH/3T3s. Dilutions of virus was plated on NIH/3T3s, and cells were placed in an incubator on a rocker for 2 hrs. At 2 hpi, a CMC overlay was added to the cells, and the cells were incubated for 5-7 days, until plaques were formed, prior to fixing and staining with methylene blue.

**Adenovirus vectors.** Replication-defective human Ad5 adenoviruses (del E1, E3) were generated using the AdMax HiIQ system (Microbix). Genes of interest were cloned into the shuttle plasmid pDC316(io) and co-transfected with pBHGlox $\Delta$ E1,3Cre plasmid into 293 IQ cells to reconstitute virus as previously described (485, 489). Transfections were performed using the PureFection kit (System Biosciences) according to the manufacturer's protocol, and adenovirus plaques were observed after 10-14 days in cell culture. Viruses were passaged four times in 293 IQ cells prior to ultracentrifugation. Constructs were screened by PCR and sequenced to confirm the presence of the insert. Adenovirus titers were calculated using limiting dilution assays on 293 IQs in 96-well plates.

**Mice.** All mouse experiments were performed at OHSU in ABSL3 laboratories in compliance with IACUC protocols. The small lab animal unit at OHSU is accredited by the Association for the Accreditation and Assessment of Laboratory Animal Care (AALAC) International. Animals were housed in ventilated racks and monitored daily by veterinary staff. C57BL/6J mice were vaccinated as indicated with MCMV delivered intraperitoneally ( $10^6$  PFU,

i.p.), and/or AdV injected intramuscularly in the thigh ( $10^8$  PFU, i.m.). Mice were challenged with  $10^3$  PFU CHIKV in a 20  $\mu$ l volume in the footpad (f.p.), or they were challenged (i.m.) with  $10^3$  or  $10^4$  PFU in a 20  $\mu$ l volume in the calf muscle. Footpad measurements were taken with calipers. For T cell depletion experiments, mice were administered T cell depleting antibodies diluted in PBS in a 100  $\mu$ l volume (i.p.). Vaccinated groups were injected with 300  $\mu$ g anti-CD4 (GK1.5, BioXCell), 300  $\mu$ g anti-CD8 (2.43, BioXCell), 300  $\mu$ g Rat IgG2b Isotype Control (LTF-2, BioXCell), or a combination of 300  $\mu$ g anti-CD4 and 300  $\mu$ g anti-CD8. T cell depletions were confirmed by flow cytometry. To confirm T cell depletions, splenocytes were stained with fluorophore-conjugated antibodies specific for mouse CD3, CD4, CD8, and CD19. Fluorescent markers were detected on an LSRII instrument (BD Pharmingen) and data was analyzed using FlowJo (TreeStar).

**Western Blot Analysis.** NIH/3T3's were left uninfected or infected with MCMV CHKVf5 or AdV CHKVf5. Cells were lysed in 1x Cell Lysis buffer (Cell Signaling) supplemented with 1mM Phenylmethylsulfonyl fluoride (PMSF) (Fisher), scraped, and incubated on ice for 15 min. Lysates were centrifuged (4°C, 10 min, 16,000 x g), and supernatants were transferred to a new tube containing Laemmli buffer. Samples were boiled 10 minutes and loaded onto 4-12% Bis-Tris SDS-PAGE gels (Thermo/Fisher). Samples were transferred onto Immobilon-P Transfer Membranes (Fisher). Membranes were blocked in 5 % milk powder in Tris-buffered saline supplemented with 0.1% Tween 20 (TBST), and membranes were probed with anti-HA antibody (Roche, clone 3F10) at 1:1000 dilution followed by rabbit anti-Rat HRP-conjugated secondary antibody or anti-GAPDH-HRP (Cell Signaling) for a loading control. Blots were washed with TBST, and the membrane was incubated with chemiluminescent substrate to visualize the bands. The membrane was exposed with X-ray film.

**Neutralization Assays.** Blood samples were collected and left at room temperature for 30 minutes to allow for clotting. Blood was centrifuged (5 min, 3,000 x g) and sera was transferred to a new tube. Sera was heat-inactivated at 56°C for 30 minutes. Following heat-inactivation, sera was serially diluted in DMEM supplemented with 5% FBS and PSG. Roughly 100 plaque forming units of CHIKV 181/25 were added to serum dilutions, and the complexes were incubated at 37°C for 2 hrs. Following incubation, complexes were added to Vero cells and placed on a rocker for 2 hrs at 37°C. After 2 hrs, CMC-containing media was added to the cells, and cells were placed in a 37°C incubator for two days prior to fixing and staining.

**ELISpot Assays.** ELISpot assays were performed as previously described (490). Briefly, a single cell splenocyte suspension was prepared by pushing whole spleen through a 70 µm cell strainer and rinsing with 15 ml RPMI complete media (10% FBS, PSG). Cells were pelleted (10 min at 650 x g), and red blood cells were lysed with 1x Red Blood Cell Lysis Buffer (Bioleged) for 3 min. Splenocytes were replenished with 10 ml RPMI complete and pelleted as before. Cells were resuspended into 5 ml RPMI complete, counted, and samples were normalized to cell count. Splenocytes were added to prewashed Mouse IFN $\gamma$  ELISpot plates (MabTech) with 1 µl peptide (10 µg/well), 1 µl DMSO, or 1 µl of phorbol 12-myristate 13-acetate/Ionomycin stock as a positive control. Splenocytes were incubated on ELISpot plates for 24-48 hrs. Plates were washed and incubated with anti-mouse IFN $\gamma$  biotin antibody for 2 hrs and streptavidin-ALP antibody for 1 hr according to the manufacturer's protocol. Spots were visualized using BCIP/NPT-plus substrate, and plates were rinsed with water and dried prior to counting with an AID ELISpot plate reader.

## CHAPTER 5 DISCUSSION AND FUTURE DIRECTIONS

### 5.1 SMALL MOLECULE KINASE INHIBITORS AND CHIKV

We found that dasatinib blocked translation of CHIKV sgmRNAs, while translation of the viral genomic mRNA and host mRNAs was not affected by the kinase inhibitor. These data imply that SFKs play crucial roles in translation of viral sgmRNAs in human fibroblasts. In contrast to my *in vitro* data, dasatinib appeared to enhance viral replication *in vivo*. Dasatinib has many targets *in vivo*, including blocking SFKs, which are important for induction of adaptive immunity. B and T cells are essential for controlling virus infections in the blood and tissues. Therefore, it was not surprising that dasatinib did not inhibit viral replication *in vivo*. This finding raises the question as to whether dasatinib could be effective in mice lacking B and T cells (Rag1<sup>-/-</sup> or Rag2<sup>-/-</sup> mice), wherein virus persists for the lifetime of the mouse. However, future studies will work towards identifying a specific host factor that dasatinib blocks in NHDFs that is required for translation of viral sgmRNAs. Blocking this host factor using a more specific inhibitor may show better efficacy *in vivo*.

Other future studies will be devoted to characterizing the host kinase landscape during CHIKV replication. Recent advances in kinome screening have shown that enrichment of cellular kinases, using multiplexed kinase inhibitor beads, followed by MS detection (MIB-MS) allows for the identification of kinase abundance as well as the kinase activation status in a large proportion of the cellular kinome (491-495). We are currently working with Dr. Nathaniel Moorman and Dr. Mark Heise to map changes that occur in the human kinome during CHIKV infection in human fibroblasts using this multiplexed kinase inhibitor bead assay (MIB-MS). My goal is to identify new kinase pathways that are important for viral replication, which will open opportunities for using other kinase inhibitors as therapies to treat alphavirus infections.

## 5.2 MONOCLONAL ANTIBODIES AS THERAPIES OR PROPHYLACTICS

We showed that a humanized antibody therapy is effective as a therapeutic in rhesus macaques if given at days 1 and 3 post infection. The therapeutic reduced viral replication in the blood and tissues, and as a result, the antiviral therapy reduced joint inflammation. In addition to these findings, our study showed that CHIKV could be partially cleared from tissues that were already infected with CHIKV, demonstrating that potent antiviral antibodies may be able to clear virus in infected tissues to some degree. Future studies could test whether changing the Fc portion of the antibody optimizes Fc-mediated effector functions to promote viral clearance in infected tissues, and whether modifications that increase the antibody half-life improve efficacy.

Future studies will also work towards defining the therapeutic window by which the antibody therapy remains effective. Given that neutralizing antibodies are very effective in clearing virus in the blood, the therapeutic window may be related to the length of the viremic phase. Patients with more severe CHIKV infections tend to have higher viral titers during the acute phase, and some patients experience longer viremic phases (> 5 days). Therefore, the therapeutic window may be longer or shorter depending on the severity of the CHIKV infection. This mAb therapy could be highly effective in vulnerable populations, such as the neonates or patients over 60 years of age, that are at risk for more severe disease or in patients experiencing severe acute infections. In addition, the monoclonal antibody could be given prophylactically to vulnerable populations who are at risk during CHIKV outbreaks. Overall, this therapy is highly effective in treating CHIKV infection and preventing disease *in vivo*.

## 5.3 VACCINE OPTIONS FOR CHIKV

In Chapter 4, we showed that a vaccine containing a synthetic polypeptide comprised of T cell epitopes from CHIKV, called CHIKVf5, elicited protective immunity that is mediated by both CD4+ and CD8+ T cells. However, we still do not know whether the protective response is

mediated by single CD4 or CD8 epitopes or whether a combination of both types of responses are required for the observed protective immunity against CHIKV. Future experiments will address which T cell epitopes, alone or in combination, elicit protection. In order to dissect the protective responses elicited by CHIKVf5, we generated replication-defective adenoviruses that express individual CHIKV peptides 47, 256, 260, 416, and 451, which each containing an in-frame HA tag for detection. Mice were vaccinated with individual peptide AdV vectors or in combination. At 14 days post vaccination, splenocytes recovered from the vaccinated animals were analyzed for T cell responses using IFN $\gamma$  ELISpot assays for each individual peptide (**Fig 5-1A**). Mice vaccinated with AdV 47, AdV 260 and AdV 451 produced robust IFN $\gamma$  responses after stimulation with their corresponding CHIKV peptide. Based upon these findings, another set of mice was vaccinated with a control adenovirus, AdV 47, AdV 260, or AdV 451. Alternatively, mice were vaccinated with combinations AdV 47 + AdV 260, AdV 47 + AdV 451, AdV 260 + AdV 451, or AdV 47 + AdV 260 + AdV 451 (**Fig 5-1B**). Completion of this experiment will determine if peptides 47, 260, and/or 451 are necessary for protection in the muscle tissue.

A second set of future experiments will determine whether CHIKVf5 vaccines can protect therapeutically. For these experiments, mice will be infected with CHIKV in the footpad or in the calf and vaccinated at 14 dpi with AdV CHIKVf5. Mice will be sacrificed at different times post vaccination to measure whether the T cells elicited by vaccination promoted viral clearance in ankle or leg muscle tissues.

Additional studies may be devoted to determining the importance of T cells in the rhesus macaque model of CHIKV infection. Using this model, rhesus cytomegalovirus (RhCMV) vectors could be used to deliver T cell antigens to macaques prior to CHIKV challenge. Similarly, a T cell vaccine could be tested therapeutically in a cynomolgus macaque model to determine if a therapeutic vaccine could affect viral persistence in the tissues. Completion of these studies would provide evidence as to whether a prophylactic and/or therapeutic vaccine is feasible in

humans to clear persistent virus in the joints and muscles. A therapeutic vaccine could help patients recover from chronic CHIKV infection and improve the quality of life of patients experiencing chronic CHIKV-induced arthritis.

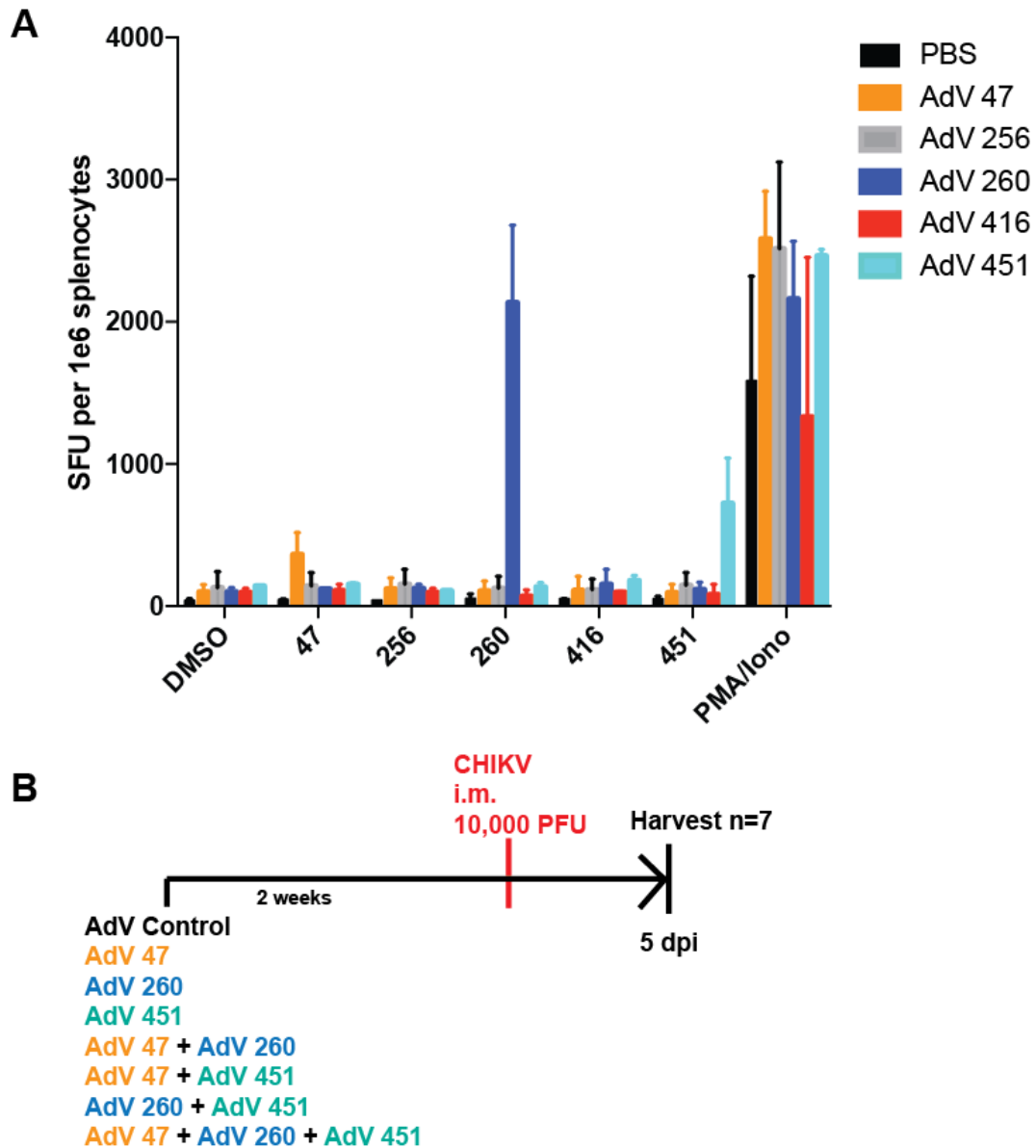


**Figure 5-1: Adenoviruses vaccines expressing CHIKV 18-mer peptides were tested for their ability to block CHIKV infection in the calf.**

(A) Mice were vaccinated with AdV peptide vaccines. At 2 wpi, splenocytes were collected and stimulated with CHIKV peptides, and their IFN $\gamma$  production was measured by IFN $\gamma$  ELISpot. (B) Mice were vaccinated with 10<sup>8</sup> PFU adenovirus i.m. as indicated. Two weeks post vaccination, mice were challenged i.m. with 10,000 PFU CHIKV SL15649.

Data produced by Rebecca Broeckel.

# APPENDIX I

## SUPPLEMENTAL DATA: DASATINIB PROJECT

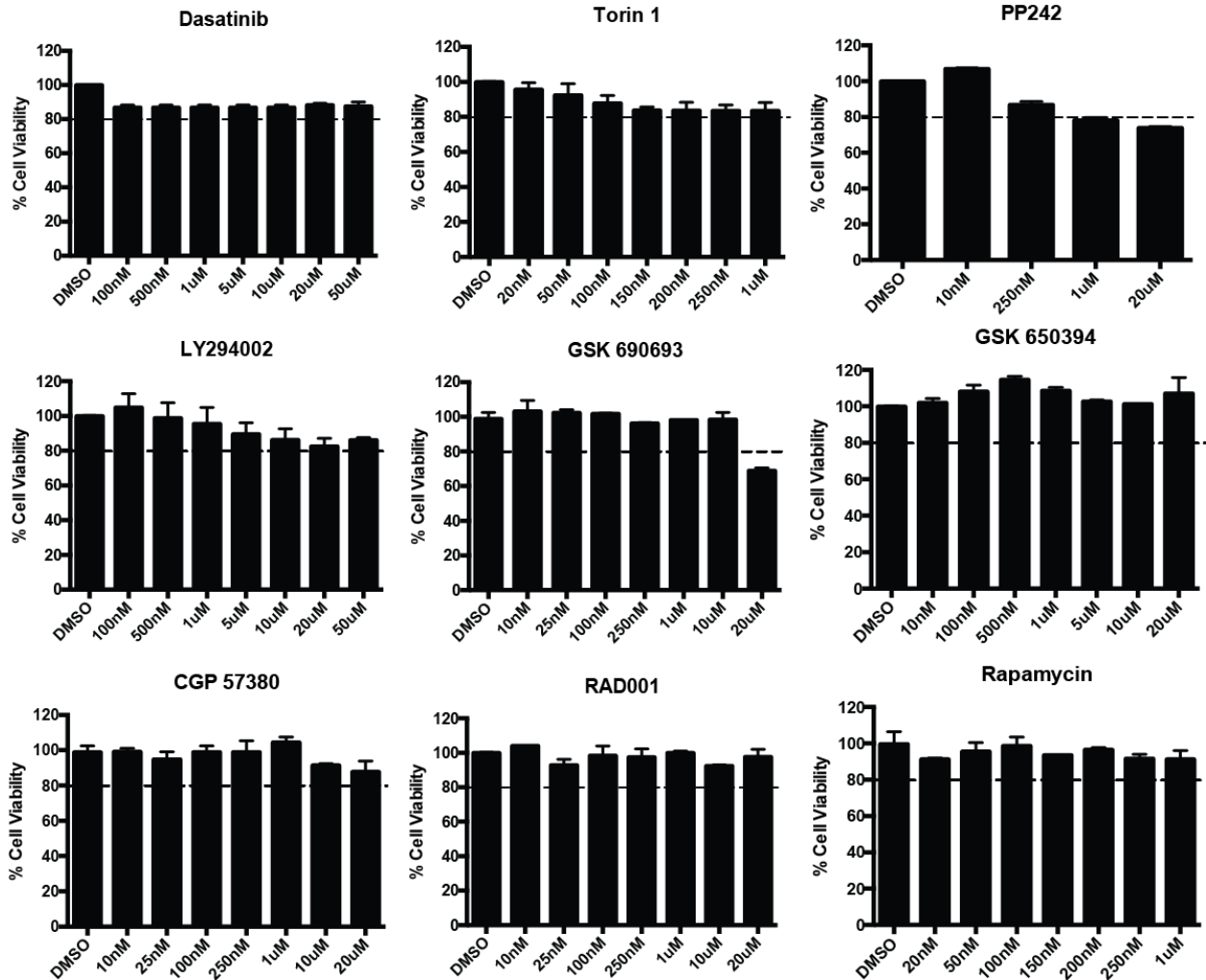
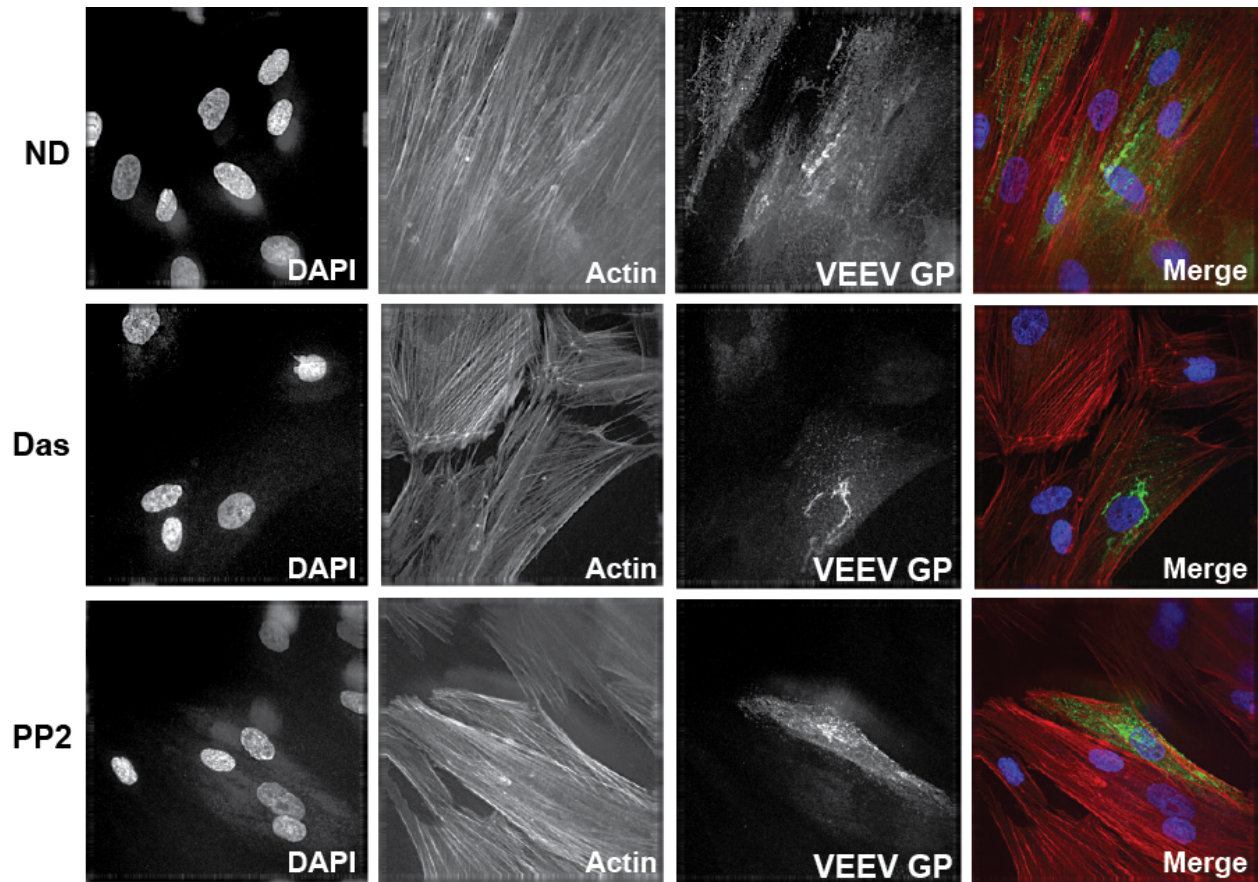


Figure S-1: Cell viability in NHDFs after treatment with different inhibitors.

Cells were treated with the indicated concentrations of inhibitors. At 24 hrs post treatment, cell viability was measured with the CellTiter-Glo Luminiscent Cell Viability Assay kit. The dotted line marks 80% cell viability, which was the viability cutoff for our assay.

Data produced by Rebecca Broeckel.



**Figure S-2: Dasatinib and PP2 block viral spread from infected cells.**

Cells were infected with VEEV (MOI = 1). At 2 hpi, cells were washed with PBS and treated with 10  $\mu$ M Dasatinib or 10  $\mu$ M PP2. At 24 hpi, cells were fixed, permeabilized, and stained for VEEV glycoproteins and counterstained with DAPI and Phalloidin to highlight host DNA and Actin filaments.

Data generated by Rebecca Broeckel and Patricia Smith and analyzed by Rebecca Broeckel.

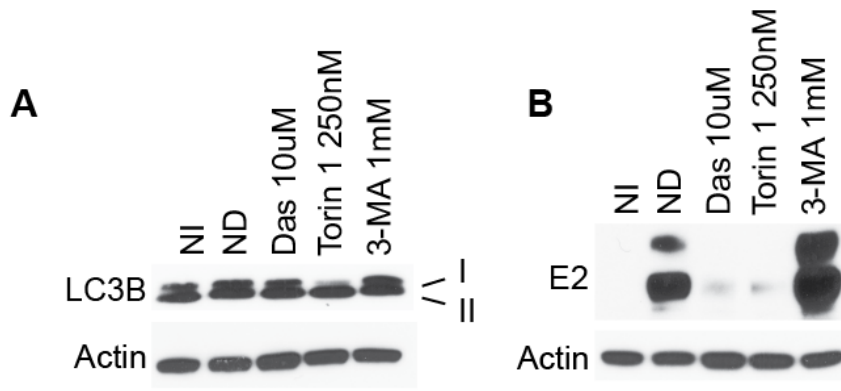


**Figure S-3: Dasatinib and Torin 1 differentially affect autophagy.**

NHDFs were infected with CHIKV (MOI = 3) or left uninfected (NI). At 2 hpi, cells were washed with PBS, and media containing drug was added to the cells as indicated. At 7 hpi, lysates were analyzed for **(A)** LC3 or **(B)** E2.

Data produced and analyzed by Rebecca Broeckel.

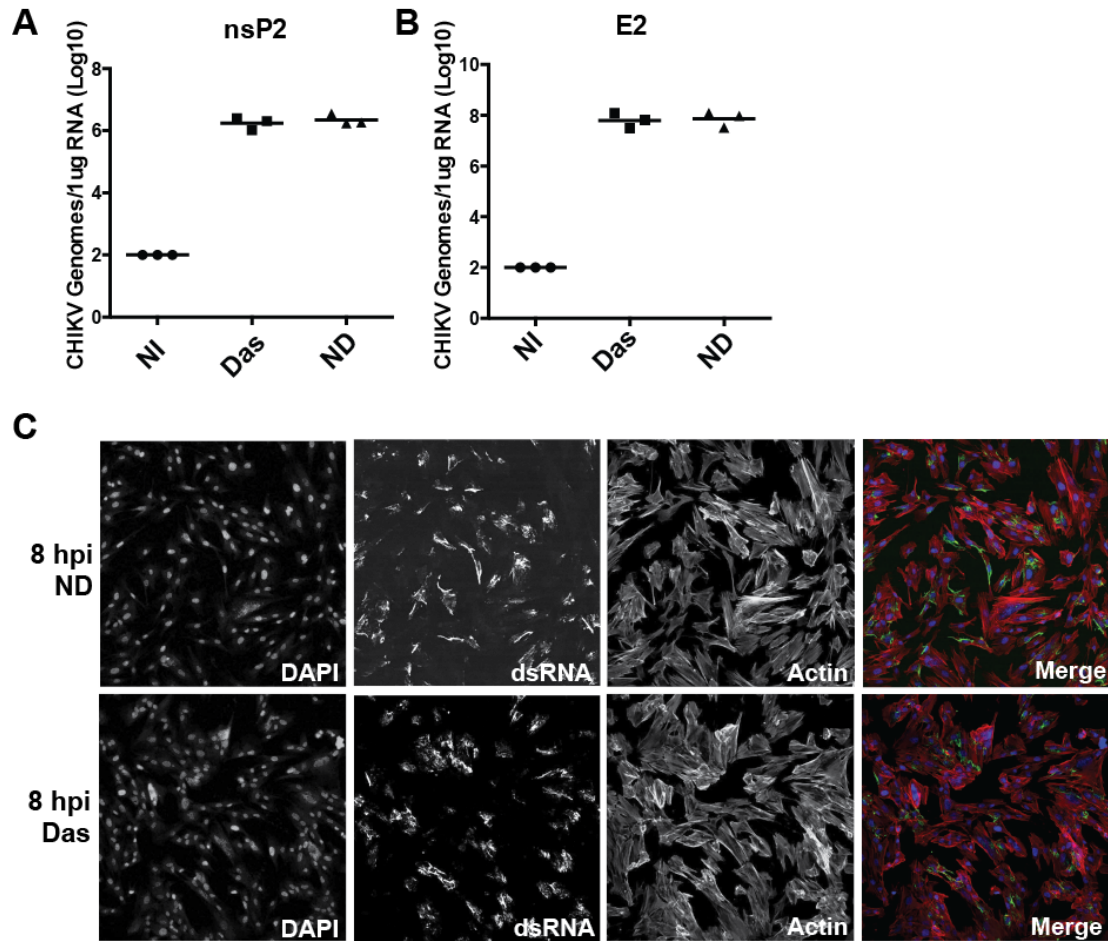


**Figure S-4: Dasatinib does not affect RNA levels and dsRNA complexes.**

NHDFs were infected with CHIKV 181-25 (MOI = 3). At 2 hpi, cells were washed with PBS, and media with no inhibitor or 10  $\mu$ M dasatinib was added back to the cells. At 12 hpi, cells were washed extensively in PBS, and cell lysates were scraped in Trizol. CHIKV nsp2 (**A**) and E2 (**B**) RNA levels were measured in cell lysates. (**C**) NHDFs were infected with CHIKV (MOI = 25), and cells were treated with dasatinib at 2 hpi or untreated. At 8 hpi, cells were fixed and analyzed for levels of dsRNA and counterstained with DAPI and Phalloidin (NI = uninfected, ND = no drug).

Panel A and B produced and analyzed by Thomas Morrison's group. Panel C produced and analyzed by Rebecca Broeckel.

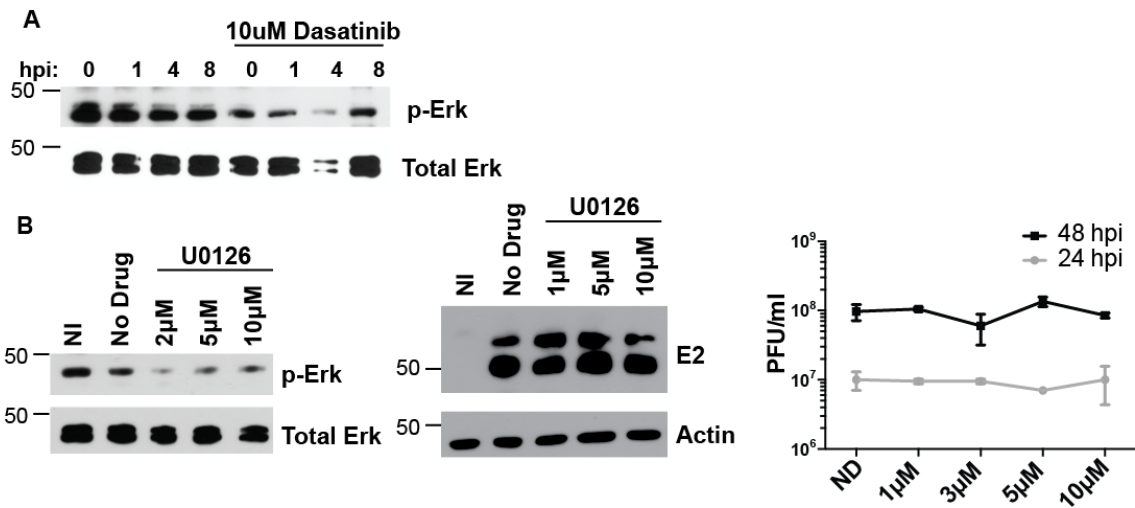


**Figure S-5: Erk inhibitor U0126 does not block CHIKV infection.**

(A) NHDFs were treated with dasatinib 30 minutes prior to infection and infected with CHIKV (MOI = 1). Phosphorylation of Erk and total Erk protein levels were detected by western blotting. (B) NHDFs were treated with U0126 at 2 hpi, and cell lysates were analyzed at 24 hpi for p-Erk and total Erk (left panel), CHIKV E2 and Actin (center panel) by western blotting. (Right panel) NHDFs were infected with CHIKV (MOI = 1), treated with U0126 at 2 hpi, and supernatants were collected at 24 hpi and 48 hpi and titered on Vero cells.

Data produced and analyzed by Rebecca Broeckel.

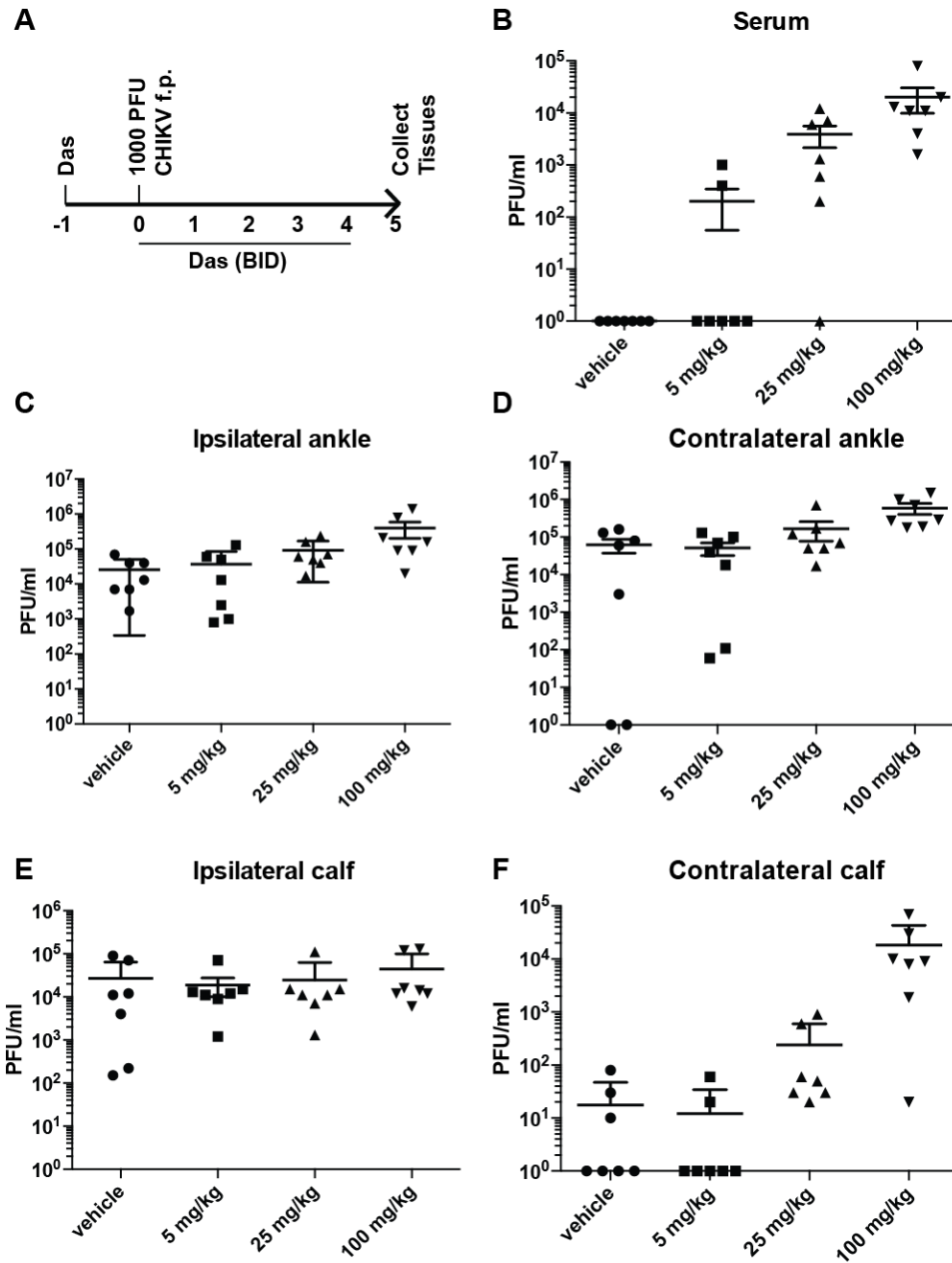


**Figure S-6: Dasatinib enhances viral replication in vivo.**

(A) C57BL/6 mice were treated with the indicated doses of dasatinib p.o. in a propylene glycol/water emulsion (1:1) once on the day prior to challenge and then twice daily (BID). At 5 dpi, mice were sacrificed and tissue viral burdens were measured by plaque assay. (B) 5 dpi sera was collected from CHIKV infected and treated mice, and CHIKV was measured by plaque assay. (C-F) Whole tissues were collected at 5 dpi, and they were homogenized in 1 ml media. The homogenate was then titered by plaque assay. Shown are the titers from ipsilateral ankle, contralateral ankle, ipsilateral calf, and contralateral calf, respectively.

Data produced and analyzed by Rebecca Broeckel.

SUPPLEMENTAL DATA: MONOCLONAL ANTIBODY THERAPY PROJECT

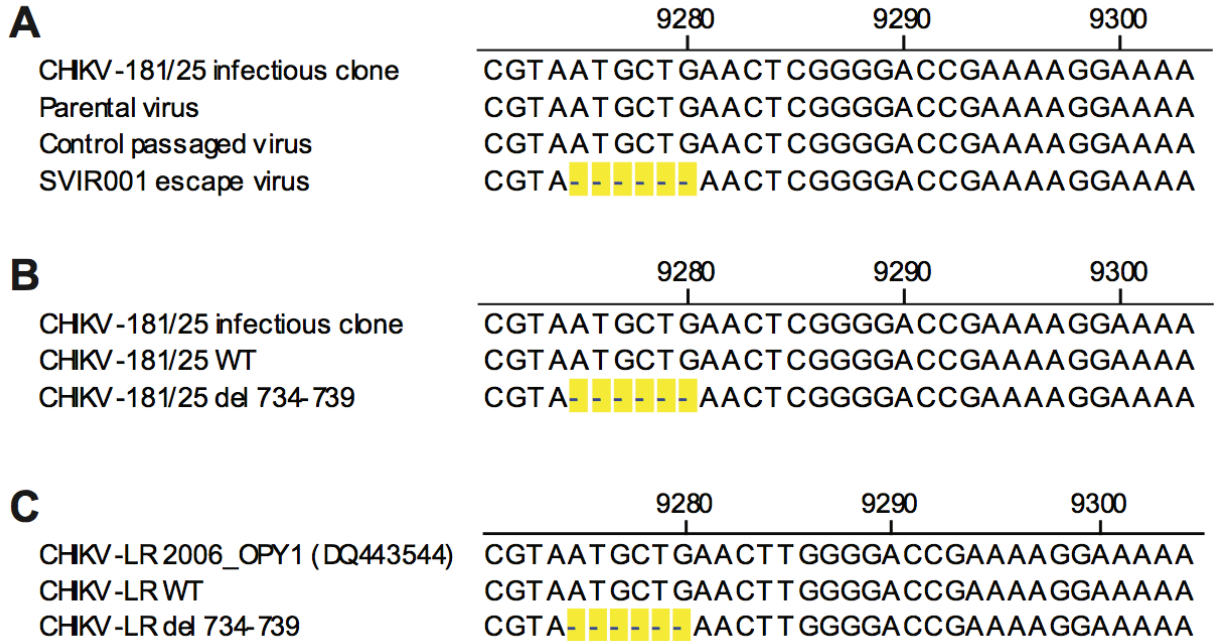


**Figure S-7: Sequence alignment of SVIR001 escape variant viruses.**

(A) Viral RNA was isolated from CHIKV-181/25 passaged in the presence of SVIR001, control passaged 181/25, or parental 181/25. cDNA was produced and sequenced to identify the escape mutation(s). The sequences were aligned to the CHIKV 181/25 infectious clone using MegAlign (DNASar). (B-C) Results of mutagenesis. The six nucleotide deletion (del 734-739) was introduced into the CHIKV-181/25 (B) or CHIKV-LR (C) infectious clone. WT or deletion mutant viruses were generated in BHK21 cells. Viral RNA was isolated from stocks, cDNA was produced, and sequenced to confirm mutation. The sequences were aligned to the CHIKV 181/25 infectious clone (B) or CHIKV strain LR2006\_OPY1 (accession number DQ443544) (C) using MegAlign (DNASar). Deletion is highlighted in yellow.

Data produced and analyzed by Julie Fox.

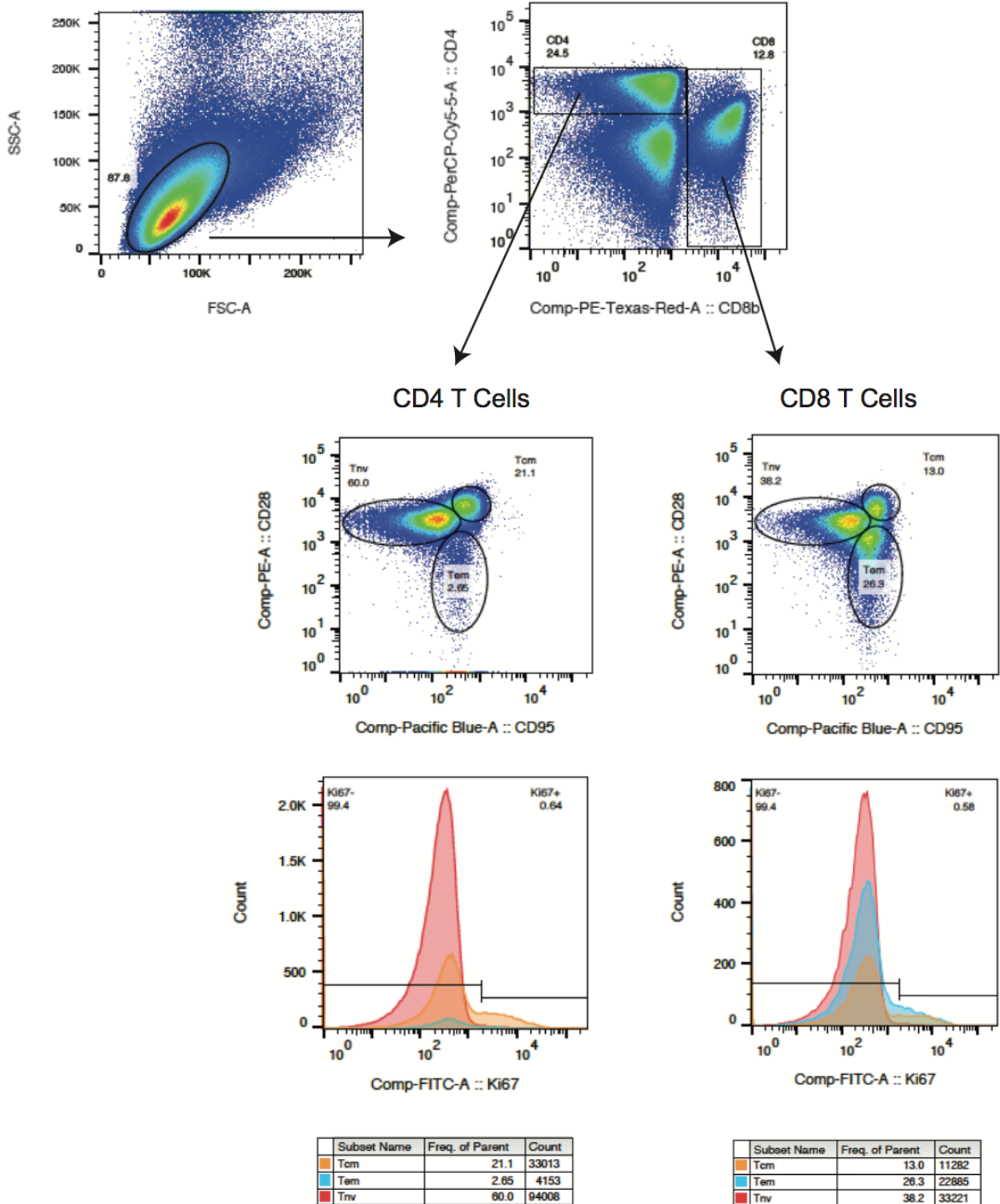


**Figure S-8: T cell gating strategy.**

PBMCs were stained for surface levels of CD4, CD8 $\beta$ , CD95, CD28, CD127 and for intracellular levels of Ki67. The lymphocyte subset was identified and CD4<sup>+</sup> and CD8<sup>+</sup> T subsets are shown (top panel). Within the CD4<sup>+</sup> and CD8<sup>+</sup> T cell subsets, the naïve (CD28<sup>+</sup>CD95<sup>-</sup>), central memory (CD28<sup>+</sup>CD95<sup>+</sup>), and effector memory (CD28<sup>-</sup>CD95<sup>+</sup>) subsets are indicated. The percentage of proliferating (Ki67<sup>+</sup>) T cells within each subset was calculated.

Data produced and analyzed by Nicole Haese.

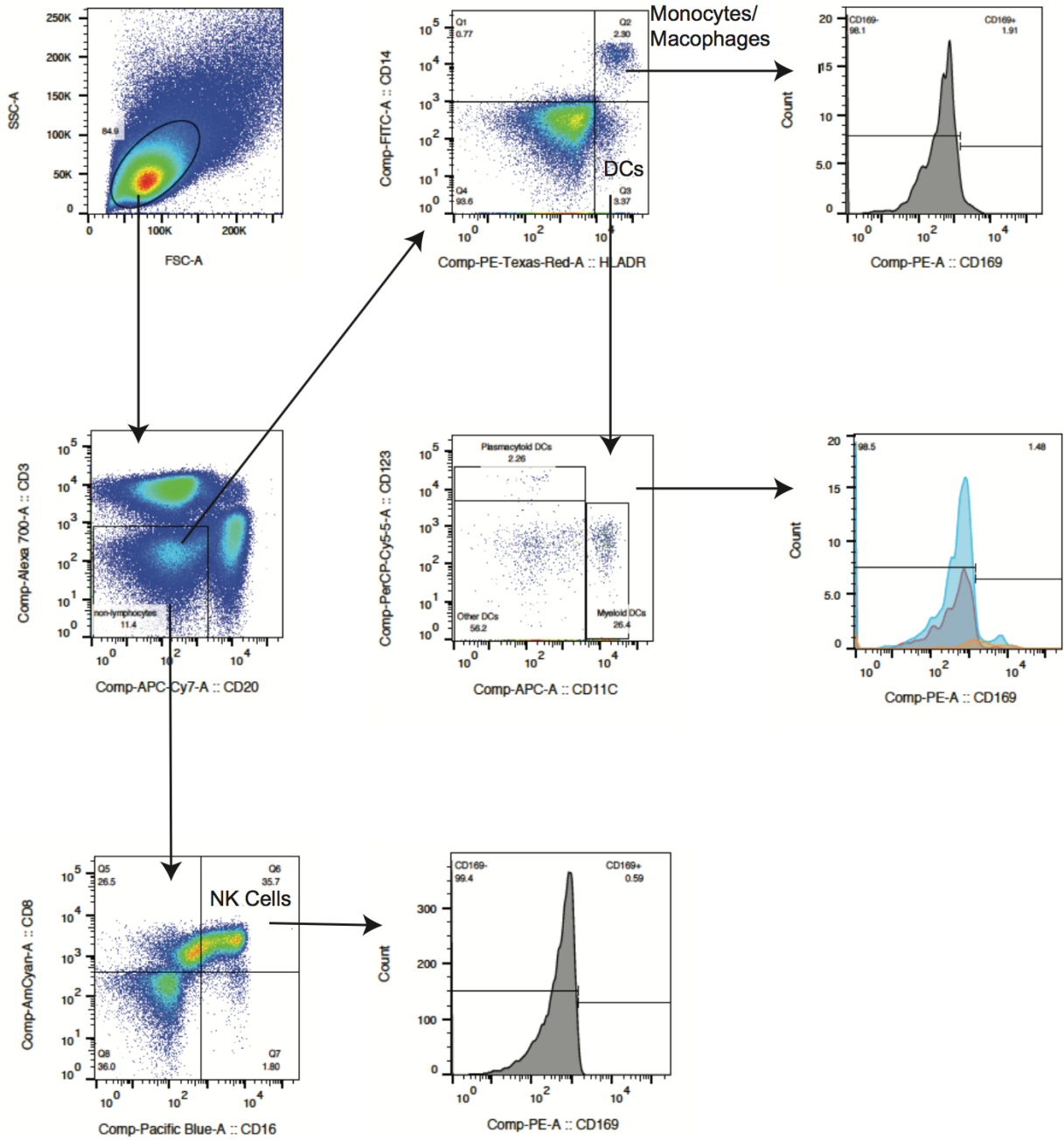


**Figure S-9: Gating strategy for NK cells, macrophages, and DCs.**

PBMCs were stained with HLA-DR, CD14, CD11c, CD123, CD20, CD3, CD8, CD16, and CD169 to differentiate monocyte/macrophages, DCs, and NK cells using the following gating strategy: monocyte/macrophages (CD3<sup>-</sup>CD20<sup>-</sup>CD14<sup>+</sup>HLA-DR<sup>+</sup>), plasmacytoid DCs (CD3<sup>-</sup>CD20<sup>-</sup>CD14<sup>+</sup>HLA-DR<sup>+</sup>CD123<sup>+</sup>), myeloid DCs (CD3<sup>-</sup>CD20<sup>-</sup>CD14<sup>+</sup>HLA-DR<sup>+</sup>CD11c<sup>+</sup>), and NK cells (CD3<sup>-</sup>CD20<sup>-</sup>CD8<sup>+</sup>CD16<sup>+</sup>). The percentage of activated cells (CD169<sup>+</sup>) within each subset was calculated. The gating strategy and definition of the different cellular subsets are shown.

Data produced and analyzed by Nicole Haese.

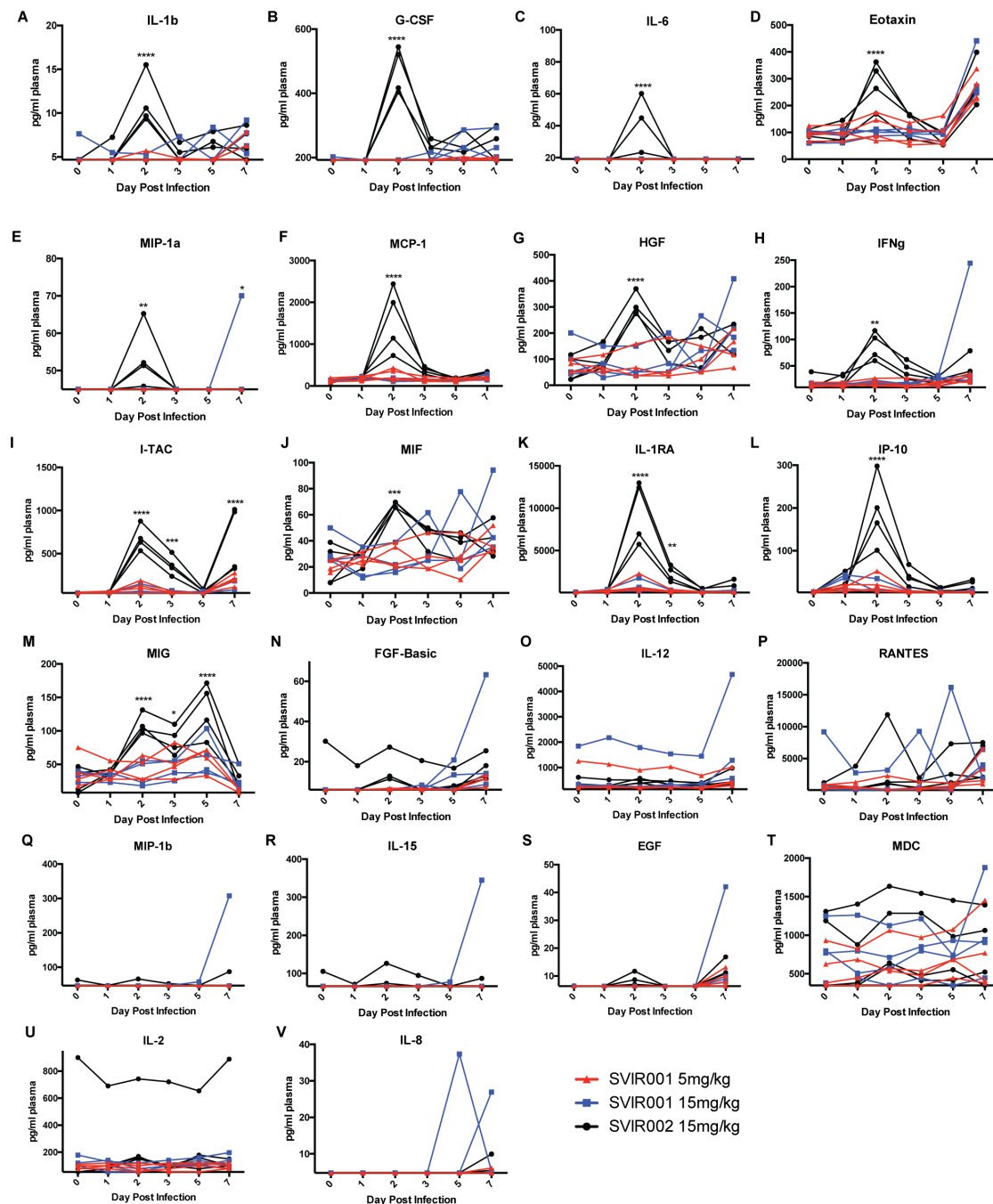


**Figure S-10: Plasma cytokines and chemokine analysis.**

Cytokine analysis from 29-plex-cytokine magnetic bead assay was performed on plasma from animals treated with SVIR001 or control mAb SVIR002. Cytokine analysis revealed changes in plasma cytokine levels of **(A)** IL-1 $\beta$ , **(B)** G-CSF, **(C)** IL-6, **(D)** eotaxin, **(E)** MIP-1 $\alpha$ , **(F)** MCP-1, **(G)** HGF, **(H)** IFN $\gamma$ , **(I)** I-TAC, **(J)** MIF, **(K)** IL-1RA, **(L)** IP-10, and **(M)** MIG. Differences were analyzed using Sidak's multiple comparison tests, and adjusted *P* values are reported (*n* = 4; \*\*\*\*, *P* < 0.0001, \*\*\*, *P* < 0.0005, \*\*, *P* < 0.01, \*, *P* < 0.05). Individual animals are graphed. Plasma cytokine levels of **(N)** FGF-Basic, **(O)** IL-12, **(P)** RANTES, **(Q)** MIP-1 $\beta$ , **(R)** IL-15, **(S)** EGF, **(T)** MDC, **(U)** IL-2, and **(V)** IL-8 did not demonstrate any significant changes between treatment groups. IL-10, IL-17, GM-CSF, VEGF, TNF $\alpha$ , and IL-4 remained below the limit of detection and are not shown.

Data produced and analyzed by Rebecca Broeckel.

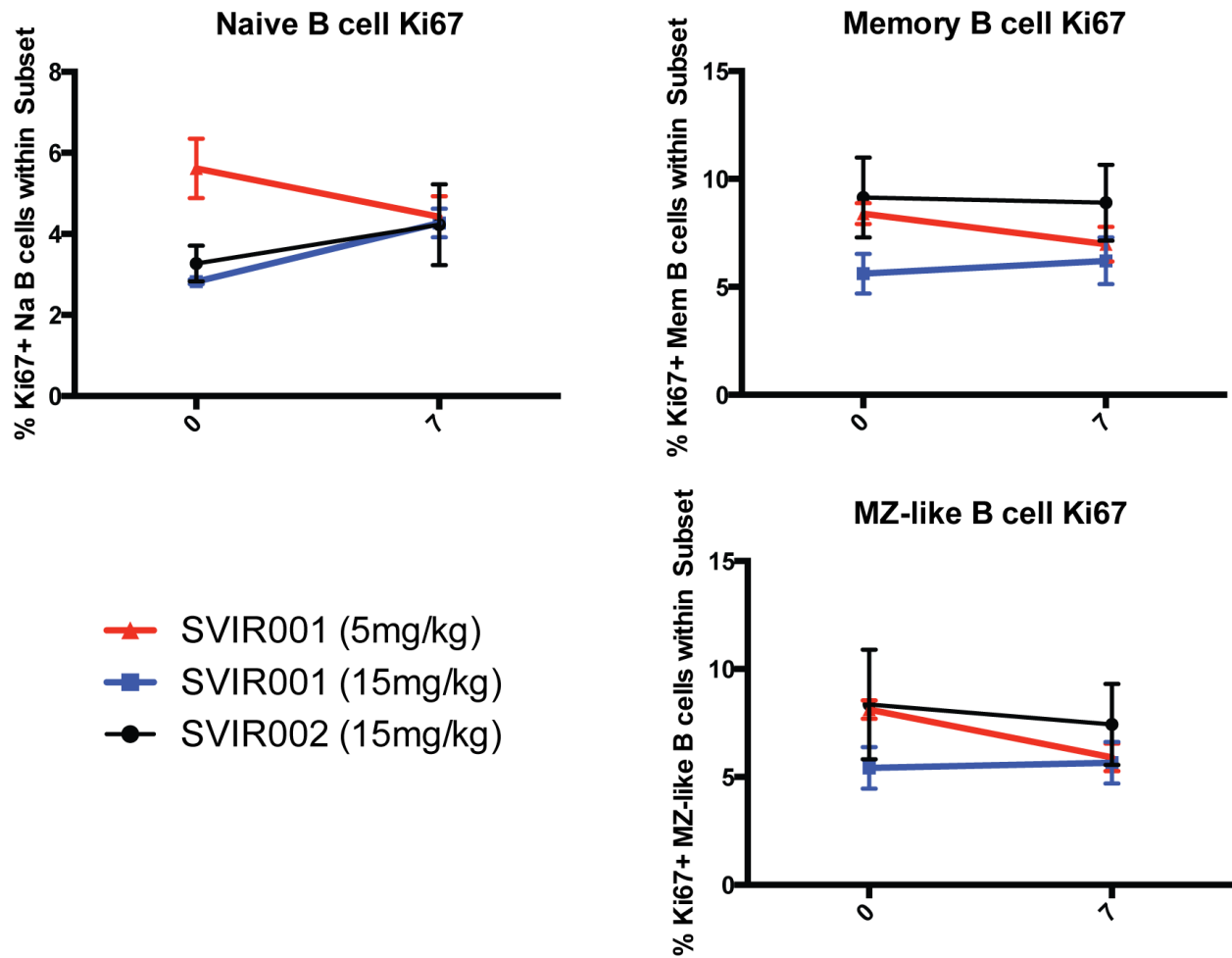


**Figure S-11: B cell proliferative responses were not affected by SVIR001 therapy.**

Total peripheral blood mononuclear cells were analyzed by flow cytometry for the presence of B cell proliferative responses following CHIKV infection in control and anti-CHIKV treated NHP. B cells were stained with antibodies directed against CD3, CD20, CD27, IgD and HLA-DR as well as Ki67 in order to identify proliferating (Ki67+) cells in naïve B cells, memory B cells and marginal zone like B cells. The percentage of actively proliferating cells within cell type was calculated using FlowJo software and the data was graphed in GraphPad Prism v6 software.

Data produced and analyzed by Nicole Haese.

<b>Sequencing Primer</b>	<b>5'- Sequence- 3'</b>
1: 5'- 8248F	GTTTTAGGAGGAGCTAATGAAGGAG
2: 5'- 8573F	CCATAAGACCGTACCTAGCTCACTGTCC
3: 5'- 8912F	CATGTACGCACCCATTTCCACC
4: 5'- 9924F	CGGTCACCAATCACAAAAAAT
5: 5'- 9500F	CCGTGCCGACTGAAGGG
6: 5'- 9802F	GCTAAAGCGGCCACATACC
7: 5'- 10101F	CACTTTGGAGCCAACGCTATCG
8: 5'- 10389F	GCTCCGCGTCCTTTACCA
9: 5'- 10676F	CGGTGCACGTGCCGTACTIONCTCAGG
10: 5'- 11017F	GCTGAAATAGAAGTAGAAGGGA

<b>PCR Primer</b>	<b>5'- Sequence- 3'</b>
5'- 8248F	GTTTTAGGAGGAGCTAATGAAGGAGCCCGT
5'- 11359R	GTGTGTCTCTTAGGGGACACATATACCTTCGTACCT

**Table S-1: Primers used for sequencing and amplifying the E2 and E1 genes of CHIKV-181/25**

Data produced and analyzed by Julie Fox.

<b>Mutagenesis Primers</b>	<b>5'- Sequence- 3'</b>
CHIKV-181/25 E2 del 734-739	For- ctggtcccgcgtaaactcggggacc Rev- ggtccccgagtttacgcgggaccag
CHIKV-LR E2 del 734-739	For- tctggtcccgcgtaaacttggggaccg Rev- cgtccccaagtttacgcgggaccaga

**Table S-2: Oligonucleotide primers for mutagenesis of CHIKV infectious clones**

Data produced and analyzed by Julie Fox.

mAb	SVIR002 (15 mg/ kg)				SVIR001 (15 mg/ kg)				SVIR001 (5 mg/ kg)			
Animal	31559	31055	31289	31333	31078	31296	31312	31302	31651	30430	31088	31335
Right finger	3 *#	2 *	0	1 *	0	0	1	3	0	0	0	1
Left finger	2	0	1 #	3	0	0	2 *	1	0	1	0	0
Right wrist	0	1	0	1	0	0	0	1	0	0	0	1
Left wrist	1	0	1	1	2	1	1	1	1	0	1	2 #
Right elbow	0	1	0	0	1	0	0	0	1 *	1	0 #	1
Left elbow	1	3	1	1	1	0	1	1	0	0	0	1
Right toe	1	0	1	0	0	0	0	0	0	0	0	0
Left toe	2	0	0	1	0	0	0	0	0	0	0	0
Right ankle	1	1	0	0	0	0	0	0	0	0	0	0
Left ankle	1	2	0	0	1	0	0	0	0	0	0	0
Right knee	2 *	2	0	1	0	0	0	0	0 #	1	0	0
Left knee	1	1	1	1	0	0	0	1	0	0	0	1 #
<b>Total score</b>	<b>15</b>	<b>13</b>	<b>5</b>	<b>10</b>	<b>5</b>	<b>1</b>	<b>5</b>	<b>8</b>	<b>2</b>	<b>3</b>	<b>1</b>	<b>7</b>
<b># joints affected</b>	<b>10</b>	<b>8</b>	<b>5</b>	<b>8</b>	<b>4</b>	<b>1</b>	<b>4</b>	<b>6</b>	<b>2</b>	<b>3</b>	<b>1</b>	<b>6</b>

**Table S-3: Detailed histological findings reported per animal.**

H&E stained joint sections were scored as described in **Table 3-2**. Additional findings such as the presence of granulocytes or hemosiderin are indicated but were not used in the calculation of scores. \* Granulocytes (eosinophils and/or neutrophils), # Hemosiderin

Data produced by Lois Colgin, Rebecca Ducore, and Anne Lewis.

SUPPLEMENTAL DATA: T CELL VACCINE PROJECT

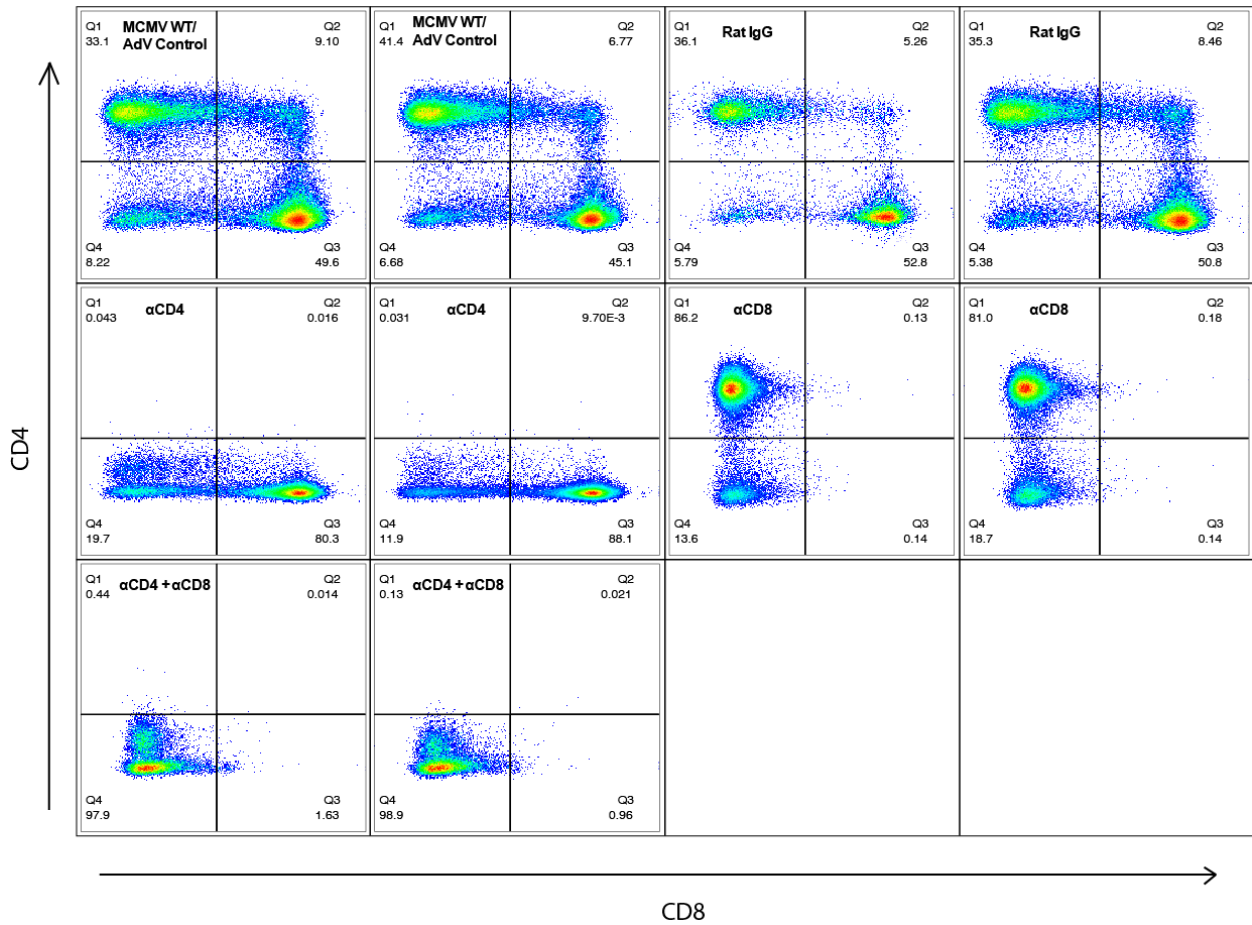


**Figure S-12: T cell depletions were confirmed in mice receiving CD4+ and CD8+ T cell depleting antibodies.**

Mice were administered 300 μg Rat IgG, anti-CD4, anti-CD8, or anti-CD4 plus anti-CD8 depleting antibodies two days prior to infection and two days post infection. At 5 dpi, splenocytes from two mice per group were fixed and stained with fluorophore-conjugated antibodies to CD3, CD19, CD4, and CD8. Representative flow cytometry plots are shown of CD3+CD19- cells.

Data produced and analyzed by Rebecca Broeckel.

## REFERENCES

1. Arnold K, Bordoli L, Kopp J, Schwede T. 2006. The SWISS-MODEL workspace: a web-based environment for protein structure homology modelling. *Bioinformatics* 22:195-201.
2. Bienert S, Waterhouse A, de Beer TA, Tauriello G, Studer G, Bordoli L, Schwede T. 2017. The SWISS-MODEL Repository-new features and functionality. *Nucleic Acids Res* 45:D313-D319.
3. Biasini M, Bienert S, Waterhouse A, Arnold K, Studer G, Schmidt T, Kiefer F, Gallo Cassarino T, Bertoni M, Bordoli L, Schwede T. 2014. SWISS-MODEL: modelling protein tertiary and quaternary structure using evolutionary information. *Nucleic Acids Res* 42:W252-8.
4. Kiefer F, Arnold K, Künzli M, Bordoli L, Schwede T. 2009. The SWISS-MODEL Repository and associated resources. *Nucleic Acids Res* 37:D387-92.
5. Tang J, Jose J, Chipman P, Zhang W, Kuhn RJ, Baker TS. 2011. Molecular links between the E2 envelope glycoprotein and nucleocapsid core in Sindbis virus. *J Mol Biol* 414:442-59.
6. Li L, Jose J, Xiang Y, Kuhn RJ, Rossmann MG. 2010. Structural changes of envelope proteins during alphavirus fusion. *Nature* 468:705-8.
7. Mancini EJ, Clarke M, Gowen BE, Rutten T, Fuller SD. 2000. Cryo-electron microscopy reveals the functional organization of an enveloped virus, Semliki Forest virus. *Mol Cell* 5:255-66.
8. Roussel A, Lescar J, Vaney MC, Wengler G, Rey FA. 2006. Structure and interactions at the viral surface of the envelope protein E1 of Semliki Forest virus. *Structure* 14:75-86.
9. Gibbons DL, Vaney MC, Roussel A, Vigouroux A, Reilly B, Lepault J, Kielian M, Rey FA. 2004. Conformational change and protein-protein interactions of the fusion protein of Semliki Forest virus. *Nature* 427:320-5.
10. Powers A, Huang H, Roehrig J, Weaver S. 2012. Togaviridae, p 1105-1110. *In* King AMQ, Adams MJ, Carstens EB, Lefkowitz EJ (ed), *Virus Taxonomy: Ninth Report of the International Committee on Taxonomy of Viruses*. Elsevier Academic Press, London, United Kingdom.
11. Haddow A, Davies C, Walker A. 1960. O'nyong nyong fever: an epidemic virus disease in West Africa: Introduction. *Transactions of the Royal Society of Tropical Medicine and Hygiene* 54:517-522.
12. ANDERSON CR, DOWNS WG, WATTLEY GH, AHIN NW, REESE AA. 1957. Mayaro virus: a new human disease agent. II. Isolation from blood of patients in Trinidad, B.W.I. *Am J Trop Med Hyg* 6:1012-6.
13. Kurkela S, Manni T, Myllynen J, Vaheri A, Vapalahti O. 2005. Clinical and laboratory manifestations of Sindbis virus infection: prospective study, Finland, 2002-2003. *J Infect Dis* 191:1820-9.
14. Przelomski MM, O'Rourke E, Grady GF, Berardi VP, Markley HG. 1988. Eastern equine encephalitis in Massachusetts: a report of 16 cases, 1970-1984. *Neurology* 38:736-9.

15. Weaver SC, Salas R, Rico-Hesse R, Ludwig GV, Oberste MS, Boshell J, Tesh RB. 1996. Re-emergence of epidemic Venezuelan equine encephalomyelitis in South America. VEE Study Group. *Lancet* 348:436-40.
16. Zacks MA, Paessler S. 2010. Encephalitic alphaviruses. *Vet Microbiol* 140:281-6.
17. La Linn M, Gardner J, Warrilow D, Darnell GA, McMahon CR, Field I, Hyatt AD, Slade RW, Suhrbier A. 2001. Arbovirus of marine mammals: a new alphavirus isolated from the elephant seal louse, *Lepidophthirus macrorhini*. *J Virol* 75:4103-9.
18. Forrester NL, Palacios G, Tesh RB, Savji N, Guzman H, Sherman M, Weaver SC, Lipkin WI. 2012. Genome-scale phylogeny of the alphavirus genus suggests a marine origin. *J Virol* 86:2729-38.
19. Powers AM, Brault AC, Shirako Y, Strauss EG, Kang W, Strauss JH, Weaver SC. 2001. Evolutionary relationships and systematics of the alphaviruses. *J Virol* 75:10118-31.
20. Nasar F, Palacios G, Gorchakov RV, Guzman H, Da Rosa AP, Savji N, Popov VL, Sherman MB, Lipkin WI, Tesh RB, Weaver SC. 2012. Eilat virus, a unique alphavirus with host range restricted to insects by RNA replication. *Proc Natl Acad Sci U S A* 109:14622-7.
21. Calisher CH, Karabatsos N, Lazuick JS, Monath TP, Wolff KL. 1988. Reevaluation of the western equine encephalitis antigenic complex of alphaviruses (family *Togaviridae*) as determined by neutralization tests. *Am J Trop Med Hyg* 38:447-52.
22. Jacups SP, Whelan PI, Currie BJ. 2008. Ross River virus and Barmah Forest virus infections: a review of history, ecology, and predictive models, with implications for tropical northern Australia. *Vector Borne Zoonotic Dis* 8:283-97.
23. Kay BH, Boyd AM, Ryan PA, Hall RA. 2007. Mosquito feeding patterns and natural infection of vertebrates with Ross River and Barmah Forest viruses in Brisbane, Australia. *Am J Trop Med Hyg* 76:417-23.
24. Marshall ID, Woodroffe GM, Hirsch S. 1982. Viruses recovered from mosquitoes and wildlife serum collected in the Murray Valley of South-eastern Australia, February 1974, during an epidemic of encephalitis. *Aust J Exp Biol Med Sci* 60 (Pt 5):457-70.
25. Armstrong PM, Andreadis TG. 2010. Eastern equine encephalitis virus in mosquitoes and their role as bridge vectors. *Emerg Infect Dis* 16:1869-74.
26. Arrigo NC, Adams AP, Weaver SC. 2010. Evolutionary patterns of eastern equine encephalitis virus in North versus South America suggest ecological differences and taxonomic revision. *J Virol* 84:1014-25.
27. Luciani K, Abadía I, Martínez-Torres AO, Cisneros J, Guerra I, García M, Estripeaut D, Carrera JP. 2015. Madariaga virus infection associated with a case of acute disseminated encephalomyelitis. *Am J Trop Med Hyg* 92:1130-2.
28. Samina I, Margalit J, Peleg J. 1986. Isolation of viruses from mosquitoes of the Negev, Israel. *Trans R Soc Trop Med Hyg* 80:471-2.

29. Nasar F, Gorchakov RV, Tesh RB, Weaver SC. 2015. Eilat virus host range restriction is present at multiple levels of the virus life cycle. *J Virol* 89:1404-18.
30. Attoui H, Sailleau C, Mohd Jaafar F, Belhouchet M, Biagini P, Cantaloube JF, de Micco P, Mertens P, Zientara S. 2007. Complete nucleotide sequence of Middelburg virus, isolated from the spleen of a horse with severe clinical disease in Zimbabwe. *J Gen Virol* 88:3078-88.
31. KOKERNOT RH, MCINTOSH BM, WORTH CB. 1961. Ndumu virus, a hitherto unknown agent, isolated from culicine mosquitoes collected in northern Natal. Union of South Africa. *Am J Trop Med Hyg* 10:383-6.
32. Crabtree M, Sang R, Lutomiah J, Richardson J, Miller B. 2009. Arbovirus surveillance of mosquitoes collected at sites of active Rift Valley fever virus transmission: Kenya, 2006-2007. *J Med Entomol* 46:961-4.
33. Lutomiah J, Ongus J, Linthicum KJ, Sang R. 2014. Natural vertical transmission of ndumu virus in *Culex pipiens* (Diptera: Culicidae) mosquitoes collected as larvae. *J Med Entomol* 51:1091-5.
34. STANLEY NF, CHOO SB. 1964. STUDIES OF ARBOVIRUSES IN WESTERN AUSTRALIA. SEROLOGICAL EPIDEMIOLOGY. *Bull World Health Organ* 30:221-6.
35. Jupp PG, McIntosh BM. 1990. *Aedes furcifer* and other mosquitoes as vectors of chikungunya virus at Mica, northeastern Transvaal, South Africa. *J Am Mosq Control Assoc* 6:415-20.
36. Diallo M, Thonnon J, Traore-Lamizana M, Fontenille D. 1999. Vectors of Chikungunya virus in Senegal: current data and transmission cycles. *Am J Trop Med Hyg* 60:281-6.
37. WEINBREN MP, HADDOW AJ, WILLIAMS MC. 1958. The occurrence of Chikungunya virus in Uganda. I. Isolation from mosquitoes. *Trans R Soc Trop Med Hyg* 52:253-7.
38. Coffey LL, Failloux AB, Weaver SC. 2014. Chikungunya virus-vector interactions. *Viruses* 6:4628-63.
39. Li XD, Qiu FX, Yang H, Rao YN, Calisher CH. 1992. Isolation of Getah virus from mosquitos collected on Hainan Island, China, and results of a serosurvey. *Southeast Asian J Trop Med Public Health* 23:730-4.
40. Bannai H, Ochi A, Nemoto M, Tsujimura K, Yamanaka T, Kondo T. 2016. A 2015 outbreak of Getah virus infection occurring among Japanese racehorses sequentially to an outbreak in 2014 at the same site. *BMC Vet Res* 12:98.
41. CAUSEY OR, MAROJA OM. 1957. Mayaro virus: a new human disease agent. III. Investigation of an epidemic of acute febrile illness on the river Guama in Pará, Brazil, and isolation of Mayaro virus as causative agent. *Am J Trop Med Hyg* 6:1017-23.
42. de Thoisy B, Gardon J, Salas RA, Morvan J, Kazanji M. 2003. Mayaro virus in wild mammals, French Guiana. *Emerg Infect Dis* 9:1326-9.
43. WILLIAMS MC, WOODALL JP, CORBET PS, GILLETT JD. 1965. O'NYONG-NYONG FEVER: AN EPIDEMIC VIRUS DISEASE IN EAST AFRICA. 8. VIRUS ISOLATIONS FROM ANOPHELES MOSQUITOES. *Trans R Soc Trop Med Hyg* 59:300-6.

44. Johnson BK, Gichogo A, Gitau G, Patel N, Ademba G, Kirui R, Highton RB, Smith DH. 1981. Recovery of o'nyong-nyong virus from *Anopheles funestus* in Western Kenya. *Trans R Soc Trop Med Hyg* 75:239-41.
45. Lindsay M, Oliveira N, Jasinska E, Johansen C, Harrington S, Wright AE, Smith D. 1996. An outbreak of Ross River virus disease in Southwestern Australia. *Emerg Infect Dis* 2:117-20.
46. Mathiot CC, Grimaud G, Garry P, Bouquety JC, Mada A, Daguisy AM, Georges AJ. 1990. An outbreak of human Semliki Forest virus infections in Central African Republic. *Am J Trop Med Hyg* 42:386-93.
47. Powers AM, Aguilar PV, Chandler LJ, Brault AC, Meakins TA, Watts D, Russell KL, Olson J, Vasconcelos PF, Da Rosa AT, Weaver SC, Tesh RB. 2006. Genetic relationships among Mayaro and Una viruses suggest distinct patterns of transmission. *Am J Trop Med Hyg* 75:461-9.
48. Forrester NL, Wertheim JO, Dugan VG, Auguste AJ, Lin D, Adams AP, Chen R, Gorchakov R, Leal G, Estrada-Franco JG, Pandya J, Halpin RA, Hari K, Jain R, Stockwell TB, Das SR, Wentworth DE, Smith MD, Kosakovsky Pond SL, Weaver SC. 2017. Evolution and spread of Venezuelan equine encephalitis complex alphavirus in the Americas. *PLoS Negl Trop Dis* 11:e0005693.
49. Ehrenkranz NJ, Sinclair MC, Buff E, Lyman DO. 1970. The natural occurrence of Venezuelan equine encephalitis in the United States. *N Engl J Med* 282:298-302.
50. Coffey LL, Crawford C, Dee J, Miller R, Freier J, Weaver SC. 2006. Serologic evidence of widespread everglades virus activity in dogs, Florida. *Emerg Infect Dis* 12:1873-9.
51. SHOPE RE, CAUSEY OR, DE ANDRADE AH. 1964. THE VENEZUELAN EQUINE ENCEPHALOMYELITIS COMPLEX OF GROUP A ARTHROPOD-BORNE VIRUSES, INCLUDING MUCAMBO AND PIXUNA FROM THE AMAZON REGION OF BRAZIL. *Am J Trop Med Hyg* 13:723-7.
52. DEMUCHA MACIAS J, S'ANCHEZ SPINDOLA I. 1965. TWO HUMAN CASES OF LABORATORY INFECTION WITH MUCAMBO VIRUS. *Am J Trop Med Hyg* 14:475-8.
53. Pisano MB, Spinsanti LI, Díaz LA, Farías AA, Almirón WR, Ré VE, Contigiani MS. 2012. First detection of Rio Negro virus (Venezuelan equine encephalitis complex subtype VI) in Córdoba, Argentina. *Mem Inst Oswaldo Cruz* 107:125-8.
54. Pisano MB, Dantur MJ, Ré VE, Díaz LA, Farías A, Sánchez Seco MP, Tenorio A, Almirón WR, Contigiani MS. 2010. Cocirculation of Rio Negro Virus (RNV) and Pixuna Virus (PIXV) in Tucumán province, Argentina. *Trop Med Int Health* 15:865-8.
55. Talarmin A, Trochu J, Gardon J, Laventure S, Hommel D, Lelarge J, Labeau B, Digoutte JP, Hulin A, Sarthou JL. 2001. Tonate virus infection in French Guiana: clinical aspects and seroepidemiologic study. *Am J Trop Med Hyg* 64:274-9.
56. Weaver SC, Ferro C, Barrera R, Boshell J, Navarro JC. 2004. Venezuelan equine encephalitis. *Annu Rev Entomol* 49:141-74.
57. Brault AC, Powers AM, Ortiz D, Estrada-Franco JG, Navarro-Lopez R, Weaver SC. 2004. Venezuelan equine encephalitis emergence: enhanced vector infection from a single amino acid substitution in the envelope glycoprotein. *Proc Natl Acad Sci U S A* 101:11344-9.

58. Scherer WF, Dickerman RW, Cupp EW, Ordonez JV. 1985. Ecologic observations of Venezuelan encephalitis virus in vertebrates and isolations of Nepuyo and Patois viruses from sentinel hamsters at Pacific and Atlantic habitats in Guatemala, 1968-1980. *Am J Trop Med Hyg* 34:790-8.
59. Rumenapf T, Strauss EG, Strauss JH. 1994. Subgenomic mRNA of Aura alphavirus is packaged into virions. *J Virol* 68:56-62.
60. Scott TW, Bowen GS, Monath TP. 1984. A field study on the effects of Fort Morgan virus, an arbovirus transmitted by swallow bugs, on the reproductive success of cliff swallows and symbiotic house sparrows in Morgan County, Colorado, 1976. *Am J Trop Med Hyg* 33:981-91.
61. Ip HS, Wiley MR, Long R, Palacios G, Shearn-Bochsler V, Whitehouse CA. 2014. Identification and characterization of Highlands J virus from a Mississippi sandhill crane using unbiased next-generation sequencing. *J Virol Methods* 206:42-5.
62. Meehan PJ, Wells DL, Paul W, Buff E, Lewis A, Muth D, Hopkins R, Karabatsos N, Tsai TF. 2000. Epidemiological features of and public health response to a St. Louis encephalitis epidemic in Florida, 1990-1. *Epidemiol Infect* 125:181-8.
63. Blackburn NK, Foggin CM, Searle L, Smith PN. 1982. Isolation of Sindbis virus from bat organs. *Cent Afr J Med* 28:201.
64. TAYLOR RM, HURLBUT HS, WORK TH, KINGSTON JR, FROTHINGHAM TE. 1955. Sindbis virus: a newly recognized arthropodtransmitted virus. *Am J Trop Med Hyg* 4:844-62.
65. Kurkela S, Manni T, Vaheri A, Vapalahti O. 2004. Causative agent of Pogosta disease isolated from blood and skin lesions. *Emerg Infect Dis* 10:889-94.
66. Travassos da Rosa AP, Turell MJ, Watts DM, Powers AM, Vasconcelos PF, Jones JW, Klein TA, Dohm DJ, Shope RE, Degallier N, Popov VL, Russell KL, Weaver SC, Guzman H, Calampa C, Brault AC, Lemon AP, Tesh RB. 2001. Trocara virus: a newly recognized Alphavirus (Togaviridae) isolated from mosquitoes in the Amazon Basin. *Am J Trop Med Hyg* 64:93-7.
67. Miles JA. 1973. The ecology of Whataroa virus, an alphavirus, in South Westland, New Zealand. *J Hyg (Lond)* 71:701-13.
68. Weston JH, Welsh MD, McLoughlin MF, Todd D. 1999. Salmon pancreas disease virus, an alphavirus infecting farmed Atlantic salmon, *Salmo salar* L. *Virology* 256:188-95.
69. Dubin DT, Stollar V. 1975. Methylation of Sindbis virus "26S" messenger RNA. *Biochem Biophys Res Commun* 66:1373-9.
70. Dubin DT, Stollar V, Hsueh CC, Timko K, Guild GM. 1977. Sindbis virus messenger RNA: the 5'-termini and methylated residues of 26 and 42 S RNA. *Virology* 77:457-70.
71. Hefti E, Bishop DH, Dubin DT, Stollar V. 1975. 5' nucleotide sequence of sindbis viral RNA. *J Virol* 17:149-59.
72. Pettersson RF, Söderlund H, Kääriäinen L. 1980. The nucleotide sequences of the 5'-terminal T1 oligonucleotides of Semliki-Forest-virus 42-S and 26-S RNAs are different. *Eur J Biochem* 105:435-43.

73. Hyde JL, Chen R, Trobaugh DW, Diamond MS, Weaver SC, Klimstra WB, Wilusz J. 2015. The 5' and 3' ends of alphavirus RNAs--Non-coding is not non-functional. *Virus Res* 206:99-107.
74. Niesters HG, Strauss JH. 1990. Defined mutations in the 5' nontranslated sequence of Sindbis virus RNA. *J Virol* 64:4162-8.
75. Frolov I, Hardy R, Rice CM. 2001. Cis-acting RNA elements at the 5' end of Sindbis virus genome RNA regulate minus- and plus-strand RNA synthesis. *RNA* 7:1638-51.
76. Pfeffer M, Kinney RM, Kaaden OR. 1998. The alphavirus 3'-nontranslated region: size heterogeneity and arrangement of repeated sequence elements. *Virology* 240:100-8.
77. Hardy RW, Rice CM. 2005. Requirements at the 3' end of the sindbis virus genome for efficient synthesis of minus-strand RNA. *J Virol* 79:4630-9.
78. Hardy RW. 2006. The role of the 3' terminus of the Sindbis virus genome in minus-strand initiation site selection. *Virology* 345:520-31.
79. Sokoloski KJ, Dickson AM, Chaskey EL, Garneau NL, Wilusz CJ, Wilusz J. 2010. Sindbis virus usurps the cellular HuR protein to stabilize its transcripts and promote productive infections in mammalian and mosquito cells. *Cell Host Microbe* 8:196-207.
80. Barnhart MD, Moon SL, Emch AW, Wilusz CJ, Wilusz J. 2013. Changes in cellular mRNA stability, splicing, and polyadenylation through HuR protein sequestration by a cytoplasmic RNA virus. *Cell Rep* 5:909-17.
81. Fayzulin R, Frolov I. 2004. Changes of the secondary structure of the 5' end of the Sindbis virus genome inhibit virus growth in mosquito cells and lead to accumulation of adaptive mutations. *J Virol* 78:4953-64.
82. Sokoloski KJ, Nease LM, May NA, Gebhart NN, Jones CE, Morrison TE, Hardy RW. 2017. Identification of Interactions between Sindbis Virus Capsid Protein and Cytoplasmic vRNA as Novel Virulence Determinants. *PLoS Pathog* 13:e1006473.
83. Levis R, Schlesinger S, Huang HV. 1990. Promoter for Sindbis virus RNA-dependent subgenomic RNA transcription. *J Virol* 64:1726-33.
84. Ou JH, Rice CM, Dalgarno L, Strauss EG, Strauss JH. 1982. Sequence studies of several alphavirus genomic RNAs in the region containing the start of the subgenomic RNA. *Proc Natl Acad Sci U S A* 79:5235-9.
85. Wielgosz MM, Raju R, Huang HV. 2001. Sequence requirements for Sindbis virus subgenomic mRNA promoter function in cultured cells. *J Virol* 75:3509-19.
86. von Bonsdorff CH, Harrison SC. 1975. Sindbis virus glycoproteins form a regular icosahedral surface lattice. *J Virol* 16:141-5.
87. Cheng RH, Kuhn RJ, Olson NH, Rossmann MG, Choi HK, Smith TJ, Baker TS. 1995. Nucleocapsid and glycoprotein organization in an enveloped virus. *Cell* 80:621-30.
88. Paredes AM, Simon MN, Brown DT. 1992. The mass of the Sindbis virus nucleocapsid suggests it has T = 4 icosahedral symmetry. *Virology* 187:329-32.

89. Gaedigk-Nitschko K, Schlesinger MJ. 1990. The Sindbis virus 6K protein can be detected in virions and is acylated with fatty acids. *Virology* 175:274-81.
90. Gaedigk-Nitschko K, Ding MX, Levy MA, Schlesinger MJ. 1990. Site-directed mutations in the Sindbis virus 6K protein reveal sites for fatty acylation and the underacylated protein affects virus release and virion structure. *Virology* 175:282-91.
91. Kääriäinen L, Söderlund H. 1971. Properties of Semliki Forest virus nucleocapsid. 1. Sensitivity to pancreatic ribonuclease. *Virology* 43:291-9.
92. Lee S, Owen KE, Choi HK, Lee H, Lu G, Wengler G, Brown DT, Rossmann MG, Kuhn RJ. 1996. Identification of a protein binding site on the surface of the alphavirus nucleocapsid and its implication in virus assembly. *Structure* 4:531-41.
93. Skoging U, Vihinen M, Nilsson L, Liljeström P. 1996. Aromatic interactions define the binding of the alphavirus spike to its nucleocapsid. *Structure* 4:519-29.
94. Wilkinson TA, Tellinghuisen TL, Kuhn RJ, Post CB. 2005. Association of sindbis virus capsid protein with phospholipid membranes and the E2 glycoprotein: implications for alphavirus assembly. *Biochemistry* 44:2800-10.
95. Wengler G, Boege U, Bischoff H, Wahn K. 1982. The core protein of the alphavirus Sindbis virus assembles into core-like nucleoproteins with the viral genome RNA and with other single-stranded nucleic acids in vitro. *Virology* 118:401-10.
96. Tellinghuisen TL, Hamburger AE, Fisher BR, Ostendorp R, Kuhn RJ. 1999. In vitro assembly of alphavirus cores by using nucleocapsid protein expressed in *Escherichia coli*. *J Virol* 73:5309-19.
97. Linger BR, Kunovska L, Kuhn RJ, Golden BL. 2004. Sindbis virus nucleocapsid assembly: RNA folding promotes capsid protein dimerization. *RNA* 10:128-38.
98. Mukhopadhyay S, Zhang W, Gabler S, Chipman PR, Strauss EG, Strauss JH, Baker TS, Kuhn RJ, Rossmann MG. 2006. Mapping the structure and function of the E1 and E2 glycoproteins in alphaviruses. *Structure* 14:63-73.
99. Voss JE, Vaney MC, Duquerroy S, Vonrhein C, Girard-Blanc C, Crublet E, Thompson A, Bricogne G, Rey FA. 2010. Glycoprotein organization of Chikungunya virus particles revealed by X-ray crystallography. *Nature* 468:709-12.
100. Lescar J, Roussel A, Wien MW, Navaza J, Fuller SD, Wengler G, Rey FA. 2001. The Fusion glycoprotein shell of Semliki Forest virus: an icosahedral assembly primed for fusogenic activation at endosomal pH. *Cell* 105:137-48.
101. Wahlberg JM, Bron R, Wilschut J, Garoff H. 1992. Membrane fusion of Semliki Forest virus involves homotrimers of the fusion protein. *J Virol* 66:7309-18.
102. Paredes AM, Heidner H, Thuman-Commike P, Prasad BV, Johnston RE, Chiu W. 1998. Structural localization of the E3 glycoprotein in attenuated Sindbis virus mutants. *J Virol* 72:1534-41.
103. Sjöberg M, Lindqvist B, Garoff H. 2011. Activation of the alphavirus spike protein is suppressed by bound E3. *J Virol* 85:5644-50.

104. Hahn CS, Lustig S, Strauss EG, Strauss JH. 1988. Western equine encephalitis virus is a recombinant virus. *Proc Natl Acad Sci U S A* 85:5997-6001.
105. Gérardin P, Fianu A, Malvy D, Mussard C, Boussaïd K, Rollot O, Michault A, Gaüzere BA, Bréart G, Favier F. 2011. Perceived morbidity and community burden after a Chikungunya outbreak: the TELECHIK survey, a population-based cohort study. *BMC Med* 9:5.
106. Harley D, Sleigh A, Ritchie S. 2001. Ross River virus transmission, infection, and disease: a cross-disciplinary review. *Clin Microbiol Rev* 14:909-32, table of contents.
107. Soden M, Vasudevan H, Roberts B, Coelen R, Hamlin G, Vasudevan S, La Brooy J. 2000. Detection of viral ribonucleic acid and histologic analysis of inflamed synovium in Ross River virus infection. *Arthritis Rheum* 43:365-9.
108. Fraser JR, Ratnamohan VM, Dowling JP, Becker GJ, Varigos GA. 1983. The exanthem of Ross River virus infection: histology, location of virus antigen and nature of inflammatory infiltrate. *J Clin Pathol* 36:1256-63.
109. Fraser JR, Cunningham AL, Clarris BJ, Aaskov JG, Leach R. 1981. Cytology of synovial effusions in epidemic polyarthritis. *Aust N Z J Med* 11:168-73.
110. Hoarau JJ, Jaffar Bandjee MC, Krejbich Trotot P, Das T, Li-Pat-Yuen G, Dassa B, Denizot M, Guichard E, Ribera A, Henni T, Tallet F, Moiton MP, Gauzere BA, Bruniquet S, Jaffar Bandjee Z, Morbidelli P, Martigny G, Jolivet M, Gay F, Grandadam M, Tolou H, Vieillard V, Debre P, Autran B, Gasque P. 2010. Persistent chronic inflammation and infection by Chikungunya arthritogenic alphavirus in spite of a robust host immune response. *J Immunol* 184:5914-27.
111. Ozden S, Huerre M, Riviere JP, Coffey LL, Afonso PV, Mouly V, de Monredon J, Roger JC, El Amrani M, Yvin JL, Jaffar MC, Frenkiel MP, Sourisseau M, Schwartz O, Butler-Browne G, Desprès P, Gessain A, Ceccaldi PE. 2007. Human muscle satellite cells as targets of Chikungunya virus infection. *PLoS One* 2:e527.
112. Sissoko D, Malvy D, Ezzedine K, Renault P, Moscetti F, Ledrans M, Pierre V. 2009. Post-epidemic Chikungunya disease on Reunion Island: course of rheumatic manifestations and associated factors over a 15-month period. *PLoS Negl Trop Dis* 3:e389.
113. Marimoutou C, Ferraro J, Javelle E, Deparis X, Simon F. 2015. Chikungunya infection: self-reported rheumatic morbidity and impaired quality of life persist 6 years later. *Clin Microbiol Infect* 21:688-93.
114. Kurkela S, Helve T, Vaheri A, Vapalahti O. 2008. Arthritis and arthralgia three years after Sindbis virus infection: clinical follow-up of a cohort of 49 patients. *Scand J Infect Dis* 40:167-73.
115. Marks M, Marks JL. 2016. Viral arthritis. *Clin Med (Lond)* 16:129-34.
116. Aletaha D, Neogi T, Silman AJ, Funovits J, Felson DT, Bingham CO, Birnbaum NS, Burmester GR, Bykerk VP, Cohen MD, Combe B, Costenbader KH, Dougados M, Emery P, Ferraccioli G, Hazes JM, Hobbs K, Huizinga TW, Kavanaugh A, Kay J, Kvien TK, Laing T, Mease P, Ménard HA, Moreland LW, Naden RL, Pincus T, Smolen JS, Stanislawska-Biernat E, Symmons D, Tak PP, Upchurch KS, Vencovský J, Wolfe F, Hawker G. 2010. 2010 Rheumatoid arthritis classification

- criteria: an American College of Rheumatology/European League Against Rheumatism collaborative initiative. *Arthritis Rheum* 62:2569-81.
117. McInnes IB, Schett G. 2017. Pathogenetic insights from the treatment of rheumatoid arthritis. *Lancet* 389:2328-2337.
  118. Chen W, Foo SS, Rulli NE, Taylor A, Sheng KC, Herrero LJ, Herring BL, Lidbury BA, Li RW, Walsh NC, Sims NA, Smith PN, Mahalingam S. 2014. Arthritogenic alphaviral infection perturbs osteoblast function and triggers pathologic bone loss. *Proc Natl Acad Sci U S A* 111:6040-5.
  119. Chen W, Foo SS, Taylor A, Lulla A, Merits A, Hueston L, Forwood MR, Walsh NC, Sims NA, Herrero LJ, Mahalingam S. 2015. Bindarit, an inhibitor of monocyte chemotactic protein synthesis, protects against bone loss induced by chikungunya virus infection. *J Virol* 89:581-93.
  120. Ravindran V, Alias G. 2017. Efficacy of combination DMARD therapy vs. hydroxychloroquine monotherapy in chronic persistent chikungunya arthritis: a 24-week randomized controlled open label study. *Clin Rheumatol* 36:1335-1340.
  121. Chopra A, Saluja M, Venugopalan A. 2014. Effectiveness of chloroquine and inflammatory cytokine response in patients with early persistent musculoskeletal pain and arthritis following chikungunya virus infection. *Arthritis Rheumatol* 66:319-26.
  122. Miner JJ, Cook LE, Hong JP, Smith AM, Richner JM, Shimak RM, Young AR, Monte K, Poddar S, Crowe JE, Lenschow DJ, Diamond MS. 2017. Therapy with CTLA4-Ig and an antiviral monoclonal antibody controls chikungunya virus arthritis. *Sci Transl Med* 9.
  123. Condon RJ, Rouse IL. 1995. Acute symptoms and sequelae of Ross River virus infection in South-Western Australia: a follow-up study. *Clin Diagn Virol* 3:273-84.
  124. Hawkes RA, Boughton CR, Naim HM, Stallman ND. 1985. A major outbreak of epidemic polyarthritis in New South Wales during the summer of 1983/1984. *Med J Aust* 143:330-3.
  125. Choi YH, Comiskey C, Lindsay MD, Cross JA, Anderson M. 2002. Modelling the transmission dynamics of Ross River virus in Southwestern Australia. *IMA J Math Appl Med Biol* 19:61-74.
  126. Morrison TE, Whitmore AC, Shabman RS, Lidbury BA, Mahalingam S, Heise MT. 2006. Characterization of Ross River virus tropism and virus-induced inflammation in a mouse model of viral arthritis and myositis. *J Virol* 80:737-49.
  127. Gresíková M, Sekeyová M, Tempera G, Guglielmino S, Castro A. 1978. Identification of a Sindbis virus strain isolated from *Hyalomma marginatum* ticks in Sicily. *Acta Virol* 22:231-2.
  128. Niklasson B, Espmark A, LeDuc JW, Gargan TP, Ennis WA, Tesh RB, Main AJ. 1984. Association of a Sindbis-like virus with Ockelbo disease in Sweden. *Am J Trop Med Hyg* 33:1212-7.
  129. Lvov DK, Vladimirtseva EA, Butenko AM, Karabatsos N, Trent DW, Calisher CH. 1988. Identity of Karelian fever and Ockelbo viruses determined by serum dilution-plaque reduction neutralization tests and oligonucleotide mapping. *Am J Trop Med Hyg* 39:607-10.

130. Brummer-Korvenkontio M, Vapalahti O, Kuusisto P, Saikku P, Manni T, Koskela P, Nygren T, Brummer-Korvenkontio H, Vahe A. 2002. Epidemiology of Sindbis virus infections in Finland 1981-96: possible factors explaining a peculiar disease pattern. *Epidemiol Infect* 129:335-45.
131. Kurkela S, Rätti O, Huhtamo E, Uzcátegui NY, Nuorti JP, Laakkonen J, Manni T, Helle P, Vahe A, Vapalahti O. 2008. Sindbis virus infection in resident birds, migratory birds, and humans, Finland. *Emerg Infect Dis* 14:41-7.
132. Griffin DE. 1976. Role of the immune response in age-dependent resistance of mice to encephalitis due to Sindbis virus. *J Infect Dis* 133:456-64.
133. Suthar MS, Shabman R, Madric K, Lambeth C, Heise MT. 2005. Identification of adult mouse neurovirulence determinants of the Sindbis virus strain AR86. *J Virol* 79:4219-28.
134. Thach DC, Kimura T, Griffin DE. 2000. Differences between C57BL/6 and BALB/cBy mice in mortality and virus replication after intranasal infection with neuroadapted Sindbis virus. *J Virol* 74:6156-61.
135. Griffin DE. 2016. Alphavirus Encephalomyelitis: Mechanisms and Approaches to Prevention of Neuronal Damage. *Neurotherapeutics* 13:455-60.
136. Sanders EJ, Rwaguma EB, Kawamata J, Kiwanuka N, Lutwama JJ, Ssengooba FP, Lamunu M, Najjemba R, Were WA, Bagambisa G, Campbell GL. 1999. O'nyong-nyong fever in south-central Uganda, 1996-1997: description of the epidemic and results of a household-based seroprevalence survey. *J Infect Dis* 180:1436-43.
137. WILLIAMS MC, WOODALL JP. 1961. O'nyong-nyong fever: an epidemic virus disease in East Africa. II. Isolation and some properties of the virus. *Trans R Soc Trop Med Hyg* 55:135-41.
138. Saxton-Shaw KD, Ledermann JP, Borland EM, Stovall JL, Mossel EC, Singh AJ, Wilusz J, Powers AM. 2013. O'nyong nyong virus molecular determinants of unique vector specificity reside in non-structural protein 3. *PLoS Negl Trop Dis* 7:e1931.
139. LaBeaud AD, Banda T, Brichard J, Muchiri EM, Mungai PL, Mutuku FM, Borland E, Gildengorin G, Pfeil S, Teng CY, Long K, Heise M, Powers AM, Kitron U, King CH. 2015. High rates of o'nyong nyong and Chikungunya virus transmission in coastal Kenya. *PLoS Negl Trop Dis* 9:e0003436.
140. Seymour RL, Rossi SL, Bergren NA, Plante KS, Weaver SC. 2013. The role of innate versus adaptive immune responses in a mouse model of O'nyong-nyong virus infection. *Am J Trop Med Hyg* 88:1170-9.
141. Binn LN, Harrison VR, Randall R. 1967. Patterns of viremia and antibody observed in rhesus monkeys inoculated with chikungunya and other serologically related group A arboviruses. *Am J Trop Med Hyg* 16:782-5.
142. Fox JM, Long F, Edeling MA, Lin H, van Duijl-Richter MK, Fong RH, Kahle KM, Smit JM, Jin J, Simmons G, Doranz BJ, Crowe JE, Fremont DH, Rossmann MG, Diamond MS. 2015. Broadly Neutralizing Alphavirus Antibodies Bind an Epitope on E2 and Inhibit Entry and Egress. *Cell* 163:1095-107.

143. ROSS RW. 1956. The Newala epidemic. III. The virus: isolation, pathogenic properties and relationship to the epidemic. *J Hyg (Lond)* 54:177-91.
144. Weaver SC, Forrester NL. 2015. Chikungunya: Evolutionary history and recent epidemic spread. *Antiviral Res* 120:32-39.
145. Powers AM, Logue CH. 2007. Changing patterns of chikungunya virus: re-emergence of a zoonotic arbovirus. *J Gen Virol* 88:2363-77.
146. Weaver SC, Forrester NL. 2015. Chikungunya: Evolutionary history and recent epidemic spread. *Antiviral Res* 120:32-9.
147. Gardner J, Anraku I, Le TT, Larcher T, Major L, Roques P, Schroder WA, Higgs S, Suhrbier A. 2010. Chikungunya virus arthritis in adult wild-type mice. *J Virol* 84:8021-32.
148. Morrison TE, Oko L, Montgomery SA, Whitmore AC, Lotstein AR, Gunn BM, Elmore SA, Heise MT. 2011. A mouse model of chikungunya virus-induced musculoskeletal inflammatory disease: evidence of arthritis, tenosynovitis, myositis, and persistence. *Am J Pathol* 178:32-40.
149. Messaoudi I, Vomasse J, Totonchy T, Kreklywich CN, Haberthur K, Springgay L, Brien JD, Diamond MS, Defilippis VR, Streblow DN. 2013. Chikungunya virus infection results in higher and persistent viral replication in aged rhesus macaques due to defects in anti-viral immunity. *PLoS Negl Trop Dis* 7:e2343.
150. Labadie K, Larcher T, Joubert C, Mannioui A, Delache B, Brochard P, Guigand L, Dubreil L, Lebon P, Verrier B, de Lamballerie X, Suhrbier A, Cherel Y, Le Grand R, Roques P. 2010. Chikungunya disease in nonhuman primates involves long-term viral persistence in macrophages. *J Clin Invest* 120:894-906.
151. Rivas F, Diaz LA, Cardenas VM, Daza E, Bruzon L, Alcalá A, De la Hoz O, Caceres FM, Aristizabal G, Martinez JW, Revelo D, De la Hoz F, Boshell J, Camacho T, Calderon L, Olano VA, Villarreal LI, Roselli D, Alvarez G, Ludwig G, Tsai T. 1997. Epidemic Venezuelan equine encephalitis in La Guajira, Colombia, 1995. *J Infect Dis* 175:828-32.
152. Bowen GS, Fashinell TR, Dean PB, Gregg MB. 1976. Clinical aspects of human Venezuelan equine encephalitis in Texas. *Bull Pan Am Health Organ* 10:46-57.
153. Casamassima AC, Hess LW, Marty A. 1987. TC-83 Venezuelan equine encephalitis vaccine exposure during pregnancy. *Teratology* 36:287-9.
154. Greene IP, Paessler S, Austgen L, Anishchenko M, Brault AC, Bowen RA, Weaver SC. 2005. Envelope glycoprotein mutations mediate equine amplification and virulence of epizootic Venezuelan equine encephalitis virus. *J Virol* 79:9128-33.
155. Weaver SC, Bellew LA, Rico-Hesse R. 1992. Phylogenetic analysis of alphaviruses in the Venezuelan equine encephalitis complex and identification of the source of epizootic viruses. *Virology* 191:282-90.
156. Kinney RM, Tsuchiya KR, Sneider JM, Trent DW. 1992. Genetic evidence that epizootic Venezuelan equine encephalitis (VEE) viruses may have evolved from enzootic VEE subtype I-D virus. *Virology* 191:569-80.

157. Charles PC, Walters E, Margolis F, Johnston RE. 1995. Mechanism of neuroinvasion of Venezuelan equine encephalitis virus in the mouse. *Virology* 208:662-71.
158. Charles PC, Trgovcich J, Davis NL, Johnston RE. 2001. Immunopathogenesis and immune modulation of Venezuelan equine encephalitis virus-induced disease in the mouse. *Virology* 284:190-202.
159. Monath TP, Calisher CH, Davis M, Bowen GS, White J. 1974. Experimental studies of rhesus monkeys infected with epizootic and enzootic subtypes of Venezuelan equine encephalitis virus. *J Infect Dis* 129:194-200.
160. Reed DS, Lind CM, Sullivan LJ, Pratt WD, Parker MD. 2004. Aerosol infection of cynomolgus macaques with enzootic strains of venezuelan equine encephalitis viruses. *J Infect Dis* 189:1013-7.
161. GLEISER CA, GOCHENOUR WS, BERGE TO, TIGERTT WD. 1962. The comparative pathology of experimental Venezuelan equine encephalomyelitis infection in different animal hosts. *J Infect Dis* 110:80-97.
162. Steele KE, Twenhafel NA. 2010. REVIEW PAPER: pathology of animal models of alphavirus encephalitis. *Vet Pathol* 47:790-805.
163. Helenius A, Kartenbeck J, Simons K, Fries E. 1980. On the entry of Semliki forest virus into BHK-21 cells. *J Cell Biol* 84:404-20.
164. Marsh M, Bolzau E, Helenius A. 1983. Penetration of Semliki Forest virus from acidic prelysosomal vacuoles. *Cell* 32:931-40.
165. Zheng Y, Sánchez-San Martín C, Qin ZL, Kielian M. 2011. The domain I-domain III linker plays an important role in the fusogenic conformational change of the alphavirus membrane fusion protein. *J Virol* 85:6334-42.
166. Bron R, Wahlberg JM, Garoff H, Wilschut J. 1993. Membrane fusion of Semliki Forest virus in a model system: correlation between fusion kinetics and structural changes in the envelope glycoprotein. *EMBO J* 12:693-701.
167. Vancini R, Wang G, Ferreira D, Hernandez R, Brown DT. 2013. Alphavirus genome delivery occurs directly at the plasma membrane in a time- and temperature-dependent process. *J Virol* 87:4352-9.
168. Paredes AM, Ferreira D, Horton M, Saad A, Tsuruta H, Johnston R, Klimstra W, Ryman K, Hernandez R, Chiu W, Brown DT. 2004. Conformational changes in Sindbis virions resulting from exposure to low pH and interactions with cells suggest that cell penetration may occur at the cell surface in the absence of membrane fusion. *Virology* 324:373-86.
169. Silva LA, Khomandiak S, Ashbrook AW, Weller R, Heise MT, Morrison TE, Dermody TS. 2014. A single-amino-acid polymorphism in Chikungunya virus E2 glycoprotein influences glycosaminoglycan utilization. *J Virol* 88:2385-97.
170. Klimstra WB, Ryman KD, Johnston RE. 1998. Adaptation of Sindbis virus to BHK cells selects for use of heparan sulfate as an attachment receptor. *J Virol* 72:7357-66.

171. Gardner CL, Ebel GD, Ryman KD, Klimstra WB. 2011. Heparan sulfate binding by natural eastern equine encephalitis viruses promotes neurovirulence. *Proc Natl Acad Sci U S A* 108:16026-31.
172. Bernard KA, Klimstra WB, Johnston RE. 2000. Mutations in the E2 glycoprotein of Venezuelan equine encephalitis virus confer heparan sulfate interaction, low morbidity, and rapid clearance from blood of mice. *Virology* 276:93-103.
173. Levitt NH, Ramsburg HH, Hasty SE, Repik PM, Cole FE, Lupton HW. 1986. Development of an attenuated strain of chikungunya virus for use in vaccine production. *Vaccine* 4:157-62.
174. Gorchakov R, Wang E, Leal G, Forrester NL, Plante K, Rossi SL, Partidos CD, Adams AP, Seymour RL, Weger J, Borland EM, Sherman MB, Powers AM, Osorio JE, Weaver SC. 2012. Attenuation of Chikungunya virus vaccine strain 181/clone 25 is determined by two amino acid substitutions in the E2 envelope glycoprotein. *J Virol* 86:6084-96.
175. Ashbrook AW, Burrack KS, Silva LA, Montgomery SA, Heise MT, Morrison TE, Dermody TS. 2014. Residue 82 of the Chikungunya virus E2 attachment protein modulates viral dissemination and arthritis in mice. *J Virol* 88:12180-92.
176. Jose J, Snyder JE, Kuhn RJ. 2009. A structural and functional perspective of alphavirus replication and assembly. *Future Microbiol* 4:837-56.
177. Kielian M, Chanel-Vos C, Liao M. 2010. Alphavirus Entry and Membrane Fusion. *Viruses* 2:796-825.
178. Rose PP, Hanna SL, Spiridigliozzi A, Wannissorn N, Beiting DP, Ross SR, Hardy RW, Bambina SA, Heise MT, Cherry S. 2011. Natural resistance-associated macrophage protein is a cellular receptor for sindbis virus in both insect and mammalian hosts. *Cell Host Microbe* 10:97-104.
179. Orchard RC, Wilen CB, Doench JG, Baldrige MT, McCune BT, Lee YC, Lee S, Pruett-Miller SM, Nelson CA, Fremont DH, Virgin HW. 2016. Discovery of a proteinaceous cellular receptor for a norovirus. *Science* 353:933-6.
180. Frolova EI, Gorchakov R, Pereboeva L, Atasheva S, Frolov I. 2010. Functional Sindbis virus replicative complexes are formed at the plasma membrane. *J Virol* 84:11679-95.
181. Spuul P, Balistreri G, Kääriäinen L, Ahola T. 2010. Phosphatidylinositol 3-kinase-, actin-, and microtubule-dependent transport of Semliki Forest Virus replication complexes from the plasma membrane to modified lysosomes. *J Virol* 84:7543-57.
182. Kujala P, Ikäheimonen A, Ehsani N, Vihinen H, Auvinen P, Kääriäinen L. 2001. Biogenesis of the Semliki Forest virus RNA replication complex. *J Virol* 75:3873-84.
183. Jose J, Taylor AB, Kuhn RJ. 2017. Spatial and Temporal Analysis of Alphavirus Replication and Assembly in Mammalian and Mosquito Cells. *MBio* 8.
184. Froshauer S, Kartenbeck J, Helenius A. 1988. Alphavirus RNA replicase is located on the cytoplasmic surface of endosomes and lysosomes. *J Cell Biol* 107:2075-86.
185. Li ML, Stollar V. 2007. Distinct sites on the Sindbis virus RNA-dependent RNA polymerase for binding to the promoters for the synthesis of genomic and subgenomic RNA. *J Virol* 81:4371-3.

186. Li G, Rice CM. 1993. The signal for translational readthrough of a UGA codon in Sindbis virus RNA involves a single cytidine residue immediately downstream of the termination codon. *J Virol* 67:5062-7.
187. Tuittila M, Hinkkanen AE. 2003. Amino acid mutations in the replicase protein nsP3 of Semliki Forest virus cumulatively affect neurovirulence. *J Gen Virol* 84:1525-33.
188. de Groot RJ, Hardy WR, Shirako Y, Strauss JH. 1990. Cleavage-site preferences of Sindbis virus polyproteins containing the non-structural proteinase. Evidence for temporal regulation of polyprotein processing in vivo. *EMBO J* 9:2631-8.
189. Sawicki DL, Sawicki SG. 1980. Short-lived minus-strand polymerase for Semliki Forest virus. *J Virol* 34:108-18.
190. Vasiljeva L, Merits A, Golubtsov A, Sizemskaja V, Kääriäinen L, Ahola T. 2003. Regulation of the sequential processing of Semliki Forest virus replicase polyprotein. *J Biol Chem* 278:41636-45.
191. Lemm JA, Rumenapf T, Strauss EG, Strauss JH, Rice CM. 1994. Polypeptide requirements for assembly of functional Sindbis virus replication complexes: a model for the temporal regulation of minus- and plus-strand RNA synthesis. *EMBO J* 13:2925-34.
192. Strauss JH, Strauss EG. 1994. The alphaviruses: gene expression, replication, and evolution. *Microbiol Rev* 58:491-562.
193. Ahola T, Kääriäinen L. 1995. Reaction in alphavirus mRNA capping: formation of a covalent complex of nonstructural protein nsP1 with 7-methyl-GMP. *Proc Natl Acad Sci U S A* 92:507-11.
194. Mi S, Durbin R, Huang HV, Rice CM, Stollar V. 1989. Association of the Sindbis virus RNA methyltransferase activity with the nonstructural protein nsP1. *Virology* 170:385-91.
195. Vasiljeva L, Merits A, Auvinen P, Kääriäinen L. 2000. Identification of a novel function of the alphavirus capping apparatus. RNA 5'-triphosphatase activity of Nsp2. *J Biol Chem* 275:17281-7.
196. Lampio A, Kilpeläinen I, Pesonen S, Karhi K, Auvinen P, Somerharju P, Kääriäinen L. 2000. Membrane binding mechanism of an RNA virus-capping enzyme. *J Biol Chem* 275:37853-9.
197. Ahola T, Kujala P, Tuittila M, Blom T, Laakkonen P, Hinkkanen A, Auvinen P. 2000. Effects of palmitoylation of replicase protein nsP1 on alphavirus infection. *J Virol* 74:6725-33.
198. Spuul P, Salonen A, Merits A, Jokitalo E, Kääriäinen L, Ahola T. 2007. Role of the amphipathic peptide of Semliki forest virus replicase protein nsP1 in membrane association and virus replication. *J Virol* 81:872-83.
199. Gomez de Cedrón M, Ehsani N, Mikkola ML, García JA, Kääriäinen L. 1999. RNA helicase activity of Semliki Forest virus replicase protein NSP2. *FEBS Lett* 448:19-22.
200. Rikkinen M, Peränen J, Kääriäinen L. 1994. ATPase and GTPase activities associated with Semliki Forest virus nonstructural protein nsP2. *J Virol* 68:5804-10.
201. Hardy WR, Strauss JH. 1989. Processing the nonstructural polyproteins of sindbis virus: nonstructural proteinase is in the C-terminal half of nsP2 and functions both in cis and in trans. *J Virol* 63:4653-64.

202. Akhrymuk I, Kulemzin SV, Frolova EI. 2012. Evasion of the innate immune response: the Old World alphavirus nsP2 protein induces rapid degradation of Rpb1, a catalytic subunit of RNA polymerase II. *J Virol* 86:7180-91.
203. Egloff MP, Malet H, Putics A, Heinonen M, Dutartre H, Frangeul A, Gruez A, Campanacci V, Cambillau C, Ziebuhr J, Ahola T, Canard B. 2006. Structural and functional basis for ADP-ribose and poly(ADP-ribose) binding by viral macro domains. *J Virol* 80:8493-502.
204. Malet H, Coutard B, Jamal S, Dutartre H, Papageorgiou N, Neuvonen M, Ahola T, Forrester N, Gould EA, Lafitte D, Ferron F, Lescar J, Gorbalenya AE, de Lamballerie X, Canard B. 2009. The crystal structures of Chikungunya and Venezuelan equine encephalitis virus nsP3 macro domains define a conserved adenosine binding pocket. *J Virol* 83:6534-45.
205. Shin G, Yost SA, Miller MT, Elrod EJ, Grakoui A, Marcotrigiano J. 2012. Structural and functional insights into alphavirus polyprotein processing and pathogenesis. *Proc Natl Acad Sci U S A* 109:16534-9.
206. Vihinen H, Ahola T, Tuittila M, Merits A, Kääriäinen L. 2001. Elimination of phosphorylation sites of Semliki Forest virus replicase protein nsP3. *J Biol Chem* 276:5745-52.
207. Fros JJ, Domeradzka NE, Baggen J, Geertsema C, Flipse J, Vlak JM, Pijlman GP. 2012. Chikungunya virus nsP3 blocks stress granule assembly by recruitment of G3BP into cytoplasmic foci. *J Virol* 86:10873-9.
208. Panas MD, Varjak M, Lulla A, Eng KE, Merits A, Karlsson Hedestam GB, McInerney GM. 2012. Sequestration of G3BP coupled with efficient translation inhibits stress granules in Semliki Forest virus infection. *Mol Biol Cell* 23:4701-12.
209. Kamer G, Argos P. 1984. Primary structural comparison of RNA-dependent polymerases from plant, animal and bacterial viruses. *Nucleic Acids Res* 12:7269-82.
210. Tomar S, Hardy RW, Smith JL, Kuhn RJ. 2006. Catalytic core of alphavirus nonstructural protein nsP4 possesses terminal adenylyltransferase activity. *J Virol* 80:9962-9.
211. Hahn YS, Grakoui A, Rice CM, Strauss EG, Strauss JH. 1989. Mapping of RNA- temperature-sensitive mutants of Sindbis virus: complementation group F mutants have lesions in nsP4. *J Virol* 63:1194-202.
212. Hardy WR, Strauss JH. 1988. Processing the nonstructural polyproteins of Sindbis virus: study of the kinetics in vivo by using monospecific antibodies. *J Virol* 62:998-1007.
213. de Groot RJ, Rümenapf T, Kuhn RJ, Strauss EG, Strauss JH. 1991. Sindbis virus RNA polymerase is degraded by the N-end rule pathway. *Proc Natl Acad Sci U S A* 88:8967-71.
214. Shirako Y, Strauss JH. 1998. Requirement for an aromatic amino acid or histidine at the N terminus of Sindbis virus RNA polymerase. *J Virol* 72:2310-5.
215. Nicola AV, Chen W, Helenius A. 1999. Co-translational folding of an alphavirus capsid protein in the cytosol of living cells. *Nat Cell Biol* 1:341-5.

216. Sánchez IE, Morillas M, Zobeley E, Kiefhaber T, Glockshuber R. 2004. Fast folding of the two-domain semliki forest virus capsid protein explains co-translational proteolytic activity. *J Mol Biol* 338:159-67.
217. Melancon P, Garoff H. 1987. Processing of the Semliki Forest virus structural polyprotein: role of the capsid protease. *J Virol* 61:1301-9.
218. Liljeström P, Garoff H. 1991. Internally located cleavable signal sequences direct the formation of Semliki Forest virus membrane proteins from a polyprotein precursor. *J Virol* 65:147-54.
219. Ozden S, Lucas-Hourani M, Ceccaldi PE, Basak A, Valentine M, Benjannet S, Hamelin J, Jacob Y, Mamchaoui K, Mouly V, Desprès P, Gessain A, Butler-Browne G, Chrétien M, Tangy F, Vidalain PO, Seidah NG. 2008. Inhibition of Chikungunya virus infection in cultured human muscle cells by furin inhibitors: impairment of the maturation of the E2 surface glycoprotein. *J Biol Chem* 283:21899-908.
220. Zhang X, Fugère M, Day R, Kielian M. 2003. Furin processing and proteolytic activation of Semliki Forest virus. *J Virol* 77:2981-9.
221. Snyder JE, Kulcsar KA, Schultz KL, Riley CP, Neary JT, Marr S, Jose J, Griffin DE, Kuhn RJ. 2013. Functional characterization of the alphavirus TF protein. *J Virol* 87:8511-23.
222. Firth AE, Chung BY, Fleeton MN, Atkins JF. 2008. Discovery of frameshifting in Alphavirus 6K resolves a 20-year enigma. *Virol J* 5:108.
223. Liljeström P, Lusa S, Huylebroeck D, Garoff H. 1991. In vitro mutagenesis of a full-length cDNA clone of Semliki Forest virus: the small 6,000-molecular-weight membrane protein modulates virus release. *J Virol* 65:4107-13.
224. Sonenberg N, Hinnebusch AG. 2009. Regulation of translation initiation in eukaryotes: mechanisms and biological targets. *Cell* 136:731-45.
225. Frolov I, Schlesinger S. 1994. Comparison of the effects of Sindbis virus and Sindbis virus replicons on host cell protein synthesis and cytopathogenicity in BHK cells. *J Virol* 68:1721-7.
226. Frolova EI, Fayzulin RZ, Cook SH, Griffin DE, Rice CM, Frolov I. 2002. Roles of nonstructural protein nsP2 and Alpha/Beta interferons in determining the outcome of Sindbis virus infection. *J Virol* 76:11254-64.
227. Ventoso I, Sanz MA, Molina S, Berlanga JJ, Carrasco L, Esteban M. 2006. Translational resistance of late alphavirus mRNA to eIF2alpha phosphorylation: a strategy to overcome the antiviral effect of protein kinase PKR. *Genes Dev* 20:87-100.
228. White LK, Sali T, Alvarado D, Gatti E, Pierre P, Streblow D, Defilippis VR. 2011. Chikungunya virus induces IPS-1-dependent innate immune activation and protein kinase R-independent translational shutoff. *J Virol* 85:606-20.
229. Sanz MA, Castelló A, Ventoso I, Berlanga JJ, Carrasco L. 2009. Dual mechanism for the translation of subgenomic mRNA from Sindbis virus in infected and uninfected cells. *PLoS One* 4:e4772.

230. Taniuchi S, Miyake M, Tsugawa K, Oyadomari M, Oyadomari S. 2016. Integrated stress response of vertebrates is regulated by four eIF2 $\alpha$  kinases. *Sci Rep* 6:32886.
231. Gorchakov R, Frolova E, Williams BR, Rice CM, Frolov I. 2004. PKR-dependent and -independent mechanisms are involved in translational shutoff during Sindbis virus infection. *J Virol* 78:8455-67.
232. Sanz MA, González Almela E, Carrasco L. 2017. Translation of Sindbis Subgenomic mRNA is Independent of eIF2, eIF2A and eIF2D. *Sci Rep* 7:43876.
233. McInerney GM, Kedersha NL, Kaufman RJ, Anderson P, Liljeström P. 2005. Importance of eIF2 $\alpha$  phosphorylation and stress granule assembly in alphavirus translation regulation. *Mol Biol Cell* 16:3753-63.
234. Frolov I, Schlesinger S. 1996. Translation of Sindbis virus mRNA: analysis of sequences downstream of the initiating AUG codon that enhance translation. *J Virol* 70:1182-90.
235. Ventoso I. 2012. Adaptive changes in alphavirus mRNA translation allowed colonization of vertebrate hosts. *J Virol* 86:9484-94.
236. Toribio R, Díaz-López I, Boskovic J, Ventoso I. 2016. An RNA trapping mechanism in Alphavirus mRNA promotes ribosome stalling and translation initiation. *Nucleic Acids Res* 44:4368-80.
237. Parisien M, Major F. 2008. The MC-Fold and MC-Sym pipeline infers RNA structure from sequence data. *Nature* 452:51-5.
238. Castelló A, Sanz MA, Molina S, Carrasco L. 2006. Translation of Sindbis virus 26S mRNA does not require intact eukaryotic initiation factor 4G. *J Mol Biol* 355:942-56.
239. Novoa I, Carrasco L. 1999. Cleavage of eukaryotic translation initiation factor 4G by exogenously added hybrid proteins containing poliovirus 2Apro in HeLa cells: effects on gene expression. *Mol Cell Biol* 19:2445-54.
240. Garcia-Moreno M, Sanz MA, Pelletier J, Carrasco L. 2013. Requirements for eIF4A and eIF2 during translation of Sindbis virus subgenomic mRNA in vertebrate and invertebrate host cells. *Cell Microbiol* 15:823-40.
241. Sanz MA, Castelló A, Carrasco L. 2007. Viral translation is coupled to transcription in Sindbis virus-infected cells. *J Virol* 81:7061-8.
242. Gorchakov R, Frolova E, Frolov I. 2005. Inhibition of transcription and translation in Sindbis virus-infected cells. *J Virol* 79:9397-409.
243. Hong EM, Perera R, Kuhn RJ. 2006. Alphavirus capsid protein helix I controls a checkpoint in nucleocapsid core assembly. *J Virol* 80:8848-55.
244. Suomalainen M, Liljeström P, Garoff H. 1992. Spike protein-nucleocapsid interactions drive the budding of alphaviruses. *J Virol* 66:4737-47.
245. Zhao H, Lindqvist B, Garoff H, von Bonsdorff CH, Liljeström P. 1994. A tyrosine-based motif in the cytoplasmic domain of the alphavirus envelope protein is essential for budding. *EMBO J* 13:4204-11.

246. Dryga SA, Dryga OA, Schlesinger S. 1997. Identification of mutations in a Sindbis virus variant able to establish persistent infection in BHK cells: the importance of a mutation in the nsP2 gene. *Virology* 228:74-83.
247. Frolov I, Agapov E, Hoffman TA, Prágai BM, Lippa M, Schlesinger S, Rice CM. 1999. Selection of RNA replicons capable of persistent noncytopathic replication in mammalian cells. *J Virol* 73:3854-65.
248. Rikkinen M. 1996. Functional significance of the nuclear-targeting and NTP-binding motifs of Semliki Forest virus nonstructural protein nsP2. *Virology* 218:352-61.
249. Garmashova N, Atasheva S, Kang W, Weaver SC, Frolova E, Frolov I. 2007. Analysis of Venezuelan equine encephalitis virus capsid protein function in the inhibition of cellular transcription. *J Virol* 81:13552-65.
250. Garmashova N, Gorchakov R, Volkova E, Paessler S, Frolova E, Frolov I. 2007. The Old World and New World alphaviruses use different virus-specific proteins for induction of transcriptional shutoff. *J Virol* 81:2472-84.
251. ROBINSON MC. 1955. An epidemic of virus disease in Southern Province, Tanganyika Territory, in 1952-53. I. Clinical features. *Trans R Soc Trop Med Hyg* 49:28-32.
252. Carey DE. 1971. Chikungunya and dengue: a case of mistaken identity? *J Hist Med Allied Sci* 26:243-62.
253. Halstead SB. 2015. Reappearance of chikungunya, formerly called dengue, in the Americas. *Emerg Infect Dis* 21:557-61.
254. Laras K, Sukri NC, Larasati RP, Bangs MJ, Kosim R, Djauzi, Wandra T, Master J, Kosasih H, Hartati S, Beckett C, Sedyaningsih ER, Beecham HJ, Corwin AL. 2005. Tracking the re-emergence of epidemic chikungunya virus in Indonesia. *Trans R Soc Trop Med Hyg* 99:128-41.
255. Sumathy K, Ella KM. 2012. Genetic diversity of Chikungunya virus, India 2006-2010: evolutionary dynamics and serotype analyses. *J Med Virol* 84:462-70.
256. Tsetsarkin KA, Chen R, Weaver SC. 2016. Interspecies transmission and chikungunya virus emergence. *Curr Opin Virol* 16:143-150.
257. Vazeille M, Moutailler S, Coudrier D, Rousseaux C, Khun H, Huerre M, Thiria J, Dehecq JS, Fontenille D, Schuffenecker I, Despres P, Failloux AB. 2007. Two Chikungunya isolates from the outbreak of La Reunion (Indian Ocean) exhibit different patterns of infection in the mosquito, *Aedes albopictus*. *PLoS One* 2:e1168.
258. Grandadam M, Caro V, Plumet S, Thiberge JM, Souarès Y, Failloux AB, Tolou HJ, Budelot M, Cosserat D, Leparç-Goffart I, Desprès P. 2011. Chikungunya virus, southeastern France. *Emerg Infect Dis* 17:910-3.
259. Rezza G, Nicoletti L, Angelini R, Romi R, Finarelli AC, Panning M, Cordioli P, Fortuna C, Boros S, Magurano F, Silvi G, Angelini P, Dottori M, Ciufolini MG, Majori GC, Cassone A, group Cs. 2007. Infection with chikungunya virus in Italy: an outbreak in a temperate region. *Lancet* 370:1840-6.

260. Díaz-González EE, Kautz TF, Dorantes-Delgado A, Malo-García IR, Laguna-Aguilar M, Langsjoen RM, Chen R, Auguste DI, Sánchez-Casas RM, Danis-Lozano R, Weaver SC, Fernández-Salas I. 2015. First Report of *Aedes aegypti* Transmission of Chikungunya Virus in the Americas. *Am J Trop Med Hyg* 93:1325-9.
261. Higgs S, Vanlandingham D. 2015. Chikungunya virus and its mosquito vectors. *Vector Borne Zoonotic Dis* 15:231-40.
262. Anonymous. Chikungunya: Statistics Data, on Pan American Health Organization. [http://www.paho.org/hq/index.php?option=com\\_topics&view=readall&cid=5927&Itemid=40931&lang=en](http://www.paho.org/hq/index.php?option=com_topics&view=readall&cid=5927&Itemid=40931&lang=en). Accessed November.
263. Mowatt L, Jackson ST. 2014. Chikungunya in the Caribbean: An Epidemic in the Making. *Infect Dis Ther*.
264. Chen R, Puri V, Fedorova N, Lin D, Hari KL, Jain R, Rodas JD, Das SR, Shabman RS, Weaver SC. 2016. Comprehensive Genome Scale Phylogenetic Study Provides New Insights on the Global Expansion of Chikungunya Virus. *J Virol* 90:10600-10611.
265. Leparc-Goffart I, Nougairede A, Cassadou S, Prat C, de Lamballerie X. 2014. Chikungunya in the Americas. *Lancet* 383:514.
266. Nunes MR, Faria NR, de Vasconcelos JM, Golding N, Kraemer MU, de Oliveira LF, Azevedo RoS, da Silva DE, da Silva EV, da Silva SP, Carvalho VL, Coelho GE, Cruz AC, Rodrigues SG, Vianez JL, Nunes BT, Cardoso JF, Tesh RB, Hay SI, Pybus OG, Vasconcelos PF. 2015. Emergence and potential for spread of Chikungunya virus in Brazil. *BMC Med* 13:102.
267. Diallo D, Sall AA, Buenemann M, Chen R, Faye O, Diagne CT, Ba Y, Dia I, Watts D, Weaver SC, Hanley KA, Diallo M. 2012. Landscape ecology of sylvatic chikungunya virus and mosquito vectors in southeastern Senegal. *PLoS Negl Trop Dis* 6:e1649.
268. Apandi Y, Nazni WA, Noor Asleen ZA, Vythilingam I, Noorazian MY, Azahari AH, Zainah S, Lee HL. 2009. The first isolation of chikungunya virus from non-human primates in Malaysia. *Journal of General and Molecular Virology* 1:35.
269. Inoue S, Morita K, Matias RR, Tuplano JV, Resuello RR, Candelario JR, Cruz DJ, Mapua CA, Hasebe F, Igarashi A, Natividad FF. 2003. Distribution of three arbovirus antibodies among monkeys (*Macaca fascicularis*) in the Philippines. *J Med Primatol* 32:89-94.
270. Marchette NJ, Rudnick A, Garcia R, MacVean DW. 1978. Alphaviruses in Peninsular Malaysia: I. Virus isolations and animal serology. *Southeast Asian J Trop Med Public Health* 9:317-29.
271. Lourenço-de-Oliveira R, Failloux AB. 2017. High risk for chikungunya virus to initiate an enzootic sylvatic cycle in the tropical Americas. *PLoS Negl Trop Dis* 11:e0005698.
272. Vega-Rúa A, Zouache K, Girod R, Failloux AB, Lourenço-de-Oliveira R. 2014. High level of vector competence of *Aedes aegypti* and *Aedes albopictus* from ten American countries as a crucial factor in the spread of Chikungunya virus. *J Virol* 88:6294-306.
273. Vega-Rúa A, Lourenço-de-Oliveira R, Mousson L, Vazeille M, Fuchs S, Yébakima A, Gustave J, Girod R, Dusfour I, Leparc-Goffart I, Vanlandingham DL, Huang YJ, Lounibos LP, Mohamed Ali S,

- Nougairede A, de Lamballerie X, Failloux AB. 2015. Chikungunya virus transmission potential by local *Aedes* mosquitoes in the Americas and Europe. *PLoS Negl Trop Dis* 9:e0003780.
274. Dong S, Kantor AM, Lin J, Passarelli AL, Clem RJ, Franz AW. 2016. Infection pattern and transmission potential of chikungunya virus in two New World laboratory-adapted *Aedes aegypti* strains. *Sci Rep* 6:24729.
275. Dubrulle M, Mousson L, Moutailler S, Vazeille M, Failloux AB. 2009. Chikungunya virus and *Aedes* mosquitoes: saliva is infectious as soon as two days after oral infection. *PLoS One* 4:e5895.
276. Reiter P, Fontenille D, Paupy C. 2006. *Aedes albopictus* as an epidemic vector of chikungunya virus: another emerging problem? *Lancet Infect Dis* 6:463-4.
277. Tsetsarkin KA, Vanlandingham DL, McGee CE, Higgs S. 2007. A single mutation in chikungunya virus affects vector specificity and epidemic potential. *PLoS Pathog* 3:e201.
278. Niyas KP, Abraham R, Unnikrishnan RN, Mathew T, Nair S, Manakkadan A, Issac A, Sreekumar E. 2010. Molecular characterization of Chikungunya virus isolates from clinical samples and adult *Aedes albopictus* mosquitoes emerged from larvae from Kerala, South India. *Virology* 40:189.
279. Ratsitorahina M, Harisoa J, Ratovonjato J, Biacabe S, Reynes JM, Zeller H, Raelina Y, Talarmin A, Richard V, Louis Soares J. 2008. Outbreak of dengue and Chikungunya fevers, Toamasina, Madagascar, 2006. *Emerg Infect Dis* 14:1135-7.
280. Thavara U, Tawatsin A, Pengsakul T, Bhakdeenuan P, Chanama S, Anantapreecha S, Molito C, Chompoonsri J, Thammapalo S, Sawanpanyalert P, Siriyasatien P. 2009. Outbreak of chikungunya fever in Thailand and virus detection in field population of vector mosquitoes, *Aedes aegypti* (L.) and *Aedes albopictus* Skuse (Diptera: Culicidae). *Southeast Asian J Trop Med Public Health* 40:951-62.
281. Mourya DT. 1987. Absence of transovarial transmission of Chikungunya virus in *Aedes aegypti* & *Ae. albopictus* mosquitoes. *Indian J Med Res* 85:593-5.
282. Vazeille M, Mousson L, Failloux AB. 2009. Failure to demonstrate experimental vertical transmission of the epidemic strain of Chikungunya virus in *Aedes albopictus* from La Réunion Island, Indian Ocean. *Mem Inst Oswaldo Cruz* 104:632-5.
283. Agarwal A, Dash PK, Singh AK, Sharma S, Gopalan N, Rao PV, Parida MM, Reiter P. 2014. Evidence of experimental vertical transmission of emerging novel ECSA genotype of Chikungunya Virus in *Aedes aegypti*. *PLoS Negl Trop Dis* 8:e2990.
284. Mavale M, Parashar D, Sudeep A, Gokhale M, Ghodke Y, Geevarghese G, Arankalle V, Mishra AC. 2010. Venereal transmission of chikungunya virus by *Aedes aegypti* mosquitoes (Diptera: Culicidae). *Am J Trop Med Hyg* 83:1242-4.
285. Simon F, Javelle E, Oliver M, Leparç-Goffart I, Marimoutou C. 2011. Chikungunya virus infection. *Curr Infect Dis Rep* 13:218-28.
286. Simon F, Parola P, Grandadam M, Fourcade S, Oliver M, Brouqui P, Hance P, Kraemer P, Ali Mohamed A, de Lamballerie X, Charrel R, Tolou H. 2007. Chikungunya infection: an emerging

- rheumatism among travelers returned from Indian Ocean islands. Report of 47 cases. *Medicine* 86:123-37.
287. Borgherini G, Poubeau P, Staikowsky F, Lory M, Le Moullec N, Becquart JP, Wengling C, Michault A, Paganin F. 2007. Outbreak of chikungunya on Reunion Island: early clinical and laboratory features in 157 adult patients. *Clin Infect Dis* 44:1401-7.
288. Bandyopadhyay D, Ghosh SK. 2008. Mucocutaneous features of Chikungunya fever: a study from an outbreak in West Bengal, India. *Int J Dermatol* 47:1148-52.
289. Economopoulou A, Dominguez M, Helynck B, Sissoko D, Wichmann O, Quenel P, Germonneau P, Quatresous I. 2009. Atypical Chikungunya virus infections: clinical manifestations, mortality and risk factors for severe disease during the 2005-2006 outbreak on Reunion. *Epidemiol Infect* 137:534-41.
290. Rajapakse S, Rodrigo C, Rajapakse A. 2010. Atypical manifestations of chikungunya infection. *Trans R Soc Trop Med Hyg* 104:89-96.
291. Gérardin P, Barau G, Michault A, Bintner M, Randrianaivo H, Choker G, Lenglet Y, Touret Y, Bouveret A, Grivard P, Le Roux K, Blanc S, Schuffenecker I, Couderc T, Arenzana-Seisdedos F, Lecuit M, Robillard PY. 2008. Multidisciplinary prospective study of mother-to-child chikungunya virus infections on the island of La Réunion. *PLoS Med* 5:e60.
292. Borgherini G, Poubeau P, Jossaume A, Gouix A, Cotte L, Michault A, Arvin-Berod C, Paganin F. 2008. Persistent arthralgia associated with chikungunya virus: a study of 88 adult patients on reunion island. *Clin Infect Dis* 47:469-75.
293. Schilte C, Staikowsky F, Staikovskiy F, Couderc T, Madec Y, Carpentier F, Kassab S, Albert ML, Lecuit M, Michault A. 2013. Chikungunya virus-associated long-term arthralgia: a 36-month prospective longitudinal study. *PLoS Negl Trop Dis* 7:e2137.
294. Manimunda SP, Vijayachari P, Uppoor R, Sugunan AP, Singh SS, Rai SK, Sudeep AB, Muruganandam N, Chaitanya IK, Guruprasad DR. 2010. Clinical progression of chikungunya fever during acute and chronic arthritic stages and the changes in joint morphology as revealed by imaging. *Trans R Soc Trop Med Hyg* 104:392-9.
295. Chaithanya IK, Muruganandam N, Raghuraj U, Sugunan AP, Rajesh R, Anwesh M, Rai SK, Vijayachari P. 2014. Chronic inflammatory arthritis with persisting bony erosions in patients following chikungunya infection. *Indian J Med Res* 140:142-5.
296. Kee AC, Yang S, Tambyah P. 2010. Atypical chikungunya virus infections in immunocompromised patients. *Emerg Infect Dis* 16:1038-40.
297. Rampal, Sharda M, Meena H. 2007. Neurological complications in Chikungunya fever. *J Assoc Physicians India* 55:765-9.
298. Das T, Jaffar-Bandjee MC, Hoarau JJ, Krejbich Trotot P, Denizot M, Lee-Pat-Yuen G, Sahoo R, Guiraud P, Ramful D, Robin S, Alessandri JL, Gauzere BA, Gasque P. 2010. Chikungunya fever: CNS infection and pathologies of a re-emerging arbovirus. *Prog Neurobiol* 91:121-9.

299. Ramful D, Carbonnier M, Pasquet M, Bouhmani B, Ghazouani J, Noormahomed T, Beullier G, Attali T, Samperiz S, Fourmaintraux A, Alessandri JL. 2007. Mother-to-child transmission of Chikungunya virus infection. *Pediatr Infect Dis J* 26:811-5.
300. Robin S, Ramful D, Zettor J, Benhamou L, Jaffar-Bandjee MC, Rivière JP, Marichy J, Ezzedine K, Alessandri JL. 2010. Severe bullous skin lesions associated with Chikungunya virus infection in small infants. *Eur J Pediatr* 169:67-72.
301. Valampampil JJ, Chirakkarot S, Letha S, Jayakumar C, Gopinathan KM. 2009. Clinical profile of Chikungunya in infants. *Indian J Pediatr* 76:151-5.
302. Couderc T, Chrétien F, Schilte C, Disson O, Brigitte M, Guivel-Benhassine F, Touret Y, Barau G, Cayet N, Schuffenecker I, Desprès P, Arenzana-Seisdedos F, Michault A, Albert ML, Lecuit M. 2008. A mouse model for Chikungunya: young age and inefficient type-I interferon signaling are risk factors for severe disease. *PLoS Pathog* 4:e29.
303. Hawman DW, Stoermer KA, Montgomery SA, Pal P, Oko L, Diamond MS, Morrison TE. 2013. Chronic joint disease caused by persistent Chikungunya virus infection is controlled by the adaptive immune response. *J Virol* 87:13878-88.
304. Rudd PA, Wilson J, Gardner J, Larcher T, Babarit C, Le TT, Anraku I, Kumagai Y, Loo YM, Gale M, Akira S, Khromykh AA, Suhrbier A. 2012. Interferon response factors 3 and 7 protect against Chikungunya virus hemorrhagic fever and shock. *J Virol* 86:9888-98.
305. Lum FM, Teo TH, Lee WW, Kam YW, Rénia L, Ng LF. 2013. An essential role of antibodies in the control of Chikungunya virus infection. *J Immunol* 190:6295-302.
306. Teo TH, Lum FM, Claser C, Lulla V, Lulla A, Merits A, Rénia L, Ng LF. 2013. A pathogenic role for CD4+ T cells during Chikungunya virus infection in mice. *J Immunol* 190:259-69.
307. Ziegler SA, Lu L, da Rosa AP, Xiao SY, Tesh RB. 2008. An animal model for studying the pathogenesis of chikungunya virus infection. *Am J Trop Med Hyg* 79:133-9.
308. Poo YS, Rudd PA, Gardner J, Wilson JA, Larcher T, Colle MA, Le TT, Nakaya HI, Warrilow D, Allcock R, Bielefeldt-Ohmann H, Schroder WA, Khromykh AA, Lopez JA, Suhrbier A. 2014. Multiple immune factors are involved in controlling acute and chronic chikungunya virus infection. *PLoS Negl Trop Dis* 8:e3354.
309. Uhrlaub JL, Pulko V, DeFilippis VR, Broeckel R, Streblow DN, Coleman GD, Park BS, Lindo JF, Vickers I, Anzinger JJ, Nikolich-Zugich J. 2016. Dysregulated TGF- $\beta$  Production Underlies the Age-Related Vulnerability to Chikungunya Virus. *PLoS Pathog* 12:e1005891.
310. Broeckel R, Haese N, Messaoudi I, Streblow DN. 2015. Nonhuman Primate Models of Chikungunya Virus Infection and Disease (CHIKV NHP Model). *Pathogens* 4:662-81.
311. Broeckel R, Fox JM, Haese N, Kreklywich CN, Sukulpovi-Petty S, Legasse A, Smith PP, Denton M, Corvey C, Krishnan S, Colgin LMA, Ducore RM, Lewis AD, Axthelm MK, Mandron M, Cortez P, Rothblatt J, Rao E, Focken I, Carter K, Sapparapau G, Crowe JE, Diamond MS, Streblow DN. 2017. Therapeutic administration of a recombinant human monoclonal antibody reduces the severity of chikungunya virus disease in rhesus macaques. *PLoS Negl Trop Dis* 11:e0005637.

312. Chen CI, Clark DC, Pesavento P, Lerche NW, Luciw PA, Reisen WK, Brault AC. 2010. Comparative pathogenesis of epidemic and enzootic Chikungunya viruses in a pregnant Rhesus macaque model. *Am J Trop Med Hyg* 83:1249-58.
313. Messaoudi I, Vomaske J, Totonchy T, Kreklywich CN, Haberthur K, Springgay L, Brien JD, Diamond MS, Defilippis VR, Streblow DN. 2013. Chikungunya virus infection results in higher and persistent viral replication in aged rhesus macaques due to defects in anti-viral immunity. *PLoS Negl Trop Dis* 7.
314. Pal P, Fox JM, Hawman DW, Huang YJ, Messaoudi I, Kreklywich C, Denton M, Legasse AW, Smith PP, Johnson S, Axthelm MK, Vanlandingham DL, Streblow DN, Higgs S, Morrison TE, Diamond MS. 2014. Chikungunya viruses that escape monoclonal antibody therapy are clinically attenuated, stable, and not purified in mosquitoes. *J Virol* 88:8213-26.
315. Kam YW, Lee WW, Simarmata D, Le Grand R, Tolou H, Merits A, Roques P, Ng LF. 2014. Unique epitopes recognized by antibodies induced in Chikungunya virus-infected non-human primates: implications for the study of immunopathology and vaccine development. *PLoS One* 9:e95647.
316. Gérardin P, Guernier V, Perrau J, Fianu A, Le Roux K, Grivard P, Michault A, de Lamballerie X, Flahault A, Favier F. 2008. Estimating Chikungunya prevalence in La Réunion Island outbreak by serosurveys: two methods for two critical times of the epidemic. *BMC Infect Dis* 8:99.
317. Schilte C, Couderc T, Chretien F, Sourisseau M, Gangneux N, Guivel-Benhassine F, Kraxner A, Tschopp J, Higgs S, Michault A, Arenzana-Seisdedos F, Colonna M, Peduto L, Schwartz O, Lecuit M, Albert ML. 2010. Type I IFN controls chikungunya virus via its action on nonhematopoietic cells. *J Exp Med* 207:429-42.
318. Fox JM, Diamond MS. 2016. Immune-Mediated Protection and Pathogenesis of Chikungunya Virus. *J Immunol* 197:4210-4218.
319. Her Z, Teng TS, Tan JJ, Teo TH, Kam YW, Lum FM, Lee WW, Gabriel C, Melchiotti R, Andiappan AK, Lulla V, Lulla A, Win MK, Chow A, Biswas SK, Leo YS, Lecuit M, Merits A, Rénia L, Ng LF. 2015. Loss of TLR3 aggravates CHIKV replication and pathology due to an altered virus-specific neutralizing antibody response. *EMBO Mol Med* 7:24-41.
320. Klimstra WB, Nangle EM, Smith MS, Yurochko AD, Ryman KD. 2003. DC-SIGN and L-SIGN can act as attachment receptors for alphaviruses and distinguish between mosquito cell- and mammalian cell-derived viruses. *J Virol* 77:12022-32.
321. Wu SJ, Grouard-Vogel G, Sun W, Mascola JR, Brachtel E, Putvatana R, Louder MK, Filgueira L, Marovich MA, Wong HK, Blauvelt A, Murphy GS, Robb ML, Innes BL, Birx DL, Hayes CG, Frankel SS. 2000. Human skin Langerhans cells are targets of dengue virus infection. *Nat Med* 6:816-20.
322. Shabman RS, Morrison TE, Moore C, White L, Suthar MS, Hueston L, Rulli N, Lidbury B, Ting JP, Mahalingam S, Heise MT. 2007. Differential induction of type I interferon responses in myeloid dendritic cells by mosquito and mammalian-cell-derived alphaviruses. *J Virol* 81:237-47.
323. Konopka JL, Penalva LO, Thompson JM, White LJ, Beard CW, Keene JD, Johnston RE. 2007. A two-phase innate host response to alphavirus infection identified by mRNP-tagging in vivo. *PLoS Pathog* 3:e199.

324. Gardner JP, Frolov I, Perri S, Ji Y, MacKichan ML, zur Megede J, Chen M, Belli BA, Driver DA, Sherrill S, Greer CE, Otten GR, Barnett SW, Liu MA, Dubensky TW, Polo JM. 2000. Infection of human dendritic cells by a sindbis virus replicon vector is determined by a single amino acid substitution in the E2 glycoprotein. *J Virol* 74:11849-57.
325. Sourisseau M, Schilte C, Casartelli N, Trouillet C, Guivel-Benhassine F, Rudnicka D, Sol-Foulon N, Le Roux K, Prevost MC, Fsihi H, Frenkiel MP, Blanchet F, Afonso PV, Ceccaldi PE, Ozden S, Gessain A, Schuffenecker I, Verhasselt B, Zamborlini A, Saïb A, Rey FA, Arenzana-Seisdedos F, Desprès P, Michault A, Albert ML, Schwartz O. 2007. Characterization of reemerging chikungunya virus. *PLoS Pathog* 3:e89.
326. Poo YS, Nakaya H, Gardner J, Larcher T, Schroder WA, Le TT, Major LD, Suhrbier A. 2014. CCR2 deficiency promotes exacerbated chronic erosive neutrophil-dominated chikungunya virus arthritis. *J Virol* 88:6862-72.
327. Stoermer KA, Burrack A, Oko L, Montgomery SA, Borst LB, Gill RG, Morrison TE. 2012. Genetic ablation of arginase 1 in macrophages and neutrophils enhances clearance of an arthritogenic alphavirus. *J Immunol* 189:4047-59.
328. Chow A, Her Z, Ong EK, Chen JM, Dimatatac F, Kwek DJ, Barkham T, Yang H, Rénia L, Leo YS, Ng LF. 2011. Persistent arthralgia induced by Chikungunya virus infection is associated with interleukin-6 and granulocyte macrophage colony-stimulating factor. *J Infect Dis* 203:149-57.
329. Teo TH, Her Z, Tan JJ, Lum FM, Lee WW, Chan YH, Ong RY, Kam YW, Leparç-Goffart I, Gallian P, Rénia L, de Lamballerie X, Ng LF. 2015. Caribbean and La Réunion Chikungunya Virus Isolates Differ in Their Capacity To Induce Proinflammatory Th1 and NK Cell Responses and Acute Joint Pathology. *J Virol* 89:7955-69.
330. Chua CL, Sam IC, Chiam CW, Chan YF. 2017. The neutralizing role of IgM during early Chikungunya virus infection. *PLoS One* 12:e0171989.
331. Kam YW, Lum FM, Teo TH, Lee WW, Simarmata D, Harjanto S, Chua CL, Chan YF, Wee JK, Chow A, Lin RT, Leo YS, Le Grand R, Sam IC, Tong JC, Roques P, Wiesmüller KH, Rénia L, Röttschke O, Ng LF. 2012. Early neutralizing IgG response to Chikungunya virus in infected patients targets a dominant linear epitope on the E2 glycoprotein. *EMBO Mol Med* 4:330-43.
332. Fong RH, Banik SS, Mattia K, Barnes T, Tucker D, Liss N, Lu K, Selvarajah S, Srinivasan S, Mabila M, Miller A, Muench MO, Michault A, Rucker JB, Paes C, Simmons G, Kahle KM, Doranz BJ. 2014. Exposure of epitope residues on the outer face of the chikungunya virus envelope trimer determines antibody neutralizing efficacy. *J Virol* 88:14364-79.
333. Couderc T, Khandoudi N, Grandadam M, Visse C, Gangneux N, Bagot S, Prost JF, Lecuit M. 2009. Prophylaxis and therapy for Chikungunya virus infection. *J Infect Dis* 200:516-23.
334. Pal P, Dowd KA, Brien JD, Edeling MA, Gorlatov S, Johnson S, Lee I, Akahata W, Nabel GJ, Richter MK, Smit JM, Fremont DH, Pierson TC, Heise MT, Diamond MS. 2013. Development of a highly protective combination monoclonal antibody therapy against Chikungunya virus. *PLoS Pathog* 9:e1003312.

335. Galatas B, Ly S, Duong V, Baisley K, Nguon K, Chan S, Huy R, Sorn S, Som L, Buchy P, Tarantola A. 2016. Long-Lasting Immune Protection and Other Epidemiological Findings after Chikungunya Emergence in a Cambodian Rural Community, April 2012. *PLoS Negl Trop Dis* 10:e0004281.
336. Kam YW, Simarmata D, Chow A, Her Z, Teng TS, Ong EK, Rénia L, Leo YS, Ng LF. 2012. Early appearance of neutralizing immunoglobulin G3 antibodies is associated with chikungunya virus clearance and long-term clinical protection. *J Infect Dis* 205:1147-54.
337. Wauquier N, Becquart P, Nkoghe D, Padilla C, Ndjoyi-Mbiguino A, Leroy EM. 2011. The acute phase of Chikungunya virus infection in humans is associated with strong innate immunity and T CD8 cell activation. *J Infect Dis* 204:115-23.
338. Hoarau JJ, Gay F, Pellé O, Samri A, Jaffar-Bandjee MC, Gasque P, Autran B. 2013. Identical strength of the T cell responses against E2, nsP1 and capsid CHIKV proteins in recovered and chronic patients after the epidemics of 2005-2006 in La Reunion Island. *PLoS One* 8:e84695.
339. Miner JJ, Aw-Yeang HX, Fox JM, Taffner S, Malkova ON, Oh ST, Kim AHJ, Diamond MS, Lenschow DJ, Yokoyama WM. 2015. Chikungunya viral arthritis in the United States: a mimic of seronegative rheumatoid arthritis. *Arthritis Rheumatol* 67:1214-1220.
340. Teo TH, Chan YH, Lee WW, Lum FM, Amrun SN, Her Z, Rajarethinam R, Merits A, Röttschke O, Rénia L, Ng LF. 2017. Fingolimod treatment abrogates chikungunya virus-induced arthralgia. *Sci Transl Med* 9.
341. Lee WW, Teo TH, Her Z, Lum FM, Kam YW, Haase D, Rénia L, Röttschke O, Ng LF. 2015. Expanding regulatory T cells alleviates chikungunya virus-induced pathology in mice. *J Virol*.
342. Pfender N, Jelcic I, Linnebank M, Schwarz U, Martin R. 2015. Reactivation of herpesvirus under fingolimod: A case of severe herpes simplex encephalitis. *Neurology* 84:2377-8.
343. Burrack KS, Montgomery SA, Homann D, Morrison TE. 2015. CD8+ T cells control Ross River virus infection in musculoskeletal tissues of infected mice. *J Immunol* 194:678-89.
344. Binder GK, Griffin DE. 2001. Interferon-gamma-mediated site-specific clearance of alphavirus from CNS neurons. *Science* 293:303-6.
345. Yun NE, Peng BH, Bertke AS, Borisevich V, Smith JK, Smith JN, Poussard AL, Salazar M, Judy BM, Zacks MA, Estes DM, Paessler S. 2009. CD4+ T cells provide protection against acute lethal encephalitis caused by Venezuelan equine encephalitis virus. *Vaccine* 27:4064-73.
346. Sokka T, Envalds M, Pincus T. 2008. Treatment of rheumatoid arthritis: a global perspective on the use of antirheumatic drugs. *Mod Rheumatol* 18:228-39.
347. Brown PM, Pratt AG, Isaacs JD. 2016. Mechanism of action of methotrexate in rheumatoid arthritis, and the search for biomarkers. *Nat Rev Rheumatol* 12:731-742.
348. Javelle E, Ribera A, Degasne I, Gaüzère BA, Marimoutou C, Simon F. 2015. Specific management of post-chikungunya rheumatic disorders: a retrospective study of 159 cases in Reunion Island from 2006-2012. *PLoS Negl Trop Dis* 9:e0003603.

349. Lauring AS, Jones JO, Andino R. 2010. Rationalizing the development of live attenuated virus vaccines. *Nat Biotechnol* 28:573-9.
350. Edelman R, Tacket CO, Wasserman SS, Bodison SA, Perry JG, Mangiafico JA. 2000. Phase II safety and immunogenicity study of live chikungunya virus vaccine TSI-GSD-218. *Am J Trop Med Hyg* 62:681-5.
351. Hallengård D, Kakoulidou M, Lulla A, Kümmerer BM, Johansson DX, Mutso M, Lulla V, Fazakerley JK, Roques P, Le Grand R, Merits A, Liljeström P. 2014. Novel attenuated Chikungunya vaccine candidates elicit protective immunity in C57BL/6 mice. *J Virol* 88:2858-66.
352. Piper A, Ribeiro M, Smith KM, Briggs CM, Huitt E, Nanda K, Spears CJ, Quiles M, Cullen J, Thomas ME, Brown DT, Hernandez R. 2013. Chikungunya virus host range E2 transmembrane deletion mutants induce protective immunity against challenge in C57BL/6J mice. *J Virol* 87:6748-57.
353. Plante K, Wang E, Partidos CD, Weger J, Gorchakov R, Tsetsarkin K, Borland EM, Powers AM, Seymour R, Stinchcomb DT, Osorio JE, Frolov I, Weaver SC. 2011. Novel chikungunya vaccine candidate with an IRES-based attenuation and host range alteration mechanism. *PLoS Pathog* 7:e1002142.
354. Roy CJ, Adams AP, Wang E, Plante K, Gorchakov R, Seymour RL, Vinet-Oliphant H, Weaver SC. 2014. Chikungunya vaccine candidate is highly attenuated and protects nonhuman primates against telemetrically monitored disease following a single dose. *J Infect Dis* 209:1891-9.
355. Mallilankaraman K, Shedlock DJ, Bao H, Kawalekar OU, Fagone P, Ramanathan AA, Ferraro B, Stabenow J, Vijayachari P, Sundaram SG, Muruganandam N, Sarangan G, Srikanth P, Khan AS, Lewis MG, Kim JJ, Sardesai NY, Muthumani K, Weiner DB. 2011. A DNA vaccine against chikungunya virus is protective in mice and induces neutralizing antibodies in mice and nonhuman primates. *PLoS Negl Trop Dis* 5:e928.
356. Tretyakova I, Hearn J, Wang E, Weaver S, Pushko P. 2014. DNA vaccine initiates replication of live attenuated chikungunya virus in vitro and elicits protective immune response in mice. *J Infect Dis* 209:1882-90.
357. Akahata W, Yang ZY, Andersen H, Sun S, Holdaway HA, Kong WP, Lewis MG, Higgs S, Rossmann MG, Rao S, Nabel GJ. 2010. A virus-like particle vaccine for epidemic Chikungunya virus protects nonhuman primates against infection. *Nat Med* 16:334-8.
358. Wang E, Volkova E, Adams AP, Forrester N, Xiao SY, Frolov I, Weaver SC. 2008. Chimeric alphavirus vaccine candidates for chikungunya. *Vaccine* 26:5030-9.
359. Erasmus JH, Auguste AJ, Kaelber JT, Luo H, Rossi SL, Fenton K, Leal G, Kim DY, Chiu W, Wang T, Frolov I, Nasar F, Weaver SC. 2017. A chikungunya fever vaccine utilizing an insect-specific virus platform. *Nat Med* 23:192-199.
360. Wang D, Suhrbier A, Penn-Nicholson A, Woraratanadharm J, Gardner J, Luo M, Le TT, Anraku I, Sakalian M, Einfeld D, Dong JY. 2011. A complex adenovirus vaccine against chikungunya virus provides complete protection against viraemia and arthritis. *Vaccine* 29:2803-9.

361. García-Arriaza J, Cepeda V, Hallengård D, Sorzano C, Kümmerer BM, Liljeström P, Esteban M. 2014. A novel poxvirus-based vaccine, MVA-CHIKV, is highly immunogenic and protects mice against chikungunya infection. *J Virol* 88:3527-47.
362. Gardner CL, Hritz J, Sun C, Vanlandingham DL, Song TY, Ghedin E, Higgs S, Klimstra WB, Ryman KD. 2014. Deliberate attenuation of chikungunya virus by adaptation to heparan sulfate-dependent infectivity: a model for rational arboviral vaccine design. *PLoS Negl Trop Dis* 8:e2719.
363. Roques P, Ljungberg K, Kümmerer BM, Gosse L, Dereuddre-Bosquet N, Tchitchek N, Hallengård D, García-Arriaza J, Meinke A, Esteban M, Merits A, Le Grand R, Liljeström P. 2017. Attenuated and vectored vaccines protect nonhuman primates against Chikungunya virus. *JCI Insight* 2:e83527.
364. Harrison VR, Eckels KH, Bartelloni PJ, Hampton C. 1971. Production and evaluation of a formalin-killed Chikungunya vaccine. *J Immunol* 107:643-7.
365. Nakao E, Hotta S. 1973. Immunogenicity of purified, inactivated chikungunya virus in monkeys. *Bull World Health Organ* 48:559-62.
366. Kumar M, Sudeep AB, Arankalle VA. 2012. Evaluation of recombinant E2 protein-based and whole-virus inactivated candidate vaccines against chikungunya virus. *Vaccine* 30:6142-9.
367. Muthumani K, Lankaraman KM, Laddy DJ, Sundaram SG, Chung CW, Sako E, Wu L, Khan A, Sardesai N, Kim JJ, Vijayachari P, Weiner DB. 2008. Immunogenicity of novel consensus-based DNA vaccines against Chikungunya virus. *Vaccine* 26:5128-34.
368. Chang LJ, Dowd KA, Mendoza FH, Saunders JG, Sitar S, Plummer SH, Yamshchikov G, Sarwar UN, Hu Z, Enama ME, Bailer RT, Koup RA, Schwartz RM, Akahata W, Nabel GJ, Mascola JR, Pierson TC, Graham BS, Ledgerwood JE, Team VS. 2014. Safety and tolerability of chikungunya virus-like particle vaccine in healthy adults: a phase 1 dose-escalation trial. *Lancet* 384:2046-52.
369. Metz SW, Gardner J, Geertsema C, Le TT, Goh L, Vlak JM, Suhrbier A, Pijlman GP. 2013. Effective chikungunya virus-like particle vaccine produced in insect cells. *PLoS Negl Trop Dis* 7:e2124.
370. Metz SW, Martina BE, van den Doel P, Geertsema C, Osterhaus AD, Vlak JM, Pijlman GP. 2013. Chikungunya virus-like particles are more immunogenic in a lethal AG129 mouse model compared to glycoprotein E1 or E2 subunits. *Vaccine* 31:6092-6.
371. Khan M, Dhanwani R, Rao PV, Parida M. 2012. Subunit vaccine formulations based on recombinant envelope proteins of Chikungunya virus elicit balanced Th1/Th2 response and virus-neutralizing antibodies in mice. *Virus Res* 167:236-46.
372. van den Doel P, Volz A, Roose JM, Sewbalaksing VD, Pijlman GP, van Middelkoop I, Duiverman V, van de Wetering E, Sutter G, Osterhaus AD, Martina BE. 2014. Recombinant modified vaccinia virus Ankara expressing glycoprotein E2 of Chikungunya virus protects AG129 mice against lethal challenge. *PLoS Negl Trop Dis* 8:e3101.
373. Weger-Lucarelli J, Chu H, Aliota MT, Partidos CD, Osorio JE. 2014. A novel MVA vectored Chikungunya virus vaccine elicits protective immunity in mice. *PLoS Negl Trop Dis* 8:e2970.

374. Chattopadhyay A, Wang E, Seymour R, Weaver SC, Rose JK. 2013. A chimeric vesiculo/alphavirus is an effective alphavirus vaccine. *J Virol* 87:395-402.
375. Smith SA, Silva LA, Fox JM, Flyak AI, Kose N, Sapparapu G, Khomandiak S, Khomadiak S, Ashbrook AW, Kahle KM, Fong RH, Swayne S, Doranz BJ, McGee CE, Heise MT, Pal P, Brien JD, Austin SK, Diamond MS, Dermody TS, Crowe JE. 2015. Isolation and Characterization of Broad and Ultrapotent Human Monoclonal Antibodies with Therapeutic Activity against Chikungunya Virus. *Cell Host Microbe* 18:86-95.
376. Manning G, Whyte DB, Martinez R, Hunter T, Sudarsanam S. 2002. The protein kinase complement of the human genome. *Science* 298:1912-34.
377. Playford MP, Schaller MD. 2004. The interplay between Src and integrins in normal and tumor biology. *Oncogene* 23:7928-46.
378. Parsons SJ, Parsons JT. 2004. Src family kinases, key regulators of signal transduction. *Oncogene* 23:7906-9.
379. Ingley E. 2008. Src family kinases: regulation of their activities, levels and identification of new pathways. *Biochim Biophys Acta* 1784:56-65.
380. Pagano MA, Tibaldi E, Palù G, Brunati AM. 2013. Viral proteins and Src family kinases: Mechanisms of pathogenicity from a "liaison dangereuse". *World J Virol* 2:71-8.
381. Strunk U, Saffran HA, Wu FW, Smiley JR. 2013. Role of herpes simplex virus VP11/12 tyrosine-based motifs in binding and activation of the Src family kinase Lck and recruitment of p85, Grb2, and Shc. *J Virol* 87:11276-86.
382. Macdonald A, Crowder K, Street A, McCormick C, Harris M. 2004. The hepatitis C virus NS5A protein binds to members of the Src family of tyrosine kinases and regulates kinase activity. *J Gen Virol* 85:721-9.
383. Greenway A, Azad A, Mills J, McPhee D. 1996. Human immunodeficiency virus type 1 Nef binds directly to Lck and mitogen-activated protein kinase, inhibiting kinase activity. *J Virol* 70:6701-8.
384. Deininger MW, Goldman JM, Melo JV. 2000. The molecular biology of chronic myeloid leukemia. *Blood* 96:3343-56.
385. Savage DG, Antman KH. 2002. Imatinib mesylate--a new oral targeted therapy. *N Engl J Med* 346:683-93.
386. Lombardo LJ, Lee FY, Chen P, Norris D, Barrish JC, Behnia K, Castaneda S, Cornelius LA, Das J, Doweiko AM, Fairchild C, Hunt JT, Inigo I, Johnston K, Kamath A, Kan D, Klei H, Marathe P, Pang S, Peterson R, Pitt S, Schieven GL, Schmidt RJ, Tokarski J, Wen ML, Wityak J, Borzilleri RM. 2004. Discovery of N-(2-chloro-6-methyl-phenyl)-2-(6-(4-(2-hydroxyethyl)-piperazin-1-yl)-2-methylpyrimidin-4-ylamino)thiazole-5-carboxamide (BMS-354825), a dual Src/Abl kinase inhibitor with potent antitumor activity in preclinical assays. *J Med Chem* 47:6658-61.
387. Luo FR, Yang Z, Camuso A, Smykla R, McGlinchey K, Fager K, Flefle C, Castaneda S, Inigo I, Kan D, Wen ML, Kramer R, Blackwood-Chirchir A, Lee FY. 2006. Dasatinib (BMS-354825)

- pharmacokinetics and pharmacodynamic biomarkers in animal models predict optimal clinical exposure. *Clin Cancer Res* 12:7180-6.
388. Fraser CK, Blake SJ, Diener KR, Lyons AB, Brown MP, Hughes TP, Hayball JD. 2009. Dasatinib inhibits recombinant viral antigen-specific murine CD4+ and CD8+ T-cell responses and NK-cell cytolytic activity in vitro and in vivo. *Exp Hematol* 37:256-65.
389. An X, Tiwari AK, Sun Y, Ding PR, Ashby CR, Chen ZS. 2010. BCR-ABL tyrosine kinase inhibitors in the treatment of Philadelphia chromosome positive chronic myeloid leukemia: a review. *Leuk Res* 34:1255-68.
390. Hirsch AJ, Medigeshi GR, Meyers HL, DeFilippis V, Früh K, Briese T, Lipkin WI, Nelson JA. 2005. The Src family kinase c-Yes is required for maturation of West Nile virus particles. *J Virol* 79:11943-51.
391. de Wispelaere M, LaCroix AJ, Yang PL. 2013. The small molecules AZD0530 and dasatinib inhibit dengue virus RNA replication via Fyn kinase. *J Virol* 87:7367-81.
392. Chu JJ, Yang PL. 2007. c-Src protein kinase inhibitors block assembly and maturation of dengue virus. *Proc Natl Acad Sci U S A* 104:3520-5.
393. Bermejo M, López-Huertas MR, García-Pérez J, Climent N, Descours B, Ambrosioni J, Mateos E, Rodríguez-Mora S, Rus-Bercial L, Benkirane M, Miró JM, Plana M, Alcamí J, Coiras M. 2016. Dasatinib inhibits HIV-1 replication through the interference of SAMHD1 phosphorylation in CD4+ T cells. *Biochem Pharmacol* 106:30-45.
394. Reeves PM, Smith SK, Olson VA, Thorne SH, Bornmann W, Damon IK, Kalman D. 2011. Variola and monkeypox viruses utilize conserved mechanisms of virion motility and release that depend on abl and SRC family tyrosine kinases. *J Virol* 85:21-31.
395. Dyall J, Coleman CM, Hart BJ, Venkataraman T, Holbrook MR, Kindrachuk J, Johnson RF, Olinger GG, Jahrling PB, Laidlaw M, Johansen LM, Lear-Rooney CM, Glass PJ, Hensley LE, Frieman MB. 2014. Repurposing of clinically developed drugs for treatment of Middle East respiratory syndrome coronavirus infection. *Antimicrob Agents Chemother* 58:4885-93.
396. Diehl N, Schaal H. 2013. Make yourself at home: viral hijacking of the PI3K/Akt signaling pathway. *Viruses* 5:3192-212.
397. Thaa B, Biasiotto R, Eng K, Neuvonen M, Götte B, Rheinemann L, Mutso M, Utt A, Varghese F, Balistreri G, Merits A, Ahola T, McInerney GM. 2015. Differential Phosphatidylinositol-3-Kinase-Akt-mTOR Activation by Semliki Forest and Chikungunya Viruses Is Dependent on nsP3 and Connected to Replication Complex Internalization. *J Virol* 89:11420-37.
398. Judith D, Mostowy S, Bourai M, Gangneux N, Lelek M, Lucas-Hourani M, Cayet N, Jacob Y, Prévost MC, Pierre P, Tangy F, Zimmer C, Vidalain PO, Couderc T, Lecuit M. 2013. Species-specific impact of the autophagy machinery on Chikungunya virus infection. *EMBO Rep* 14:534-44.
399. Jhanwar-Uniyal M, Amin AG, Cooper JB, Das K, Schmidt MH, Murali R. 2017. Discrete signaling mechanisms of mTORC1 and mTORC2: Connected yet apart in cellular and molecular aspects. *Adv Biol Regul* 64:39-48.

400. Joubert PE, Stapleford K, Guivel-Benhassine F, Vignuzzi M, Schwartz O, Albert ML. 2015. Inhibition of mTORC1 Enhances the Translation of Chikungunya Proteins via the Activation of the MnK/eIF4E Pathway. *PLoS Pathog* 11:e1005091.
401. Krejbich-Trotot P, Gay B, Li-Pat-Yuen G, Hoarau JJ, Jaffar-Bandjee MC, Briant L, Gasque P, Denizot M. 2011. Chikungunya triggers an autophagic process which promotes viral replication. *Virology* 432:432-439.
402. Thoreen CC, Kang SA, Chang JW, Liu Q, Zhang J, Gao Y, Reichling LJ, Sim T, Sabatini DM, Gray NS. 2009. An ATP-competitive mammalian target of rapamycin inhibitor reveals rapamycin-resistant functions of mTORC1. *J Biol Chem* 284:8023-32.
403. Sun SY, Rosenberg LM, Wang X, Zhou Z, Yue P, Fu H, Khuri FR. 2005. Activation of Akt and eIF4E survival pathways by rapamycin-mediated mammalian target of rapamycin inhibition. *Cancer Res* 65:7052-8.
404. Jung CH, Ro SH, Cao J, Otto NM, Kim DH. 2010. mTOR regulation of autophagy. *FEBS Lett* 584:1287-95.
405. Glick D, Barth S, Macleod KF. 2010. Autophagy: cellular and molecular mechanisms. *J Pathol* 221:3-12.
406. Joubert PE, Werneke SW, de la Calle C, Guivel-Benhassine F, Giodini A, Peduto L, Levine B, Schwartz O, Lenschow DJ, Albert ML. 2012. Chikungunya virus-induced autophagy delays caspase-dependent cell death. *J Exp Med* 209:1029-47.
407. Dupuis-Maguiraga L, Noret M, Brun S, Le Grand R, Gras G, Roques P. 2012. Chikungunya disease: infection-associated markers from the acute to the chronic phase of arbovirus-induced arthralgia. *PLoS Negl Trop Dis* 6:e1446.
408. de la Monte S, Castro F, Bonilla NJ, Gaskin de Urdaneta A, Hutchins GM. 1985. The systemic pathology of Venezuelan equine encephalitis virus infection in humans. *Am J Trop Med Hyg* 34:194-202.
409. Doxsey SJ, Brodsky FM, Blank GS, Helenius A. 1987. Inhibition of endocytosis by anti-clathrin antibodies. *Cell* 50:453-63.
410. DeTulleo L, Kirchhausen T. 1998. The clathrin endocytic pathway in viral infection. *EMBO J* 17:4585-93.
411. Kääriäinen L, Ahola T. 2002. Functions of alphavirus nonstructural proteins in RNA replication. *Prog Nucleic Acid Res Mol Biol* 71:187-222.
412. Grimley PM, Berezesky IK, Friedman RM. 1968. Cytoplasmic structures associated with an arbovirus infection: loci of viral ribonucleic acid synthesis. *J Virol* 2:1326-38.
413. Ahlquist P. 2006. Parallels among positive-strand RNA viruses, reverse-transcribing viruses and double-stranded RNA viruses. *Nat Rev Microbiol* 4:371-82.
414. Garoff H, Simons K, Dobberstein B. 1978. Assembly of the Semliki Forest virus membrane glycoproteins in the membrane of the endoplasmic reticulum in vitro. *J Mol Biol* 124:587-600.

415. Bonatti S, Migliaccio G, Blobel G, Walter P. 1984. Role of signal recognition particle in the membrane assembly of Sindbis viral glycoproteins. *Eur J Biochem* 140:499-502.
416. Liu LN, Lee H, Hernandez R, Brown DT. 1996. Mutations in the endo domain of Sindbis virus glycoprotein E2 block phosphorylation, reorientation of the endo domain, and nucleocapsid binding. *Virology* 222:236-46.
417. Garoff H, Sjöberg M, Cheng RH. 2004. Budding of alphaviruses. *Virus Res* 106:103-16.
418. Keating JA, Striker R. 2012. Phosphorylation events during viral infections provide potential therapeutic targets. *Rev Med Virol* 22:166-81.
419. Le Sage V, Cinti A, Amorim R, Moulard AJ. 2016. Adapting the Stress Response: Viral Subversion of the mTOR Signaling Pathway. *Viruses* 8.
420. Ubersax JA, Ferrell JE. 2007. Mechanisms of specificity in protein phosphorylation. *Nat Rev Mol Cell Biol* 8:530-41.
421. Manning G, Plowman GD, Hunter T, Sudarsanam S. 2002. Evolution of protein kinase signaling from yeast to man. *Trends Biochem Sci* 27:514-20.
422. Chong YP, Ia KK, Mulhern TD, Cheng HC. 2005. Endogenous and synthetic inhibitors of the Src-family protein tyrosine kinases. *Biochim Biophys Acta* 1754:210-20.
423. Frame MC. 2002. Src in cancer: deregulation and consequences for cell behaviour. *Biochim Biophys Acta* 1602:114-30.
424. Yeatman TJ. 2004. A renaissance for SRC. *Nat Rev Cancer* 4:470-80.
425. Weiss RA, Vogt PK. 2011. 100 years of Rous sarcoma virus. *J Exp Med* 208:2351-5.
426. Koegl M, Zlatkine P, Ley SC, Courtneidge SA, Magee AI. 1994. Palmitoylation of multiple Src-family kinases at a homologous N-terminal motif. *Biochem J* 303 ( Pt 3):749-53.
427. Luttrell DK, Luttrell LM. 2004. Not so strange bedfellows: G-protein-coupled receptors and Src family kinases. *Oncogene* 23:7969-78.
428. Bromann PA, Korkaya H, Courtneidge SA. 2004. The interplay between Src family kinases and receptor tyrosine kinases. *Oncogene* 23:7957-68.
429. Wagner MJ, Smiley JR. 2009. Herpes simplex virus requires VP11/12 to induce phosphorylation of the activation loop tyrosine (Y394) of the Src family kinase Lck in T lymphocytes. *J Virol* 83:12452-61.
430. Fruehling S, Swart R, Dolwick KM, Kremmer E, Longnecker R. 1998. Tyrosine 112 of latent membrane protein 2A is essential for protein tyrosine kinase loading and regulation of Epstein-Barr virus latency. *J Virol* 72:7796-806.
431. García M, Cooper A, Shi W, Bornmann W, Carrion R, Kalman D, Nabel GJ. 2012. Productive replication of Ebola virus is regulated by the c-Abl1 tyrosine kinase. *Sci Transl Med* 4:123ra24.

432. Pogliaghi M, Papagno L, Lambert S, Calin R, Calvez V, Katlama C, Autran B. 2014. The tyrosine kinase inhibitor Dasatinib blocks in-vitro HIV-1 production by primary CD4+ T cells from HIV-1 infected patients. *AIDS* 28:278-81.
433. Lupberger J, Zeisel MB, Xiao F, Thumann C, Fofana I, Zona L, Davis C, Mee CJ, Turek M, Gorke S, Royer C, Fischer B, Zahid MN, Lavillette D, Fresquet J, Cosset FL, Rothenberg SM, Pietschmann T, Patel AH, Pessaux P, Doffoël M, Raffelsberger W, Poch O, McKeating JA, Brino L, Baumert TF. 2011. EGFR and EphA2 are host factors for hepatitis C virus entry and possible targets for antiviral therapy. *Nat Med* 17:589-95.
434. Jilg N, Chung RT. 2012. Adding to the toolbox: receptor tyrosine kinases as potential targets in the treatment of hepatitis C. *J Hepatol* 56:282-4.
435. Magnuson B, Ekim B, Fingar DC. 2012. Regulation and function of ribosomal protein S6 kinase (S6K) within mTOR signalling networks. *Biochem J* 441:1-21.
436. Ruvinsky I, Meyuhos O. 2006. Ribosomal protein S6 phosphorylation: from protein synthesis to cell size. *Trends Biochem Sci* 31:342-8.
437. O'Hare T, Walters DK, Stoffregen EP, Jia T, Manley PW, Mestan J, Cowan-Jacob SW, Lee FY, Heinrich MC, Deininger MW, Druker BJ. 2005. In vitro activity of Bcr-Abl inhibitors AMN107 and BMS-354825 against clinically relevant imatinib-resistant Abl kinase domain mutants. *Cancer Res* 65:4500-5.
438. Roskoski R. 2004. Src protein-tyrosine kinase structure and regulation. *Biochem Biophys Res Commun* 324:1155-64.
439. Anishchenko M, Paessler S, Greene IP, Aguilar PV, Carrara AS, Weaver SC. 2004. Generation and characterization of closely related epizootic and enzootic infectious cDNA clones for studying interferon sensitivity and emergence mechanisms of Venezuelan equine encephalitis virus. *J Virol* 78:1-8.
440. Deuber SA, Pavlovic J. 2007. Virulence of a mouse-adapted Semliki Forest virus strain is associated with reduced susceptibility to interferon. *J Gen Virol* 88:1952-9.
441. Li X, Yang M, Yu Z, Tang S, Wang L, Cao X, Chen T. 2017. The tyrosine kinase Src promotes phosphorylation of the kinase TBK1 to facilitate type I interferon production after viral infection. *Sci Signal* 10.
442. Sali TM, Pryke KM, Abraham J, Liu A, Archer I, Broeckel R, Staverosky JA, Smith JL, Al-Shammari A, Amsler L, Sheridan K, Nilsen A, Streblow DN, DeFilippis VR. 2015. Characterization of a Novel Human-Specific STING Agonist that Elicits Antiviral Activity Against Emerging Alphaviruses. *PLoS Pathog* 11:e1005324.
443. Karaman MW, Herrgard S, Treiber DK, Gallant P, Atteridge CE, Campbell BT, Chan KW, Ciceri P, Davis MI, Edeen PT, Faraoni R, Floyd M, Hunt JP, Lockhart DJ, Milanov ZV, Morrison MJ, Pallares G, Patel HK, Pritchard S, Wodicka LM, Zarrinkar PP. 2008. A quantitative analysis of kinase inhibitor selectivity. *Nat Biotechnol* 26:127-32.
444. Marais R, Light Y, Paterson HF, Marshall CJ. 1995. Ras recruits Raf-1 to the plasma membrane for activation by tyrosine phosphorylation. *EMBO J* 14:3136-45.

445. Yori JL, Lozada KL, Seachrist DD, Mosley JD, Abdul-Karim FW, Booth CN, Flask CA, Keri RA. 2014. Combined SFK/mTOR inhibition prevents rapamycin-induced feedback activation of AKT and elicits efficient tumor regression. *Cancer Res* 74:4762-71.
446. Chen B, Xu X, Luo J, Wang H, Zhou S. 2015. Rapamycin Enhances the Anti-Cancer Effect of Dasatinib by Suppressing Src/PI3K/mTOR Pathway in NSCLC Cells. *PLoS One* 10:e0129663.
447. Pyronnet S. 2000. Phosphorylation of the cap-binding protein eIF4E by the MAPK-activated protein kinase Mnk1. *Biochem Pharmacol* 60:1237-43.
448. Duncia JV, Santella JB, Higley CA, Pitts WJ, Wityak J, Fietze WE, Rankin FW, Sun JH, Earl RA, Tabaka AC, Teleha CA, Blom KF, Favata MF, Manos EJ, Daulerio AJ, Stradley DA, Horiuchi K, Copeland RA, Scherle PA, Trzaskos JM, Magolda RL, Trainor GL, Wexler RR, Hobbs FW, Olson RE. 1998. MEK inhibitors: the chemistry and biological activity of U0126, its analogs, and cyclization products. *Bioorg Med Chem Lett* 8:2839-44.
449. Wan X, Harkavy B, Shen N, Grohar P, Helman LJ. 2007. Rapamycin induces feedback activation of Akt signaling through an IGF-1R-dependent mechanism. *Oncogene* 26:1932-40.
450. Stead RL, Proud CG. 2013. Rapamycin enhances eIF4E phosphorylation by activating MAP kinase-interacting kinase 2a (Mnk2a). *FEBS Lett* 587:2623-8.
451. Klinghoffer RA, Sachsenmaier C, Cooper JA, Soriano P. 1999. Src family kinases are required for integrin but not PDGFR signal transduction. *EMBO J* 18:2459-71.
452. Igarashi A. 1978. Isolation of a Singh's Aedes albopictus cell clone sensitive to Dengue and Chikungunya viruses. *J Gen Virol* 40:531-44.
453. Kinney RM, Johnson BJ, Welch JB, Tsuchiya KR, Trent DW. 1989. The full-length nucleotide sequences of the virulent Trinidad donkey strain of Venezuelan equine encephalitis virus and its attenuated vaccine derivative, strain TC-83. *Virology* 170:19-30.
454. Gerardin P, Guernier V, Perrau J, Fianu A, Le Roux K, Grivard P, Michault A, de Lamballerie X, Flahault A, Favier F. 2008. Estimating Chikungunya prevalence in La Reunion Island outbreak by serosurveys: two methods for two critical times of the epidemic. *BMC Infect Dis* 8:99.
455. Sergon K, Yahaya AA, Brown J, Bedja SA, Mlindasse M, Agata N, Allaranger Y, Ball MD, Powers AM, Ofula V, Onyango C, Konongoi LS, Sang R, Njenga MK, Breiman RF. 2007. Seroprevalence of Chikungunya virus infection on Grande Comore Island, union of the Comoros, 2005. *Am J Trop Med Hyg* 76:1189-93.
456. Sergon K, Njuguna C, Kalani R, Ofula V, Onyango C, Konongoi LS, Bedno S, Burke H, Dumilla AM, Konde J, Njenga MK, Sang R, Breiman RF. 2008. Seroprevalence of Chikungunya virus (CHIKV) infection on Lamu Island, Kenya, October 2004. *Am J Trop Med Hyg* 78:333-7.
457. Anonymous. Chikungunya Fever Situation in the Country during 2006 (Prov.), *on National Vector Borne Disease Control Programme*, Delhi, 2006. <http://www.nvbdc.gov.in/Chikun-cases.html>. Accessed

458. Laurent P, Le Roux K, Grivard P, Bertil G, Naze F, Picard M, Staikowsky F, Barau G, Schuffenecker I, Michault A. 2007. Development of a sensitive real-time reverse transcriptase PCR assay with an internal control to detect and quantify chikungunya virus. *Clin Chem* 53:1408-14.
459. Ozden S, Huerre M, Riviere JP, Coffey LL, Afonso PV, Mouly V, de Monredon J, Roger JC, El Amrani M, Yvin JL, Jaffar MC, Frenkiel MP, Sourisseau M, Schwartz O, Butler-Browne G, Despres P, Gessain A, Ceccaldi PE. 2007. Human muscle satellite cells as targets of Chikungunya virus infection. *PLoS ONE* 2:e527.
460. Chu H, Das SC, Fuchs JF, Suresh M, Weaver SC, Stinchcomb DT, Partidos CD, Osorio JE. 2013. Deciphering the protective role of adaptive immunity to CHIKV/IRES a novel candidate vaccine against Chikungunya in the A129 mouse model. *Vaccine* 31:3353-60.
461. Yoon IK, Alera MT, Lago CB, Tac-An IA, Villa D, Fernandez S, Thaisomboonsuk B, Klungthong C, Levy JW, Velasco JM, Roque VG, Salje H, Macareo LR, Hermann LL, Nisalak A, Srikiatkachorn A. 2015. High rate of subclinical chikungunya virus infection and association of neutralizing antibody with protection in a prospective cohort in the Philippines. *PLoS Negl Trop Dis* 9:e0003764.
462. Kam YW, Simarmata D, Chow A, Her Z, Teng TS, Ong EK, Renia L, Leo YS, Ng LF. 2012. Early appearance of neutralizing immunoglobulin G3 antibodies is associated with chikungunya virus clearance and long-term clinical protection. *J Infect Dis* 205:1147-54.
463. Kam YW, Lum FM, Teo TH, Lee WW, Simarmata D, Harjanto S, Chua CL, Chan YF, Wee JK, Chow A, Lin RT, Leo YS, Le Grand R, Sam IC, Tong JC, Roques P, Wiesmuller KH, Renia L, Rotzschke O, Ng LF. 2012. Early neutralizing IgG response to Chikungunya virus in infected patients targets a dominant linear epitope on the E2 glycoprotein. *EMBO Mol Med* 4:330-43.
464. Kam YW, Lee WW, Simarmata D, Harjanto S, Teng TS, Tolou H, Chow A, Lin RT, Leo YS, Renia L, Ng LF. 2012. Longitudinal analysis of the human antibody response to Chikungunya virus infection: implications for serodiagnosis and vaccine development. *J Virol* 86:13005-15.
465. Kam YW, Pok KY, Eng KE, Tan LK, Kaur S, Lee WW, Leo YS, Ng LC, Ng LF. 2015. Sero-prevalence and cross-reactivity of chikungunya virus specific anti-E2EP3 antibodies in arbovirus-infected patients. *PLoS Negl Trop Dis* 9.
466. Partidos CD, Weger J, Brewoo J, Seymour R, Borland EM, Ledermann JP, Powers AM, Weaver SC, Stinchcomb DT, Osorio JE. 2011. Probing the attenuation and protective efficacy of a candidate chikungunya virus vaccine in mice with compromised interferon (IFN) signaling. *Vaccine* 29:3067-73.
467. Selvarajah S, Sexton NR, Kahle KM, Fong RH, Mattia KA, Gardner J, Lu K, Liss NM, Salvador B, Tucker DF, Barnes T, Mabila M, Zhou X, Rossini G, Rucker JB, Sanders DA, Suhrbier A, Sambri V, Michault A, Muench MO, Doranz BJ, Simmons G. 2013. A neutralizing monoclonal antibody targeting the acid-sensitive region in chikungunya virus E2 protects from disease. *PLoS Negl Trop Dis* 7:e2423.
468. Venugopalan A, Ghorpade RP, Chopra A. 2014. Cytokines in acute chikungunya. *PLoS One* 9:e111305.

469. Kelvin AA, Banner D, Silvi G, Moro ML, Spataro N, Gaibani P, Cavrini F, Pierro A, Rossini G, Cameron MJ, Bermejo-Martin JF, Paquette SG, Xu L, Danesh A, Farooqui A, Borghetto I, Kelvin DJ, Sambri V, Rubino S. 2011. Inflammatory cytokine expression is associated with chikungunya virus resolution and symptom severity. *PLoS Negl Trop Dis* 5:e1279.
470. Ng LF, Chow A, Sun YJ, Kwek DJ, Lim PL, Dimatatac F, Ng LC, Ooi EE, Choo KH, Her Z, Kourilsky P, Leo YS. 2009. IL-1beta, IL-6, and RANTES as biomarkers of Chikungunya severity. *PLoS One* 4:21.
471. Appassakij H, Khuntikij P, Kemapunmanus M, Wutthanarungsan R, Silpapojakul K. 2013. Viremic profiles in asymptomatic and symptomatic chikungunya fever: a blood transfusion threat? *Transfusion* 53:2567-74.
472. Panning M, Grywna K, van Esbroeck M, Emmerich P, Drosten C. 2008. Chikungunya fever in travelers returning to Europe from the Indian Ocean region, 2006. *Emerg Infect Dis* 14:416-22.
473. Bellini R, Medici A, Calzolari M, Bonilauri P, Cavrini F, Sambri V, Angelini P, Dottori M. 2012. Impact of Chikungunya virus on *Aedes albopictus* females and possibility of vertical transmission using the actors of the 2007 outbreak in Italy. *PLoS One* 7:e28360.
474. Larghi OP, Nebel AE. 1980. Rabies virus inactivation by binary ethylenimine: new method for inactivated vaccine production. *J Clin Microbiol* 11:120-2.
475. Habib M, Hussain I, Irshad H, Yang ZZ, Shuai JB, Chen N. 2006. Immunogenicity of formaldehyde and binary ethylenimine inactivated infectious bursal disease virus in broiler chicks. *J Zhejiang Univ Sci B* 7:660-4.
476. Bahnemann HG. 1975. Binary ethylenimine as an inactivant for foot-and-mouth disease virus and its application for vaccine production. *Arch Virol* 47:47-56.
477. Couturier E, Guillemin F, Mura M, Léon L, Virion JM, Letort MJ, De Valk H, Simon F, Vaillant V. 2012. Impaired quality of life after chikungunya virus infection: a 2-year follow-up study. *Rheumatology (Oxford)* 51:1315-22.
478. Weaver SC. 2014. Arrival of chikungunya virus in the new world: prospects for spread and impact on public health. *PLoS Negl Trop Dis* 8:e2921.
479. Pratheek BM, Suryawanshi AR, Chattopadhyay S. 2015. In silico analysis of MHC-I restricted epitopes of Chikungunya virus proteins: Implication in understanding anti-CHIKV CD8(+) T cell response and advancement of epitope based immunotherapy for CHIKV infection. *Infect Genet Evol* 31:118-26.
480. Tsuda Y, Caposio P, Parkins CJ, Botto S, Messaoudi I, Cicin-Sain L, Feldmann H, Jarvis MA. 2011. A replicating cytomegalovirus-based vaccine encoding a single Ebola virus nucleoprotein CTL epitope confers protection against Ebola virus. *PLoS Negl Trop Dis* 5:e1275.
481. Karrer U, Wagner M, Siervo S, Oxenius A, Hengel H, Dumrese T, Freigang S, Koszinowski UH, Phillips RE, Klenerman P. 2004. Expansion of protective CD8+ T-cell responses driven by recombinant cytomegaloviruses. *J Virol* 78:2255-64.
482. Yang TC, Dayball K, Wan YH, Bramson J. 2003. Detailed analysis of the CD8+ T-cell response following adenovirus vaccination. *J Virol* 77:13407-11.

483. Tatsis N, Fitzgerald JC, Reyes-Sandoval A, Harris-McCoy KC, Hensley SE, Zhou D, Lin SW, Bian A, Xiang ZQ, Iparraguirre A, Lopez-Camacho C, Wherry EJ, Ertl HC. 2007. Adenoviral vectors persist in vivo and maintain activated CD8+ T cells: implications for their use as vaccines. *Blood* 110:1916-23.
484. Farrington LA, Smith TA, Grey F, Hill AB, Snyder CM. 2013. Competition for antigen at the level of the APC is a major determinant of immunodominance during memory inflation in murine cytomegalovirus infection. *J Immunol* 190:3410-6.
485. Matthews DA, Cummings D, Eveleigh C, Graham FL, Prevec L. 1999. Development and use of a 293 cell line expressing lac repressor for the rescue of recombinant adenoviruses expressing high levels of rabies virus glycoprotein. *J Gen Virol* 80 ( Pt 2):345-53.
486. Messerle M, Crnkovic I, Hammerschmidt W, Ziegler H, Koszinowski UH. 1997. Cloning and mutagenesis of a herpesvirus genome as an infectious bacterial artificial chromosome. *Proc Natl Acad Sci U S A* 94:14759-63.
487. Paredes AM, Yu D. 2012. Human cytomegalovirus: bacterial artificial chromosome (BAC) cloning and genetic manipulation. *Curr Protoc Microbiol* Chapter 14:Unit14E.4.
488. Warming S, Costantino N, Court DL, Jenkins NA, Copeland NG. 2005. Simple and highly efficient BAC recombineering using galK selection. *Nucleic Acids Res* 33:e36.
489. Safronetz D, Hegde NR, Ebihara H, Denton M, Kobinger GP, St Jeor S, Feldmann H, Johnson DC. 2009. Adenovirus vectors expressing hantavirus proteins protect hamsters against lethal challenge with andes virus. *J Virol* 83:7285-95.
490. Pelliccia M, Andreozzi P, Paulose J, D'Alicarnasso M, Cagno V, Donalisio M, Civra A, Broeckel RM, Haese N, Jacob Silva P, Carney RP, Marjomäki V, Streblow DN, Lembo D, Stellacci F, Vitelli V, Krol S. 2016. Additives for vaccine storage to improve thermal stability of adenoviruses from hours to months. *Nat Commun* 7:13520.
491. Zawistowski JS, Graves LM, Johnson GL. 2014. Assessing adaptation of the cancer kinome in response to targeted therapies. *Biochem Soc Trans* 42:765-9.
492. Duncan JS, Whittle MC, Nakamura K, Abell AN, Midland AA, Zawistowski JS, Johnson NL, Granger DA, Jordan NV, Darr DB, Usary J, Kuan PF, Smalley DM, Major B, He X, Hoadley KA, Zhou B, Sharpless NE, Perou CM, Kim WY, Gomez SM, Chen X, Jin J, Frye SV, Earp HS, Graves LM, Johnson GL. 2012. Dynamic reprogramming of the kinome in response to targeted MEK inhibition in triple-negative breast cancer. *Cell* 149:307-21.
493. Bantscheff M, Eberhard D, Abraham Y, Bastuck S, Boesche M, Hobson S, Mathieson T, Perrin J, Raida M, Rau C, Reader V, Sweetman G, Bauer A, Bouwmeester T, Hopf C, Kruse U, Neubauer G, Ramsden N, Rick J, Kuster B, Drewes G. 2007. Quantitative chemical proteomics reveals mechanisms of action of clinical ABL kinase inhibitors. *Nat Biotechnol* 25:1035-44.
494. Stuhlmiller TJ, Miller SM, Zawistowski JS, Nakamura K, Beltran AS, Duncan JS, Angus SP, Collins KA, Granger DA, Reuther RA, Graves LM, Gomez SM, Kuan PF, Parker JS, Chen X, Sciaky N, Carey LA, Earp HS, Jin J, Johnson GL. 2015. Inhibition of Lapatinib-Induced Kinome Reprogramming in ERBB2-Positive Breast Cancer by Targeting BET Family Bromodomains. *Cell Rep* 11:390-404.

495. Cooper MJ, Cox NJ, Zimmerman EI, Dewar BJ, Duncan JS, Whittle MC, Nguyen TA, Jones LS, Ghose Roy S, Smalley DM, Kuan PF, Richards KL, Christopherson RI, Jin J, Frye SV, Johnson GL, Baldwin AS, Graves LM. 2013. Application of multiplexed kinase inhibitor beads to study kinome adaptations in drug-resistant leukemia. *PLoS One* 8:e66755.